Numerical and experimental performance evaluation of ventilated packages

by
Tobi Samuel Fadiji

Dissertation presented for the degree of Doctor of Philosophy in the Faculty of Engineering at Stellenbosch University

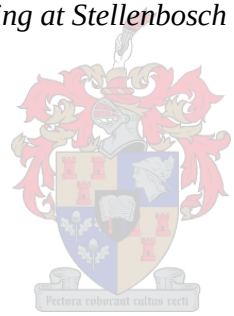

Supervisors: Prof. Corné Coetzee
Prof. Umezuruike Linus Opara

April 2019

DECLARATION

By submitting this dissertation electronically, I declare that the entirety of the work contained therein is my own, original work, that I am the sole author thereof (save to the extent explicitly otherwise stated), that reproduction and publication thereof by Stellenbosch University will not infringe any third party rights and that I have not previously in its entirety or in part submitted it for obtaining any qualification.

This dissertation includes three original papers published in peer-reviewed journals or books and three unpublished publications. The development and writing of the papers (published and unpublished) were the principal responsibility of myself and, for each of the cases where this is not the case, a declaration is included in the dissertation indicating the nature and extent of the contributions of co-authors.

Date: April 2019

UNIVERSITEIT•STELLENBOSCH•UNIVERSITY
jou kennisvennoot • your knowledge partner

Plagiaatverklaring / *Plagiarism Declaration*

1 Plagiaat is die oorneem en gebruik van die idees, materiaal en ander intellektuele eiendom van ander persone asof dit jou eie werk is.
Plagiarism is the use of ideas, material and other intellectual property of another's work and to present is as my own.

2 Ek erken dat die pleeg van plagiaat 'n strafbare oortreding is aangesien dit 'n vorm van diefstal is.
I agree that plagiarism is a punishable offence because it constitutes theft.

3 Ek verstaan ook dat direkte vertalings plagiaat is.
I also understand that direct translations are plagiarism.

4 Dienooreenkomstig is alle aanhalings en bydraes vanuit enige bron (ingesluit die internet) volledig verwys (erken). Ek erken dat die woordelikse aanhaal van teks sonder aanhalingstekens (selfs al word die bron volledig erken) plagiaat is.
Accordingly all quotations and contributions from any source whatsoever (including the internet) have been cited fully. I understand that the reproduction of text without quotation marks (even when the source is cited) is plagiarism.

5 Ek verklaar dat die werk in hierdie skryfstuk vervat, behalwe waar anders aangedui, my eie oorspronklike werk is en dat ek dit nie vantevore in die geheel of gedeeltelik ingehandig het vir bepunting in hierdie module/werkstuk of 'n ander module/werkstuk nie.
I declare that the work contained in this assignment, except otherwise stated, is my original work and that I have not previously (in its entirety or in part) submitted it for grading in this module/assignment or another module/assignment.

TS Fadiji	April 2019
Voorletters en van / *Initials and surname*	**Datum / *Date***

PAPER CONTRIBUTION DECLARATION

Declaration by the candidate

Declaration with regard to parts of the dissertation in which, in addition to the candidate, other authors were involved. With regard to the following chapters in the dissertation, the nature and scope of my contribution were as follows:

Dissertation Chapter	Contribution Nature	Extent (~%)
Chapter 2	Main author and Primary Researcher	75%
Chapter 3	Main author and Primary Researcher	70%
Chapter 4	Main author and Primary Researcher	70%
Chapter 5	Main author and Primary Researcher	75%
Chapter 6	Main author and Primary Researcher	80%
Chapter 7	Main author and Primary Researcher	80%

The following co-authors have contributed to the following chapters in the dissertation:

Name	e-mail	Chapters	Contribution	Extent (~ %)
C. Coetzee	ccoetzee@sun.ac.za	2,3,4,5,6,7	Advice/Mentoring	10 %, 10 %, 10 %, 10 %, 10 %, 10 % respectively
U. L. Opara	opara@sun.ac.za	2,3,4,5,6,7	Advice/Mentoring	10 %, 10 %, 10 %, 10 %, 10 %, 10 % respectively
T. M. Berry	tarl@sun.ac.za	2,3,4,5	Advice/Mentoring	5 %, 5 %, 5 %, 10 % respectively
A. Ambaw	tsige@sun.ac.za	3,4	Advice/Mentoring	5 %, 5 % respectively

Signature of candidate: Date: 25-02-2019

Declaration by the candidate

The undersigned hereby confirm that:

1. The declaration above accurately reflects the nature and extent of the contributions of the candidate and co-authors to the Chapters as indicated in the table above,
2. No other authors contributed to Chapters as indicated, besides those specified above,
3. Potential conflicts of interest have been revealed to all interested parties and that the necessary arrangements have been made to use the material indicated in the table above in the relevant Chapters of this dissertation.

Name	Signature	Institutional Affiliation	Date
C. Coetzee	Signed electronically	Stellenbosch University	25-02-2019
U. L. Opara	Signed electronically	Stellenbosch University	25-02-2019
T. M. Berry	Signed electronically	Stellenbosch University	25-02-2019
A. Ambaw	Signed electronically	Stellenbosch University	25-02-2019

ABSTRACT

Packaging serves a crucial role in reducing postharvest losses, particularly in the handling of fresh horticultural produce, and would be difficult to do without. Packaging protects the produce against mechanical hazards such as compression, impact, drop or vibration during distribution, ensuring its safe delivery to the consumers in a sound condition, at a minimum cost. Ventilated corrugated paperboard (VCP) packaging is being used extensively for handling fresh produce due to its capability to promote uniform and rapid cooling. However, the presence of ventilation openings jeopardises the strength of the package which could result in produce damage. As it is of utmost importance to ensure that the produce reaches its final destination without damage, continuous improvement in the package strength is paramount. Hence, this project aimed to gain a better understanding of the structural performance of VCP packaging to enhance the development of better and improved package designs.

Firstly, a validated finite element analysis (FEA) model was developed to study the structural performance of an existing VCP package. This model incorporated some geometrical nonlinearities of the package. Paper and paperboard characterisations were done to determine the tensile properties, edge compression resistance and flat crush resistance. The tensile properties were used as input parameters in the model. The model was able to predict the compression strength of the package, and showed good agreement with experimental results, within 10%. Package liner thickness had a linear relationship with the compression strength. The stress in the package was found to be concentrated and a maximum at the corners.

Subsequently, the FEA model was used to assess the strength of different package designs with emphasis on the influence of different geometrical configuration. The model was validated with experimental results. Increasing the vent area of the package reduced its compression strength. Packages manufactured with double-walled corrugated board performed better than single-walled board irrespective of the design, with the difference in strength as high as 72%. This study showed the importance of knowing the paperboard properties in the design of a package to improve its strength.

Furthermore, the creep behaviour of different package designs was evaluated, and results showed load and environment conditions as significant factors affecting the creep rate. Increasing the applied load and relative humidity (RH) as well as reducing the temperature, accelerated the creep rate of the package. Also, package configuration also had a significant effect on the creep rate.

Finally, to understand the deformation phenomenon of packages subjected to compression load, the displacement field of different designs was studied using digital image correlation (DIC), a full-field non-contact optical measurement technique. Findings showed that the distribution of the package displacement is

largely heterogeneous. The displacement field in the out-of-plane direction was the largest while that in the horizontal direction was the smallest. Buckling was found to be a predominant phenomenon occurring at the centre of the package panels.

Overall, this study provided empirical and numerical evidence for the design of improved packages, balancing the need for adequate structural performance and optimum cooling functionalities of the package.

OPSOMMING

Verpakking speel 'n deurslaggewende rol in die vermindering van na-oesverliese, veral in die hantering van vars tuinbouprodukte, en dit sal moeilik wees om daar sonder klaar te kom. Verpakking beskerm die produk teen meganiese skade as gevolg van druk, impak, val of vibrasie tydens verspreiding. Dit verseker die veilige aflewering van die produk, in ‘n veilige toestand en teen minimum koste, aan die verbruiker. Geventileerde gegolfde karton (GGK) verpakking word omvattend gebruik vir die hantering van vars produkte as gevolg van sy vermoë om uniforme en vinnige verkoeling te bevorder. Die teenwoordigheid van ventilasie openinge belemmer egter die sterkte van die verpakking wat tot skade aan die produk kan lei. Aangesien dit van uiterste belang is om te verseker dat die produk sy eindbestemming sonder skade bereik, is voortdurende verbetering in die verpakkig se sterkte van die grootste belang. Daarom was die doel van hierdie proefskrif om 'n beter begrip van die strukturele vermoeë van GGK verpakking te verkry en om sodoende die ontwikkeling van beter verpakking te bevorder.

Eerstens is 'n gevalideerde eindige element-analise (EEA) model ontwikkel om die strukturele vermoeë van bestaande GGK-verpakking te bestudeer. Hierdie model het sommige geometriese nie-lineariteite van die verpakking ingesluit. Papier- en kartonkarakterisasie is gedoen om die trek eienskappe, rand drukweerstand en plat breekweerstand te bepaal. Die trek eienskappe is gebruik as invoer veranderlikes in die model. Die model was in staat om die druksterkte van die verpakking te voorspel en het binne 10% goeie ooreenkoms met eksperimentele resultate getoon. Die dikte van die verpakkingvoering het 'n lineêre verband met die druksterkte gehad. Die spanning in die verpakking was gekonsentreer en ‘n maksimum in die hoeke.

Vervolgens is die EEA-model gebruik om die sterkte van verskillende verpakkingsontwerpe te bepaal, met die klem op die invloed van verskillende geometriese konfigurasies. Die model is gevalideer met eksperimentele resultate. Verhoging van die ventilasie area van die verpakking het die druksterkte verlaag. Verpakking wat met dubbelwandige golfkarton vervaardig is, het beter gevaar as enkelwandige karton, ongeag die ontwerp, met 'n verskil in sterkte van tot 72%. Hierdie studie het getoon dat dit belangrik is om die karton-eienskappe te weet gedurende die ontwerp van verpakking om sodeoende sy sterkte te verbeter.

Verder is die kruipgedrag van verskillende verpakkingsontwerpe geëvalueer, en resultate het las- en omgewingsomstandighede as belangrike faktore wat die kruipkoers beïnvloed, getoon. Verhoging van die aangewende las en relatiewe humiditeit (RH) asook die verlaging van die temperatuur, versnel die kruipkoers van die verpakking. Verpakkingskonfigurasie het ook 'n beduidende uitwerking op die kruipkoers gehad.

Ten slotte, om die vervormingsverskynsel van verpakking onder druklas te verstaan, is die verplasingsveld van verskillende ontwerpe bestudeer aan die hand

van digitale beeldkorrelasie (DBK), 'n nie-kontak optiese metingstegniek. Bevindinge het getoon dat die verdeling van die verpakking se verplasing hoofsaaklik heterogeen is. Die verplasingsveld in die uit-vlak rigting was die grootste terwyl dit in die horisontale rigting die kleinste was. Daar was gevind dat knik ‘n oorheersende fenomeen in die middel van die verpakkingpanele was.

In die algemeen het hierdie studie empiriese en numeriese bewyse verskaf vir die ontwerp van verbeterde verpakking, wat die behoefte aan voldoende strukturele vermoeë en optimale afkoelfunksies van die verpakking balanseer.

ACKNOWLEDGEMENTS

My sincere gratitude to the National Research Foundation (NRF), South Africa for the award of postgraduate scholarship through the DST/NRF South African Research Chair in Postharvest Technology at Stellenbosch University.

To my supervisors Prof. Corné Coetzee and Prof. Umezuruike Linus Opara, thank you for the invaluable input, ingenuity and mentorship towards the success of my research. For all the esteemed professional advice, support, encouragement, patience and kind interactions that has helped me through this ambitious effort, I want to say thank you. To Dr. Tarl Berry and Dr. Alemayehu Ambaw, that you for the willingness and enthusiasm to assist me anytime I walk into your offices.

My adorable wife, Angelina Wilson Fadiji, I sincerely appreciate your love, encouragement, support and helping to read through this thesis. Most importantly, thank you for all the sacrifices during this PhD journey. To my mother Mrs Juliana Bola Fadiji and to a precious daddy, Alhaji Salman Adelodun Ibrahim, I appreciate all the effort to make sure I went through school even through thick and thin. You have been a source of immense help and a pillar of strength throughout my entire life. My profound appreciation goes to all my relatives, who in one way or the other have inspired and encouraged me.

I would also like to thank the following organisations and people for sharing their assistance, technical advice and experience: Paper Sciences (Sappi Technology Centre), Pretoria and APL-Cartons, Cape Town. To Mr Jason Knock and Rene van der Westhuizen from Paper Sciences (Sappi Technology Centre), thank you for hosting and your time during some of the experiments. Many thanks to Stefan Boshoff, Roche' Kenny and Dewald Grobbelaar from APL-Carton, for helping with the package manufacturing and for all the insights gained from the various discussions. Many thanks to Dr. Oluwafemi Caleb for the words of encouragement and advice. To Pastor Funlola Olojede from RCCG Desire of Nations, thank you for the spiritual nurturing. And to the big family and friends at RCCG Desire of Nations, Stellenbosch, I appreciate you all. To Nazneen at SARChI, thank you for the effective administration. Finally, to the wonderful team at SARChI Postharvest Technology, I thank you all for the wonderful and unforgettable moments we had together.

This work was based upon research supported by the South African Research Chairs Initiative of the Department of Science and Technology and National Research Foundation.

To my wife Angelina Wilson Fadiji, for all your unending love, encouragement, understanding and support; you are a rare gem. To the Lord God Almighty for all your grace and blessings.

Table of Contents

List of Figures

List of Tables

NOTE

This thesis presents a compilation of manuscripts where each chapter is an individual entity and some repetition between chapters, therefore, has been unavoidable.

List of contributions

A. Publications – Peer-reviewed journal papers (published and submitted)

1. **Fadiji, T.,** Berry, T. M., Coetzee, C. J., & Opara, U. L. (2018). Mechanical design and performance testing of corrugated paperboard packaging for the postharvest handling of horticultural produce. *Biosystems Engineering*, *171*, 220–244.
2. **Fadiji, T.,** Coetzee, C. J., Berry, T. M., Ambaw, A., & Opara, U. L. (2018). The efficacy of finite element analysis (FEA) as a design tool for food packaging: A review. *Biosystems engineering*, *174*, 20–40.
3. **Fadiji, T.**, Ambaw, A., Coetzee, C. J., Berry, T. M., & Opara, U. L. (2018). Application of finite element analysis to predict the mechanical strength of ventilated corrugated paperboard packaging for handling fresh produce. *Biosystems Engineering*, *174*, 260–281.
4. Berry, T. M., **Fadiji, T.,** Defraeye, T., & Opara, U.L. (2017). The role of horticultural carton vent hole design on cooling efficiency and compression strength: A multi-parameter approach. *Postharvest Biology and Technol*ogy, *124*, 62–74.
5. **Fadiji, T.,** Coetzee, C. J., Berry, T. M., & Opara, U. L. (2018). Investigating the role of geometrical configurations of ventilated fresh produce packaging to improve the mechanical strength – Experimental and numerical approaches. *Food Packaging and Shelf Life* (under review).
6. **Fadiji, T.,** Coetzee, C. J., & Opara, U. L. (2018). Analysis of the creep behaviour of ventilated corrugated paperboard packaging for handling fresh produce – an experimental study. *Food and Bioproducts Processing* (under review).
7. **Fadiji, T.,** Coetzee, C. J., & Opara, U. L. (2018). Evaluating the displacement field of paperboard packages subjected to mechanical loading using digital image correlation (DIC). *Biosystems Engineering* (submitted).

B. Publications - Peer-reviewed conference proceedings

1. Berry, T. M., **Fadiji, T.,** Defraeye, T., Coetzee, C., & Opara, U. L. (2016, June). A multi-parameter approach to vent hole design for cartons packed with internal packaging. In *VIII International Postharvest Symposium: Enhancing Supply Chain and Consumer Benefits-Ethical and Technological Issues 1194* (pp. 1307–1314).
2. **Fadiji, T.,** Berry, T. M., Ambaw, A., Coetzee, C., & Opara, U. L. (2017, September). Finite element modelling of the structural performance of ventilated paperboard packaging. In *VII International Conference on Managing Quality in Chains (MQUIC2017) and II International Symposium on Ornamentals in 1201* (pp. 237–244).

3. **Fadiji, T.,** Berry, T. M., Ambaw, A., Coetzee, C., & Opara, U. L. (2017, September). Finite element analysis (FEA)–an effective and efficient design tool in food packaging industries: a review. In *VII International Conference on Managing Quality in Chains (MQUIC2017) and II International Symposium on Ornamentals in 1201* (pp. 245–252).

C. Conferences - Posters/Presentations

1. **Fadiji, T.,** Coetzee, C. J., & Opara, U. L. (2016). *To protect and preserve – Studies to improve the mechanical design of ventilated fresh produce packaging*, 5th African Higher Education Week and RUFORUM Biennial Conference, 17–21 October, Cape Town, South Africa.
2. **Fadiji, T.,** Coetzee, C. J., & Opara, U. L. (2016). *Modelling the structural behaviour of ventilated paperboard packaging*, Engineering and Technology Innovation for Global Food Security, 24–27 October, Cape Town, South Africa.
3. Berry, T., **Fadiji, T.,** Defraeye, T., Ambaw, A., & Opara, U. L. (2016). *Impact of vent hole design on fruit cooling rate and carton strength: A multi-parameter evaluation*, Engineering and Technology Innovation for Global Food Security, 24–27 October, Cape Town, South Africa.
4. Berry, T., **Fadiji, T.,** Defraeye, T., Coetzee, C., & Opara, U. L. (2016). *A multi-parameter approach to vent hole design for cartons packed with internal packaging*, VIII International Postharvest Symposium, 21–24 June, Cartagena, Spain.
5. **Fadiji, T.,** Berry, T. Ambaw, A., Coetzee, C., & Opara, L. (2017). *Finite element analysis (FEA) – an effective and efficient design tool in food packaging industries: a review*, VII International Conference on Managing Quality in Chains (MQUIC2017), 4–7 September 2017, Stellenbosch, South Africa.
6. **Fadiji, T.,** Berry, T., Ambaw, A., Coetzee, C., & Opara, L. (2017). *Finite element modelling of the structural performance of ventilated paperboard packaging*, VII International Conference on Managing Quality in Chains (MQUIC2017), 4–7 September 2017, Stellenbosch, South Africa.
7. **Fadiji, T.,** Berry, T., Coetzee, C., & Opara, U. L. (2018). *The role of horticultural package vent hole design on structural performance*, 12th CIGR Section VI Postharvest Technology and Bio-Process Engineering International Symposium, 22–25 October 2018, Ibadan, Nigeria.
8. **Fadiji, T.,** Coetzee, C., & Opara, U. L. (2018). *Deformation field of corrugated paperboard horticultural packages using digital image correlation*, 12th CIGR Section VI Postharvest Technology and Bio-Process Engineering International Symposium, 22–25 October 2018, Ibadan, Nigeria.

Chapter 1. General Introduction

1.1 Background

Food security is one of the numerous factors inhibiting sustainable development for humanity and the planet earth as a whole. The ability to provide sufficient quality, quantity and safe food to the world's growing population, predicted to rise above 9 billion in 2050, is an enormous challenge (Opara, 2011; FAO, 2009). It has been projected that food production will have to increase by more than 70% to meet the future demand (Opara, 2011; FAO, 2009; Gilland, 2002). For the current population, adequate food is being produced to meet the dietary requirements and the credit goes to advancement in major agricultural and postharvest technologies. Despite this advancement, over 1 billion people (Africa's current population) still do not have enough to eat and frequently go to bed hungry, eventually leading to starvation and in worst scenario death may occur. Most of the projected increase in food production would have to come from the intensive application of technological innovations, given the increasing competition for fresh water and agricultural land for urbanisation, and development of new infrastructure networks (Satterthwaite et al., 2010).

About 12% of South Africa's gross domestic product (GDP) is from the agricultural sector, with more than 3% from the fresh horticultural produce industry (SADAFF, 2014; PPECB, 2013). The fresh horticultural produce such as fruit and vegetables are consumed locally, however, the industry is export-oriented. Often, the satisfaction a consumer derives from high quality produce in sound condition is the major aim of production, handling, storage, transportation and distribution of fresh horticultural produce (Opara & Pathare, 2014). Consumer perception of fresh produce is influenced by numerous factors such as texture quality, shape and appearance (Fadiji et al., 2016a; Opara & Pathare, 2014). Consequently, these factors affect the purchasing decision of the consumers. For example, high quality produce free from mechanical damage (bruise, puncture, and cuts), pathogens and physiological disorders will receive higher consumer attention and could lead to significant economic growth (Fadiji et al., 2016a; Van Zeebroeck et al., 2007; Prusky, 2011; Matzinger & Tong, 1993; Timm et al., 1996). A reduction in the aesthetic appeal of a produce may be caused by the presence of bruising or any physical damage. In addition, bruised fruit are highly susceptible to extreme moisture loss (about 400 times greater than intact fruit), and to bacteria or fungi infestation (Wilson et al., 1995). Some studies have also shown the loss in nutritional value of fresh produce as a function of the presence of mechanical damage (Opara & Pathare, 2014; Sablani et al., 2006). For example, Sablani et al. (2006) reported higher vitamin C in unbruised tomato compared to bruised tomato.

In order to reduce produce damage, package design must be carefully considered. In the generalised optimisation criteria for package design and performance evaluation (Figure 1.1), cooling, produce, and mechanical performance as well as energy efficiency need to be ensured. Produce performance is closely linked to

mechanical performance through the effects of compression, impact and vibration. Several studies have classified the loads that cause mechanical damage as impact, compression and vibration loadings (Opara & Fadiji, 2018; Fadiji et al., 2016a, b; Lu et al., 2012; Ahmadi, 2012; Chonhenchob et al., 2009; Jarimopas et al., 2007; Lee et al., 2005; Ragni & Berardinelli, 2001; Bajema & Hyde, 1998; Ruiz Altisent, 1991; Brusewitz et al., 1991; Armstrong et al., 1991; Holt & Schoorl, 1984). Impact damage commonly occurs due to free fall of fruit from trees or during collision between the fruit and the package (Fadiji et al., 2018a; 2016a, Li & Thomas, 2014). Compression damage could occur during and after packaging, when the exerted force on the fruit and package is greater than the threshold the fruit or the package can withstand (Fadiji et al., 2018a; Li & Thomas, 2014). Vibration damage occurs when the package and the produce go through continuous movement during transit, which may lead to package/produce damage (Fadiji et al., 2018a, 2016b, Sittipod et al., 2009; Jarimopas et al., 2007, 2005).

Mechanical damage to fresh produce is a major contributing factor to postharvest losses (Opara & Pathare, 2014; Kader, 2002). Losses can be referred to as the quantitative and qualitative food loss in the postharvest system. This system comprises interconnected activities from the time of harvest through crop processing (transportation, handling, packaging and storage), marketing and food preparation, to the final decision by the consumer to eat or discard the food. In the supply chain of fresh horticultural produce, postharvest losses and disposed produce can be as high as 40% before getting to the final end-user (Defraeye et al., 2015; Fox & Fimeche, 2013; Gustavsson & Stage, 2011; Barchi et al., 2002). In South Africa, postharvest losses were reported to be between 20–25% (Oelofse & Nahman, 2013).

Among various postharvest operations, packaging is very important in minimising mechanical damage to fresh produce, consequently reducing postharvest losses (Fadiji et al., 2018a; Opara & Pathare, 2014; Pathare et al., 2012b). The main aim of packaging is to protect the produce against damage that may arise through inadequacies in handling and transportation (Opara & Pathare, 2014). Mangaraj et al. (2009) described packaging as a crucial step in protecting produce from external factors such as contaminants, spoilage micro-organisms and gas composition. Furthermore, packaging was defined by Opara and Mditshwa (2013) as an important element of food security, which ensures that packed fresh produce are delivered in sound condition to the consumers. In addition to the protection capability of packaging, it should also be able to promote rapid cooling, remove the respiration heat build-up within the package, facilitate metabolic gas exchange, enhance produce shelf life, maintain produce quality as well as maintain the cold chain (Defraeye et al., 2015; Opara, 2011). With diverse packaging types that exist such as paper, metals, glass, and plastics, paper packaging has been widely adopted in the fresh produce industry (Rhim, 2010; Pascall, 2010).

As part of the advancement in innovative packaging, ventilated corrugated paperboard packaging has emanated as the most prevalent type used for packaging fresh horticultural produce (Opara, 2011). The placement of vent holes in a package helps to maintain a balance in the airflow outside and inside of the package and reduces the resistance to airflow. This has been shown to increase the preserving capabilities of the package (Berry et al., 2017; Han & Park, 2007). Although, vent holes allow for uniform cooling of the packed produce, if not properly designed, it can jeopardise the mechanical strength of the package. Pathare and Opara (2014) outlined some factors to consider in designing vent holes to enhance cooling efficiency while still providing sufficient protection to the packed produce. The factors include: vent area, location, shape and size. During the handling, storage and transportation of fresh produce, these packages are stacked on top of each other on a pallet and are exposed to static and dynamic loads under varying environmental conditions (Fadiji et al., 2018a; Jarimopas et al., 2007; Navaranjan & Johnson, 2006). These may occur in either short or long durations. Static load eventuates as compression due to the pressure exerted on the stacked package. Greater loads beyond what the package can carry, particularly the bottom package, will result in damage to the package and consequently to the packed produce. Opara and Fadiji (2018) studied the produce (apple fruit) and package interactions when subjected to compressive load. The combination of package dimensions and type of paperboard was reported to influence the resistance of the package to compression loading. High mechanical damage to the fruit in the form of bruises was greatest at the top of the package. Dynamic load arises from vertical and horizontal acceleration during distribution and transportation (Navaranjan & Johnson, 2006). Additionally, long-term storage of stacked packages can result to creep which could in turn lead to package collapse. All these factors may reduce the value of the packed produce due to damage.

Another major challenge to the structural strength of ventilated corrugated paperboard packaging is the complexity of the mechanical behaviour of paper material in relation to varying environmental conditions (temperature and relative humidity). This can lead to an adverse effect by drastically reducing the stacking strength (Pathare & Opara, 2014; Dongmei et al., 2013). Haslach (2000) stated the complexity in the structural performance of paper packaging was due to its time-dependent characteristics making reference to moisture content, load, and temperature whether constant or combined. High humidity and low temperature increase the moisture content in the package, hence causing a reduction in its mechanical strength (Bronlund et al., 2013). Allaoui et al. (2009a) showed a reduction as high as 50% in the Young's modulus of paper on changing the relative humidity from 50–90%. In the study by Zhang et al. (2011), the edge compressive resistance of corrugated paperboard reduced by about 19% after uniformly increasing the relative humidity from 30% to 90%. Therefore, the design of packages should be such that it can survive the life cycle in a cold chain without damage.

Amidst the challenges faced in the fresh horticultural produce industry, the demand for high quality horticultural produce, including fruit and vegetables has increased in recent years. As a general rule, paper-based packages are over-sized in order to avoid time-dependent failure, and the use of objective package designs and performance evaluation methods are minimal (Han & Park, 2007). This results in limited innovation, which may reduce competitiveness. In order for the packaging industries to ensure a sustainable competitive advantage, it is crucial to advance their products and services. With the enhancement of affordable computing power and efficiency, numerical modelling has been accepted as a successful method in engineering (Ambaw et al., 2013; Delele et al., 2010). Furthermore, modelling has proven successful because experimental layout or setup is resource-intensive and time consuming (Delele et al., 2010). Finite element analysis (FEA) has been considered as a vital tool in the corrugated board and packaging industries for accurate predictions of the strength of packages (Biancolini et al., 2010; Urbanik & Saliklis, 2007; Biancolini, 2005). FEA can also be applied to predict the structural performance of packages under load for various test cases such as predicting the effect of complex package design features (vent holes).

The South African Research Chair (SARChI) Postharvest Technology Laboratory at Stellenbosch University have in recent times conducted experimental and numerical studies to investigate the performance of ventilated corrugated paperboard packages. Heat and mass transfer, cooling rates and airflow patterns inside multi-scale ventilated packages used by South African fruit industry were investigated to provide a better understanding of the cold chain performance of these packages and shipping containers (Getahun et al., 2018, 2017a, b; Delele et al., 2013a, b; Ngcobo et al., 2013; Ngcobo, 2012). The susceptibility of both package and fresh fruit to impact, compression and vibration loads was investigated to provide insights on the mechanical integrity of the packages (Opara & Fadiji, 2018; Fadiji, 2015; Fadiji et al., 2016a, b, c). More recently, Berry (2017) developed computational fluid dynamics (CFD) models to evaluate the cooling rate, to quantify spatio-temporal moisture distributions in packages during shipping and to increase packing densities in refrigerated freight containers (RFC). While these studies provide a preliminary understanding of the performance of VCP packages, more research is required to evaluate the resistance of the package to mechanical loads in order to enhance package designs. In addition, this will provide opportunity to simultaneously optimise the integrated performance of ventilated horticultural packages in maintaining the cold chain while preventing damage to the package and the produce.

In addition to optimising packaging design, other specific challenges have necessitated investigating the mechanical performance of different package design. These challenges include the package deformation due to compression that has the paucity of evidence of its effects on packages. Another challenge is the insufficient evidence on appropriate models for understanding the mechanical behaviour of

packages as compared to cooling, produce performance and energy efficiency that have been extensively studied.

1.2 Aim and objectives

The aim of the study was to gain a better insight into the structural performance of ventilated paperboard packaging to enhance the development of improved next-generation packaging for the key role players in the fruit packaging value chain.

The specific objectives were to:

a) Develop an experimentally validated finite element model that predicts the mechanical strength of ventilated corrugated packaging.
b) Apply the validated finite element model to investigate the performance of different package design configuration.
c) Investigate the effects of package design and environmental conditions on the creep behaviour of ventilated packages.

A secondary objective was also to provide preliminary evidence on the potential of digital image correlation (DIC) in investigating package deformation.

1.3 Outline of the research presented

The outline for this research is presented as follows:

Chapter 2 presents an overview of the performance of corrugated paperboard packaging, enumerating the various testing for evaluating its mechanical strength, including the influence of manufacturing processes and environmental conditions on its performance. Chapter 3 gives an overview of the application of finite element analysis (FEA) as a design tool in food packaging, with emphasis on corrugated paperboard packaging, and also the challenges encountered by the users of FEA in food and packaging industries are highlighted. Chapter 4 covers the development and validation of FEA model to study the structural performance of corrugated paperboard packages subjected to compression load.

Chapter 5 presents an application of the validated model from Chapter 4 to investigate the effects of different package geometrical configuration on package performance. Results are compared with physical package compression tests. Building on Chapter 5, this research further presents the effects of package design and environmental conditions on the creep behaviour of ventilated packages in chapter 6. In Chapter 7, this study also presents preliminary evidence on the potential of using digital image correlation (DIC) to investigate deformation phenomenon of the packages under compression. Finally, chapter 8 gives the concluding summary of the research, and recommendation for future prospects.

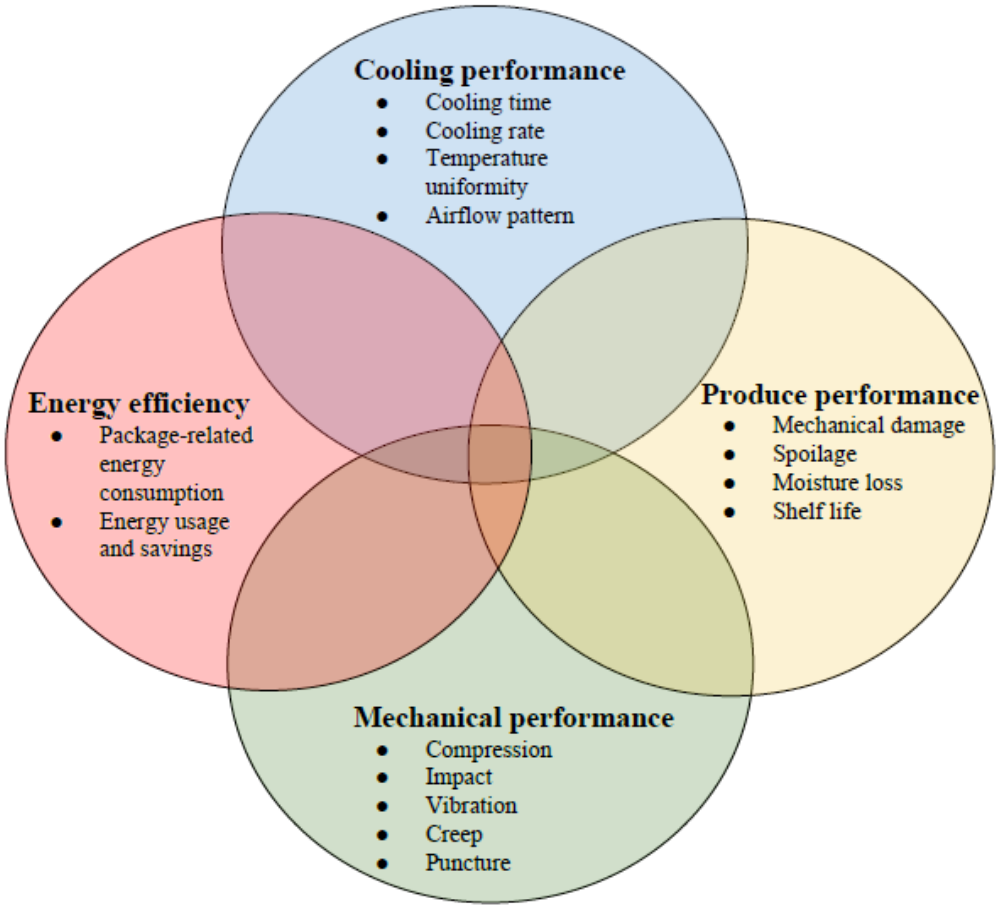

Figure 1.1: Generalised criteria for optimal package design and performance evaluation.

Chapter 2. Mechanical design and performance testing of corrugated paperboard packaging for the postharvest handling of horticultural produce*

Abstract

Corrugated paperboard is the primary material used in the transportation, distribution and storage of many products, particularly horticultural produce. Corrugated paperboard packages provide protection to packed produce against mechanical loadings at all phases of distribution. These packages filled with produce are exposed to different hazards such as being dropped from height, transportation shocks, compression during stacking and exposure to the weight of other packed produce, all of which can damage produce. This review discusses performance testing of corrugated paperboard packaging, and highlights the manufacturing process and cold chain environment factors affecting the strength of corrugated paperboard packaging. The performance requirements for corrugated paperboard packages include appearance, structural stability and protection of contents. Testing the quality of corrugated paperboard and its various components, maintaining good control of manufacturing operations and environmental factors such as moisture, humidity and temperature are necessary for better understanding the performance of corrugated paperboard packaging. Advances in numerical techniques such as finite element analysis (FEA) offer new prospects and opportunities for replacing tedious, time-consuming and expensive experiments to improve the performance of corrugated paperboard packaging.

Keywords: corrugated paperboard packaging; cold chain; horticultural produce; box compression test; tensile test.

---

*Publication:

Fadiji, T., Berry, T. M., Coetzee, C. J., & Opara, U. L. (2018). Mechanical design and performance testing of corrugated paperboard packaging for the postharvest handling of horticultural produce. *Biosystems Engineering*, *171*, 220–244.

2.1 Introduction

Packaging is an essential requirement for fresh and processed food products to provide vital protection from external factors arising from contaminants, gas composition, spoilage microorganisms, mechanical loadings and physical damage (Samanta et al., 2016; Mangaraj et al., 2009; Farber, 1991). Opara and Mditshwa (2013) described packaging as an essential food security component, which assures safe handling and delivery of fresh and processed products from point of production to the end-users. Thus, packaging plays a vital function in the postharvest handling and transportation of fresh and processed food and other biomaterials (Defraeye et al., 2015; Pathare & Opara, 2014; Pathare et al., 2012b; Opara, 2011).

A wide variety of packaging materials are used for handling fresh and processed horticultural products including polymeric film pouches, tin cans, paper and paperboard, wooden crates, baskets, plastics, trays and metallic films. Paper and paperboard are the most widely used for packaging food, particularly fresh horticultural produce (Chamberlain & Kirwan, 2013). These packages must meet various criteria for successful packaging that ensure the safety of the packed products (Rhim, 2010; Pascall, 2010).

The use of corrugated paperboard remains a dominant packaging material in the horticultural industry due to its versatility (Kaushal et al, 2015; Pathare & Opara, 2014). Corrugated paperboard packaging has been employed widely to protect products against damage that may arise from handling, transportation, storage, hazards and environmental conditions (Navaranjan & Johnson, 2006). Some advantages of corrugated paperboard which make its usage widely acceptable, particularly in horticultural industry include; low weight and hence very easy to handle, inexpensive, fully recyclable in nature (making them eco-friendly), strong and stiff compared to its weight, easily available and easily customisable to any specific requirement (Pathare & Opara, 2014; Thompson et al., 2010; Navaranjan & Johnson, 2006; Biancolini, 2005; Biancolini et al., 2005; Aboura et al., 2004).

In recent times, corrugated paperboard has been used for the manufacture of ventilated paperboard cartons for handling perishable produce. Pathare et al. (2012b) reported that ventilated corrugated paperboard (VCP) packaging is commonly used and adopted globally in handling fresh produce. VCP packaging is an important technological innovation that rapidly promotes efficient and uniform cooling of horticultural produce (Fadiji et al., 2016a, b, c; Pathare & Opara, 2014; Pathare et al., 2012b; Ngcobo et al., 2012; Ferrua & Singh, 2011; Thompson et al., 2010; De Castro et al., 2005). Vent holes help to maintain balance in airflow channels between the surrounding and inside of the carton/package to reduce the resistance to airflow and has been shown to strengthen the package, hence preserving the packed product (Han & Park, 2007).

During postharvest handling, transportation and storage of fresh produce packed inside paper cartons, they are exposed to static and dynamic loads, under varying

environmental conditions, which can occur over either short or long durations (Fadiji et al., 2016a, b, c; Viguié et al., 2011; Jarimopas et al., 2007; Navaranjan & Johnson, 2006). Static loads are mainly a result of pressures exerted on stacked packages (compression) that cause short and long-term creep buckling. Dynamic load arises from vertical and horizontal acceleration during transportation. The value of the packed produce may reduce due to these factors as a result of the presence of mechanical damage such as bruise defects on fruit which may lead to economic loss of the fruit due to downgrading or rejection by consumers (Opara & Fadiji, 2018; Jarimopas et al., 2007; Van Zeebroeck et al., 2007). However, corrugated paperboard cartons are still preferred, as they have been established to have good strength when dry (Pathare & Opara, 2014; Twede & Harte, 2003).

The complexity of the mechanical behaviour of corrugated paperboard is observed when the surrounding environmental conditions such as temperature and relative humidity (RH) vary. Changes in humidity have considerable degradative effects on the mechanical strength of the paper package and its operational life span. Increased moisture content reduces the fibre network strength, mechanical properties and the life of the package (Defraeye et al., 2015; Jo et al., 2012; Navaranjan & Johnson, 2006), which can increase the susceptibility of the packed produce to damage (Opara & Fadiji, 2018; Fadiji et al., 2016a, b; Opara & Pathare, 2014; Pathare & Opara, 2014; Chonhenchob & Singh, 2003). The complexity of the structural performance of paper packaging was discussed by Haslach (2000). The complex behaviour of paper packaging was reported to be due to its time-dependent characteristics with reference to moisture content, load, and temperature, whether constant or variably combined. Pathare and Opara (2014) reported that one of the main objectives of a ventilated packaging system for fresh horticultural produce is to minimise mechanical damage of the packed produce during postharvest handling and enhance the overall packaging performance in maintaining a balance between the mechanical integrity of the package and uniform air distribution within the package system.

The strength and performance of a corrugated package depend on numerous factors, such as the quality of the input cellulose fibre, the mechanical properties of the components and the combined board, the manufacturing quality control protocol, machine precision, and the human factor involved in the corrugation process (Fadiji et al. 2017; Zhang et al., 2014; Pathare & Opara, 2014; Biancolini et al., 2010; Rahman & Abubakr, 2007). Knowledge about these vital attributes will help improve the structural performance of the package by both minimising the amount of material utilised for making corrugated paperboard packages and guiding the design of packages with improved performance attributes (Fadiji et al., 2017). The high susceptibility of packed fresh produce to mechanical damage is prevalent and is a major cause of postharvest losses during export (Fadiji et al., 2016a, b; Pathare & Opara, 2014; Pathare et al., 2012b). Therefore, the design of packaging that can facilitate logistical handling, while still reliably protecting the produce from mechanical damage is thus a high priority to the fresh produce industry. This review

provides an overview of the performance testing of corrugated paperboard packaging towards minimising damage to horticultural produce, and discusses the effects of manufacturing processes and cold chain environmental factors affecting the strength of paperboard packaging and packaging materials.

2.2 Fresh produce packaging

2.2.1 Types of packaging materials – brief overview

There exist a wide range of packaging materials used for handling fresh produce and processed products from the farm to the end-user (Opara & Mditshwa, 2013). The design and construction of packages influence and play a significant role in determining the shelf life of a product (Marsh & Bugusu, 2007; Hotchkiss, 1997). All packaging types can be classified into two groups: (a) retail packages: These packages protect the packed contents from damage and at the same time advertise the contents for sale. They include glass bottles, metal cans, plastic bottles, sachets and wraps; (b) shipping packages: The packed contents are protected from damage during transportation, distribution, and other marketing functions. They include sacks, drums, barrels, foil bags, shrink wrapped containers and corrugated paperboard cartons (Paine & Paine, 1992).

Different product packaging materials possess a range of performance properties that influence the quality or shelf-life of the content (Robertson, 2012). Paper and paperboard packaging represents 40% of the packaging market and are the most common material in use (Pathare & Opara, 2014). Plastics and glass compete for second place with about 30%, and rigid plastics take a share of about 18% (Pathare & Opara, 2014; Robertson, 2012; World Packaging Organisation, 2008). Metal, glass and others are about 18%, 7% and 5%, respectively (World Packaging Organisation, 2008). Approximately 70% of all consumer packaging is used in the food industry, 48% of all the packaging is made from paperboard (Opara & Mditshwa, 2013; World Packaging Organisation, 2008; Kirwan, 2003).

Glass packages are impervious to moisture, gases, odour and microorganisms and hence are prevalently used in food industries to store products like beverages and liquid foodstuff. These are very useful as they are inert and do not migrate into the food product, recyclable, reusable, resealable, suitable for heat processing and are transparent to display packed products (Marsh & Bugusu, 2007). Some drawbacks of glass packages include the high cost of glass materials and their manufacturing cost. Although metals are considered the most versatile of all packaging forms, the high cost of metals and the cost of manufacturing makes metal packages expensive (Marsh & Bugusu, 2007). In addition, the heavy weight of metals increases the transportation cost. However, they have a number of advantages: they are strong, they are also convenient for ambient storage and are tamperproof. Plastic are ideal for food packaging because they are resistant to breakage, resistant to corrosion, relatively inexpensive because they are chemically resistant, waterproof and light weight. They are heat sealable, easy to print on and can be combined into production

processes where the package is formed, filled, and sealed in the same production line (Marsh & Bugusu, 2007; Kirwan & Strawbridge, 2003). However, some disadvantages of plastic as food packaging material include: easy bend, crush or crack properties, little heat resistance, and costly laminates. In addition, when compared to metal and glass, plastics are relatively permeable to light, gases (for example, oxygen and carbon dioxide), water vapour and low molecular weight molecules (Opara & Mditshwa, 2013; Marsh & Bugusu, 2007; EPA, 2006). Therefore, when selecting the right plastic to use, knowledge of how sensitive the product is to either loss or absorption of these substances is crucial.

Paper is composed of a network of bonded fibres that is formed by draining a suspension of fibres through a filter screen. Cellulose fibres are the main constituents of paper. Paperboard is a paper material that often consists of several plies bonded together by an adhesive material. Paper and paperboard are orthotropic in nature, with different mechanical properties in the three principal directions (Figure 2.1) (Pathare & Opara, 2014; Jiménez-Caballero et al., 2009; Harrysson & Ristinmaa, 2008; Stenberg, 2003; Xia et al., 2002). This directional dependence of paper and paperboard are (a) the direction of machine or the roll press (MD), (b) cross or perpendicular to the machine direction (CD), and (c) out of plane direction shown in Figure 2.1.

Strength properties usually depend on the selection of the fibre sources and the treatment applied at the paper mill (Side, 2008). Paper usually shows differences between the in-plane and out-of-plane material behaviour (Mäkelä & Östlund, 2003). The mechanical response of paper and paperboard is dominated by the stress components in the in-plane direction, i.e. (MD and CD), while the response in the out-of-plane or thickness direction (ZD) is insignificant or negligible. This is because the dimension of paper in the thickness direction is smaller than the dimension in the other directions (Phongphinittana & Jearanaisilawong, 2013; Jiménez-Caballero et al., 2009; Nygårds et al., 2009). Figure 2.2 shows a typical representation of the mechanical response of paper depicted by the stress-strain curve under uniaxial tensile loading.

Two important zones are illustrated in Figure 2.2: the linear elastic zone, which represents a recoverable deformation, caused by the stretching of the starch or adhesive. Following this zone is the nonlinear plastic zone, which corresponds to an unrecoverable deformation arising from a combination of fibre slip, fibre rupture and matrix breakage (Phongphinittana & Jearanaisilawong, 2013; Gooren, 2006). Due to the orientation of the fibres in the paper material, the mechanical response will differ depending upon the loading direction (Allaoui et al., 2009b; Mäkelä & Östlund, 2003). Figure 2.2 also shows other characteristics and properties of paper such as the high nonlinearity in the stress-strain relationship and the lack of clear transition between the pure elastic and the elastic-plastic deformation (Gooren, 2006; Mäkelä & Östlund, 2003). Mäkelä and Östlund (2003) and Tryding (1996) stated that permanent deformation could occur when there is an unloading on the

nonlinear part of the stress-strain curve from some point. The stiffness (papers ability to resist deformation) during unloading usually coincides with the elastic modulus (Gooren, 2006; Mäkelä & Östlund, 2003; Tryding, 1996). The strength of paper generally reduces with increasing moisture content and decreasing temperature (Fadiji et al., 2017; Allaoui et al., 2009a).

The numerous uses of paper and paperboard includes bags, sacks, wrapping, tissue, rigid boxes, fibre drums, moulded pulp containers, cushioning materials, corrugated boxes and folding cartons (Robertson, 2005). Due to the strength and economic advantages of paper and paperboard, bulk packaging of sugar, powder, dried fruit and vegetables have been pervasive (Raheem, 2012). The various main types of packaging paper used in food packaging are summarised in Table 2.1. To allow for proper ventilation of horticultural products such as fresh fruit and vegetables that respire and remain alive after harvest, VCP packages have been developed. However, the major drawback is in optimising package designs with respect to mechanical strength, produce protection, ventilation and cost (Biancolini & Brutti, 2003).

2.2.2 Corrugated paperboard as a packaging material

Corrugated paperboard is an important application of paper and paperboard and has been used for the production of carton boxes since 1897 (Talbi et al., 2009; Beldie et al., 2001; Gilchrist et al., 1999). Gällstedt and Hedenqvist (2006) referred to corrugated paperboard as one of the most common renewable packaging materials. Corrugated paperboard is widely used and considered the best choice for the manufacturing of carton boxes used mostly in fresh food industry (Biancolini, 2005). Corrugated paperboard manufacturing involves the use of a high precision corrugator (combination of several machines) to form a machinery line process. A corrugator consists of the following subassemblies: single facer, double backer, heating and drying section, longitudinal cutter, cross cutter and a plier (Garg et al., 2016; Fadiji, 2015). Paper, the main raw material used in manufacturing corrugated paperboard is humidified by means of high-pressure steam. The humidification process allows for the softening of the paper fibres to facilitate the formation of the corrugated medium and the gluing process. The sandwich-like structure of a corrugated paperboard consists of a flute-shaped corrugated medium (providing the shear stiffness) formed using heat, pressure and moisture to retain the flute structure, and two outside sheets called the linerboards which provide bending stiffness.

The manufacturing process of corrugated paperboard involves both wet and dry parts. The fluting is corrugated between two rolls and then glued to the liners in the wet part while heat is applied to dry the corrugated board and remove the humidity in the dry part. Starch-based adhesive is used as glue for binding the liners and the fluting medium. The production process is shown in Figure 2.3. Warping and washing are two problems that occur during corrugated paperboard manufacturing, and result due to moisture content imbalance in the different layers of the

paperboard. Warping occurs when the corrugated board can deform to a buckling shape and Washboarding occurs when there is a dip in the facing between the corrugations (Garg et al., 2016; Fadiji, 2015). The moisture imbalance in the different layers of the corrugated paperboard is due to the hygroscopic nature of paper and hence affects the dimension stability of the corrugated paperboard. Therefore, controlling the moisture level at the various stages during the manufacturing process of corrugated paperboard ensures the quality of the board (Thompson et al., 2010).

Usually, the number of layers in a corrugated board depends on the packaging requirements. In a single-faced corrugated paperboard, there are two layers: the liner and the corrugated fluting medium. The single-wall corrugated board consists of three layers: two liners and corrugated fluting medium (core). As reported by Niskanen (2012), about 80% of corrugated paperboard is manufactured as single-wall board. Double and triple-wall corrugated paperboards consist of five and seven layers, respectively (Figure 2.4). The double-wall and triple-wall boards are produced for more demanding packaging solutions (Twede & Selke, 2005; Nordstrand, 2003). Corrugated board is manufactured in several flute profile standards. The flute profiles are characterised by letters A, B, C, E or F (Pathare & Opara, 2014; Hägglund & Carlsson, 2012; Campbell, 2010; Nordstrand, 2003). The letter designations are not related to the relative sizes of the flutes but relate to the order in which the flutes were invented. The properties of the flute types are shown in Table 2.2. A specification of the corrugated board grade includes information on the flute type and the basis weight (mass per unit area) of the flute and of the liners. The grade of corrugated board significantly affects the performance of the corrugated paperboard package in the distribution environment (Nordstrand, 2003). As shown in Table 2.2, A-flute has the tallest core profile, and is usually used for heavy duty boxes. The most commonly used board grades are the B and C-flutes. C-flute is used in conventional transport packages where compression strength is required while B-flute is used where high compression strength is not required, for example, canned products. The E and F-flutes are relatively small and are usually used for manufacturing smaller boxes (Nordstrand, 2003). Usually, corrugated boards with smaller flutes have more flutes per unit length (Hägglund & Carlsson, 2012). The wavelength also known as flute pitch is the horizontal distance between adjacent flute troughs. Also listed in Table 2.2 are the take-up factors which quantify the length of the fluting per unit length of the corrugated board.

Corrugated paperboard is an orthotropic sandwich structure, however, depending on the research, corrugated paperboard is often treated as a single structure (Haj-Ali et al., 2009; Biancolini, 2005; Beldie et al., 2001; Beldie, 2001), as a sandwich (Nordstrand, 1995) or as a monolithic material (Aboura et al., 2004). However irrespective of the approach, the properties of the components (liners and fluting) influence and govern the mechanical behaviour of the sandwich structure. Corrugated paperboard is also characterised by three principal directions namely: the machine direction (MD) and cross direction (CD), which are in the in-plane

directions; and the out-of-plane direction, which refers to the thickness direction (ZD). MD corresponds to the direction of manufacturing of the material while CD corresponds to the transverse direction as shown in Figure 2.5 (Talbi, et al., 2009; Thakkar et al., 2008; Aboura et al., 2004).

The structure of corrugated paperboard gives it the ability to resist buckling and a high stacking strength. The space in the corrugated core helps to facilitate air movement and serves as thermal insulator, which provides protection against fluctuating atmospheric conditions during handling and storage. This makes it an ideal choice for packaging in many industries, including the fresh fruit industry (Sek et al., 2005). As reported by Little and Holmes (2000), over 90% of the packaging in the USA used in the fruit industry is corrugated paperboard. Berry et al. (2015) also reported that corrugated paperboard cartons are most commonly used in export handling of pome fruits (apples and pears) for the South African fruit industry. Sek et al. (2005) and Lu et al. (2001) regarded corrugated paperboard as packaging material for the future.

2.3 Factors affecting paper and paperboard performance

2.3.1 Effects of manufacturing process on the strength of corrugated paperboard

2.3.1.1 Paper and paperboard thickness

The thickness or “calliper” of the paper or board determines the bulkiness and the density of the paper. Paper calliper is the perpendicular distance between two plane parallel surfaces under a pressure of about 98 kPa – equivalent to 1 kg-force cm^2. It is often measured using a micrometer. Variations in calliper can influence several basic paper performance properties, such as quality of roll and strength. The thickness of corrugated paperboard depends on flute height and the calliper of the linerboards (Nevins, 2008; Urbanik, 2001). Manufacturing process could reduce the thickness of the board by compression. The wet pressing process during manufacturing of paper and paperboard increases the fibre-to-fibre bond and the paper density. The increase in density because of wet pressing decreases the thickness, which frequently counterbalances the increase in elastic moduli obtained by densification. Increased densification results in large reduction in the bending stiffness of the linerboards of a corrugated paperboard and has been reported to lower the edge compression resistance (section 2.4.1.7) of the corrugated paperboard and the box compression resistance (section 2.4.2.1) (Popil, 2012; Popil & Hojjatie, 2010; Dimitrov & Heydenrych, 2009; Nevins, 2008; Shallhorn et al., 2004; Whitsitt, 1988). However, compression strength has also been reported to increase with increased wet pressing (Shallhorn et al., 2004). Due to crushing, a reduction of about 1.27 mm in the thickness of paperboard was reported by Batelka (1994a) and this resulted in a reduction of about 13% in the edge compression strength of the paperboard. A study by Kroeschell (1992) stated that the crushing of corrugated paperboard reduced the thickness to height ratio of the board, which

may adversely affect the edge compression strength of the board. The author reported the effect of corrugated paperboard crushing on the edge compression strength was variable. About 15% reduction in edge compression strength of corrugated paperboard was reported to be due to a reduction in thickness of about 30% while with less than 10% reduction in thickness, an insignificant reduction in the edge compression strength was observed. About 20% reduction in flute height resulted in about 3% reduction in the edge compression strength and bending stiffness of corrugated paperboard (Urbanik, 2001). The author suggested this might be caused by excessive tension on the fluting medium and the use of corrugated rolls with a flute profile that is smaller. Guo et al. (2010) demonstrated the effect of thickness on the flat crush strength, edge compression strength, bursting strength, and puncture resistance of honeycomb composite paperboard and corrugated paperboard. The flat crush strength increased when the thickness of corrugated and honeycomb composite paperboard was raised from 10 mm to 15 mm and 20 mm. For the same thicknesses, an increase in bursting strength and puncture resistance was also reported for both honeycomb composite and corrugated paperboards. Budimir et al. (2012) reported a 20% reduction in transportation cost when the thickness of corrugated paperboard is reduced. Some researchers used equations to show the relationship between thickness and bending stiffness of paperboard:

Whitsitt (1988) showed that the bending stiffness of corrugated paperboard was proportional to the thickness of the paper and paperboard:

$$BS_W = \frac{E_L C_L C_B^2}{2} \tag{2.1}$$

where BS_W is the bending stiffness of the corrugated paperboard (N m), E_L is the elastic modulus of the linerboards (N m^{-2}), C_L is the thickness of the linerboard (m) and C_B is the thickness of the board (m).

Fellers and Carlsson (1983) presented the proportionality of thickness to the bending stiffness of a homogenised corrugated paperboard strip:

$$BS_{HS} = \frac{E_{HS} C_{HS}^3}{12} \tag{2.2}$$

where BS_{HS} is the bending stiffness of the homogenous strip (N m), E_{HS} is the elastic modulus of the homogenous strip (N m^{-2}) and C_{HS} is the thickness of the homogenous strip (m).

Markström (1999) presented a relationship between the bending stiffness of the corrugated paperboard to be proportional to the thickness of the board and the tensile stiffness of the liners:

$$BS_{HS} = 0.5 TS_L C_B^2 \quad (2.3)$$

where BS_{HS} is the bending stiffness of the corrugated paperboard (N m), TS_L is the tensile stiffness of the liner (N m^{-1}) and C_B is the thickness of the corrugated paperboard (m).

2.3.1.2 Fluting medium shape

The flute describes the structure of a wave-shaped paperboard material that makes up the corrugation. The reason for the shape of flute (Figure 2.5) that runs parallel to the depth of the package is due to the strength of the wave. Furthermore, the wave created, gives rigidity and stacking strength to corrugated paperboard packages and the hollow space created by the wave-like structure allows air to insulate the content of the corrugated paperboard package. Flutes usually come in different sizes, referred to as profiles (Table 2.2). The standard profiles range from A-flute (the largest) to F-flute (Pathare & Opara, 2014; Budimir et al., 2012; Hägglund & Carlsson, 2012; Nordstrand, 2003). Mechanical properties and the strength of corrugated paperboard depend directly on the flute profiles (Bivainis & Jankauskas, 2015; Budimir et al., 2012). Generally, larger flute profiles provide greater strength to the corrugated paperboard while a better foldability and printability is achieved by smaller flute profiles (Park et al., 2016; Budimir et al., 2012). A-flute boards are reported to show greater strength towards bending and buckling while paperboards with fluting smaller or equal to E have low resistance to bending and are used for the manufacture of primary packaging (i.e. the layer of packaging in immediate contact with the packaged content) (Budimir et al., 2012).

Urbanik (2001) modelled the influence of flute geometry on strength and stiffness of corrugated paperboard. The author developed a mathematical model for the optimisation of flute shape in correlation with the edge compression strength of the corrugated paperboard and the model predicted that the edge compression strength depends on flank angle, take-up factor and flute height to pitch ratio. The model is less applicable when an existing single facer is to be optimised; however, it is very useful when a new pair of corrugator rolls is to be designed. Mechanical properties and material savings change for the flute profiles were predicted by the strength and stiffness models. The results from the study was used to quantify the balance in runnability, cost, strength and stiffness with an optimum flute profile.

2.3.1.3 Linerboard to fluting bond

Bonding is simply defined as the process of binding one material to another material (Ramos-gonzalez et al., 2015; Vishnuvarthanan & Rajeswari, 2013; Vähä-Nissi & Kuusipalo, 1997; Bennett et al., 1989; Koichiro, 1972; Gander et al., 1969). The adhesive bonding between linerboard and the fluting medium is a fundamental process in the production of corrugated paperboard packaging (Johnson & Popil, 2015). In a corrugator bond, the tips of the fluting medium stick to the linerboard facings at two different locations; the double-backer and the single-facer. The starch

adhesive used to bond the linerboard and the fluting medium constitute about 2% of the weight of corrugated paperboards and is one of the least expensive materials used in corrugated paperboard package plants (Johnson & Popil, 2015; Vishnuvarthanan & Rajeswari, 2013; Perkins et al., 2000). Luo et al. (2011) described starch adhesive as being the most extensively used adhesive in the corrugated paperboard industry because of the abundant supply, low cost, biodegradability, ease of chemical modification and renewability. The process of corrugator bonding obtains a strong bond that will increase the productivity of the corrugator, minimise waste and provide consistency in package performance (Johnson & Popil, 2015; Vishnuvarthanan & Rajeswari, 2013; Batelka, 1994b; Kroeschell, 1990; Gartaganis, 1976). Johnson and Popil (2015) also stated that good bonding occurs from a matrix combination of different operating parameters such as moisture, tension, temperature, speed and nip roll pressure. The characteristics of the adhesive formulation and the mechanical alignment of adhesive and corrugating roll mechanism are additional parameters that are crucial in obtaining a good bond between the linerboards and fluting medium.

Corrugation bond quality has a considerable effect on package stacking strength and production speed and is thus a critical factor during manufacturing. Kroeschell (1990) reported that the strength of liner adhesion to the fluting medium was not affected by starch composition, the properties of the liners and fluting medium, corrugation speed or the contents of the starch solids. However, the author reported that the liner adhesion strength was singularly affected by the quantity of starch applied. Although it should be noted, that corrugation quality can be adversely affected by overabundance of adhesive application during the bonding process; the corrugated paperboard may experience washboarding which can cause poor print quality, warping of the board, and crushing of the board due to damping of the fluting medium during slotting and scoring (Johnson & Popil, 2015; Batelka, 1994b; Kroeschell, 1990; Marcille-Lorenz, & Whitsitt, 1990; Daub & Gottsching, 1988; Sprague, 1982; Gartaganis, 1976).

The edge compression strength of corrugated paperboard was affected by the adhesion strength of linerboards to a value of about 400 N m^{-1}, above which there was no significant effect (Kroeschell, 1990). In contrast, Schaepe (2000) reported that liner adhesive strength of up to 730 N m^{-1} significantly influenced the edge compression strength of corrugated paperboard. An 8% reduction in edge compression strength of corrugated paperboard was reported by Batelka (1994b), which was attributed to a ~54% decrease in the adhesion strength of a single-facer linerboard to medium board. The bond between the linerboards and the fluting medium in a corrugated paperboard can be measured by the pin adhesion test, which measures the force required to separate linerboards from the flute tips. The effects of pin adhesion loss on edge compression tests and box compression tests can be magnified by glue line skip and intermittent glue application, and in combination with heavy board weight would result in severe impact on compression performance of the corrugated paperboard (Schaepe, 2000). Schaepe (2000)

reported a pin adhesion strength of 876 N m^{-1} and 730 N m^{-1} to be considered as good and low respectively. The author also stated that corrugated paperboard with liner adhesion strength less than 438 N m^{-1} is at risk of delamination.

2.3.1.4 Web tension

Web tension is referred to as the tension stress applied to the fluting medium as it is transported from the roll of paperboard through the single facer to the corrugating rolls (Godshall & Koning, 1972). The operation speed in the process of manufacturing a single-faced corrugated paperboard is dependent on the flute fracture characteristics or runnability of the fluting medium (Batelka, 1994a; Godshall & Koning, 1972; Gander et al., 1969; McKee & Gander, 1967). Flute fracture occurs due to high tension on the fluting medium between the top and bottom tips of the corrugating rolls within the single facer (Nevins, 2008; Kruger & Lacourse, 1990; Whitsitt et al., 1982; Sprague & Whitsitt, 1982). This becomes further evident as fracture of the fluting medium flanks and when bending stress is high beyond the bearable limit, fracture occurs at the flute tips (Whitsitt et al., 1982; Sprague & Whitsitt, 1982). The amount of web or the transport tension on the corrugating fluting medium is one of the factors that influences runnability as it passes through the labyrinth of the corrugating rolls. Undesirable speed at the labyrinth can lead to bad or poor corrugation due to inadequate time for flute formation and adhesive pick up by such flutes. Furthermore, resultant delamination and poor bonding between the linerboards and the fluting medium could be an after effect (Kruger & Lacourse, 1990; Touzinsky et al., 1982; Whitsitt et al., 1982; Sprague & Whitsitt, 1982; Godshall & Koning, 1972).

Resulting defects due to tension on the fluting medium just before the single facer were studied by several researchers (Norfariza, 2012; Biancolini et al., 2010; Nevins, 2008; Alava & Niskanen, 2006; Waterhouse, 1985; Whitsitt et al., 1982). The tension of fluting medium in-between the corrugating tips depends on the coefficient of friction caused by the impact between the corrugating rolls and the fluting medium (Nevins, 2008). To reduce the coefficient of friction that subsequently minimises the tension, lubricants can be applied to the surface of the fluting medium. Controlling the speed of the pre-feeders and the brakes of the roll stand are other measures to reduce the tension on the fluting medium (Nevins, 2008). Temperature and moisture content was reported by Nevins (2008) and Whitsitt et al. (1982) to be factors that affect the coefficient of friction, as increasing temperature and decreasing moisture content reduces the coefficient of friction. Ideally, to avoid flute fracture during flute formation, the fluting medium should have high tensile strength and a low coefficient of friction (Nevins, 2008; Eagleton, 1995; Whitsitt et al., 1982; Sprague & Whitsitt, 1982).

High web tension produced flute fracture at slower corrugator speeds (Batelka, 1994a). In comparison with different flute profiles, A-flute fractured at a slower corrugator speed than B-flute, with B-flute fracturing at a slower corrugator speed than C-flute (Batelka, 1994a; Godshall & Koning, 1972). Web tension was

identified as one of the factors that enhances the flute moulding characteristics of the corrugating fluting medium (Batelka, 1994a) which makes web tension a critical factor in the manufacture of corrugated paperboard. During cold corrugation process of paperboard, cracks develop at the tip of the corrugation when the tension is high (Batelka, 1994a; Whitsitt et al., 1982). This is because the paper is not moistened and heated during cold corrugation process to allow for pliability of the cellulose and lignin. The nature of paper is less plastic and brittle in cold condition and hence when the paper is fluted in such conditions under high tension, cracks are bound to occur at the flute tips. In order to avoid the problem of cracks at flute tips, pre-feeder may be required to keep the speed steady and control the tension. Furthermore, pre-feeder and regular break tension adjustment may be required to even out any piping in paper to keep the flute nip line at constant tension to avoid high-low flutes and creasing (Vishtal et al., 2014; Vishtal & Retulainen 2012; Kruger & Lacourse, 1990; Touzinsky et al., 1982).

2.3.1.5 Moisture

The properties of corrugated paperboard are adversely affected by moisture, weakening the highly porous paper fibres, and consequently reducing corrugated paperboard strength (Fadiji et al., 2017; Rhim, 2010; Pascal, 2010; Wang, 2010; Twede & Selke, 2005). During the production of corrugated paperboard, inaccurate control of moisture content can lead to many problems. Too much moisture content could cause the softening of the paperboard leading to collapse and flute exposure after production while low moisture content could lead to the paperboard being crisp and easy to breakdown. Therefore, during the production and processing of corrugated paperboard, controlling the moisture content is very crucial. The starch-based adhesive used to bind the linerboards and the fluting medium are typically inexpensive and hence allows for easy recycling of the corrugated paperboard (Natarajan et al., 2014; Emblem & Emblem 2012; Soroka, 2002).

The effects of steaming on high-density linerboards and the fluting medium before the single-facer manufacture were studied by Wallace et al. (1995). Steaming was applied to increase the moisture content of the linerboards and the fluting medium, with care taken to ensure preconditioner and preheater operation not to increase the temperature of the linerboards and the fluting medium. When compared to the strength of corrugated paperboard made from unsteamed linerboards and fluting medium, steaming the singer-facer linerboards increased the edge compression strength and liner adhesion strength by 2.2% and 5%, respectively. Steaming the fluting medium resulted in an increase of about 18% and 1% in liner adhesion strength and edge compression strength, respectively. Wallace et al. (1995) further stated that during the process of corrugation, increasing the moisture reduces the damage to the linerboards and the fluting medium thus resulting in production of a stronger corrugated paperboard. Steaming the paperboards during manufacture helps to relieve built-in stresses in the paper sheets, which can decrease the compression strength and modulus of elasticity of the sheets by 5 – 13% (Dimitrov, 2010).

2.3.1.6 Temperature

Temperature is a decisive factor that influences the quality of corrugated paperboard. The moisture content of paper is affected by the temperature (Linvill & Östlund, 2014; Wendler, 2006; Netz, 1998; Batelka, 1994a). Hence, the production line of corrugated paperboard is equipped with pre-heaters that may be used for adjusting the water content of the paper and single-facer board and bonding of the different layers of the corrugated paperboard. Whitsitt et al. (1982) stated the importance of temperature during the production process of corrugated paperboard in setting the adhesive for bonding between the linerboards and the fluting medium. Furthermore, temperature is a crucial factor during the manufacture of corrugated paperboard to plasticise the fluting medium to minimise damage during flute formation (Johnson & Popil, 2015; Haslach, 2009, 2000; Morgan, 2005; Dunn, 2003; Whitsitt et al., 1982).

Whitsitt et al. (1982) developed a cold corrugating process that produces corrugated flutes at room temperature. The authors found the performance of the resulting corrugated paperboard to be better than the normal (hot) corrugated paperboard. Temperature of a single-facer linerboard measured after a preheater had a significant effect on the edge compression strength and liner adhesive strength of the corrugated paperboard. A temperature range of 85 °C – 100 °C was reported to be optimum using high-density liners for the manufacture of corrugated paperboard. In a study by Johnson and Popil (2015), manufacturing operations that produce excessive temperatures for the paper (>93 °C) result in a brittle bond in which too much heat inhibits penetration of the dissolved portion of the adhesive slurry into the gaps of the linerboards and fluting medium interface and the adhesive remains and cures on the surface. Another resulting defect is the zipper bond in which the linerboards pull apart without visible fibre tear of the fluting medium and the linerboards (Johnson & Popil, 2015). Low corrugating roll temperature could lead to white glue-lines on the corrugated paperboard and are characterised by symptoms such as: adhesives appearing white, low bond strength and no gelatinisation (Johnson & Popil, 2015).

2.3.2 Mechanical hazards affecting packaging and fresh produce in the cold chain during postharvest handling

When designing efficient packages, it is crucial to determine the damage severity of the handling and distribution environment (Jamialahmadi et al., 2008). A distribution environment includes all the environmental conditions the package and produce encounter during the postharvest journey from the grower to the consumer (Ragulskis et al., 2012; Jamialahmadi et al., 2011; Eagleton, 1995). Package handling, storage and transportation can result in various hazards within the distribution environment. These may include, among others, horizontal impacts or vertical drops, compression loads, transport vibration and shocks (Opara & Fadiji, 2018; Fadiji et al., 2016a, b, c; Pathare & Opara, 2014; Singh et al., 2009; Van Zeebroeck et al., 2007; Vergano et al., 1991). Any of these hazards or a combination

of two or more can lead to package and produce damage. Assessing the distribution method and understanding the supply chain environment of a produce, can help to determine the type of hazards the produce will be subjected to and the extent of the hazards, which will consequently assist in designing the package that will effectively protect the produce (Jamialahmadi et al., 2008). Trucks, trains, ships and aircrafts are the main modes of transportation that have the potential of causing various hazards. It is important that package designers have an upfront knowledge on the modes of transportation to predict the likelihood of these hazards. An ideal package should be able to provide adequate protection needed by the produce, at the lowest possible overall cost (Robertson, 2012; Han & Park, 2007).

2.3.2.1 Vibration hazards

Vibration is an oscillating motion over time. During the postharvest journey of packaged produce inside corrugated paperboard packages, the produce undergo continuous movement during transit which may lead to package/produce damage (Fadiji et al., 2016b; Sittipod et al., 2009; Jarimopas et al., 2007). Packages being transported by truck, rail or aircraft are generally exposed to vibration. During transportation of packaged produce, vibration is affected by a number of factors such as the road roughness, travelling speed, number and load of axles, truck suspension (Idah et al., 2012; Vursavuş & Özgüven, 2004; Berardinelli et al., 2005, 2003a, b). Produce damage during vibration occurs when the acceleration the produce experiences is more than the acceleration of gravity (9.8 m s^{-2}). When the acceleration is below this level, the packed produce does not move with respect to the carton or the nearest produce. During vehicle transportation, acceleration impact is experienced more at the top of the stacked cartons because the peak acceleration increases from the bottom of the carton to the top (Fadiji et al., 2016b; Van Zeebroeck et al., 2007; Slaughter et al., 1993; Hinsch et al., 1993).

To understand the behaviour of corrugated paperboard packaging under vibration, Park et al. (2011) characterised the properties of corrugated paperboard such as vibration transmissibility, resonant frequency, damping ratio and maximum dynamic stress, which are relevant to its application for protective packaging during transportation. A similar study by Guo and Zhang (2004) evaluated the dynamic cushion curve and analysed the resonance and vibration transmissibility of honeycomb paperboards. The authors reported the large effect honeycomb paperboard had in diminishing vibration in the high frequency region because vibration transmissibility at resonant frequencies that exist over 350 Hz is insignificant. In a recent study by Fadiji et al. (2016b), the authors determined the transmissibility of corrugated paperboard packages and incidence of apple bruise damage at three frequencies: 9, 12 and 15 Hz. The authors reported the range of packaging transmissibility to be from 100 to 250%, with the highest observed at 12 Hz. The incidence and severity of the apple bruising was also reported to be dependent on the type of package and the frequency of excitation. Table 2.3 shows range of vertical frequencies and maximum accelerations, which are encountered during transportation and distribution. Immobilising or restricting the movement of

the produce, cautious handling and proper packaging have shown to minimise the losses of produce due to vibration hazard damage (Chonhenchob et al., 2009; Chonhenchob & Singh, 2003; Singh & Singh, 1992; Singh et al., 1992). In transport trailers, air-ride suspension has been used to minimise vibration hazards particularly during the shipment of produce that are sensitive to vibration injury (Pathare & Opara, 2014; Hinsch et al., 1993).

2.3.2.2 Impact/drop hazards

Impact hazards may occur during handling, storage and transportation due to impacts from racks, forklifts, dropping of the packages, sudden braking and accelerating transportation system and shocks during transportation. The resulting effect of an impact hazard include bursting of the packages or bruising of the packed produce. There is no particular stage during the handling and distribution process at which impact hazard occurs, as it may occur at each stage of the process and is usually difficult to eliminate (Fadiji et al., 2016a; Opara & Pathare, 2014; Gołacki et al., 2009). Opening of package flaps causing the package to lose its function, distortion in package shape thereby reducing stacking abilities, and the splitting of the seams are among the adverse effects of impact hazards on corrugated paperboard packages (Fadiji et al., 2016a; Opara & Pathare, 2014; Pathare & Opara, 2014; Walker, 1992). During handling and transportation, some level of protection against shock may be required to prevent damage caused by impact depending on the packed produce. The use of rigid packages and adequate cushioning can reduce damage that may arise from impact hazard.

It is crucial to determine the potential drop height that packed produce may experience, the fragility of the produce and the resistance of the package to shock damage due to free fall. This is necessary because during transportation and storage, packages can fall onto the floor resulting in damage (Fadiji et al., 2016a; Pathare & Opara, 2014; Hammou et al., 2012). Some other factors such as forklifts bumping pallets, tossing the package horizontally during palletisation and sudden breaking or entering potholes during transportation could result in impacts. Drop testing is used to measure the ability of the package to retain and protect the packed produce from free fall (Fadiji et al., 2016a; Pathare & Opara, 2014; Hammou et al., 2012). Recently, an extensive impact study was done by Fadiji et al. (2016a) to determine the susceptibility of apple fruit packed inside ventilated corrugated paperboard packages at different drop heights. The authors reported that the incidence and susceptibility to bruise damage of apples was affected by package design and drop heights. In drop testing, the product of the weight of the packed produce and the drop height determines the potential energy of the package (Pathare & Opara, 2014; Poustis, 2005). The drop height is the vertical distance from the point the package was released to the impact surface, falling under the influence of gravity. During handling operations, imposed loads on the package are usually reported in terms of equivalent drop height (EDH). This is defined as the free fall height that is required to produce the same total velocity change as measured on the shock waveform (Eagleton, 1995). EDH is used for comparison between impacts by forces other

than gravitational force. For an ideal free-falling package, the relationship between the total velocity change and EDH is given as:

$$\Delta V = (1+e)\sqrt{2gh_{eq}} \tag{2.4}$$

where e is the coefficient of restitution, g is the acceleration due to gravity (m s^{-2}), ΔV is the change in total velocity (m s^{-1}) and h_{eq} is the equivalent drop height (m).

Researchers have correlated several other mechanical parameters with the damage caused by impact hazards. Such parameters are the energy absorbed (Jarimopas et al., 2007; Bollen et al., 2001, 1999) and force (Brusewitz et al., 1991). The amount of absorbed energy by the impacted surface during drop is referred to as the coefficient of restitution:

$$e = \frac{V_r}{V_i} \tag{2.5}$$

where V_r is the rebound velocity (m s^{-1}) and V_i is the impact velocity (m s^{-1}). For packed produce, the range of the coefficient of restitution is usually from 0.3 to 0.75. In packaging design, the value of 1 for coefficient of restitution is considered a worst-case value (Garcia-Romeu-Martinez et al., 2007; Brusewitz et al., 1991; Eagleton, 1995).

2.3.2.3 Compression hazards

Compression is said to occur when a pushing force reduces the volume of an object. Compression hazards occurs during postharvest handling and distribution if the package at the bottom of the stack on the pallet is not sufficiently strong enough to withstand the load of the carton stacked on it. Compression loads on packages are generally associated with storage stacking (Eagleton, 1995). Static compression is a loading force that a package will endure when it is stacked vertically for an amount of time. The force being applied is not moving. A package may also encounter dynamic compression while being transported in the back of a truck. Dynamic compression occurs when there is a moving force being pressed against the object and can be observed during cushion testing. This form of compression may result from vibration and shocks in transportation by load amplification when the packages vibrate at the critical resonant frequencies. It is important to mention that very low vibration frequencies from transport operations such as the response of aircraft to gusts and ships rolling or pitching may result in dynamic compression loads on the packages (Eagleton, 1995). Equipment for mechanical handling such as slings, cargo nets, clamps on trucks, rail car coupling and strapping of the package could result in dynamic compression loads (Eagleton, 1995).

To minimise this, carton boxes should not be stacked above their design requirements (Kader, 2002). In a report by Kader (2002), designing corrugated paperboard cartons to withstand more than four pallets high, particularly during storage is not economically feasible. Appropriate package design systems and good packaging offer vital protection to package and produce against compression hazards, and utilising strong packages able to withstand multiple stacking can help minimise this hazard thereby reducing the incidence and the extent of produce damage. The shallowness of packaging also determines the extent of damage as it should be shallow enough to prevent the packed produce in the bottom from damage that may arise from weight of the packages in the top layers.

2.4 Testing for assessing the mechanical strength of packaging and packaging materials

The performance properties of corrugated paperboard packaging are related to varying factors such as the level of efficiency achieved during manufacture of the paperboard and package, creasing and packing operations (Sukumaran, 2015). Furthermore, performance properties of corrugated paperboard packaging are also related to the strength of the package during handling, transportation, storage, point of sale of packed products and in usage by consumers (Sukumaran, 2015; Pathare & Opara, 2014). This section discusses some of the different parameters and tests used to describe the mechanical strength of corrugated paperboard packaging with a multiscale approach (i.e. applied to paper–corrugated paperboard–corrugated paperboard package).

2.4.1 Paper and paperboard

2.4.1.1 Tensile tests

Tensile tests are performed on paper and paperboard to provide information on the ductility property, yield strength and the tensile strength. Tensile strength is an indication of strength of paper and paperboard, which are dependent on factors such as bonding, fibre length and fibre strength (Tappi, 2006; Aboura, et al., 2004). Furthermore, tensile strength also indicates the resistance of paper and paperboard to web breaking of papers. When evaluating the tensile strength, the extension and the tensile energy absorption for these parameters can aid in predicting the performance of paper and paperboard, particularly when the material (paper and paperboard) is subjected to uneven stress (Tappi, 2006). When low ductility is observed in a tensile test, it is often accompanied by low resistance to fracture under other forms of loading.

The in-plane elastic constants or properties of paper and paperboard can also be obtained using tensile tests (Mäkelä & Östlund, 2003). The stiffness and strength properties are anisotropic and in most cases, the fibre orientation is approximately symmetric which indicates that the stiffness properties can be assumed orthotropic and different in all directions (Fadiji et al., 2017; Mäkelä & Östlund, 2003).

Therefore, the elastic properties should be obtained at the different in-plane orientations of the paper and paperboard (MD and CD). A recent study by Fadiji et al. (2017) evaluated the elastic properties of five different paper grammages as a function of two environmental conditions (standard room and cold chain condition) and found significant differences between the different fibre orientations. MD exhibited higher elastic properties compared to the CD. This was explained by Salminen (2003) to be due to the straining behaviour of MD, which is less plastic and ductile. The stiffer and higher resistance to stress in the MD was reported to be due to the distribution and orientation of fibres in the MD during the paper forming process (Pathare & Opara, 2014; Stenberg et al., 2001). Moisture absorption by paper was also reported by Fadiji et al. (2017) to have a great influence on the elastic properties of paper and paperboard at different fibre orientations. When paper absorbs moisture, the material softens and alters the paper fibre behaviour of the stress-strain curve thus reducing the tensile strength and elastic moduli (Vishtal & Retulainen, 2012; Allaoui et al., 2009b).

To perform tensile tests for paper and paperboard, standard test methods have been established by various standard organisations. Some organisations include; American Society for Testing and Materials International (ASTM International), International Organisation for Standardisation (ISO) and Technical Association of the Pulp and Paper Industry (TAPPI), with specific methods for tensile tests of paper and paperboard as ASTM D828, ISO 1924 and TAPPI T494, respectively. The tensile test of paper and paperboard is usually performed using rectangular samples of 180 × 15 mm under a constant displacement velocity of 20 ± 5 mm min^{-1}.

2.4.1.2 Ring crush test

Ring crush tests (RCT) are used to determine the ring crush resistance of a paper strip formed into a ring with a standardised length and width. According to the Australian paperboard industry, RCT is a vital and relevant indication of package stacking performance compared to the Short-span compression test (SCT; section 2.4.1.3) (Shallhorn et al., 2005; Parker & Jackson, 2005; Jackson & Parker, 1998). TAPPI T822 and ISO 12192 standards are used for measuring ring crush resistance and RCT specimen is a paper strip 152 mm in length and 12.7 mm in width, rolled to form a cylindrical radius of 24.64 mm inserted in a circular groove of 6.35 mm in depth. A compression load is applied to the edge of the paper strip whose bottom half is supported by the holder. Shallhorn et al. (2005) developed a quantitative model for the ring crush resistance of paperboard and found the mode of failure to be localised at the top edge, initiated by the development of a bending moment at the unsupported edge, at higher calliper.

According to Popil (2010), a general form of a combined compression and buckling model for RCT was proposed as:

$$RCT = C(SCT)^{b}\left(\sigma_{cr}R\right)^{1-b} \tag{2.6}$$

where C and b are empirical constants, SCT is the short-span compression test value, R is the radius of the fixed ring, σ_{cr} is the buckling load of a thin shell ring given by Timoshenko and Gere (1961) as:

$$\sigma_{cr} = \frac{E_{CD}}{\sqrt{1-\nu_{12}\nu_{21}}}\frac{t}{R} \tag{2.7}$$

where E_{CD} is the modulus of elasticity in the cross direction obtained by tensile testing, ν is the Poisson ratio and t is the thickness of the paperboard.

2.4.1.3 Short-span compression test

The compression strength of paper in compression mode is determined using the short-span compression test. It is applied to fluting and liner papers. Due to the buckling stability provided by SCT, the compressive strength material characteristic is commonly obtained using SCT (Sukumaran, 2015). TAPPI T826 and ISO 9895 are standards used for SCT and the value is expressed in kN m^{-1}. A 15 mm wide strip of the paper material is clamped between two clamps, a distance 0.7 mm apart and a compressive force is applied until collapse to measure the maximum force (Hämäläinen et al., 2017). According to Šarčević et al. (2016), SCT is considered the most reliable method for estimating the compressive strength of paperboard. However, RCT is still widely used in characterising the compressing strength of linerboard and fluting medium (Dimitrov & Heydenrych, 2009). The RCT combines both compression and buckling failure while SCT excludes any bending and buckling. Popil (2010) compared SCT and RCT with the basic weight of paper and reported a linear relationship for SCT, however RCT deviated from linearity with increase in basic weights and this was reported to be due to a larger prevalence of edge rolling at larger basis weights. SCT, in combination with a bending stiffness model gives a good estimation of the edge compression test (ECT) value of corrugated paperboard (Popil et al., 2004; Whitsitt, 1988).

Rennie (1995) showed a strong correlation between SCT and RCT if the thickness of the paper and bending stiffness are included in empirical model:

$$SCT = RCT + 0.005\frac{T}{t^{2}} \tag{2.8}$$

where T is the bending stiffness (N m) and t is the thickness of the paper (m).

2.4.1.4 Concora crush test for fluting medium

The concora crush test (CCT) evaluates the crush resistance of flutes. Flutes are exposed to compression on the long edge until buckling occurs (Mark & Borch, 2001). CCT gives a measurement of the performance characteristics of corrugated paperboards used in packaging for transporting and stacking of packed product. The measured force indicates how much force is required to break the fibres of the flutes. TAPPI T824 standard is used for CCT and the test employs a 152 × 12.7 mm flute sample placed in the holder of the crush tester with the long edge uppermost. Due to heating and moulding of the flute in the corrugator, edge effect occurs at the two vertical edges in CCT, thereby adversely affecting the compression strength.

2.4.1.5 Concora liner test (CLT)

The concora liner test (CLT) measures the resistance of a flat strip of paper in the axial direction (Marín et al., 2009; Mark & Borch, 2001). The CLT is used in both the MD and CD directions of the liners. For CLT, one edge of a paper strip of length 152 mm and width 12.7 mm is clamped between two metal strips so that a free upper part of 6.3 mm protrudes above the clamp and load is applied to the free edge of the paper strip. Edge crushing or bending failure is always a phenomenon that occurs during CLT, which tend to limit the effectiveness of the test method as the response reduces the CLT value below the compression strength of the paper strip (Mark & Borch, 2001).

2.4.1.6 Flat crush test

Flat crush tests (FCT) can be used for measuring the flat crush resistance of corrugated paperboard. The FCT is a measure of the resistance of the flutes in corrugated board to a crushing force applied perpendicular to the surface of the board. FCT is a measure of the corrugated paperboard flute rigidity. A high crush value indicates a combination of good flute formation and at least adequate strength medium while a low FCT value is an indication of low strength medium, crushed flutes and leaning flutes. The test is satisfactory for single-faced or single wall corrugated paperboard, but not suitable for double wall or triple wall corrugated paperboard, because of the lateral motion of the single facing or facings (Syed & Bhoomkar, 2013; Guo et al., 2010; Jiménez-Caballero et al., 2009; Krusper et al. 2007). Syed and Bhoomkar (2013) analysed the effect of fluting on flat crush resistance in single wall corrugated paperboard and concluded that flute profiles have great influence on the strength of the corrugated paperboard. FCT is usually performed with ISO 3035 and TAPPI T825 standards on circular paperboard samples and measured in kg cm^2 or kPa.

2.4.1.7 Edge compression test

Edge compression test (ECT), otherwise known as the edge crush test, evaluates the in-plane compressive strength of corrugated paperboard. The ECT measures the ability of a vertically placed corrugated paperboard sample to sustain a top-to-

bottom load. ECT of the corrugated paperboard plays the most important role in the overall performance of the package compressive strength. It is usually a dominant factor in the compression strength of a package and widely used for quality control and package designs via the Mckee formula, which is dependent on the package geometry characteristics (calliper and perimeter) (Fadiji et al., 2017; Kołakowski et al., 2015; Ristinmaa et al., 2012; Urbanik & Frank, 2006; Twede & Selke, 2005; Biancolini et al., 2005; Biancolini & Brutti, 2003; McKee et al., 1963). ECT can be performed on any of the flute profiles (Table 2.2) for different board combinations (Figure 2.4). ECT is typically expressed in units of force per unit length N m^{-1}.

Several industry standard tests are available for performing ECT. Some of which include: TAPPI T811, European Federation of Corrugated Board Manufacturers (FEFCO No 8) and ISO 3037. ECT is performed using rectangular corrugated paperboard samples cut to 100 mm long and 25 mm wide. The corrugated paperboard is held in the test fixture between two metal guide blocks. The blocks align the board samples vertically so that the applied force is parallel to the cross direction (CD). The clamping force on the bottom and top of the corrugated paperboard holds it perpendicular to the test force so there is no chance of tipping that causes lower results. In addition, as proposed by Biancolini and Brutti (2003), mathematical calculation can be used in estimating ECT value:

$$ECT_{theoretic} = RCT_{INlin} + RCT_{OUTlin} + RCT_{flu} \times C.O \qquad (2.9)$$

where $INlin$ and $OUTlin$ are the inner and outer liners respectively, flu is the fluting, RCT is the ring crush test value, $C.O$ is the wave factor of the board and $ECT_{theoretic}$ is the estimated edge compression test value.

Dimitrov and Heydenrych (2009) obtained predictive mathematical models for ECT values by correlating measured ECT values with predicted ECT values using the compression strength of the paperboard components; short-span compression test (SCT) and the ring crush test (RCT). High coefficients of determination (R^2) values of 0.9758 and 0.9625 for SCT and RCT, respectively was shown for the models, indicating the suitability of the models in predicting the compression strength of corrugated paperboard, using the measured paper compression strength (SCT or RCT) after exposure to constant climatic conditions. Furthermore, Šarčević et al. (2016) proposed a model to evaluate the edge compression resistance of paperboard and reported SCT to be a better predictor of ECT value than RCT. However, the RCT is still commonly used despite that it is established that it is affected by the buckling load of the paper.

2.4.2 Corrugated paperboard package

2.4.2.1 Box compression test

Box compression strength of corrugated paperboard packages has been the most prominent in interest and attention within the paper package industry of all the several performance requirements of corrugated paperboard package that exist (Frank, 2014; McKee et al., 1963). Box compression tests (BCT) are used in quantifying the performance of a package by measuring the maximum force the package can carry. The reason for the great significance of box compression strength are aligned with its close correlation to the stacking performance of the packages during storage and its usefulness in evaluating the overall quality of the paperboard materials (Frank, 2014; Singh et al., 2008; McKee et al., 1963). Numerous factors affect box compression strength and structural design of the package. These factors include size, dimension, flap direction and loading direction, suitability of the packed content in the package, type of secondary packaging, storage and transport conditions and material properties (compression strength and stiffness of the paperboard) (Frank, 2014; Emblem, 2012; Kirwan, 2008). These factors cause a large variation in the box compression strength thus giving room for studying the effect of different variables such as paper materials, imperfection of the package geometry and environmental conditions (Paunonen & Gregersen, 2010).

ISO 12048 and ASTM D642 standards are commonly used for BCT. In a BCT, the package is placed between two plates loaded from top to bottom and the force is recorded as a function of displacement (Fadiji et al., 2016c; Paunonen & Gregersen, 2010). BCT is performed on a single package, hence, does not account for the decrease in stacking strength due to even small stacking misalignment. However, BCT provides valuable insight into the mode of failure and the potential contribution of the various factors, for example, package panels, creases and flaps. During package compression, about 40 – 64% of the total load is carried by the edges while the remaining load is distributed and carried by the panels (Paunonen & Gregersen, 2010; Meng et al., 2007; Maltenfort, 1980). The stiffness of the whole package is a function of the stiffness of the different parts of the package, with the top and bottom section of the package having a lower stiffness compared to the middle section (Meng et al., 2007; Beldie et al., 2001).

The model developed by McKee et al. (1963) and associated experimental procedures have made a lasting contribution to the design of corrugated paperboard packages. The model predicts the compression strength of a single wall corrugated package. The formula gives the compression strength as a function of the ECT, perimeter of the package and the flexural stiffness of the board:

$$BCT = cECT^{b}\left(\sqrt{D_{MD}D_{CD}}\right)^{(1-b)} Z^{(2b-1)} \tag{2.10}$$

where C is an empirical constant and is a function of panel rigidity, b is an empirical constant and is a function of size, ECT is the edge compression test value, Z is the package perimeter, D_{MD} and D_{CD} are the geometric mean of the bending stiffness in the MD and CD, respectively.

The formula has been further simplified to relate ECT with the package perimeter as:

$$BCT = 5.87\left(ECT\right)\sqrt{h \times Z} \tag{2.11}$$

where h is the calliper of the corrugated paperboard.

2.4.2.2 Creep test

Paper packages must be designed to sufficiently withstand loads over the packages total life span. During handling, transportation and storage, corrugated paperboard packages experience a time-dependent phenomenon known as creep (Paunonen & Gregersen, 2010; Navaranjan & Johnson, 2006; Alfthan, 2004; Haslach, 2000). Creep is defined as the progressive increase in strain observed when a material is exposed to a constant load over a long duration and occurs as a result of non-recoverable deformation in paper due to its viscoelastic nature (Niskanen, 2012). Usually for paper materials, accelerated creep occurs with varying RH. This time-dependent behaviour adversely affects paperboard packaging and may lead to package failure/damage or shortening of life. Morgan (2004) stated that the main reason for damage of corrugated paperboard packages during handling is compressive creep. The mechanical creep strain response in paper materials is more significant with varying ambient conditions, such as RH and temperature compared to having a constant ambient condition at a given duration. Creep phenomenon is usually characterised by three stages: the primary creep is the first stage, where the strain rate is relatively high and increases instantaneously with the application of load. This slows down gradually with time. The secondary creep is also called the steady state, where the strain rate remains constant and a steady creep is achieved. Determining the minimum creep rate at this stage is important for structural designers, as this is when most of the creep related deformation occurs (Arvidsson & Grönvall, 2004; Eagleton, 1995). The third stage is referred to as the tertiary stage. At this stage, the creep strain rate begins to increase and this continues until fracture or creep rupture occurs. ASTM D7030 standard is used for evaluating the creep performance of corrugated paperboard packaging under constant load. Some studies of the creep of corrugated paperboard packaging are summarised in Table 2.4.

For creep to occur, a constant stress (σ_0) is applied to a material, which tends to cause deformation $(\in)$ over the period of time the stress is being applied. The creep function therefore is shown as:

$$f(t) = \frac{1}{(\sigma_0)} \in (t) \tag{2.12}$$

The creep rate of the material takes the form:

$$v = \left[\frac{\delta f(t)}{\delta t} \right] \tag{2.13}$$

This is measured in $Pa^{-1}s^{-1}$ as $t \rightarrow 0$.

Considering the creep phenomenon from a mechanical point of view, the energy released by the material when creep deformation occurs as stress can be applied as a function of the creep rate at every instant as:

$$W(t) = \frac{\sigma_0^2}{2E} + \sigma_0^2 \int_0^T v(t) dt \text{ in Pa} \tag{2.14}$$

where E is the Young's modulus of the material.

2.4.2.3 Impact test

Drop or impact tests are used to assess the ability of corrugated paperboard packages to withstand vertical impacts during postharvest handling. With drop tests, the capability of a package and its internal packing to provide protection to the packed contents during the sudden shock resulting from a free fall can also be evaluated. Different standards are available for carton drop tests. These include the International Safe Transit Association (ISTA 1A), ASTM D5276, TAPPI T802, and ISO 2248. The carton drop test involves dropping the carton from a certain height, simulating the shipping environment during which the packed contents may be subjected to falls. Accelerometers may be placed in the package to measure the acceleration forces and the shock response when dropped (Fadiji et al., 2016a). The package is inspected after dropping to visualise its performance during shipping to forecast any possible damage that may occur during handling. A package is deemed to have failed if the package and internal packing are damaged, or if scratch or deformation is visible on the packed contents. A good package is able to absorb impact energy and treat packed contents as a separate unit, avoiding internal collision and contact (Fadiji et al., 2016a; Peleg, 1985).

2.4.2.4 Vibration test

Package and contents are exposed to stresses or vibration during transportation. The vibration stresses can be measured by vibration tests and are often specified as acceleration, in g-units (1 g = 9.81 m s^{-2}). Vibration tests make use of vibration tables to simulate the vibration that occurs on a mode of transportation (e.g. truck). Vibration tests could be for random or sinusoidal vibrations (Caldicott, 1991).

Random vibration is based on the actual measurement (i.e. real world vibrations) during transportation and handling of the packages. Random vibration is comprised of vibration energy at all frequencies over a specified range and the content resonances (natural frequency equals the forcing frequency of the conveyance) are excited together. Sinusoidal vibration applies a single frequency to the package, for a specified rate and duration. Sinusoidal vibrations are easier and cheaper to perform and the results have been understood in relation to the actual distribution environment. Standard test such as ASTM D4728 and ASTM D 999 are used for random and sinusoidal vibrations, respectively.

2.5 Cold chain environment factors affecting the strength of paperboard packaging

Corrugated paperboard is very sensitive to environmental conditions because it is made of hygroscopic material (Berry et al., 2017, 2016; Fadiji et al., 2016c; Pathare et al., 2016; Pathare & Opara, 2014; Zhang et al., 2011; Thakkar et al., 2008; Kirwan, 2003). Paper being a hygroscopic material is affected by factors such as moisture content, RH and the sensible heat in the form of ambient temperature which affect properties such as stiffness and consequently the strength of paperboard and package (Vishtal & Retulainen, 2012; Rhim, 2010; Allaoui et al., 2009a, b; Gooren, 2006; Kirwan, 2003). Furthermore, the high RHs of cold storage result in board moisture contents at which paper is much weaker (Rhim, 2010). The shape or dimensions of corrugated paperboard may also be affected when exposed to variations of humidity and drying out may also cause brittleness of the corrugated paperboard (Fadiji et al., 2016c; Pathare & Opara, 2014; Navaranjan et al., 2013; Hung et al., 2010; Morgan, 2005; Uesaka, 2002; Rigdahl, 1984). Improper storage or care of the cargo may result in dimensional changes (swelling), distortion (waviness) and reduced strength (tearing). This damage is irreversible, since drying leads to warping due to inner tensions and to staining (drying rings) or to bursting/cracking of the rolls. Cold storage factors affecting the strength of corrugated paperboard packaging are discussed in this section.

2.5.1 Moisture content of paper and paperboard and cold chain humidity

The amount of water present and measurable in paper and paperboard is the moisture content. Moisture content of paper and paperboard is dependent on the environment and the amount of moisture that may have been added during the production and conversion process (Fadiji et al., 2016c; Allaoui et al., 2009a; Twede & Selke, 2005). Maintaining the original moisture content of the corrugated paperboard helps to limit changes to the characteristics of the paperboard throughout the manufacturing process, handling, and storage (Linvill & Östlund, 2014; Lyngå & Sikö, 2003). Furthermore, the time-dependent behaviour of paper-based packaging is determined strongly by its moisture content (Haslach, 2000), and changes in environmental RH was reported to have a large significant effect on moisture content (Sørensen & Hoffmann, 2003).

During storage, handling and transportation, corrugated paperboard packaging are exposed to varying environmental conditions, usually very high RH (90-95%) which in turn raises the moisture uptake, thereby influencing the strength of the packages significantly (Lyngå & Sikö, 2003). Twede and Selke (2005) reported that humidity and moisture storage conditions reduced the strength of packages in a matter of hours. In the study by Wang et al. (2013), the author reported an increase with moisture content of paper as the RH increased (Figure 2.6). The study by Rhim (2010) also stated that the moisture content of paper increases slowly when the RH is below 70% while with RH above 70%, the moisture content increases rapidly. In the study by Sørensen and Hoffmann (2003), increase in moisture content due to increase in RH affected the static compression strength of moulded fibre trays. Decreasing RH increases the maximum stacking strength of the trays. A recent study by Pathare et al. (2016) investigated the effects of cold storage (−0.5 °C at 90% RH) on the structural integrity of ventilated packaging used for handling pome fruit. Increasing moisture content reduced the package compressive strength. The study showed good correlation between change in moisture during storage and the compressive strength of the package.

Paper-based packaging swells during moisture uptake causing an increase in weight and shrinks when moisture is lost (Fadiji et al., 2016c; Rhim, 2010; Allaoui et al., 2009a; Kim et al., 2006). When cold paperboard is exposed to a warm environment the air adjacent to the board can be cooled below its dew point (point of condensation) and this moisture is then absorbed by the board. Several authors have studied the effect on moisture content on the mechanical properties and performance of paperboard components, corrugated paperboard and corrugated paperboard packages. A summary of some of the research and methodologies is shown in Table 2.5.

Paperboards are prone and susceptible to absorption of water from the environment, particularly during storage under high humidity or when in contact with food materials with high-moisture such as fresh horticultural produce (Rhim et al., 2006). Most often, water absorption minimises the physical and mechanical strength of the paperboards causing damage to the packed produce during storage and distribution (Fadiji et al., 2016c; Pathare & Opara, 2014; Rhim et al., 2006). To increase the water resistance and barrier properties of corrugated paperboard packaging, surface treatments such as protective coatings can be used.

The use of biopolymers which are renewable and biodegradable have been used to produce environmentally friendly coating materials for paperboards to increase the water resistance (Khwaldia et al., 2014; Reis et al., 2011; Havimo et al., 2011; Rhim et al., 2007, 2006). Trezza and Vergano (1994) reported the effectiveness of zein-coated paperboard. Rhim et al. (2007) highlighted the use of poly (lactide) coating to increase the water resistance of paperboards. Mechanical properties, coating homogeneity, water absorption capacity and moisture barrier properties of paperboard was evaluated using chitosan emulsion film as coating (Reis et al.,

2011). Paperboard coated with chitosan emulsion improved the water barrier properties compared to uncoated paperboard. The authors further stated that these treatments could influence the quality and integrity of the packed produce. Park et al. (2000) reported the impact of soy protein coated paperboard on water, gas and lip barriers as well as mechanical properties for extending the shelf life of food products. Furthermore, research by Gällstedt et al. (2005), Lin and Krochta (2003) and Han and Krochta (2001) reported that protein-coated paperboards improved the barrier properties including the physical, mechanical and surface colour properties. Future research lies in the development of sustainable modification techniques based on renewable resources such as green chemistry and biopolymers in controlling water absorption in paperboard packaging.

2.5.2 Cold chain temperature

For fresh horticultural produce such as fruit and vegetables, temperature is a vital environmental factor influencing the deterioration rate and postharvest life of the product (Defraeye et al., 2015). Cold chain temperatures are dependent on the produce that is being stored (Nevins, 2008). Some horticultural produce such as apples and pears are typically stored at a temperature of about 0 °C. Maintaining low-temperature conditions during cold chains is crucial to reduce respiration rate of the stored produce, consequently preserving the quality (Berry, 2017; Uchino et al., 2004; Salisbury & Ross, 1991). The hydroscopic nature of paperboard allows for moisture absorption or desorption to maintain equilibrium with the environment. In a cool store, the moisture content of paperboard packaging is influenced by the temperature. According to Defraeye et al. (2017), measuring the temperature in cold storage is essential to develop and evaluate new packaging designs. An increase in RH because of temperature reduction can cause an increase in paperboard moisture content (Fadiji et al., 2016c; Eagleton, 1995; Nevin, 2008). The effect of temperature on paperboard is therefore indirect which is observed by its influence on the moisture content. Haslach (2000) highlighted that the time-dependent mechanical properties of paperboard is most strongly determined by its moisture content and to a lesser extent by temperature. The study by Skogman and Scheie (1969) measured the moisture content of Kraft paper as a function of temperature ranging from −20 to 20° C. The authors found that with an increase in temperature for a constant RH, the moisture content decreased.

The temperature of both package and the packed fresh horticultural produce in storage, helps in determining the amount of water condensing from the atmosphere and can be easily monitored. Low temperatures affect the strength of paperboard and unless the corrugated paperboard package is specially treated, up to 75% reduction in strength can occur due to moisture sorption. For most horticultural produce, particularly fresh fruits and vegetables, low temperature and high humidity are recommended to maintain quality and extent the shelf life (Sun, 2016; Hui et al., 2004). In cool stores, mist is used for increasing humidity. However, mist from conventional humidifiers, such as ultrasonic devices wets the corrugated paperboard packages and thereby reduces their strength and performance during

storage and distribution. Sørensen and Hoffmann (2003) used a response plot to show relative static compression strength of moulded fibre trays as a function of the environmental temperature and humidity (Figure 2.7). From the plot, increasing the temperature speeds up moisture evaporation from the fibre causing the moisture content to decrease, hence strengthening the moulded fibre tray. The compression strength of the moulded fibre tray greatly reduced with increasing RH. Although the response plot was based on constant environmental conditions, it helps provide information on the variability in the stacking strength of the fibre tray.

The environmental conditions for food packaging varies in real-life situations, with high likelihood of changes in temperature and RH, either short or long in duration. Therefore, further research lies in validating mechanical behaviour of packages (for example stacking strength) in response to cyclic environmental conditions in order to obtain a better knowledge of the package functionalities.

2.5.3 Storage duration

For fresh horticultural produce, long-term storage under cyclic environmental conditions (temperature and humidity) are not desirable during distribution operations. Long transportation distances, short storage times and relatively constant (or perhaps few cycles) environmental conditions are typically the attributes of the distribution system for fresh produce (El-Ramady et al., 2015; Eagleton, 1995). In situations where the transportation times are shorter than the storage times, the performance of the package can be measured by the static or quasi-static mechanical properties (Pathare & Opara, 2014; Van Zeebroeck et al., 2007; Eagleton, 1995). Some forms of dynamic measures are required when fresh produce are distributed, as the storage times are almost the same as the transportation times (Henriod, 2006; Thompson, 2004; Eagleton, 1995). In addition, during distribution, packed product inside ventilated corrugated paperboard packages may be stored for a period of time in the cold store. During storage, the packages are superimposed or stacked one upon another. The bottom package is continually subjected to constant load and therefore must be strong enough to withstand the load during the storage duration (Fadiji et al., 2016c; Daxner et al., 2007; Sangchai, 1997).

During cold storage of fresh horticultural produce, the package must be able to resist the changes in moisture and humidity and should exhibit high stacking strength (Fadiji et al., 2017; Fadiji et al., 2016c; Pathare & Opara, 2014). It is therefore important to determine the allowable load the package can withstand without collapse within the storage time. Pathare et al. (2016) observed significant influence of storage time on the stacking strength of ventilated corrugated paperboard packages. In the study of the time effect when corrugated paperboard packages were loaded with dead weight, the authors reported that at a given RH, the total time of application of the load to the failure point depended on the dead weight applied (Eagleton, 1995; Zhao, 1993). Dead weight relatively close to the maximum compression strength of the package will cause the package to fail within minutes.

However, a life span of about 30 d before failure was recorded when a dead load of about 60% of the maximum strength of the package was applied, although the likelihood for storage of chilled horticultural produce for this period is low. A time correction factor was proposed in SPI (1980) for the compression strength of paperboard packages stored for an elongated period:

$$T_0 = 1 - 0.204t^{0.104} \tag{2.15}$$

where T_0 is the correction factor for the package storage and t is the storage period in days.

2.6 Conclusion and future prospects

Packaging performs a crucial role in protecting produce from damage during handling, transportation and storage, modifying the distribution environment and enhancing the produce transport density per volume. Packaging is thus generally considered the most flexible and cost-effective means to modify or improve a fresh produce cold chain. Corrugated paperboard is the most common fresh produce packaging type, and its successful application can be attributed to its efficacy; low cost, recyclability, biodegradability as well as good protection of the packed produce. Furthermore, the structural design of corrugated packaging is well suited to withstand the many different loading conditions present in postharvest handling of fresh produce.

This review highlighted the relevant functionality parameters of corrugated paperboard packaging towards enhancing protection to packed produce. These include the behaviour of the paperboard board components (liners and fluting medium), corrugated paperboard and the packaging by listing performance mechanical tests that can be used to evaluate the strength of corrugated paperboard packaging. The compressive strength of paperboard, corrugated paperboard and the package is an important factor to consider in achieving a better and more efficient packaging that can effectively protect the packed products.

The main contribution in this review is providing a summary for the factors that affect strength of corrugated paperboard packaging with respect to the manufacturing processes and the cold chain storage conditions. The sensitivity of corrugated paperboard to atmospheric condition, particularly the effect of moisture that is very evident on the mechanical characteristics of the corrugated paperboard packaging. The continual optimisation of the use of corrugated paperboard packaging under severe atmospheric conditions requires the knowledge of its behaviour under this condition, be it during manufacturing or handling processes.

Most often, the mechanical performance of packages are based on experimental procedures (section 2.4). In light of the need to evaluate the weaknesses of the packages to optimise the performance, the use of mathematical modelling

techniques in replacing time-consuming and expensive experiments is constantly evolving (Sun, 2016; Ambaw et al., 2013; Delele et al., 2010; Dehghannya et al., 2010; Zou et al., 2006a, b). The constant evolution of the modelling tools presents novel opportunities for studying the effects of different operating parameters once the model is validated. Some of these numerical techniques include finite element analysis (FEA), computational fluid dynamics (CFD) and discrete element method (DEM). These numerical techniques have been used to provide an efficient methodology in predicting the package and produce interactions during postharvest handling. FEA combined with other powerful numerical techniques such as CFD and DEM are becoming common and useful in studying the mechanical behaviour of corrugated paperboard packaging and packed produce. Creating a validated model that can predict the mechanical integrity and failure of corrugated paperboard packages under varying conditions will help to save time and money spent in experimental tests during the packaging design stage. Furthermore, this will help improve future package designs to the benefit of the packaging industry.

In addition, recent progress in experimental tools for corrugated paperboard packaging includes the use of artificial neural networks in predicting the box compression strength of corrugated paperboard packages. Also more recently, full field optical techniques such as digital image correlation have been used for displacement or strain measurements and for characterisation of the mechanical properties of paper and paperboard used as input parameters for the FEA, CFD or DEM simulations. Future research prospects should therefore be directed towards more powerful modelling or simulation tools that will utilise a holistic approach towards understanding the integrated behaviour of corrugated paperboard packaging to minimise damages to packed produce and make future cold chains more resource efficient.

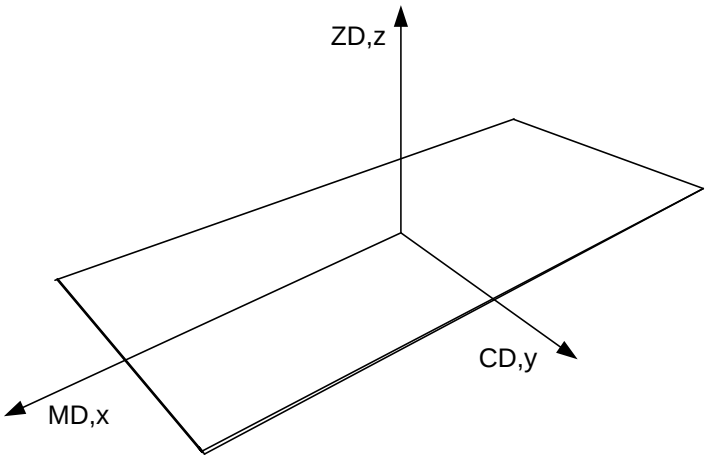

Figure 2.1: Principal material directions of paperboard (MD is the machine direction, CD is the cross direction and ZD is the thickness direction).

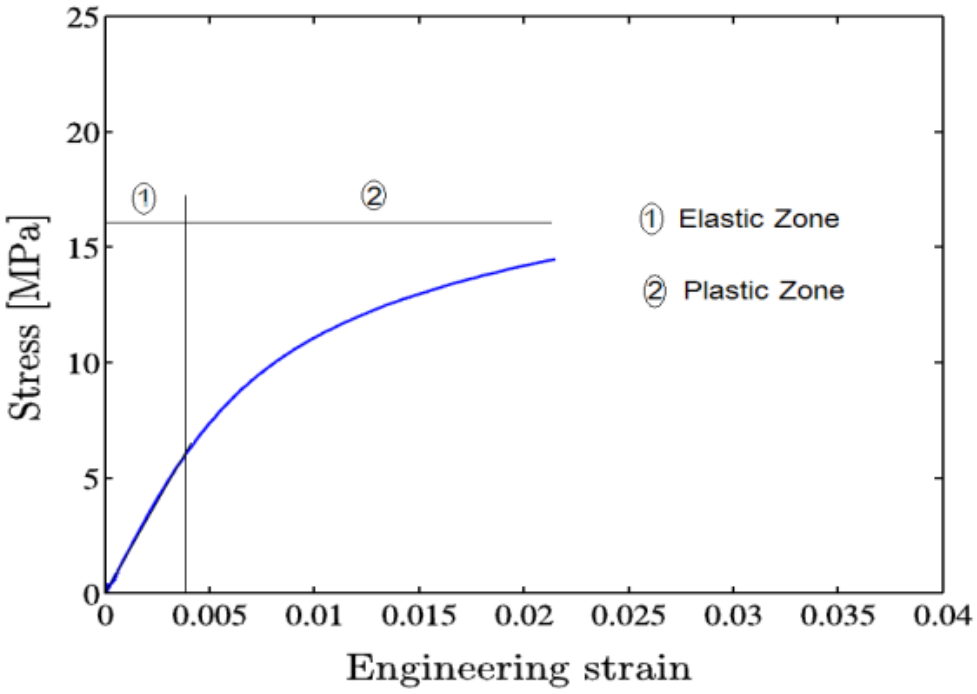

Figure 2.2: Typical representation of the response of paper under uniaxial tensile loading (Phongphinittana & Jearanaisilawong, 2013).

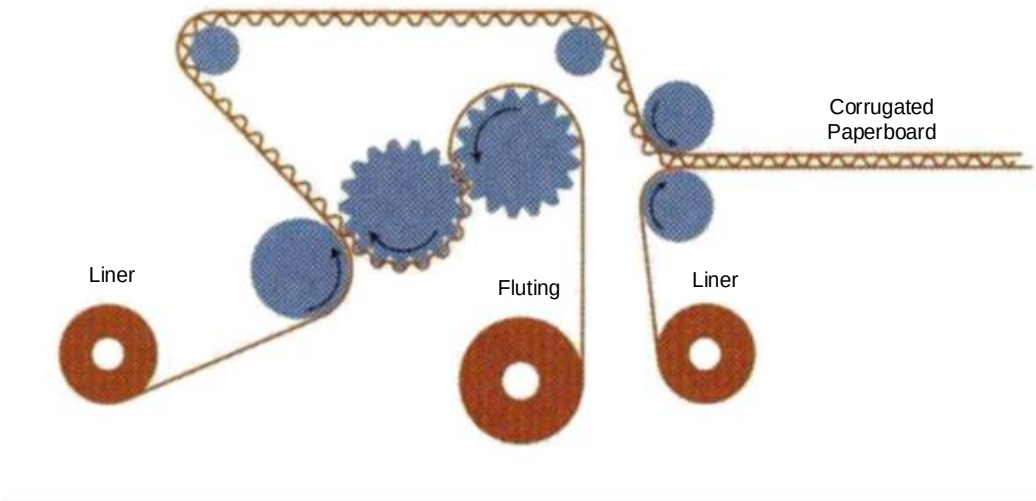

Figure 2.3: Manufacture of corrugated paperboard (Allansson & Svärd, 2001).

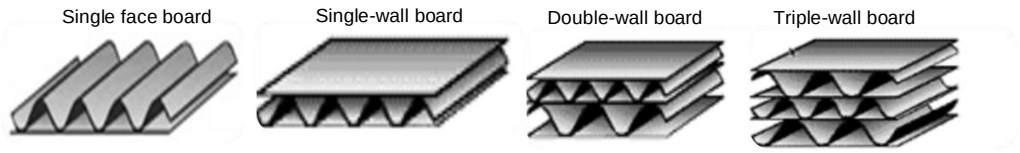

Figure 2.4: Different types of corrugated boards (Twede & Selke, 2005).

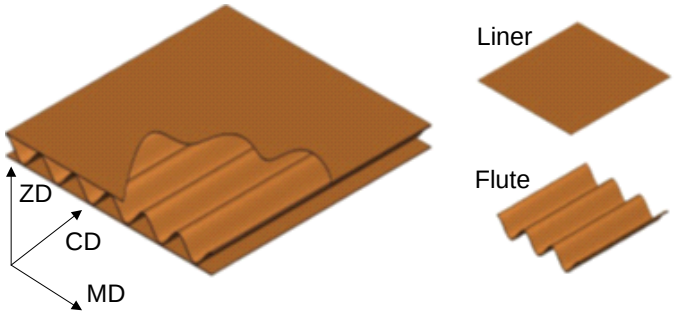

Figure 2.5: Corrugated paperboard panel geometry (MD is the machine direction, CD is the cross direction and ZD is the thickness direction) (Fadiji et al., 2016c).

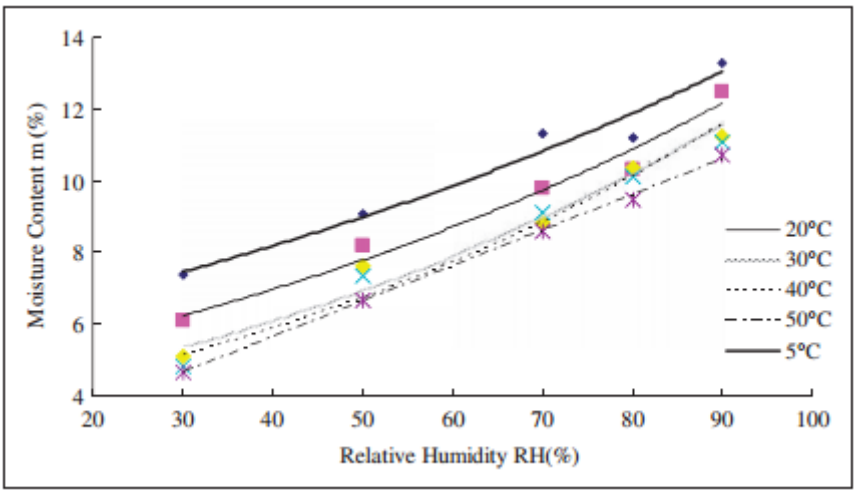

Figure 2.6: Relationship between the moisture content of paper and the relative humidity (Wang et al., 2013).

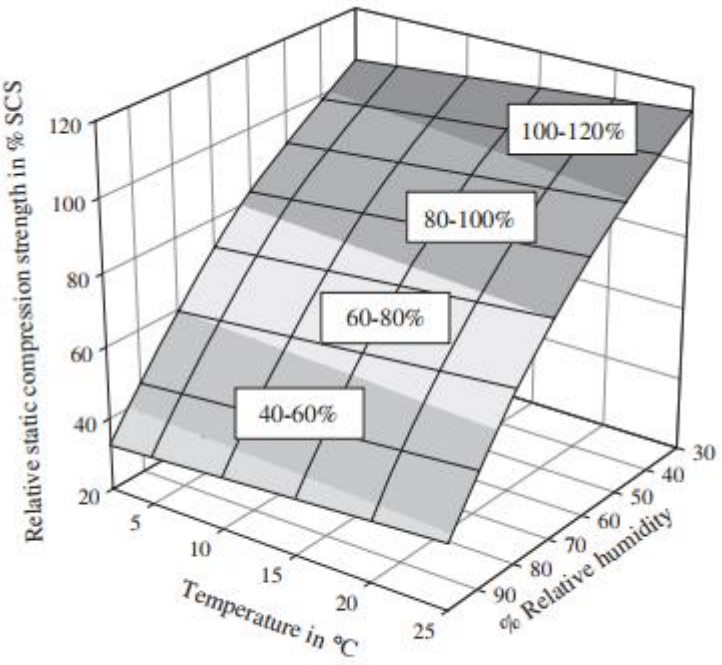

Figure 2.7: Response plot showing a relationship between relative static compression strength predicted from temperature and relative humidity (Sørensen & Hoffmann, 2003).

Table 2.1: Main types of packaging paper (Kirwan, 2008; Robertson, 2005; Paine & Paine, 1992).

Basic Material	Source	Weight range g m^{-2}	Tensile Strength kN m^{-1}	Properties and Uses
Kraft papers	Sulphate pulp from softwoods	70 – 300	2.45 – 11.28	Heavy-duty paper, bleached, natural or coloured; may be wet-strengthened or made water-repellent, strongest of all papers. Used for bags, multi-wall sacks and liners for corrugated. Bleached varieties are used for food packaging where strength is required.
Sulphite papers	Usually bleached generally made from a mixture of softwood and hardwood	35 – 300	Highly variable	Lighter and weaker than Kraft paper, clean, bright paper of excellent printing nature and used for smaller bags, pouches, envelopes, waxed paper, labels and for foil laminating.
Greaseproof papers	From heavily beaten pulp	70 – 150	1.77 – 4.41	Grease-resistant for baked goods and fatty foods.
Glassine papers	Similar to greaseproof, but super-calendared	40 – 150	1.37 – 5.25	Oil and grease resistant, used as an odour barrier for lining bags, boxes, and for greasy foods.
Parchment paper	Treatment of unsized paper with concentrated sulphuric acid	12 – 75	2.11 – 14.22	Non-toxic, high wet strength, grease and oil resistant for wet and greasy food.
Tissue paper	Lightweight paper from most pulp	20 – 50	Low strength	Lightweight, soft wrapping paper.

Table 2.2: Different flute profiles (Budimir et al., 2012; Nordstrand, 2003).

Flute types	Properties	Flute height (mm)	Take-up factor	Wavelength (mm)	Flute/m length of the corrugated board web
A	First standard board style. The largest flute, seldom used at present.	4.8	1.50 – 1.55	8.3 – 10	110
B	Most widely specified profile, difficult to crush, good compactness and high compression strength.	2.4	1.30 – 1.35	6.1 – 6.9	150
C	Larger than B flute, higher compression strength but edges can be crushed easily.	3.6	1.40 – 1.45	7.1 – 7.3	130
E	Smaller corrugations that B, with excellent flat crush resistance.	1.2	1.15 – 1.25	3.2 – 3.6	290
F	Known as the microflutes (very small corrugations), with excellent flat crush resistance and rigidity.	0.5 – 0.8	1.15 – 1.25	2.3 – 2.5	400 – 550

Table 2.3: Range of vertical frequencies and maximum acceleration encountered during transportation and distribution (Eagleton, 1995; Marcondes, 1994; Brandenburg & Lee, 1993; Tevelow, 1983; Schlue, 1968).

Transport mode	Vibrating system	Frequency range (Hz)	Maximum acceleration (g)
Rail cars	Vertical suspension	2 – 7	0.5
	Lateral suspension	0.7 – 2	0.8
	Structural	50 – 70	0.3
Trucks	Rolls	≈ 1	0.1
	Suspension	0 – 7	0.5
	Unsprang suspension	10 – 20	0.3
	Structural and tyres	50 – 100	0.3
	Damaged suspension	> 100	
Trucks on flat cars	Vertical	2 – 4.6	1
	Rolls	0.7 – 3.1	10
Aircraft	Propeller	2 – 10	0.5
	Jet	100 – 200	0.5
Ships	Sea	0.1 – 0.2	0.2
	Engines	100	0.4

Table 2.4: Examples of creep of corrugated paperboard packaging.

Study purpose	Result output	References
To evaluate the creep properties and recoverability of double-wall corrugated paperboard with A and B flutes at different combined conditions	Results showed that relative humidity and constant compression loads have evident effects on the creep properties and recoverability of double-wall corrugated paperboard. Mathematical model of creep and time curves was established.	Guo et al. (2008)
To examine the compressive and tensile creep behaviour of paperboard at cyclic and constant relative humidity	Paperboard at cyclic humidity had higher creep rate and more frequent failures than paperboard at constant humidity	Byrd (1972a, b)
To examine how compressive creep properties of corrugated paperboard package components are affected by cyclic humidity	Creep performance cannot be predicted by compressive strength, failure strain, energy absorption or stiffness	Considine et al. (1994)
To investigate the relationship between applied load and time until collapse of corrugated boxes	Increasing the applied load reduces the time until collapse of the corrugated boxes	Kellicutt and Landt (1951); Bronkhorst (1997)
To develop a model for predicting the creep behaviour of corrugated paperboard	Model was able to predict the creep performance of corrugated paperboard for a set of properties of the paperboard components and board geometry under compression load and constant RH	Navaranjan and Johnson (2006)
To analyse the creep failure of corrugated paperboard under fluctuating humidity regimes	The area under a humidity/time curve described the various humidly cycles. Maximum effect observed with increasing severity of the humidity impulse	Morgan (2005)
To examine the compressive creep of ECT samples made from recycled and virgin paper	Results showed that virgin paperboard had lower yield and deformation than recycled paperboard	Byrd and Koning (1978)

Table 2.5: Examples of moisture content effect on the performance of corrugated paperboard packaging.

Study purpose	Result output	References
To study the effect of air relative humidity on the shock absorbing properties of corrugated paperboard	Results showed significant influence of the moisture content of the corrugated paperboard material on the cushioning characteristics	Marcondes (1992)
To understand moisture sorption in moulded paper packaging for food at varying environmental temperatures and humidities, and the resultant effects on static compression strength	Increasing humidity and lowering temperatures results in moisture adsorption. Static compression strength of moulded paper packages and trays was significantly affected by moisture absorbed or dissipated and decreased with increased moisture.	Sørensen and Hoffmann (2003)
To study the effects of water content on the mechanical properties of corrugated paperboard	Corrugated paperboard showed sensitivity to relative humidity. Failure stress and ultimate strain of corrugated paperboard are significantly affected by moisture	Allaoui et al. (2009a)
Determine moisture content effect on tensile properties of three paper-based packaging materials: vegetable parchment (VP) paper, Kraft paper and solid-bleached (SBS) paper, in the MD and CD direction	VP paper was the strongest followed by the SBS paperboard and the Kraft paper in the MC direction, but the SBS paperboard was the strongest followed by the VP paper and the Kraft paper in the CD directions. Tensile strength decreased with increasing moisture content in both MD and CD directions for all paper samples	Rhim (2010)
To investigate the failure mechanism of virgin and recycled based corrugated paperboard at different environmental conditions	Virgin paper sheet components had better performance in compression than the recycled components. Compression failure at 50% and 90% RH occurs along the adhesive lines and the combination of failure mechanisms resulted in local buckling of the corrugated paperboard	Navaranjan et al. (2013)
To study the effect of storage conditions on moisture content of corrugated paperboard packages	Good correlation was found between package compression strength with change in moisture content of the package during storage	Pathare et al. (2016)
Assess the compression strength of ventilated corrugated paperboard cartons at different environmental conditions	Decrease in compression strength with increase in absorbed moisture	Fadiji et al. (2016c)

Chapter 3. The efficacy of finite element analysis (FEA) as a design tool for food packaging: a review *

Abstract

Finite element analysis (FEA) is a powerful and prevalent numerical technique that has been developed into an indispensable modern tool for the modelling and simulation of various engineering processes, particularly in food packaging industries. The advent of advanced computing power and efficient FEA software packages, coupled with the reduced cost of the software packages, has viably advanced the use of FEA in effectively and efficiently simulating various engineering design problems. In food packaging, FEA is useful for simulating and studying the structural design of packages. This numerical technique, validated with experimental results, helps package designers to improve the mechanical integrity and strength of the packages in order to protect the produce and package against damage. Advances in information and communication technologies will expand prospects by developing sophisticated and user-friendly software towards more holistic analyses of the performance of food packages. This review presents the state of the art in the research and development of FEA for use in food packaging highlighting food processing operations. The advantages of using FEA, as well as the shortcomings and challenges encountered by users of FEA in food packaging are also highlighted.

Keywords: Finite element analysis (FEA); Packaging; Corrugated paperboard; Modelling

---

*Publication:

Fadiji, T., Coetzee, C. J., Berry, T. M., Ambaw, A., & Opara, U. L. (2018). The efficacy of finite element analysis (FEA) as a design tool for food packaging: A review. *Biosystems Engineering*, *174*, 20–40.

3.1 Introduction

Finite element analysis (FEA) is a computer simulation technique used mostly by mathematicians, engineers and scientists (Pathare & Opara, 2014; Huebner et al., 2001). It is a numerical technique that can be used for predicting how a product reacts to real-world forces, vibration, heat, fluid flow, and other physical effects. FEA can show whether a product will break, wear out or function the way it was designed. While it is difficult to determine the exact date of the invention of FEA, its concept can be traced to the pioneering works of Hrennikoff (1941) and Courant (1943) in civil and aeronautical engineering with the need to solve complex elasticity and structural analysis problems. In recent years, the use of computers for high volume computations involving FEA has enabled its wide spread use (Hughes, 2012).

As with other numerical techniques such as computational fluid dynamics (CFD), FEA has in recent times become a powerful and prevalent tool in many industries, with solutions representing a rich tapestry of mathematical physics, numerical methods, user interfaces and futuristic visualisation techniques (Norton & Sun, 2006; Xia & Sun, 2002). The engineering computations in FEA have the principal goal of obtaining information concerning the response of physical systems to certain imposed conditions, which aid in making and justifying engineering designs and decisions. Despite its long history, the finite element method continues to be the predominant strategy employed by engineers to conduct structural analyses (Biancolini & Brutti, 2003). In addition to FEA gaining more ground being used extensively in the area of structural mechanics, it's application has also been successful in other areas such as fluid dynamics, heat transfer and conduction, electric and magnetic fields, food processing and packaging, among others (Fadiji et al., 2017; 2016a; Åslund et al., 2014; Pathare & Opara, 2014; Reddy, 2014; Rayfield, 2007; Han & Park, 2007; Sirkett et al., 2007; Navaranjan & Johnson, 2006; Biancolini & Brutti, 2003; Cook et al., 2002; Geng et al., 2001; Beldie et al., 2001; Pommier et al., 1991). FEA has become an integral part of many engineering designs due to its ability to predict the performance of new designs or processes before making or implementing the prototypes (Schaldach et al., 2000).

Knowledge of the strength of the structure to be analysed was highlighted to be an essential factor in making a sound decision (Kheyr & Mortezaei, 2007). The use of simple design and evaluation procedures cannot realistically assess the performance of many structures, particularly properties such as ultimate strength, inelastic behaviour and response, and load distribution characteristics. In order to predict these behaviours, the use of extensive analytical methods or experimental trials are required, which in many cases are not sufficient, economical or expedient. As a result, the potential of FEA to predict the performance of most structures has grown (De Borst et al., 2012; Hughes, 2012; Cook et al., 2002; Schaldach et al., 2000).

Food packaging is a vital requirement to provide protection to the packed product from external factors that may arise from contaminants, physical damage and

mechanical loadings (Fadiji et al., 2018a; Siddiqui & Ali, 2017; Opara & Pathare, 2014; Mangaraj et al., 2009; Farber, 1991). Boyette et al. (1996) described packaging, particularly for horticultural produce (fresh fruits and vegetables) as one of the most important operations in the long and complicated journey from the grower to the consumers. Ultimately, the main objective of packaging design is to minimise mechanical damage to packed produce during the distribution cycle and improve the overall packaging performance (Pathare & Opara, 2014; Opara & Pathare, 2014). Packaging design includes optimal selection and combination of raw materials, optimal selection of prism type, optimisation of overall design of box, and the cost control of packaging (Lertkittikul, 2017; Betancur-Muñoz et al., 2014; Chen et al., 2011a). Optimum packaging design must be able to maintain adequate mechanical strength and stability of the package.

Traditionally, to prevent impact-induced damage on a product, a reliability test is done using the 'design – prototype – test – redesign' approach which can be expensive, tedious and time consuming. Numerical modelling provides an efficient approach to predict the structural integrity of product when subjected to mechanical loadings (Hammou et al., 2012). The increased use of FEA in food packaging represents a way in which package designers can adapt and be more responsive to change (Hicks et al., 2009). FEA is continually replacing the time-consuming and costly experimental trials, and provides opportunities for studying different production processes and effects of varying parameters once the model is validated (Defraeye et al., 2013; Delele et al., 2010; Hicks et al., 2009). FEA has been used in packaging industries to simulate a wide range of processes such as; plastic bottle forming (Vaidya, 2012; Yang et al., 2004), handling of plastic films (McPherson et al., 2004; Babini et al., 2003), paper cup brim forming (Ramasubramanian & Muthuraman, 1999), behaviour of paper and paperboard at micro level (Fadiji et al., 2017; Dano & Bourque, 2009; Huang & Nygårds, 2010; Biancolini & Brutti, 2003; Gilchrist et al., 1998) and paper package structural behaviour (Fadiji et al., 2016c; Han & Park, 2007; Sirkett et al., 2007; Biancolini & Brutti, 2003; Beldie et al., 2001). Due to the usefulness of FEA in food packaging industries, there has been an increase in its development in the past years. Therefore, this review provides an overview of the recent advances in FEA application in food packaging industries, particularly the role of corrugated paperboard packaging.

3.2 Benefits of utilising FEA

FEA is often used as an alternative to various time consuming and expensive experimental tests (Delele et al., 2010) and has proven to be useful in simulating any design concept and in determining the behaviour of this concept in almost any environment (Rao, 2010; Srirekha & Bashetty, 2010). Consequently, FEA helps in evaluating the possibility of a new design once a model has been developed and validated, without the need to prototype and waste time and resources (Rao, 2010; Delele et al., 2010; Srirekha & Bashetty, 2010; Reh et al., 2006; Chandrupatla et al., 2002). As highlighted by Xia and Sun (2002) and Bakker et al. (2001), the results of most mathematical models such as FEA will help to enhance

performance, improve reliability, provide more confidence in scale-up and improve consistency of the product. For instance, mathematical models can assist in the following areas:

- Provide comprehensive results while generating the physical response of a system at any instantaneous point.
- Make it possible to perform different analyses of the same model under varying situations or conditions.
- Handle complex geometries and makes the evaluation of geometric changes possible with less time and resources as opposed to experimental tests.
- Assist in safe simulation of potentially dangerous, impractical or complex loading conditions and failure modes.
- Make extrapolation of experimental results possible through parametric analysis of the validated models.
- Provide visual representations and simulation calculations for different parameters (for example stress or temperature distribution) making it possible for rapid performance evaluation and modification.
- Provide a rapid calculation for most applications with relatively low investments making it useful in a wide range of engineering problems such as solid mechanics, dynamics, and heat transfer.

The use of FEA in food and packaging industries has provided new insights for food package designers regarding the performance of various food handling equipment, processes and packages. Problems involving food processes such as drying, heating and cooling among others have been successfully solved using FEA (Petrů et al., 2014, 2012; Fasina & Fleming, 2001; Pan et al., 2000; Zhao et al., 1998; Zhou et al., 1995). Understanding the behaviour of different produce such as apples and pears (Ahmadi et al., 2016; Yousef et al., 2016; Wei et al., 2015; Wu et al., 2013; Celik et al., 2011), tomatoes (Li et al., 2013) and cantaloupe (Seyedabadi et al., 2015) has become possible with FEA. The area of food packaging has been successfully studied using FEA, allowing for development, troubleshooting, optimisation as well as producing new, reliable, efficient and effective designs (Fadiji et al., 2016c; Viguié et al., 2010; Biancolini et al., 2009; Han & Park, 2007; Urbanik & Saliklis, 2007; Roduit et al.,2005; Beldie et al., 2001).

3.3 Basic concepts and essential elements of FEA

FEA is the application of the finite element method in which the object or system is represented by a geometrically similar model consisting of multiple-linked, simplified representations of discrete regions. This numerical analysis uses a complex system of points called nodes, which form a grid called a mesh. This mesh is programmed to contain the material and structural properties, which defines how the structure will react to certain loading conditions. Nodes are assigned at a certain density throughout the material depending on the anticipated diffusion or stress levels of a particular area (Pathare & Opara, 2014; Moaveni, 2008; Roduit et al., 2005; Cook et al., 2002; Gupta & Meek, 1996). The basic idea of FEA is to find

solutions to a complicated problem by replacing it with a simpler one. The domain (usually a physical structure) in FEA is discretised into several subdomains or finite elements and the process is known as discretisation. FEA techniques are used to obtain approximate solutions to boundary value problems (otherwise known as field problems) in engineering (Reddy, 2014; Moaveni, 2008). In a boundary value problem, the field is the domain of interest and it usually represents a physical structure (Reddy, 2014; Hughes, 2012; Moaveni, 2008).

Generally, the concept of FEA involves a piecewise polynomial interpolation. Over the entire structure, the field quantity becomes interpolated in a piecewise form and a set of simultaneous algebraic equation is generated at the nodes, which is associated with the elements (Eq. (3.1)), as in the case of a structural analysis. The functions of all the elements are then assembled to form the global matrix equation i.e., the governing algebraic equations that define and represent the entire structure under study (Eq. (3.2)).

$$\left[K\right]_e \left\{u\right\}_e = \left\{f\right\}_e \tag{3.1}$$

where, $\left[K\right]_e$ is the elementary stiffness matrix, dependent and determined by the geometry, element and material properties, $\left\{u\right\}_e$ is the elementary displacement vector which defines the nodes motion under loading and $\left\{f\right\}_e$ is the elementary force vector which defines the applied force on the element.

$$[K]\{u\} = \{f\} \tag{3.2}$$

where, $\left[K\right]$ is the global stiffness matrix, $\left\{u\right\}$ is the vector of the unknown nodal displacements (or temperature in thermal analysis) and $\left\{f\right\}$ is the vector of the applied nodal forces (or heat flux in thermal analysis).

The governing algebraic equations can be solved for the dependent variable at each node after applying the boundary conditions after which the strain and stress can be calculated based on the displacement of nodes associated with the element. Many engineering phenomena can be expressed using the governing equations and boundary conditions. However, it is important to mention that the governing equations are associated and depend on the physics of the problem being analysed and not with the method of the solution (Nikishkov, 2004). Hence, the solved governing equation depends on the physical problem to be analysed.

FEA is performed with a great accuracy since the actual shape, load and boundary conditions, as well as the material properties can be specified and applied. In order to formulate the FEA of a physical problem, certain steps are common to all analyses whether structural, heat transfer, fluid flow, or any other problem. In

practice, three principal steps are involved in FEA: pre-processing, analysis (solver), and post-processing (Srirekha & Bashetty, 2010; Cook et al., 2002).

3.3.1 Pre-processing

All the tasks prior to the numerical simulation process are referred to as pre-processing. These include the conceptualisation of the problem, meshing, and building the computational model. The pre-processing stage involves the creation of the model to be used for the analysis. The structure is created using the computer aided design (CAD) program that can come with the FEA software or be provided by another software developer. The success of the entire FEA process crucially depends at this stage on the skill of the analyst to determine the level of the simplification to be introduced or included into the model when compared with the physical situation. For a successful analysis, the software user must be able to determine the mesh and element types to be used in the model. The structure is divided into a number of discrete sub-regions known as “elements”, connected at discrete points known as “nodes”. The structure represented by nodes and elements is called the “mesh”. The elements not only represent subdivisions of the structure, but also the mechanical properties and behaviour of the structure. Most FEA software packages have the ability to perform meshing and define the shape and properties of the structure to be analysed simultaneously (Xia & Sun, 2002; Cook et al., 2002). An example of a meshed corrugated paperboard is shown in Figure 3.1.

Complex regions of the structure such as curves require a higher number of elements to accurately represent the geometry, whereas regions with simple geometry can be represented by fewer elements. Choosing an appropriate element for a structure requires some factors such as; prior knowledge of FEA, knowledge of the behaviour and properties of the structure, the elements available in the FEA software and the characteristics of the elements. In the pre-processing stage, once the meshing of the structure is completed, the constraints, loads, boundary condition and the material properties of the structure are defined. In addition, the entire structure is fully defined by the geometric model at this stage.

3.3.2 Analysis

The analysis step is the processing stage whereby the computer is used to solve the set of mathematical equations. After the meshing, the dataset such as the geometry, constraints, load, and mechanical properties of the structure generated as inputs are put into the finite element code to generate matrix equations for each element. These are then reassembled together to form a global matrix equation for the structure. That is, these datasets are used as input to the FEA code, which constructs and solves a system of linear and nonlinear algebraic equations until convergence is achieved. Nodal results such as displacement values at different nodes, temperature values at different nodes in a heat transfer problem or velocity values in a fluid dynamics analysis are also obtained at this stage (Cook et al., 2002). One of the

problems that might be encountered in the analysis stage is solving large linear systems. In modern FEA packages, algebraic or geometric multigrid methods are employed to accelerate the iterative solution process for large linear systems. Another problem that may be experienced with the FEA solver is the nonlinearity of the model to be analysed. However, certain nonlinearities may be neglected to obtain linear equations that can be solved easily. For these purposes, in most FEA software packages, segregated and continuation solvers are developed. A third problem that may be faced at the analysis stage is the model instability, which results in a poor approximation of the mathematical model being produced. One way to solve this problem is through better adaptive meshing which is an important factor in improving model behaviour.

3.3.3 Post-processing

This is the final stage involved in FEA. Raw data generated in the analysis step makes it difficult to interpret. In the post-processing stage, these data are evaluated and used to create either 2D or 3D representations such as; the deflected shape of the structure, stress plots, and other animations, which are useful in better understanding the behaviour of the problem being analysed. For example, depending on the FEA software package available, colour may be used to indicate the value of some component of stress or displacement on the analysed structure. An example of a typical model of ventilated corrugated paperboard package under buckling is shown in Figure 3.2. An outward buckling occurred on the length side of the package and was observed to originate from the middle of the length side face. The deep red colour observed on the face of the length side of the package indicates region where the greatest buckling occurred. Usually, the pre- and post-processing stages are part of the same FEA software package. An overview of the steps involved in the process of finite element analysis is shown in Figure 3.3. Estimating the error in the post-processing stage of a finite element simulation is an important task, which can be achieved by solving the equations of the mathematical model using different sizes of mesh to obtain a convergence of the numerical solution. Furthermore, sensitivity analysis of the model is very important particularly to different stages and input parameters such as the initial conditions, boundary conditions, applied loads, material properties and varying constraints. Recently, optimisation software packages are being combined into FEA software packages and are being used in iterative calculations in order to optimise critical shape or dimensions of an analysed structure.

3.4 Common commercial FEA codes used in food packaging

Because FEA involves operations where large matrices are solved it can be a very computationally intensive method (Hutton, 2004). When FEA was in its early years, mainframe computers, which were considered a powerful tool for engineering design and analysis, were used (Hutton, 2004). The first finite element software code that was developed during the 1960's was NASTRAN, which was capable of handling thousands of nodal field variable computations (Hutton, 2004). However,

in the last two decades there has been a progressive growth in the development of commercial finite element codes. This has enhanced their use in modelling complex phenomena, which consequently makes them attractive and increases their versatility for engineering design. According to Robertson (2012), the advent of finite element analysis has made the task of designing and manufacturing in food packaging easier and rapid. This has also resulted in enormous flexibilities and efficiencies through a more thorough design analysis of variables such as stresses and the mechanical performance as a whole. In today's computational environment, most of these FEA codes can be implemented on desktop computers and engineering workstations to obtain solutions to large problems in static and dynamic structural analysis, heat transfer, fluid flow and electromagnetics. Five of the commercial FEA codes that are more commonly used, particularly in food packaging are discussed below and examples of research using the software given. Although the FEA software packages highlighted have proved very useful in packaging research, we do not necessarily provide endorsement for these FEA software packages.

3.4.1 ANSYS

The flexibility and robust design analysis of ANSYS (ANSYS Incorporation, Canonsburg, PA, USA) make it a versatile FEA code across various disciplines. The multi-physics attribute of ANSYS allows the same model to be used for a variety of coupled field applications, such as thermal-structural, magneto-structural and electrical-magnetic-flow-thermal. Comprehensive graphical tools are incorporated in ANSYS. These allow for an effective visualisation of the model (Öchsner & Öchsner, 2016). Two essential optimisation types are incorporated in ANSYS and these are design and topology optimisation (Lakshmininarayana, 2004). Pathare et al. (2012a) used ANSYS to study how the strength of corrugated paper containers was affected by different ventilation openings. Maximum stress was observed on containers with the highest ventilation openings (6% of the total area of the container). The authors reported that the stress was produced at top and towards the corner of ventilated opening. Han & Park (2007) used ANSYS FEA code to investigate the principal design parameters of vent holes and hand holes in the faces of corrugated paperboard boxes. Oblong-shaped vent holes performed best in maintaining the strength of the boxes. The results from the model generally agreed well with laboratory experimental results. ANSYS was used by Zhou et al. (1995) to predict the temperature and moisture distribution in food materials during microwave heating. The behaviours and performances of concrete beams (Ibrahim & Mahmood, 2009), dental implants (Kayabaşı et al., 2006) skeletal muscles (Yucesoy et al., 2002), and human ear (Gan et al., 2004) have been studied using ANSYS FEA code. The ANSYS FEA code offers tools such as units awareness, graphical geometry modeller, graphical manual meshing, linear static analysis and nonlinear (large displacement and contact) analysis. ANSYS FEA code is also capable of performing heat transfer, electric, magnetic, fluid flow and fluid structure interaction processes, as well as material models, which include plasticity and creep, among others.

3.4.2 ABAQUS

ABAQUS (ABAQUS Incorporation, Johnston, RI, USA) is an engineering simulation program based on the finite element method. It can provide the solutions about stress and strain, heat and mass transfer, natural frequencies and mode shape, forced response, fatigue and lifetime estimation and nonlinear material. ABAQUS has been used extensively and widely for many engineering problems due to its numerous attributes such as; containing a comprehensive library of elements that can be used to model any geometry, compatibility with other computer aided design (CAD) software packages, ability to simulate the behaviour of different engineering materials (rubber, polymers, metal, reinforced concrete, composites), capacity to simulate linear, nonlinear, static as well as dynamic analysis. For instance, in a nonlinear analysis using ABAQUS, the load increments and convergence tolerances are automatically chosen to ensure an accurate and efficient solution to the problem. Furthermore, in ABAQUS, when problems involve multiple components, they are modelled by associating the geometry by defining the appropriate material models to each components and specifying the interactions between the components. Hammou et al. (2012) developed an efficient homogenisation model for corrugated paperboard, this model was implemented in the ABAQUS FEA code and the foam behaviour model, which was used to study the drop and shock resistance of corrugated paperboard boxes with different foam cushion internal configurations.

3.4.3 LS-DYNA

LS-DYNA (Livermore Software Technology Corporation, Livermore, CA, USA) is a multi-purpose explicit and implicit FEA code that can be used for analysing real world problems. The origin of LS-DYNA FEA code is highly nonlinear, transient dynamic FEA using explicit time integration. Modelling contact in LS-DYNA is fully automated. In addition, LS-DYNA has the capability to simulate a wide range of different physical phenomena using analysis techniques such as Explicit and Implicit Time Integration Schemes, Nonlinear Dynamics, Large Deformations, Sophisticated Material Models, Complex Contact Conditions, Thermal Analysis and Thermal Structural Coupling, Fluid Dynamics and Fluid Structure Interactions, Smooth Particle Hydrodynamics (SPH), Element Free Galerkin (EFG), Eigenvalue Analysis among others (Lakshmininarayana, 2004). The possibility of increasing computation speed in LS-DYNA helps to improve scalability and various third party software are compatible for pre-processing the input files of LS-DYNA. The pre- and post- processor associated with LS-DYNA is the LS-TAURUS, which was also developed by Livermore Software Technology Corporation. Using LS-DYNA, the mechanical impact loading on the behaviour of consumer structures and products has been extensively studied (Mulkoglu et al., 2015; Neumayer et al., 2006). Venter and Venter (2012) used LS-DYNA to develop numerical models for an inflatable paper dunnage bag. The model was able to predict the inflated shape and the stress condition of the dunnage bag in a constrained void. The error of the numerical model was about 6.2% when the model results were compared with

physical test results. The drop impact of a cooker with foam packaging and the thermal pre-stress analysis of plastic foil wrapping was performed by Neumayer et al. (2006) using LS-DYNA FEA code. Erdogan and Eksi (2014) used LS-DYNA software to model the thermoforming process of three-thermoformed material and the wall thickness distribution was predicted and compared with experimental results.

3.4.4 MSC MARC

MARC FEA code (MSC Software Corporation, Santa Ana, CA, USA) is a general-purpose tool capable of solving complex structural and thermal problems. It is a robust nonlinear FEA solver with the capabilities to accurately simulate the behaviour of various products under contact, large strain, static, dynamic and multi-physics loading conditions. The pre- and post-processor dedicated to support MARC solver is MENTAT. The combination of MARC and MENTAT enhance the delivery of an efficient and complete analysis (pre-processing and post-processing solution) for an implicit nonlinear FEA (Öchsner & Öchsner, 2016; Lakshmininarayana, 2004). MARC contains an extensive material model library; elastomers, linear elastic, elastic plastic, creep, composites, viscoelastic, hyperelastic, powder metallurgy, among others. Furthermore, MARC contains more than 140 elements which are accurate, modern and robust, hence can be used to represent complex problems appropriately (Lakshmininarayana, 2004). It can handle robust product testing and manufacturing simulation such as predicting damage and crack propagation, acoustics, hydrodynamic bearing, magnetostatics among others. The multi-physics attribute make modelling interactions between structural, electrical, magnetic and thermal analyses possible. MARC is therefore widely considered as complete solution that can tackle all nonlinear simulation requirements (Öchsner & Öchsner, 2016; Lakshmininarayana, 2004). Beex and Peerlings (2009) used MARC to study the creasing and folding behaviour of laminated paperboard. The breaking stress and the deformation behaviour of coated paperboard during indentation with a trapezoidal centre bevel cutter was studied by Nagasawa et al. (2006) using MARC FEA software code.

3.4.5 MSC NASTRAN

NASTRAN (MSC Software Corporation, Santa Ana, CA, USA), known in full as NASA Structural Analysis is an all-purpose FEA solution for various engineering problems ranging from small to complex. MSC Patran is the associated pre- and post-processor for MSC NASTRAN. MSC NASTRAN is widely used to perform static, dynamic, heat transfer, acoustic, thermal, aero-elastic, hydro-elastic, piezo-electric analyses and many more. NASTRAN can handle different material types from metal and plastics to hyperelastic to composites. MSC NASTRAN has a unique element technology, which provides efficient and accurate results, lowering the modelling effort, solution time and computer requirements (Lakshmininarayana, 2004). Biancolini and Brutti (2003) used MSC NASTRAN to evaluate the structural performance of corrugated board panel. In addition, the

authors reported that the numerical tool (MSC NASTRAN) is applicable to a wide range of problems including corrugated board structure and for product optimisation, because all parameter effects are taken into account, including materials, micro-geometry and macro-geometry. MSC NASTRAN was used by Fadiji et al. (2017) to study the behaviour of paperboard packaging materials under mechanical loadings. The model was able to predict the edge compression resistance of the corrugated paperboard. The authors validated the numerical results with experimental results and close agreement was reported. The experimental results and the simulation results differed by about 5.5%.

3.5 Application of FEA in food packaging industries

The importance of numerical methods such as finite element analysis (FEA) and computational fluid dynamics (CFD) was reported by Delele et al. (2010). The advantage these techniques have over time consuming and costly experiments has increased their use, particularly in food packaging. This section discusses the role of finite element analysis in food packaging with emphasis on how FEA has been used to improve corrugated paperboard packaging. A multiscale approach is used in discussing the application of FEA (i.e. paper → corrugated paperboard → corrugated paperboard package).

3.5.1 Paper and paperboard

The uniqueness of the response of paperboard load, moisture and temperature makes it one of the most complex engineering materials (Fadiji et al., 2017; Hubbe, 2013; Alava & Niskanen, 2006; Haslach, 2000; Bandyopadhyay et al., 2000). Paper and paperboard are two commonly used materials in almost every industry (Xia et al., 2002). Paper can be utilised for storage purposes in two principal ways; either as a wrapping material or converted into a container. The paper used for the manufacture of containers is usually a thick hard paper called paperboard, with grammage above 200 g m^{-2} (Hagman, 2013; Huang et al., 2014). In fresh fruit industries where packaging plays a continuous increasing role, paper and paperboard are becoming reliable and important (Raheem, 2012; Ahmed & Alam, 2012; Koutsimanis et al., 2012; Mahalik & Nambiar, 2010; Kibirkštis et al., 2007; Pré, 1992; Smith e al., 1990). Designing paperboard packages requires the analysis of the structural integrity of the various components and evaluating the strength and stiffness properties. Understanding these structural responses of paperboard is a crucial step in the design of a whole paperboard package, and over the years, FEA has been used widely to better understand the material properties of paper (Talbi et al., 2009; Biancolini, 2005).

Paper is an anisotropic, in-homogenous network consisting of cellulose fibres surrounded by fillers of different kinds (Hagman, 2013). The anisotropy and in-homogeneity properties of paper is a consequence of the manufacturing process, where a fibre suspension is deployed onto a moving web which is then pressed between rolling cylinders and dried (Hagman, 2013). This results in the paper

having different mechanical properties in three principal directions (Figure 3.4) (Pathare & Opara, 2014; Hagman, 2013; Jiménez-Caballero et al., 2009; Harrysson & Ristinmaa, 2008; Stenberg, 2003; Xia, 2002; Xia et al., 2002). This directional dependence of paper and paperboard are the direction that the paper moves through the machine (MD), direction perpendicular to the machine direction and the out of plane direction (ZD). The constitutive model of the in-plane (MD and CD), out-of-plane (ZD) properties and mechanical properties of paper and paperboard have been studied by several authors (Domaneschi et al., 2017; Pradier et al., 2016; Linvill & Östlund, 2016; Borgqvist et al., 2015; Huang & Nygårds, 2012; Giampieri et al., 2011; Beex & Peerlings, 2009; Östlund & Nygårds, 2009; Ramasubramanian & Wang, 2007; Hallbäck et al., 2006; Stenberg, 2003; Xia, 2002). Some of the properties of paper and paperboard that are typically sought are high compression strength, high bending stiffness, foldability, crease-ability and esthetical properties (such as look and feel).

During paperboard conversion, operations such as gluing, folding and cutting could be straightforward (Beex & Peerlings, 2009), however, a difficulty could be encountered during the conversion process. This difficulty is the cracking of high grammage paperboard, which may be due to the quality of the fold at the creases (Beex & Peerlings, 2009). Creasing is an important mechanical behaviour of paperboard die cutting (Nagasawa et al., 2003). Creasing (Figure 3.5), otherwise known as scoring helps to facilitate folding in paperboard and the quality of fold in paperboard is defined by the crease. The bending stiffness of the paperboard around the folding line is lowered when creased because a shear-induced delamination is produced into the paperboard structure, which weakens the paper fibre (Giampieri et al., 2011). The strength of paperboard and paperboard packages can be compromised due to cracked folds, and may affect the attractiveness to customers (Giampieri et al., 2011). Table 3.1 presents the application of FEA in studying the creasing of paperboard.

Xia et al. (2002) proposed computational hybrid models for paperboard creasing using a detailed delamination and material model. In their proposed model, in-plane elastoplastic models and the elastic behaviour in the thickness direction were used to simulate the in-plane behaviour of paperboard. In combination with an interface model, the damaging creasing and folding behaviour in the out-of-plane direction of the paperboard were studied. A numerical model using MSC MARC FEA software was developed by Beex and Peerlings (2009). The model was able to predict the behaviour of paperboard in a virtual environment for varying creasing settings. The authors used a continuum model and delamination model to describe the material behaviour of paper and to account for the opening behaviour of different paper plies, respectively. Paperboard was modelled as a fibre network by Kulachenko and Uesaka (2012). Beam elements was used to represent the modelled fibres and was able to produce the microscopic material properties of the structure. The delamination model used was based on the cohesive model by Ortiz and Pandolfi (1999). Although the model developed by the authors was capable of

studying microscale behaviour of paperboard, it was not suitable for simulating paperboard creasing and folding macroscale phenomena (Domaneschi et al., 2017). The numerical models, when compared with experimental results showed high accuracy in the prediction of paperboard response during creasing, with plasticity and multiple delamination occurring at the shear regions.

Giampieri et al. (2011) used a different FEA approach for the simulation of fold in pre-creased paperboard. This model was based on shell model with damaging line hinges. The model can be applied on a large scale for simulating paperboard package forming processes. Huang and Nygårds (2012) used FEA to investigate the behaviour of paperboard during forming of complex shaped surfaces. The numerical investigation included the effect of pressure, boundary conditions, material properties and different deformation and damage mechanisms such as delamination and plasticity. Results showed that delamination occurred at the edge and at the deepest area of the mould shape, which consequently affected the in-plane strain fields. The forming performance of the paperboard was significantly affected by the boundary conditions. Comparing the strain between the MD and CD, boundary conditions had greater effect on the strain in the MD than in the CD. Conversely, material properties affected the strain in the CD more than in the MD. Experiments were carried out and the results were in good agreement with numerical results.

With various numerical techniques available to model and understand the damage mechanisms of paperboard properties, it is ideal to combine experimental and numerical studies to enhance the understanding of paperboard properties such as creasing and folding, thereby improving the end-use of paperboard (Huang and Nygårds 2010). Huang et al. (2014) studied the creasing and folding behaviour of three commercially produced paperboards both numerically and experimentally. The studies were performed on paperboard strips in both MD and CD. The numerical model was able to predict the creasing and folding behaviour for all the three paperboards. In addition, the simulation results predicted the experiment force–displacement curves for all paperboards.

A recent study by Li et al. (2016) used FEA to investigate the pure crack opening mode and sliding mode of multi-ply paperboards. A mixed-mode method was used to analyse the behaviour of the paperboard during the creasing and folding process. The authors used four techniques to characterise the delamination property of the paperboard. The techniques were z-directional tensile test (ZDT), double-notch shear test (DNS), double-cantilever beam test (DCB) and end-notched flexure (ENF). Results showed that fracture properties in both MD and CD directions were not the same because of fibre orientation bias. Furthermore, the response of the pure sliding mode was stronger and stiffer when the fibres were oriented in the direction of the crack growth. Orienting the fibres transversely to the crack growth direction made the response highly nonlinear and softer. This was attributed to the bending

of interface fibres rather than compression and extension. In addition, the response of the pure crack opening mode was characterised fully and sufficiently by the ZDT.

3.5.2 Corrugated paperboard

Corrugated paperboard is the final product of laminating paperboard layers (two or more) using a conversion process. The outer layers are known as the liners and the corrugated core is known as fluting (Fadiji et al., 2018a; Harrysson & Ristinmaa, 2008). Due to its numerous advantages such as; recyclability, low cost to weight ratio, high stiffness per unit weight among others, corrugated paperboard is an attractive material which is commonly used for manufacturing corrugated paperboard boxes used for transporting various products (Fadiji et al., 2018a, 2017; Harrysson & Ristinmaa, 2008). The packages are exposed to different hazards and mechanical loadings during its lifetime (transportation and storage) which tend to affect the structural performance of the package components and the whole package (Opara & Fadiji, 2018; Fadiji et al., 2018a, 2017, 2016a, b, c; Pathare & Opara, 2014; Harrysson, & Ristinmaa, 2008). FEA has been used by several researchers to study the mechanical properties of corrugated paperboard such as ultimate failure, collapse, creasing, stability, buckling, elastic behaviour, and transverse shear (Fadiji et al., 2017; Åslund et al., 2014; Zhang et al., 2014; Talbi et al., 2009; Haj-Ali et al., 2009; Thakkar et al., 2008; Jiménez-Caballero et al., 2009; Biancolini et al., 2005; Aboura et al., 2004; Gilchrist et al., 1998; Pommier & Poustis, 1990; Peterson, 1983). Some examples of FEA application on corrugated paperboard are presented in Table 3.2.

An early study of the mechanical performance of corrugated paperboard by Peterson (1983) involved the use of FEA to study the stress developed under three-point bending in the MD on corrugated paperboard. The authors used symmetry in the model and only linear elastic behaviour was considered. The fluting medium was assumed to have a sinusoidal shape. The fluting under compression was reported to be the most critical component of the corrugated paperboard controlling the stress. Numerical results were validated with experimental studies. Pommier and Poustis (1990) studied the bending stiffness of a single-wall corrugated paperboard using FEA involving a linear elastic code. To simulate the perfect bonding between the liners and the fluting, nodes at contact points were merged together. Bending stresses on the board were obtained and compared with experimental results. However, the authors concluded that the model was not sufficient to determine the bending flexibility matrix of an orthotropic material.

To determine the transverse shear of corrugated paperboard using three-point bending method, Nordstrand and Carlsson (1997) used FEA and found good agreement with the experimental validation. Patel et al. (1997) used FEA to evaluate the local buckling and the failure on the facings of cylindrical corrugated paperboard. The model was able to predict the collapse stress of the corrugated board. However, the Tsai-Wu collapse stresses obtained by FEA were approximately 125% of the experimental collapse stresses. The board collapsed

when the local buckling of the inner facings occurred and unconservative results were reported for the critical buckling load from the local buckling analysis of a shear loaded board element. The mechanical performance of corrugated paperboard was investigated by Gilchrist et al. (1998) using FEA. The authors used the ABAQUS finite element code for implementing the simulation. Detailed geometry of the board was considered using 3D meshes by discretising the liners and the fluting. The model evaluated the stiffness of the board by analysing various combined board configurations, which includes the geometries of anticlastic bending test, four-point bending and edge compression test. Experimental measurements were reported to correlate with simulation results.

ABAQUS finite element software code was used by Allansson and Svärd (2001) to study the influence of the local buckling of corrugated paperboard facings on the board panels. The simulation used a linear-elastic orthotropic material model. Results from FEA was compared with experimental tests and good agreement was observed in the load-displacement paths obtained from both methods. The study by Biancolini and Brutti (2003) used FEA to gain better understanding of how a corrugated board panel deforms during compression loading with MSC NASTRAN. The authors used the elastic material properties from experiments as input material in the simulation. From the rectangular corrugated paperboard model, an equivalent in-plane and bending stiffness was developed. The ECT value predicted from the eigenvalue buckling analysis (predicts the buckling strength of an ideal linear elastic structure) was in agreement with the measured ECT value with a difference of about 1.5% and 4.8% for virgin and production corrugated paperboard, respectively.

Detailed modelling of both single and double walled corrugated paperboard subjected to compression loading was compared with simplified shell modelling with a solid core using FEA by Armentani et al. (2006). The material properties used in the model were estimated from the in-plane properties of the paper sheet and each layer was modelled as orthotropic and homogenous. The stiffness of the core was determined as an effective stiffness equivalent to the stiffness of the fluting. The results from the detailed model and simplified model were very close before buckling occurred for both board types. However, the behaviour of the simplified model differed from the detailed model in the post-buckling regime. In general, the agreement observed in the load-displacement responses for both experimental tests and numerical analysis was good. Gospodinov et al. (2011) developed a finite element model to study how the changes in mechanical characteristic of the different layers of corrugated paperboard affected its complex mechanical behaviour. A single-wall corrugated paperboard with C-flute profile was used in the study. The mechanical behaviour of the corrugated paperboard was reported to be significantly affected by the liners than the flute. Results obtained from the model were compared with experimental results and they showed good coincidence. Hernández-Pérez et al. (2014) developed a finite element model to determine the twist stiffness of corrugated paperboard with single and double web

cores. The model employed the homogenised core approach. The twist stiffness was studied with an analytical approach using the first order shear deformation theory. Numerical results were compared with the analytical model and good agreement was reported in predicting the torsional stiffness of the board. However, the authors reported that the analytical approach was significantly less computationally demanding than the FEA. In addition, the analytical solution was more viable in predicting the twist stiffness of the corrugated paperboard.

To understand the performance of corrugated paperboard, Popil et al. (2006) used FEA to model the effect of adhesive on the strength of the board. Different types of corrugating adhesives were applied in a range of basis weights on the double-backer simulator equipment. ECT and bending stiffness were measured as a function of the applied adhesive level and type. Hill anisotropic plasticity constitutive model was used to model the material response of the linerboard and flutings while the Tsai-Wu anisotropic failure criterion was used to determine the damage locations that occurred with ECT progressive loading. The simulation was able to accurately predict buckling loads, load-deflection response, and other mechanical behaviour modes to confirm the observed effects of increased glue line volume on the ECT response during the experimental tests. Rahman and Abubakr (2007) investigated the role of adhesives in the buckling failure of corrugated paperboard using FEA. In the FEA, the authors incorporated the glue material that represents the actual geometry and material properties of the corrugated paperboard. Detailed model included the different components of the corrugated paperboard (liners, fluting and adhesive). Buckling analysis of the corrugated paperboard under compression load was performed. Results showed that increasing the modulus of elasticity of the adhesive increases the buckling strength of the corrugated paperboard. An increase of about 50% in strength was reported when the adhesive modulus was about 20 times the modulus of the liners. Furthermore, there was a significant decrease in the buckling strength of the corrugated paperboard due to loss of adhesives along the paperboard gluelines.

Johnson and Popil (2015) developed a finite element model for corrugated paperboard to simulate the mechanical behaviour at the gluelines from the MD straining. The model was used to analyse the changes in adhesive or linerboard modulus and strains at the gluelines. Results from the model showed that large changes in the adhesive modulus does not have a significant effect on the axial strain. Changing the adhesive modulus from 500 MPa to 5000 MPa resulted in an 8% increase in the axial strain at the gluelines. About 33% reduction in axial strain was reported when the liner stiffness was increased by 1.5 times as expected during adhesive impregnation. The corresponding FEA transverse strain varied insignificantly with the changes in the adhesive modulus or the liner stiffness. In addition, localised modulus resulted in an increased bond strength. This was explained to be due to a combination of adhesive penetration into the substrate and formation of covalent bonds. Furthermore, the FEA of the corrugated paperboard with parametric analysis of gluelines indicated that localised decreased strain may

be attributed to an increase in liner modulus rather than changes in adhesive modulus. Experiments were used to validate the simulation results, with good agreement reported.

It has been reported that the processes involved during paperboard manufacturing can cause severe deformation on the corrugated paperboard, particularly along the folds (Thakkar et al., 2008; Beex & Peerlings, 2009). Thakkar et al. (2008) modelled the creasing of corrugated paperboard using MSC MARC FEA code. The authors adopted an orthotropic finite-strain elasto-plasticity formulation in the model. Highest tensile stresses were found to occur beneath the creaser, which is an indication for crack initiation and propagation. In addition, the model was able to accurately predict the locations where creasing and damage were likely to occur on the corrugated paperboard. The outcome of the simulations was found to agree closely with the experimental results. The study by Urbanik and Saliklis (2007) generated a simplified formula for corrugated paperboard from using FEA to model corrugated paperboard. The corrugated paperboard was simply supported and under axial compression. ANSYS FEA code was used in calculating the critical buckling load on the board.

The structural performance of paper material is strongly dependent on environmental conditions (temperature, moisture content, humidity) and if not properly managed optimally, could affect the strength of the paperboard (Pathare & Opara, 2014; Vishtal & Retulainen, 2012; Haslach, 2000). Rahman et al. (2007) developed a finite element model able to predict the permeability of moisture through the layers (linerboards and flutings) of corrugated paperboard. In addition, the model predicted the response of the board to creep and hygroexpansion to determine the overall structural behaviour of the board. ANSYS commercial finite element code was used and the corrugated paperboard used was single-walled C-flute board. The model was validated accurately with experimental tests. Navaranjan and Johnson (2006) developed a finite element model to predict the non-linear creep behaviour of corrugated paperboard. The model had the capability to predict the creep performance of corrugated paperboard for a given set of properties of the constituents and the geometry of the board, when the board was uniaxially loaded under compression at a constant relative humidity. To predict the steady-state moisture transport through corrugated paperboard, Bronlund et al. (2013) developed a finite element model. The model showed reasonable agreement with experimentally measured moisture fluxes. A recent study by Fadiji et al. (2017) reported a significant difference in the edge compression resistance of a C-fluted corrugated paperboard at standard conditions (23 °C and 50% RH) and refrigerated condition (0 °C and 90% RH). The authors used NASTRAN for the FEA and model results were in good agreement, within 10%, when compared with the experimental results.

3.5.3 Corrugated paperboard packages

Several investigations and analyses have been made to facilitate and enhance the design of corrugated paperboard packages using finite element analysis (Fadiji et al., 2016c; Han & Park, 2007; Biancolini & Brutti, 2003; Park & Lee, 1999; Patel et al., 1997; Pommier & Poustis, 1989). The top to bottom compression resistance of corrugated paperboard package was predicted by Pommier and Poustis (1989) using linear elastic finite element analysis. The model considered shear bending and bending stiffness of the corrugated paperboard. The models results were in line with experimental results. The buckling of a flapless corrugated paperboard box was modelled by Pommier et al. (1991) using FEA from the stiffness of the corrugated paperboard obtained from anticlastic bending and four point tests. Symmetry was used in the simulation by modelling a quarter of the box and shell quadratic interpolation rectangular finite elements was used. The study applied four different boundary conditions for the simulation to obtain the vertical compression strength and the model results were compared with experimental and analytical results. Linear elastic-plastic laminate was used by Beldie et al. (2001) to simulate package resistance to compression. Low stiffness was observed at the top and bottom corners of the package and the stiffness was governed by the creases on the package. Biancolini and Brutti (2003) used FEA to evaluate the buckling of corrugated paperboard package by employing the homogenisation procedure for the corrugated board. Homogenisation involves transforming the corrugated board into an equivalent homogenous layered structure (Figure 3.6) (Fadiji et al., 2016c; Hägglund & Carlsson, 2012; Patel et al., 1997). The model was able to predict the incipient buckling load of the package and the reliability was compared with experimental results. Furthermore, the study suggested that closure fins of the package must be accounted for in order to model the overall instability of the package. The closure fins were observed to have a constraining effect that imposes a parabolic buckling of the package vertical walls. The box compression strength prediction was 7.4% lower than the experimental value for high quality Kraft corrugated paperboard. The study by Cannella and Dai (2006) used FEA to investigate the integrated effect of the stiffness characteristics of creases and panels on the carton during folding and manipulation in packaging. The authors reported that a carton panel is subject to a large displacement with linear deflection.

In the study by Sirkett et al. (2006), the authors developed a finite element model to study the machine-material interactions that occur during carton production within a packaging machine. The model was used to investigate the effect of variations in machine set-up, material properties and pack geometries on the normal carton erection process. The performance of the model in response to large displacements, multiple concurrent interactions, and large deformations compared well with observed carton behaviour. In addition, the pattern of deformation of the carton and the opening force characteristics closely matched experimental validations. The model developed was suitable in modelling the behaviour of folding cartons during normal erection. Sirkett et al. (2007) further developed and validated a finite element model of cartons during packaging operation. The model

was aimed at addressing the problem of carton buckling. Linear elastic material properties with non-linear crease behaviour were used in the model. The model was able to predict the pattern of deformation of the carton during buckling and its increasing magnitude with production rate. Furthermore, the model could be used to study the effects of variation in material properties, pack properties and machine settings. The model was validated with experimental results, with a maximum error of 55%. According to the authors, the large error was due to software limitations.

For fresh produce such as fruit and vegetables that respire, the packages used must have adequate ventilation to allow for uniform airflow within the package for the preservation of the packed produce (Berry et al., 2017; 2016; Fadiji et al., 2016c; Pathare et al., 2012b). Moreover, consideration must be given to the geometrical factors of the package such as vent shape, size, area and location to enhance the design and performance of the package. Han and Park (2007) used ANSYS FEA software code to study the principal designs of vent and hand holes on the face of corrugated paperboard packages. The stress levels and distribution on the cartons under compression were investigated with 15 vent hole variations. The holes on the package represented 2% of the total surface area on the facings, irrespective of the configuration. The package was assumed empty without flaps and 3D shell elements were used for the simulation. To optimise the design of packages, results from the model were used to determine the appropriate vent location and shape. In contrast to the study by Jinkarn et al. (2006) who reported circular vent holes to have the lowest reduction in compression strength, vertical oblong-shaped vent holes, symmetrically located on the front and back face of the package, within a certain distance to the left and right from the centre performed best in the stress analysis. The authors recommended the length of the vent holes to be less than 25% the depth of the package in order to achieve a minimum reduction in the package compression strength. Model results were validated with actual experimental results, with good agreement found between both techniques.

A homogenisation model to study the drop impact of corrugated paperboard packaging with different configurations of foam cushions was implemented in ABAQUS finite element software by Hammou et al. (2012). Drop tests were instrumented to obtain the curves of deceleration versus time. Corrugated paperboard package with the corner foam cushions had more damping effect to the shock response of the packed product. The models agreed well with experimental results. Yuan et al. (2013) also established a model to study the stress and strain distribution on corrugated paperboard boxes made with three types of waveform corrugated fluted medium; U-shaped, V-shaped and UV-shaped, able to resist the pressure of the top surface stacking. Boxes made with V-shaped and U-shaped corrugated fluted medium were reported to have good rigidity and good cushioning properties, respectively. Experimental results were found to be consistent with the model results, proving the validity of the model. A recent study by Luong et al. (2018) proposed a finite element model to study the behaviour of corrugated paperboard packages subjected to shocks. The model used an elastoplastic

homogenisation approach for the corrugated paperboard package to help reduce the computational time. The model was able to predict the mechanical behaviour of corrugated cardboard packages under impact dynamics, particularly in the early stage of design development. The authors reported that the critical acceleration level and critical velocity change levels could be used for package design decisions. Drop height of the packed product was reported to be strongly related to the velocity change that products would experience in transportation and handling. Hence, proper control of the drop height of the package will help in minimising damage. The numerical results obtained were in good agreement with the experimental results.

Weigel (2001) studied the dynamic interactions between corrugated paperboard containers and wood pallets during resonant vibration within the unit load system using FEA. Unit loads consisting palletised bulk bins of apples and peaches were tested. The model was found to accurately predict the resonant frequencies of the loads. The authors also analysed the effects of product mass, container design and pallet design on the natural frequencies. In addition, the model was able to improve the efficiency of the unit load system during transportation and distribution. To understand moisture effect on the performance of corrugated paperboard packaging, FEA was used by Lyngå and Sikö (2003) to develop a method for determining the moisture dynamics due to climate fluctuations in corrugated paperboard boxes. The model assumed a still air in the cells between the paper sheets and the board and the body inside the carton, that is, there is a continuous vapour density. Model was verified with respect to vapour density. The authors reported vapour density to be the same as the whole air body within the package. Table 3.3 is a summary of some of the applications of FEA for corrugated paperboard packaging.

3.5.4 Other application areas of FEA

The application of FEA has been successful in various food processing operations such as drying, heating, thawing, freezing, cooling, and mechanical damage (Celik, 2017; Stopa et al., 2017; Salarikia et al., 2017; Ahmadi et al., 2016; Hao et al., 2016; Singha & Muthukumarappan, 2016; Aprajeeta et al., 2015; Montanuci et al., 2014; Campanone & Zaritzky, 2005; Mascarenhas et al., 1997; Zhou et al., 1995; Puri & Anantheswaran, 1993; De Alwis & Fryer, 1990). Table 3.4 shows a summary of some of the food processing operations that have been studied using FEA.

The process of drying agricultural products is one of the methods of preservation (Irudayaraj et al., 1992). Excess moisture in agricultural produce can enhance the growth of moulds and infestations that may lead to damage of the stored product (Erbay & Icier, 2010). The behaviour of fresh produce during drying process is a function of the heat and mass characteristics of the products and it is therefore important to have adequate knowledge of the moisture and temperature distributions in the products as this is vital in the selection of appropriate packaging, design of equipment, storage and handling practices, and quality control (Ranjan et

al., 2004; Irudayaraj et al., 1992). FEA is a powerful technique to aid the process of drying agricultural products. The intra-kernel moisture distribution of moisture in the drying and tempering process of rice was studied by Yang et al. (2002) using FEA. The model examined the moisture content gradients (MCGs) inside the rice kernels. The model predicted maximum MCG to be in the direction of the kernel short axis. Moisture content in the centre of the kernel was observed to have a slower smaller change compared to the moisture content on the kernel surface during tempering process. FEA has also been successfully used to investigate the performance of ventilation systems for drying agricultural crops to provide uniform air distribution. This is necessary because uneven airflow can lead to irregular drying, wastage of energy and drying air inefficiency (Faoro et al., 2013; Khatchatourian et al., 2009; Franca & Haghighi, 1995).

Sterilisation is a crucial and vital process for food storage and preservation. To protect food from spoilage, preservation is pertinent (Xia & Sun, 2002). As reported by Xia and Sun (2002), thermal processing is the most important method of sterilisation, which leads to microbial damage; however, excessive heat may produce quality loss and significant change in nutritional attributes. Fellows (2009) defined food sterilisation as the heating of food products to a sufficiently high temperature for a long period to kill enzymes and microbial activity in order to increase the shelf life. Examples of sterilised food products are evaporated milk, fruit and vegetable juice, pureed vegetables, vegetable soups and heat pasteurized beer (Kannan & Sandaka, 2008; Kumar et al., 1990). FEA is a powerful tool to improve the understanding of the phenomena involved in thermal sterilisation for better design of food operations. The natural convection heating of a canned liquid food during sterilisation was simulated using FEA by Kumar and Bhattacharya (1991). Results showed that the coldest part of the can fluctuates at about 10–12% of the can height from its base, at a radial distance relatively half-way between the centre of the can and its inner wall. Tattiyakul et al. (2001) used FEA to investigate the starch dispersion in a rotating can under stationary and continuous axial agitation. Governing mass, momentum and energy transport equations were solved. Results showed that at 15 and 146 rpm when the can was stationary and agitated continuously, uneven temperature distribution occurred with different slowest heating points in the can. In addition, high viscous gelatinised starch is formed at the can walls at 146 rpm, which hindered heat transfer in the radial direction resulting in slower heat penetration than at 0 and 15 rpm. Generally, food quality and safety can be improved with sterilisation process, and with the aid of FEA, this process can be enhanced.

Agricultural products are susceptible to mechanical damage during harvesting, packaging, handling and transportation, which may result in substantial quality reduction (Li & Thomas, 2014). According to Bollen et al. (1999), the mechanical damage on produce particularly fruit manifests as bruising. The perception of most consumers is that the quality of fruit is a function of its appearance (Opara & Fadiji, 2018; Fadiji et al., 2016a, b, c; Opara & Pathare, 2014) and little obvious damage

can affect a customer's decision to purchase the produce (Harker, 2009). It is essential to have adequate knowledge of the mechanical characteristics of horticultural products in order to design and develop farm machinery and to also limit reliance on the experimental tests which in terms of cost and time are inefficient (Salarikia et al., 2017; Delele et al., 2010). FEA has proven useful in its application to study the performance and behaviour of agricultural produce exposed to various mechanical loadings (Kabas & Vladut, 2015). Some researchers have applied FEM to simulate the drop test of fruits like pear (Celik, 2017), apples (Celik et al., 2011), peaches (Kabas & Vladut, 2015) and tomatoes (Kabas et al., 2008). Kabas et al. (2008) used FEA to estimate the deformation of cherry tomato under drop load by simplifying the tomato into a spherical solid and assuming a single material. A more recent study by Salarikia et al. (2017) assessed the stress and strain distribution fields within pear fruit generated by fruit collision when subjected to impact loading, conducted at two drop heights and four impact surfaces. The largest and smallest stresses, strains and contact forces were observed during collision with the steel and rubber surfaces, respectively. Dintwa et al. (2011) developed a model to understand the deformation behaviour of tomato cells. The model assumed the cell to be a thin liquid sphere permeable wall and used a linear elastic material behaviour for the cell wall. The model was reported to be adequate in predicting the force–deformation behaviour of a single tomato cell in compression. Li et al. (2013) reported that the internal structural properties of tomato has an apparent effect on the mechanical damage behaviour of the tissues in the multiscale FEA of the exocarp, mesocarp and locular gel tissues of tomatoes.

3.6 Limitations and the future of FEA

FEA has been widely used and proven efficient in food processing and food packaging, particularly for paper packaging industry. Some factors such as the availability of powerful FEA software packages with incorporated pre- and post-processors; sophisticated and high speed computers; accurate algorithms for solving various phenomena, have enhanced the practicability and efficiency of FEA simulation in food packaging industries, particularly corrugated paperboard packaging. Although various good results and a number of successes have been reported, some limitations are still encountered in the use of FEA, particularly in the corrugated paperboard industry, which has been slower to adopt FEA than other sectors. This has been attributed to the complex structure and mechanical behaviour of paper and corrugated paperboard (Jiménez-Caballero et al., 2009). FEA designers still have to cope with several inaccuracies due to some assumptions and approximations that are made. Although the advent of very powerful FEA software allows modelling the detailed corrugated structure with shell or solid elements, the computational time and effort required, such as in the case of the corrugated paperboard package/carton, makes it not practicable (Ye et al., 2014). More recently, the homogenisation process for corrugated paperboard to obtain an equivalent orthotropic plate has been adopted and it is replacing the complex structure of the corrugated board (Cheon & Kim, 2015). It is thus important to mention that the simulation limitations of corrugated paperboard packages are not

only related to the computational effort but also to complexity of the geometrical modelling.

The complex nonlinearity of paper material also makes simulating the mechanical response of corrugated paperboard packaging a tedious and difficult task. In addition, paper exhibits additional characteristics such as humidity dependence of the mechanical properties, creep and hygroexpansion, that increases the level of complexity in modelling. More research is required to incorporate the nonlinearity (geometrical or material, etc.) of corrugated paperboard structures. Furthermore, the dependency of paper material on time and temperature makes the material characterisation to obtain the input parameters for the FEA even more difficult.

It is claimed by many FEA software vendors that it is not necessary to require an understanding of the theory involved in different processes. However, some knowledge of the basics cannot be ignored nor discarded and is indispensable. Familiarisation with the physics involved in the modelling will be necessary to set-up a proper model closely related and able to represent the physical model. According to Xia and Sun (2002), the biggest problem in a numerical simulation may not be the mesh generation, sophisticated computers, or the FEA solvers but an adequate knowledge of the physical phenomena involved.

As discussed in section 3.3, there are many steps involved in FEA such as, selection of numerous parameters that control and enhance the analysis process. Most of these processes such as mesh generation and refinement, and suitable elements to capture various failure mechanisms have been automated and improved and require less attention of the users. Nowadays, FEA is much more streamlined than the software of former generations and is readily available to professionals, engineers, smaller enterprises and educational institutions at affordable prices. However, much is still to be done to improve the potential of FEA for the realisation of better engineering designs. The solution algorithms and user interfaces need to be continually improved and enhanced to lighten the hurdles involved in the computational details on FEA users (engineers, designers and researchers) who use FEA in various areas. In addition, new interfaces will aid experts of FEA in building application specific tools, together with an application expert, which allows the engineer to focus on design tasks.

The installation and large scale maintenance of FEA software over continuously evolving operating system (OS), processor and cluster technologies can be costly and complex for the FEA end-users (Ari & Muhtaroglu, 2013). Hence, the availability of less expensive cloud-based computing FEA resources, in combination with protected means of data transport will fast track intensified computational studies in design projects (Hashem et al., 2015; Ari & Muhtaroglu, 2013). To date, the story of FEA, with emphasis on food packaging and processing applications has been a success. The continual improvement of the next-generation software will be a significant step to enhance the engineering effort, develop more

accurate analyses, and support product development from conceptualisation to realisation.

3.7 Conclusions

This current study is a review of the application of FEA in food packaging industries, with a focus on corrugated paperboard packaging. There has been a considerable growth and usefulness of FEA to enhance the design of better packages. In addition, FEA has been useful in different food processing operations such as drying, freezing, sterilisation and mechanical damage. Although FEA has remained a powerful tool, high level of accuracy must be ensured during the simulation process and proper representation of the physical model must be attained in order to increase confidence in the FEA results and predictions. Together with the FEA model, experiments need to run concurrently to validate the simulation predictions, particularly where assumptions have been made to simplify the computational effort of the model. It is undoubtable that with the unrelenting progress in computing power and development of very powerful, user-friendly FEA software, more explanations will be provided on the mechanical behaviour of food packaging, leading to the design of better packages. By combining FEA with other numerical approaches such as computational fluid dynamics (CFD) and discrete element method (DEM), an opportunity is provided to simultaneously optimise the integrated performance of corrugated paperboard packaging in maintaining an efficient cold chain and protecting the package and packed produce against damage.

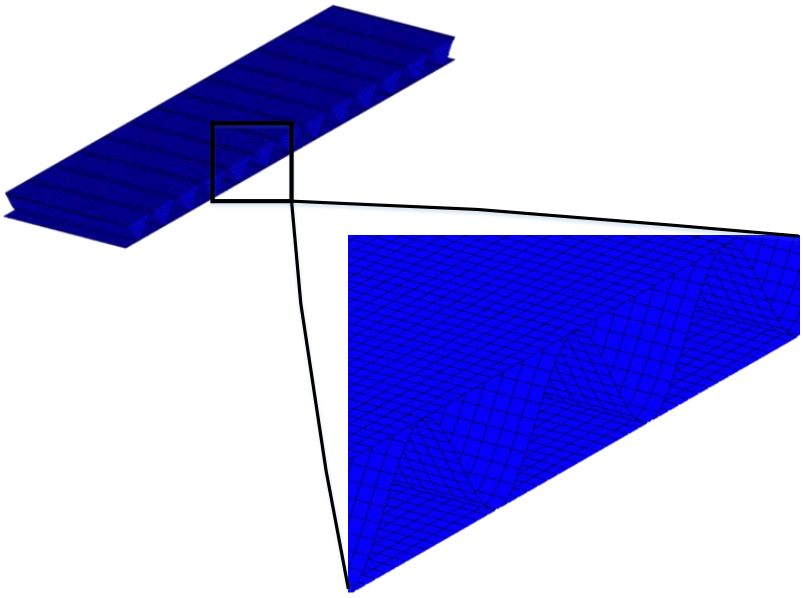

Figure 3.1: Mesh structure of a corrugated paperboard. A portion of the corrugated paperboard has been exploded to clearly illustrate the mesh structure.

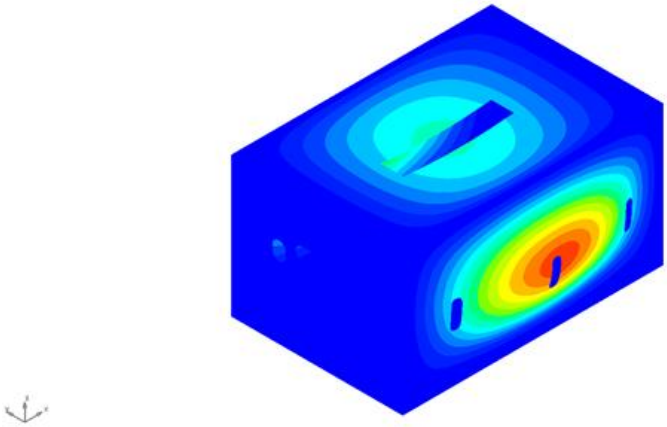

Figure 3.2: An example of a typical model for a ventilated corrugated paperboard package under buckling (Fadiji et al., 2016c). From the plot, buckling occurred on the long side of the package and it originated from the middle.

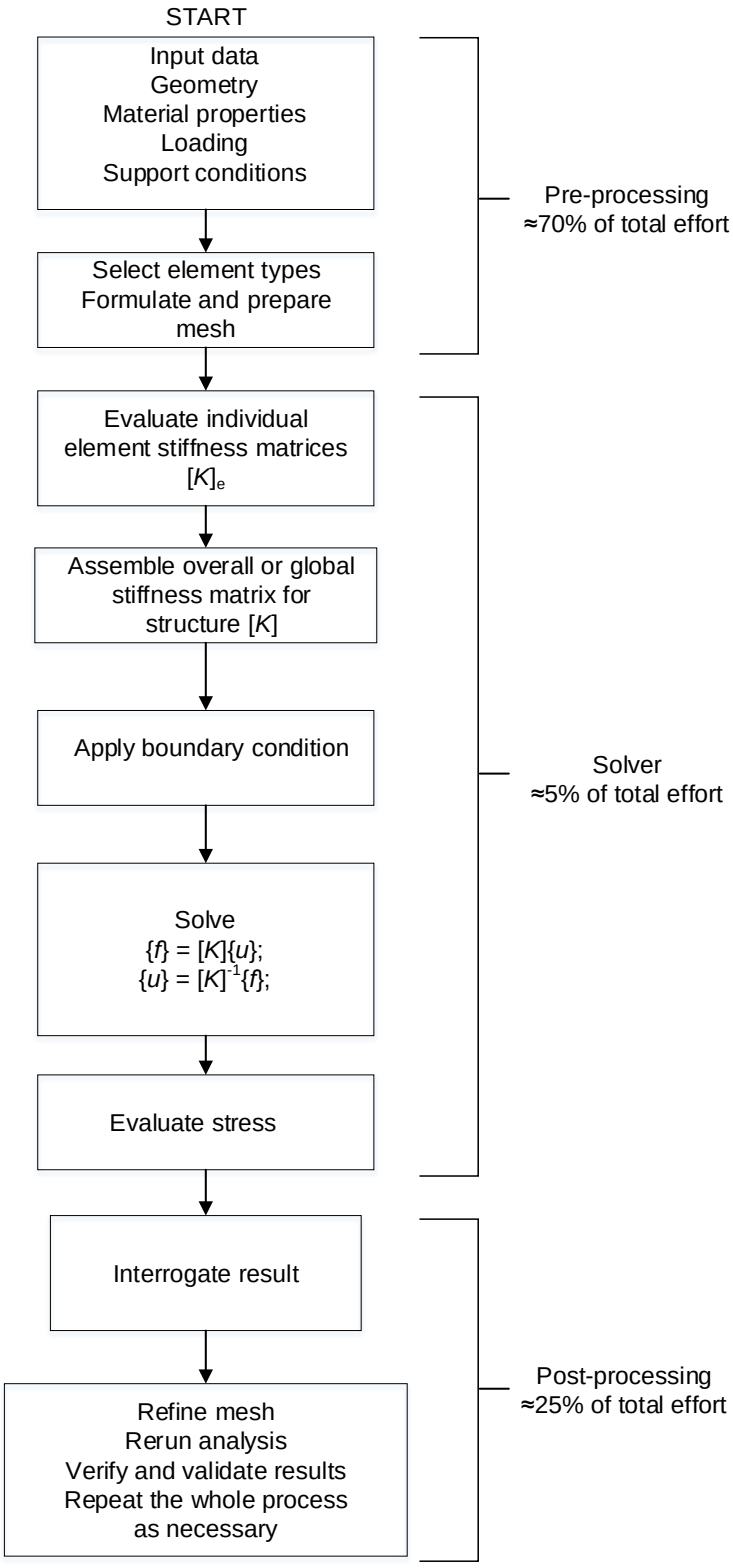

Figure 3.3: Overview of finite element analysis process – structural simulation.

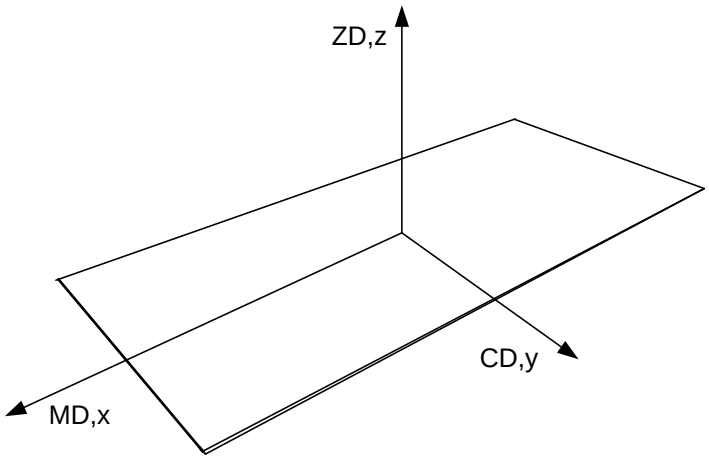

Figure 3.4: Principal material directions of paperboard: the in-plane directions are the machine direction (MD) and the cross direction (CD), while the thickness direction (ZD) is the out-of-plane direction (Fadiji et al., 2018a).

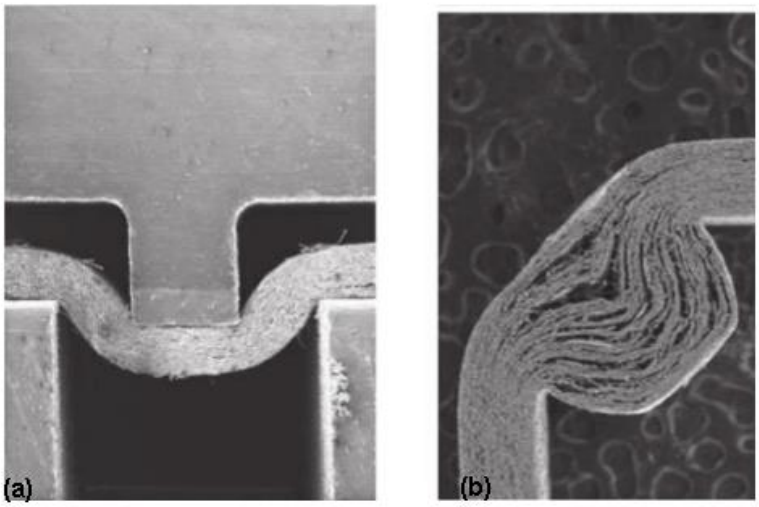

Figure 3.5: a) Typical creasing process of paperboard (Domaneschi et al., 2017; Dunn, 2000), b) Typical folding process of paperboard (Domaneschi et al., 2017; Nagasawa et al., 2003).

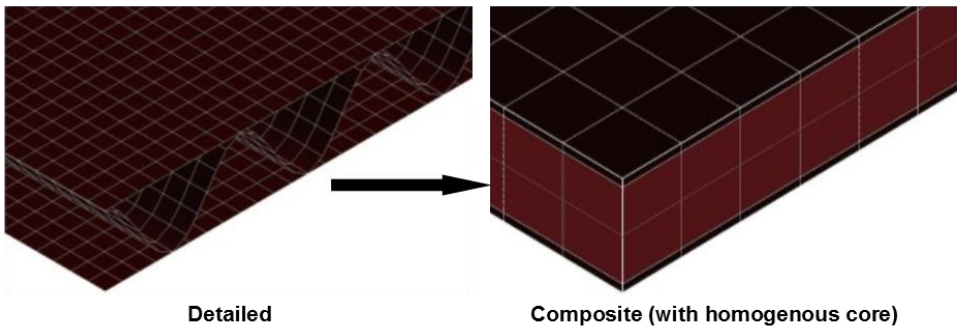

Figure 3.6: Modelling approach for the finite element simulation of the corrugated paperboard package (Fadiji et al., 2016c).

Table 3.1: Some examples of the application of finite element analysis (FEA) to study creasing and folding of paperboard.

Study purpose	Research outputs	References
Numerical investigation of folding of coated paper performed using FEA	Deformation of the coated paperboard is a function of the paper substrate and the strain levels was not influenced by the strain hardening behaviour of the coating at maximum loading	Barbier et al. (2005)
FEA of creasing and folding of paperboard	Simulations are in good agreement when compared to macroscopic experiments of creasing and folding	Nygårds et al. (2005)
Predict and understand the behaviour of a three-layer laminated paperboard during creasing and folding	Model agrees with experimental results and was validated by force–crease depth curves and strain fields during creasing and moment–angle curves and microscopic images during folding	Beex and Peerlings (2009)
Simulations of creasing of paperboard with a two dimensional finite element model	The force displacement curves from the simulations and experiments were compared, with good agreement	Huang and Nygårds (2010)
Model to study the mechanical response of crease lines	Model was validated based on the experimental tests available in the literature, with good agreement	Giampieri et al. (2011)
FEA of folding behaviour and response of paperboard	Deformation mechanisms that are active during folding are evidently important for forming packages. Bending moment measured from the folding operation was in agreement with the simulated response	Borgqvist et al. (2016)

Table 3.2: Examples of FEA application on corrugated paperboard.

Study purpose	Key findings	References
Study the stress generated in corrugated paperboard under three-point loading using FEA	Results show that the fluting under compression is the critical component of the stress field	Peterson (1983)
FEA model to study the four-point bending and twisting test for corrugated paperboard	Results were in good agreement with experimental studies. However, the board stiffness was overestimated	Gilchrist et al. (1998)
Develop FEA model for the three-point bending to assess the relevance of homogenised elastic behaviour of the corrugated cardboard	To effectively analyse corrugated paperboard and panels, simplified homogenisation method was accurate and faster than the 3D approach	Aboura et al. (2004)
FEA model to analyse corrugated paperboard materials and structural system	Good ECT response was observed for a wide range of corrugated paperboards geometries with the FEA models	Haj-Ali et al. (2009)
Develop FEA model for corrugated paperboard reliable for stress and displacement measurement	Flute shape and size have a major influence on the performance of corrugated paperboard	Zhang et al. (2014)
Predict the twist stiffness of single and double walled corrugated board	Numerical model results were found to be in good agreement with experimental results	Hernández-Pérez et al. (2014)
FEA model to investigate the edge effect and the influence on edgewise compressive strength of corrugated paperboard	Edge effect significantly affected the edgewise compression strength of corrugated paperboard. Agreement with experimental values	Hua et al. (2017)
Simulate the edge compressive resistance of corrugated paperboard at different environmental conditions using FEA	Numerical results were validated with experimental values, with good agreement. Edge compressive resistance was significantly affected by temperature and relative humidity	Fadiji et al. (2017)

Table 3.3: Examples of FEA application on corrugated paperboard packages

Study purpose	Key findings	References
Predict the top to bottom compression strength of corrugated paperboard package	Model was validated with McKee's formula using bending stiffness from four-point bending test and shear bending stiffness from anticlastic test	Pommier and Poustis (1989)
Analyse the mechanical behaviour of paperboard packages subjected to static compressive loads	Middle segment of the package had higher stiffness than the upper and lower segment and of the whole package. Failure occurred near corners with the maximum stress moving from the panel centre to the corners as panel deflected	Beldie et al. (2001)
Predict the failure loads of corrugated paperboard boxes in compression	The failure load predicted for boxes with B-flute and C-flute corrugated paperboard were 3% higher and 5% lower than the experimental results, respectively	Nordstrand et al. (2003)
Investigate the strength of corrugated paperboard packages	Model accurately predicted the experimental results of incipient buckling observed during the standard box compression test	Biancolini and Brutti (2003)
Analyse the buckling and post-buckling behaviour of corrugated paperboard box with FEA	Critical loads and load-displacement curves were obtained for panels and boxes with various geometry and materials to show their effect on compression stiffness	Biancolini et al. (2005)
FEA model to investigate the principal design parameters of vent holes and hand holes on the face of corrugated paperboard boxes	Vertically oriented oblong-shaped vent holes performed best. FEA simulation agreed well with experimental results	Han and Park (2007)
Develop a homogenisation finite element model to simulate the drop test of corrugated paperboard box containing different foam cushion configurations	Corrugated paperboard box with the corner foam cushions gave a more damping effect to the shock response of the product. FEA results agreed well with the experimental results	Hammou et al. (2012)
FEA model capable of predicting the compressive strength ventilated corrugated paperboard packages	Vent number, orientation, and shape affected the buckling of the packages. FEA model was in good agreement with experimental results	Fadiji et al. (2016c)
FEA model to study the behaviour of corrugated paperboard boxes subjected to shocks	The numerical results obtained are in good agreement with the experimental results	Luong et al. (2018)

Table 3.4: Summary of the use of FEA in food processing operations.

Process	Application	Product	References
Heating and cooling	Microwave heating	Solid food	Lin et al. (1995); Wang and Brennan (1995); Zhou et al. (1995); Oliveira and Franca (2000); Romano et al. (2005)
		Potatoes	Pandit and Prasad (2003)
		Cereal grains	Haghighi et al.(1990); Irudayaraj et al. (1992)
	Drying	Potatoes	Vagenas and Marinos-Kouris (1991); Chen et al. (1993a); Wang and Chen, (1999)
		Carrots	Vagenas and Marinos-Kouris (1991); Curcio et al. (2008)
		Rice	Yang et al. (2002)
		Mango	Janjai et al. (2008)
		Apricot	Vagenas and Marinos-Kouris (1991)
	Cooling	potatoes and tomatoes	Hayakawa and Succar (1982)
		Meat	Wang and Sun (2002)
		Pear	Nguyen et al. (2006)
		Frozen foods	Chuntranuluck et al. (1998)
Mechanical Damage	Internal mechanical damage	Apples	Li et al., 2013
	Dynamic collision		Dintwa et al. (2008)
	Bruising		Wu and Pitts (1999)
	Shock response and deformation behaviour	Pear	Yousefi et al. (2016); Salarikia et al. (2017); Celik (2017)
		Apple	Celik et al. (2011)
		Peach	Kabas and Vladut (2015)
		Tomato	Kabas et al. (2008);
	Bruising	Watermelon	Sadrnia et al. (2008)
	Dynamic behaviour	Pineapple	Chen and Baerdemaeker (1993b)
Freezing and thawing	Thawing	Food products	Zeng and Faghri 1994)
	Thawing	Frozen minced meat	Taher and Farid (2001)
	Sterilisation	Liquid food products	Kumar et al. (1990)

Chapter 4. Application of finite element analysis to predict the mechanical strength of ventilated corrugated paperboard packaging for handling fresh produce *

Abstract

The presence of vent holes in corrugated paperboard package causes material loss of the package, which compromises its strength and stability. To improve the structural design of fresh produce packages, it is important to understand the response of packages when subjected to various types and combinations of mechanical loads. This study aimed to develop a validated finite element analysis (FEA) model to study the structural behaviour of commonly used ventilated corrugated paperboard (VCP) package when subjected to compression load by considering the geometrical nonlinearities of the packages. Two package types were used: a control package without vent holes and standard vented packages. The FEA model accurately predicted the compression strength of the corrugated paperboard, control package and standard vent package. When compared with experimental results, the model predictions for the VCP package were within 10%. Compression strength of the standard vent packages were found to be linearly affected by paperboard liner thickness. Increasing and decreasing the baseline liner thickness of the standard vent package by 80% resulted in an increase and decrease in compression strength by about 15% and 19%, respectively. From the contact FEA model, maximum Von Mises stress was produced at the corners of the package. Von Mises stress was reduced by about 25% on changing the friction coefficient from 0 to 0.1. This study provides empirical evidence for package designers on how to improve the mechanical integrity of packages while at the same time aiming to maintain an optimum ventilation.

*Keywords***:** ventilated paperboard packaging; finite element analysis; package; produce; box compression test.

---

*Publication:

Fadiji, T., Ambaw, A., Coetzee, C. J., Berry, T. M., & Opara, U. L. (2018). Application of finite element analysis to predict the mechanical strength of ventilated corrugated paperboard packaging for handling fresh produce. *Biosystems Engineering*, *174*, 260–281.

4.1 Introduction

The packaging of horticultural produce such as fresh fruit remains vital and crucial particularly for products with long and complex journeys from growers to consumers and over the years, the development of horticultural packages has itself become a rapidly growing industry (Opara & Fadiji, 2018; Berry et al., 2017; Fadiji et al., 2016a, b, c; Giampieri et al., 2011; Biancolini & Brutti, 2003). Packaging provides an economic means of minimising damage and protecting packed produce during distribution. Adapting packaging as an integral part of both internal and external part of the distribution system, makes the reduction of distribution costs possible (Fadiji et al., 2016c; Robertson, 2012; Jarimopas et al., 2007). A good packaging system should be able to protect the products, be manufactured with minimal materials and tested to prove its optimum performance. Efficient, economical, and reliable packaging is a necessity during storage, transportation and distribution as it is an essential link between the producer and the end users (consumers) (Opara & Fadiji, 2018; Paine, 2012). Unless sound delivery of the product is achieved, the quality and the reliability of a product during production and manufacture will be wasted. Satisfaction of the consumer with quality product is thus the main objective of the handling, production, storage and distribution of fresh horticultural produce (Fadiji et al., 2016a, b, c; Opara & Pathare, 2014; Pathare & Opara, 2014). Increasing consciousness of the intricacies of packaging, together with the competition in this rapidly growing industry are some of the driving forces towards achieving lighter, more economic, and reliable packaging and this requires substantial investments in the development of new technical solutions (Fadiji et al., 2018a, b; Robertson, 2012; Giampieri et al., 2011; Robertson, 1993). Furthermore, the reliability of packaging is extremely crucial in the food industry (Mahalik & Nambiar, 2010; Kibirkštis et al., 2007).

In the packaging industry, particularly horticulture, paperboard is one of the most widely used materials since it can be easily converted from a flat configuration into a solid box shape (Csavajda et al., 2017; Fadiji et al., 2016c; Giampieri et al., 2011; Gilchrist et al., 1998). The most important structural application of paperboard is through corrugated paperboard packages (Fadiji et al., 2018a; Csavajda et al., 2017; Zhang et al., 2014; Talbi et al., 2009; Biancolini et al., 2009; Han & Park, 2007). Corrugated paperboard packages are usually light but very stiff with the ability to sustain significant loads (Giampieri et al., 2011). Corrugated paperboard is an orthotropic sandwich structure defined by the two surface pliers known as liners, separated by a lightweight corrugated core known as fluting (Figure 4.1) (Navaranjan & Johnson, 2006; Nordstrand, 1995). The liners provide bending stiffness to the board while the fluting provides shear stiffness (Dongmei, 2009). The liners are usually joined with the fluting using a starch-based adhesive to form a single wall corrugated board (Figure 4.1). The linerboards are usually made from test liners (recycled paper) or Kraft paperboard (of various grades) which may be bleached white, mottled white, coloured, or pre-printed (Zhang et al., 2014). The corrugated paperboard is characterised by two main principal (in-plane) directions. The first direction is the machine direction (MD) which is the machining direction,

coincides with the paperboard fibre alignment and is perpendicular to the principal axes of the corrugations. The second direction is the cross direction (CD) corresponding to the transverse direction and parallel to the corrugation axes. A third (out-of-plane) direction, is used to define the directional properties of corrugated paperboard, is the thickness direction (ZD) corresponding to the direction along the thickness (Figure 4.1) (Fadiji et al. 2016c; Talbi et al., 2009; Biancolini, 2005; Urbanik, 1996).

Due to its numerous advantages such as efficient material characteristics, high strength to low weight ratio and economical properties, corrugated paperboard is used commonly for the manufacture of shipping containers (Fadiji et al., 2016c; Talbi et al., 2009; Singh et al., 2008; Han & Park, 2007). Efficient and effective distribution of a broad variety of products ranging from fresh fruit and vegetables, industrial products and consumables has been possible due to the advent of ventilated corrugated paperboard packages (VCP). Over the years, VCP has become the most widely used packaging, particularly for horticultural produce (Pathare et al., 2017; Berry et al., 2017; Fadiji et al., 2016c; Pathare et al., 2012b; Hung et al., 2010). VCP packages has gained popularity in fresh fruit industries due to its ability to allow for rapid, uniform and efficient cooling and air distribution of the packed produce with minimum amount of material used for the internal packaging (Fadiji et al., 2016c; Thompson et al., 2010; De Castro et al., 2005). Although the presence of vent holes can produce loss of package strength (Fadiji et al., 2016c), the design of vent holes should be such that the package can maintain a balance between cooling of the produce and the structural integrity of the package (Pathare et al., 2012b; Vigneault & De Castro, 2005; Vigneault & Goyette, 2002).

VCP packages are subjected to a multitude of dynamic and static loadings such as impact, vibration and compression that could result in damage and reduce its value (Opara & Fadiji, 2018; Fadiji et al., 2016a, b; Singh et al., 2008). Numerous factors affect the structural performance of VCP packages; including the mechanical properties of the board combination (liners and fluting), the structural stability of the corrugated board and the quality of the input cellulose fibres (Zhang et al., 2014; Gilchrist et al., 1998). The uncertainties in the process of design and structural performance of corrugated paperboard was highlighted by Biancolini et al. (2005) to be due to variation in the mechanical properties of paperboard and paper combination. For corrugated paperboard packages to withstand compression load due to stacking, the structural analysis of the paperboard components and in depth knowledge of the paperboard stiffness properties are very critical (Talbi et al., 2009; Biancolini & Brutti, 2003). Stacking the packages on top of each other causes compression force to be applied on the bottom package, causing these packages to experience the greatest load (Fadiji et al., 2016c). Sufficient and adequate compression strength of the bottom package is important to avoid collapse of the stacked packages (Daxner et al., 2007). The result of the applied force is a vertical edgewise compression along the CD (Figure 4.1) and the side panels are

bent along both the MD and CD which results in buckling (Park et al., 2011). It is therefore paramount to consider buckling when determining the load bearing capabilities of the package (Ma et al., 2014; Park et al., 2011).

Regardless of the complex paper structure, the emergence of simulation models such as finite element analysis (FEA) has the advantage of saving experimental cost, time, sample production as well as detailed analysis by adjusting various parameters (Delele et al., 2010). In addition, FEA has proven to provide adequate confidence to use it as a design tool (Fadiji et al., 2016c; Pathare & Opara, 2014; Ambaw et al., 2013; Delele et al., 2010; Jiménez-Caballero et al., 2009). However, it is crucial to estimate the reliability and the reproducibility of the numerical simulation results (Fadiji et al., 2018b, 2017; Ambaw et al., 2013; Delele et al., 2010). Several previous researches have involved the use of FEA in modelling the properties of corrugated paperboard components and structures such as crush strength, compression strength, creep, recoverability, flexural stiffness, buckling, collapse, elasticity, bending and ultimate failure among others (Fadiji et al., 2016c; Ma et al., 2014; Zhang et al., 2014; Bartolozzi et al., 2013; Kueh, 2012; Huang & Nygårds, 2011; Haj-Ali et al., 2009; Jiménez-Caballero et al., 2009; Thakkar et al., 2008; Han & Park, 2007; Sirkett et al., 2007; Cannella & Dai, 2006; Biancolini et al., 2005; Aboura et al., 2004; Biancolini & Brutti, 2003; Mäkelä & Östlund, 2003; Beldie et al., 2001; Gilchrist et al., 1998). However, the nonlinearity of paper makes the mechanical response modelling of corrugated paperboard and structures a difficult and complex task (Park et al., 2011).

Pommier et al. (1991) used finite element code to evaluate the buckling of a flapless corrugated paperboard box from the stiffness of the board from which it was produced. The stiffness properties of the board were obtained experimentally by four-point bending and anticlastic bending tests. The authors used symmetry by modelling a quarter of the box using shell quadratic elements. FEA results were compared to the experimental and analytical vertical compression strength and the results correlated well. In the study by Biancolini and Brutti (2003), by means of experimental and numerical analysis, the authors evaluated the mechanical behaviour of paperboard packages. The developed FEA model was able to predict accurately the incipient buckling observed during the stacking strength test of the paper box, despite the minimal computational effort. Biancolini et al. (2005) developed a numerical model for evaluating the crushing behaviour of paperboard packages. The authors found the numerical results to be in good agreement with the homogenised corrugated board model used.

In the fresh fruit industry, a wide range of ventilated paperboard packages exist for handling various produce (Berry et al., 2015). Different factors such as the cooling energy use, cooling performance, efficiency and mechanical integrity of ventilated package designs used in handling various fresh produce have been studied and established to be crucial in delivery of good quality produce to the end-users (Getahun et al., 2017a, b; Berry et al., 2017; Fadiji et al., 2017, 2016a, b, c; Defraeye

et al., 2014, 2013; Delele et al., 2013a, b; Han et al., 2015; Zou et al., 2006a, b). In a previous study by Fadiji et al. (2016c), the authors evaluated the compression strength of ventilated paperboard packages experimentally and numerically. Linear elastic FEA model was developed to study the buckling of VCP packages, which assumed an ideal situation and found good correlation between the experimental and FEA models. However, in real world situations, nonlinearities and imperfections exist during handling the VCP packages. This present study aimed to develop a validated FEA model to study the structural behaviour of VCP packages by considering the geometrical nonlinearities of the packages.

4.2 Basic principles of buckling

4.2.1 Linear buckling

The structural instability of a material on load application is referred to as buckling. The buckling strength of a linear elastic structure is predicted by an eigenvalue buckling analysis. In eigenvalue or linear buckling analysis, the material is idealised as being elastic. The linear buckling analysis generally overestimates the strength of a structure that leads to a non-conservative result due to imperfections and nonlinearities of most real world structures. Therefore, linear buckling analysis is not feasible in most engineering activities. However, the linear buckling analysis provides information about the deformation shapes of the structure and it helps to contribute to determining the preload in nonlinear analysis. Eq. (4.1) is applied in linear buckling analysis.

$$\left(\left[K\right]-\lambda_i\left[P\right]\right)\left\{\phi_i\right\}=0 \tag{4.1}$$

where $\left[K\right]$ is the structural stiffness matrix, $\left[P\right]$ is the preset load matrix and ϕ_i is the buckling mode of the structure. The equation is solved to obtain the minimum eigenvalue, $\lambda_{\min}$ and therefore the critical load, P_{cr} can be written as:

$$\left\{P_{cr}\right\}=\lambda_{\min}\left\{P\right\} \tag{4.2}$$

4.2.2 Nonlinear buckling

Nonlinear buckling analysis provides more accuracy compared to linear buckling analysis and is therefore crucial in evaluating practical structures. In this approach, the load is applied incrementally until a small change in the load level causes a large change in deflection. When this occurs, the structure has become unstable. Nonlinear buckling analysis accounts for both material and geometric nonlinearities as depicted in Figure 4.2. Material nonlinearity is associated with nonlinear mechanical properties (elastic-plastic behaviour) while geometric nonlinearity is associated with a change in the shape (geometry) of the structure.

To understand the concept of nonlinearity mathematically, nonlinear buckling analysis can be reduced to solving Eq. (4.3).

$$[K]\{D\} = [P] \tag{4.3}$$

where $\{D\}$ is the total deformation, $[K]$ is the structural stiffness/rigidity matrix and $[P]$ is the preset load matrix. In order to solve Eq. (4.3), the critical load is divided to an incremental load step as shown in Eq. (4.4).

$$\{P_{cr}\} = \sum_{i}^{n} \{\Delta P_i\} \tag{4.4}$$

The load is applied in an incremental manner while the geometry of the structure and any nonlinear material properties are updated, and a critical load is obtained when the slope of the load–displacement curves reaches zero, with further increment in load leading to a negative slope.

4.3 Materials and methods

4.3.1 Paper materials

Five grades of paper samples were obtained from the manufacturers and used in this study. The paper samples were used in combination to form the corrugated paperboard. The paper samples were obtained from the same source and preparation process. The paper samples grammages (g m^{-2}) were; 125FL, 165SC, 175SC, 175T1 and 140T2. FL indicates fluting liner, SC indicates semi-chemical paperboard, T1 indicates fully recycled board and T2 indicates partly recycled linerboard. The inconsistency in the thickness of paper materials may be due to the fibrous structure of paper and the minor irregularities from the manufacturing process (Fadiji et al., 2017). ISO 534 standard procedures for measuring the thickness of paper and corrugated paperboard as a single sheet were used to measure the thickness of the paper materials (ISO, 2011). According to the ASTM 4332 standard, the samples were preconditioned at 30 ± 1 °C and relative humidity (RH) of 20–30% for 24 h and then conditioned at a temperature of 23 ± 1 °C and 50% RH for 24 h (ASTM, 2006). For each paper sample type, ten replicates of the thickness were measured, with the mean values and standard deviation given in Table 4.1.

4.3.2 Numerical simulation

4.3.2.1 Characterisation of the paper material

In order to determine the elastic modulus of the paperboard that is used as input parameter for the numerical simulation, the tensile properties were measured in a

tensile tester (Lorentzen & Wettre, model Code 64) where the paper sample is placed lengthwise horizontally. Most often, the fibre orientation of paper is symmetric which indicates the assumption for its orthotropic nature, that is, the elastic properties can be determined in three symmetric planes (Fadiji et al., 2017; Allaoui et al., 2009b). The constant rate of elongation was 100 ± 10 mm min-^{1} and the measurements were carried out according to ISO 1924 standard (ISO, 2008). The dimensions of the paper samples used were, width 15 mm and length 180 mm, whereof the span length in the testing machine was 100 mm. The elastic properties were determined in the in-plane directions, that is, the MD as well as in the CD, while Eq. (4.5) was used to determine the elastic properties in the out-of-plane direction or the ZD (Sirkett et al., 2007; Beldie et al., 2001; Persson, 1991; Mann et al., 1979):

$$E_{ZD} = \frac{E_{MD}}{200} \tag{4.5}$$

where E_{MD} is the elasticity modulus in the MD and E_{ZD} is the elasticity modulus in the ZD.

The shear moduli, G_{xy}, G_{xz}, G_{yz}, were determined from the elasticity moduli using Eq. (4.6) according to Sirkett et al. (2007) and Allansson and Svärd (2001).

$$\begin{aligned} G_{xy} &= 0.387\sqrt{E_{MD}E_{CD}} \\ G_{xz} &= \frac{E_{MD}}{55} \\ G_{yz} &= \frac{E_{CD}}{35} \end{aligned} \tag{4.6}$$

where E_{CD} is the elasticity modulus in the CD.

The Poisson's ratio ν_{xy} was approximated and the values given by Biancolini and Brutti (2003) for similar materials (0.33 for the flute paper and 0.34 for the liners) were used in this study. ν_{xz} and ν_{yz} were set as 0.01 according to Nordstrand (1995).

4.3.2.2 Paperboard simulation test

The model geometry was developed using ANSYS® Design Modeller™ Release 18.1 (ANSYS, Canonsburg, PA, USA) and the mesh was created using MSC Patran (MSC Software Corporation, CA, USA). Mentat/Marc (MSC Software Corporation, CA, USA), a nonlinear commercial FEA code was used for the analysis. A detailed geometry (liners and flutings) of the corrugated paper was studied. Some basic assumptions were made to enable accurate modelling of the

geometry. The geometry model of a single wall corrugated paperboard for B and C flutes with paperboard combination 140T2/175SC/165SC and 175T1/175SC/125FL, respectively were created by cementing the three layers together. The adhesive between the liner and the fluting was modelled by connecting the extreme positions of the fluting directly to the liners by sharing the same nodes. To idealise the flute wave between the fluting and the liners, a sine function was assumed. Figure 4.3 shows the general geometry of the corrugated paperboard used in the FEA. The pitch and height of the corrugated paperboards used in this study were; 7.60 mm and 4.20 mm, respectively for paperboard with C flute medium and 6.25 mm and 2.60 mm, respectively for paperboard with B flute medium.

The material was considered as orthotropic and approximated as linear elastic. The equivalent material properties of the liners and flute used as input parameters in the finite element model were obtained from tensile tests. Shell elements were used for the edge compression test (ECT) model and were oriented properly to capture the actual pattern of the paperboard of liners and the fluting. The shape of the corrugated paperboard for the ECT model was according to FEFCO No. 8 standard (100 mm x 25 mm). To obtain an accurate and effective scheme for the ECT model, attention must be given to the boundary conditions. A unit load was uniformly applied to the corrugated paperboard at the top, a fixed constraint in all directions (x, y and z) was applied at the bottom and at the outside nodes close to the top of the corrugated paperboard (Figure 4.4). Buckling analysis was performed to obtain the critical buckling load and estimate the buckling shape. The Lanczos buckle extraction technique available in Marc was used in the analysis. The material properties used as input parameters in the simulation for B and C corrugated paperboard are shown in Table 4.2 and Table 4.3, respectively.

4.3.2.3 Package simulation

The geometry was developed using ANSYS® Design Modeller™ Release 18.1 (ANSYS, Canonsburg, PA, USA) and the mesh was created using MSC Patran (MSC Software Corporation, CA, USA). Mentat/Marc (MSC Software Corporation, California, USA), a general-purpose finite element solver was used for the analysis. The choice of Mentat/Marc FEA software was due to its successful history and capabilities in nonlinear analysis. Liner elastic 3D orthotropic properties were used to model the corrugated paperboard package. Accurate simulation of the corrugated paperboard requires representing the numerical model as close as possible to the physical model. To construct an analytical model for the sandwich corrugated paperboard structure with orthotropic properties, the core should be homogenised. This was achieved with the laminate theory resulting in solid plates with equivalent properties.

For this study, the procedure suggested by Biancolini et al (2010) was used in approximating the sandwich structure as a homogenous material and to calculate the equivalent properties of the solid core. This procedure, in the event that the

function describing the sandwich structure is known, allows for calculation of the stiffness matrix. As described by Biancolini et al. (2010), a sine wave was used to represent the fluting of the corrugated paperboard (Figure 4.3). The ABD matrix of the laminate was calculated using the equivalent plate bending stiffness formula for the corrugated core as shown in Table 4.4 (Biancolini et al., 2005). The ABD matrix defines the elastic properties of the entire laminate and creates a connection between the applied loads and the associated strains in the laminate, hence allows for determining the force and moment resultants given a set of imposed strains and curvature. Matrix A represents the extensional in-plane stiffness matrix while matrix B and D represent the bending extension-coupling matrix and the bending stiffness matrix, respectively. The corrugated paperboard was approximated by ignoring the bending extension-coupling matrix assuming a symmetric laminate. Hence, the matrix B is zero. In the model for this study, the package was considered as a composite structure, which consists of three layers: the two liners and a middle solid core (Figure 4.5).

Material properties used as input parameters in the finite element simulation are shown in Table 4.2 and Table 4.3. In order to capture bending and the actual pattern of the paperboard of liners and the core properly, boxes were oriented properly and quadrilateral shell elements were used for the simulation. A mesh sensitivity analysis was performed on the standard vent package to identify the number of elements required in the finite element model in order to give satisfactory predictions. The results of the convergence study as shown in Figure 4.6 indicated a convergence in the buckling load for mesh size 4 mm and smaller, hence this mesh size was adopted for the FEA in this study. The model consisted of 39692 elements and 39990 nodes for the standard vent package while for the control package model consisted of 47626 elements and 47746 nodes.

For this study, two cases for the boundary conditions able to represent the physical model were used in the simulation:

Case A (Figures. 4.7a and 4.7b) where the top of the package was constrained along the lengthwise (long) side of the package to allow for translation in the *y* direction while the translation in the *x* and *z* directions was prevented. Rotation in the *y* and *z* direction was fixed while the rotation in the *x* direction was allowed. Similarly, along width (short) side of the package, translation in the *y* direction was allowed, while the translation in the *x* and *z* directions was fixed. However, unlike the long side of the package, rotation was fixed in the *x* any *y* directions while rotation in the *z* direction was allowed. Face pressure was applied to the top of the package. At the bottom of the package, translation and rotation were fixed in all directions;

Case B (Figures. 4.7c and 4.7d) where the conditions used in Case A, at the top (long and short sides) of the package were the same. However, at the bottom, translation and rotation were fixed for the edge nodes of the bottom hole, while only the rotation was fixed for the remaining nodes at the bottom. Linear buckling

analysis was carried out to determine the critical buckling load and estimate the most likely buckling shape of the package. In addition, a contact boundary condition was applied to study the effect of platen contact on the package strength. Nonlinear static analysis was performed and the large strain nonlinear procedure available in the Mentat/Marc (MSC Software Corporation, California, USA) finite element solver, incorporating geometric nonlinearities into the formulation was also activated.

4.3.3 Experimental procedure

4.3.3.1 Edge compression test (ECT)

The ECT measures the ability of a vertically placed sample of corrugated paperboard to sustain a top-to-bottom load. FEFCO No. 8 Standard was used for the ECT with the Lorentzen and Wettre crusher tester. Rectangular corrugated paperboard samples (Figure 4.8a) of 100 mm in length and 25 mm in width were used. The corrugated paperboard used for the test was a single wall of type C and B flutes. The corrugated paperboard was held tightly in the test fixture (two metal guide blocks). The blocks align the board samples vertically so that the applied force is parallel to the CD. The clamping force on the bottom and top of the board held it to be parallel to the direction of the applied force so there is no chance of tipping that causes lower recorded force values. The corrugated paperboard was inserted between two compression platens with no waxed edges or mechanical support beyond the initial vertical alignment at a constant speed of 12.5 ± 2.5 mm min^{-1} until instability occurred. The maximum force that the sample could resist before failure was recorded. To obtain the value for the ECT, the maximum force was normalised by the length of the sample as described by McKee et al. (1963) and Fadiji et al. (2017).

4.3.3.2 Flat crush test (FCT)

The compressive strength reflects the strength of paperboard packaging material at compression loads. The flat crush test (FCT) is a measure of the resistance of the flutes in corrugated board to a crushing force applied perpendicular to the surface of the board under prescribed conditions (Kołakowski et al., 2015; Krusper et al., 2007). The FCT was carried out according to Tappi T 825 standard method using the Lorentzen and Wettre crusher tester. For the FCT, a circular shaped corrugated paperboard of area 100 cm^2 was used (Figure 4.8b). The corrugated paperboard used for the test was a single wall of type C and B flutes. During testing, the corrugated paperboard was subjected to increasing force, which was applied perpendicular to the surface of the paperboard with a speed of 12.5 mm min^{-1}, until the fluting medium breaks. The FCT value is expressed as the force divided by the sample's surface area. Ten replicates were carried out for the FCT.

4.3.3.3 Box Compression test (BCT)

In South African pome fruit industries, telescopic packages are commonly used for export (Pathare et al., 2017; Berry et al., 2015). The packages used in this study were fabricated using a corrugated fibreboard cutting machine (KM series 6, Kasemake House, Cheshire, UK) and then assembled and glued by hand. Two types of packages were manufactured; a control package without vent voles and a standard vent package with vent holes (vent area of approximately 4%). Dimensions are shown in Figure 4.9. The BCT was evaluated in accordance with the ASTM D642 Standard (ASTM, 2010), using a box compression tester (M500-25CT, Testomatic, Rochdale, UK). Prior to the BCT, samples were preconditioned at 30 ± 1 °C and RH of 20–30% for 24 h and then conditioned at 23 ± 1 °C and 50% RH for 24 h according to ASTM D4332 standard (ASTM, 2006). The cartons were compressed by applying a continuous motion of the platen at a speed of 12.7 ± 2.5 mm min^{-1} until failure was reached. The fixed-platen method of the compression tester was used. A preload of 222 N was applied on the test cartons. The purpose of the preload is to remove the initial transient effects. Eight replications were used for the compression test.

4.3.4 Statistical analysis

The statistical evaluations were performed using Statistica (v. 13.0, Statsoft, USA). The experimental data were treated with one-way analysis of variance (ANOVA) at 95% confidence level and with the differences at $p<0.05$ considered statistically significant. Graphical representations were made using GraphicPad Prism 7 software (GraphicPad Software, Inc. San Diego, CA, USA). The standard error of the mean is indicated by error bars on the figures. Statistical difference between the mean was shown using the letters on the error bars. Means with the same letters are not statistically different.

4.4 Results and discussion

4.4.1 Material characterisation of the corrugated paperboard components

Figure 4.10 shows a typical in-plane uniaxial tensile stress-strain curve in the MD and CD for the corrugated paperboard combination used in this study. The stress-strain curve is a representation of the paper material behaviour when in tension. The curve characterises a linear and nonlinear part, and is dependent on moisture content, cellulose fibre, and the hydrogen bond (Allaoui et al., 2009a). Figure 4.10 clearly shows the strong anisotropy attribute present in paper as seen from the different loading directions (MD and CD). According to Borodulina et al. (2012), reducing the number of bond in paper fibre increases the stress variation inside the fibre network, which consequently mean that the paper fibres reach yield stress at lower fibre network stress level. From the curves (Figure 4.10), a clear difference was observed between the MD and the CD in the modulus, as the stress level of the paper was high and apparent in the MD. Salminen (2003) and Kulachenko et al. (2007) reported that this could be due to the predominant orientation of the fibre in

the MD during manufacturing process and the straining behaviour in the MD, which has a low plasticity and ductility.

As shown in Figure 4.11 for all the paper samples, MD had the highest elastic modulus, which was significantly different from the elastic moduli in the CD and the ZD. For 175T1, the percentage difference between the elastic modulus of the MD and other directions were about 144% and 198% for CD and ZD, respectively; for 175SC, the differences were about 117% and 198%, respectively; for 125SC, the differences were about 121% and 198%, respectively; for 140SC, the differences were about 136% and 198%, respectively; for 140SC, the differences were about 136% and 198%, respectively; for 165SC, the differences were about 109% and 198%, respectively. The higher stiffness and resistance to stress in the MD was reported to be due to fibre distribution during the forming process of the paper sheets (Fadiji et al., 2017; Nygards et al., 2009; Stenberg et al., 2001). The elastic moduli of the paperboard in the ZD was observed to be significantly different from the elastic moduli in the MD and ZD. According to Harrysson and Ristinmaa (2008), the out-of-plane (ZD) mechanical properties are a function of the fibre properties perpendicular to the paperboard bond strength and the longitudinal direction. The apparent difference between the mechanical properties in the in-plane (MD and CD) and out-of-plane (ZD) was reported to be due to the rather different physical phenomena governing the in-plane and out-of-plane mechanical properties (Harrysson & Ristinmaa, 2008). Usually, the mechanical properties in MD are about two to four times greater than in CD.

4.4.2 Simulation results and validation for the strength of the corrugated paperboard

The edge compression resistance and flat crush resistance obtained from the experimental study for both B and C flutes corrugated paperboard are shown Table 4.5. The edge compression resistance measures the ability of a vertically placed corrugated paperboard to sustain top-to-bottom load and helps to evaluate the in-plane compression strength of the corrugated paperboard. The strength of a corrugated paperboard package can also be predicted using the edge compression resistance value, the package geometry and the paperboard properties (Fadiji et al., 2017). As shown in Table 4.5, the ECT value for corrugated paperboard with C flute medium was higher than corrugated paperboard with B flute medium with a percentage difference of about 39%, although not statistically different (p<0.05). The same trend was observed for the FCT values for both corrugated paperboard types except for the statistical difference observed (p<0.05) with a percentage difference of about 43%. Our findings were similar to the study by Urbanik (2001) who studied the influence of flute geometry on the strength and stiffness of corrugated paperboard. The author reported the possibility of balancing cost, strength and stiffness of a corrugated paperboard with an optimum flute profile. A crucial structural performance of a package is its stacking strength and it is a function of the edgewise compression resistance and bending stiffness of the corrugated paperboard (Navaranjan et al., 2013; Urbanik, 2001) and according to

Ahmed and Bhoomkar (2013), ECT in combination with the bending stiffness of a corrugated paperboard have a direct correlation with BCT. Furthermore, certain manufacturing effects of the corrugation, as well as the strength of the paper material, can be reflected by the edge compression resistance, hence it is a realistic measure of the corrugated paperboard quality (Jinkarn et al., 2006).

Corrugated paperboard with a low flat crush resistance could lead to a reduction in package performance. From our study, a percentage reduction in the flat crush resistance of about 36% was observed in B flute corrugated paperboard when compared to the paperboard with C flute medium. Low flat crush resistance may be an indication of some paperboard conditions such as low medium strength, poorly formed flutes, crushed flutes or leaning flutes. Corrugated paperboard with leaning flutes may not result in low flat-crush resistance and adverse package performance, as lateral movement between liners must occur for leaning flute to result in low flat crush resistance. The lateral movement between liners can be restricted by the geometry of the package when a package is manufactured from corrugated paperboard with low flat crush resistance.

For the simulation of the edge compression resistance of the C flute corrugated paperboard, fringe plots of the first and second buckling mode for the large strain and the small strain model procedures are shown in Figure 4.12 and Figure 4.13, respectively. The small strain procedure for the buckling analysis assumes that the changes after displacement is significantly small so that the geometry remains unchanged, while the large strain procedure was used to capture the geometric nonlinearity of the corrugated paperboard. The edge compressive resistance for the large strain and small strain were 6.24 kN m^{-1} and 6.32 kN m^{-1} for C flute corrugated paperboard, with a percentage difference of 2.5% and 1.3%, respectively when compared with the experimental results shown in Table 4.5. For B-flute corrugated paperboard, the large strain and small strain buckling procedure resulted in edge compressive resistance of 3.89 kN m^{-1} and 3.99 kN m^{-1}, respectively. When the numerical results from large and small strains are compared with the experimental results for the B flute corrugated paperboard (Table 4.5), the percentage difference was about 11% and 8%, respectively.

4.4.3 Simulation results and validation for the strength of the corrugated paperboard package

To model the corrugated paperboard package, the numerical model must be able to represent the physical process accurately. In this study, the influence of the boundary conditions to obtain satisfactory finite element model results was checked. Two boundary conditions similar to the physical phenomenon were used (section 4.3.2.3). Figures 4.14a – h show the fringe plot of the displacement and the first buckling mode for the control package without vent holes and the package with a standard vent configuration using Cases A and B boundary conditions. The results presented are for packages with C flute medium. As shown in the plots, the package width exhibited resistance to buckling while the centre of the package length was

observed to be the origin of the buckling. An outward buckling occurred on the package length (long side of the package) while the package width (short side of the package) was observed to buckle slightly inward. According to Panyarjun and Burgess (2001), localised crushing of the package liners could lead to package failure. From the simulation, buckling of the vertical edges induced the collapse failure.

Figure 4.15 shows a typical force versus deformation response curve obtained by compressing the cartons (control and standard vent packages). An approximately linear initial response was observed which was followed by a nonlinear behaviour that eventually leads to a maximum load. This may be due to a large deformation in the out-of-plane of the package and local buckling exhibited by the liners (Åslund et al., 2014). The buckling of the package that occurs during compression loading is often produced by the greatest bending moment located around the face of the package as shown in Figures 4.14a – h. Centrally locating the vent or hand holes, will result in a significant reduction in compression strength of the package (Han & Park, 2007; Jinkarn et al., 2006; Biancolini & Brutti, 2003). Table 4.6 shows the buckling loads obtained from the finite element simulation for the packages for both Cases A and B boundary conditions, in comparison with the experimental results.

Comparing the buckling loads from the finite element model and the experiment of the control package for Case A boundary condition resulted in a percentage difference of about 13%, while for Case B boundary condition, a percentage difference of about 10% was observed. For the standard vent package, when the buckling loads from the finite element model and the experiment were compared, a percentage difference of about 10% and 5% were observed for Case A and Case B boundary conditions, respectively. For both simulation and experimental results, compared to the control package, the standard vent package had lower buckling loads. In the Case A boundary condition, compared to the control package, the buckling load for the standard vent package decreased by about 9%, while a decrease of about 20% was observed for Case B boundary conditions.

From the experimental results, mean value and standard error of buckling loads obtained for the control and standard vent package were 7268 ± 158 N and 6797 ± 151 N, with a percentage difference of about 7% and a significant difference was observed between the buckling loads ($p<0.05$) according to Duncan's multiple range tests. The reduction in compression strength of the standard vent package can be attributed to the presence of the vent hole. Although vent holes decrease the mechanical strength of the package (Pathare et al., 2012b), they consequently help to reduce materials wastage as the removed materials can be recycled (Pathare & Opara, 2014; Chen et al., 2011a). They are also a crucial factor affecting the efficiency of cooling the packed produce (Pathare et al., 2012b; Thompson et al., 2002). The design of ventilated corrugated packages should be such that it provides adequate cooling to the packed produce while maintaining its structural integrity.

Typically, unvented corrugated packages are stronger than ventilated corrugated packages. Vigneault et al. (2009) and Kader (2002) suggested that locating vent holes away from the vertical corners of the package minimises the reduction in the maximum strength in ventilated corrugated packages. In addition, the area of the ventilation openings should not account for more than 5% of the total package area, as most corrugated paperboard packages can have up to 5% ventilation area without minimising the stacking or compression strength (Thompson et al., 2002; Kader, 2002). Packages with more than 5% ventilation area must be carefully designed to provide sufficient structural strength (Pathare et al., 2012b; Thompson et al., 2002). In addition, packed produce depends on the package walls to avoid damage. It is therefore crucial to maintain and retain the strength of package walls to improve minimise produce damage during postharvest handling.

4.4.4 Effect of thickness

A parametric study was used to verify the influence of liner thickness (outer and inner) on the strength of the package using the validated finite element model. The thickness of the inner and outer liner for the validated model was used as the baseline and labelled as 100%. The baseline liner thickness was altered by 80% increase and decrease at an interval of 20%, while keeping the core thickness constant. This was done for the two cases of boundary conditions used. Figures 4.16a – d show the relationship between the liner thickness and the buckling load for the control package. The round black circles represent the buckling load at the baseline thickness used for the validated model. A linear relationship was observed between liner thickness (outer and inner) and the buckling load of the package. The coefficient of determination (R^2) was high for all the relationships; 0.984 for outer and inner thicknesses with Case A boundary conditions, and 0.990 for outer and inner thicknesses with the Case B boundary conditions.

Our findings show that increasing and decreasing the baseline thicknesses by 80% resulted in an increase and decrease in buckling load by about 13% and 16%, respectively with the Case A boundary conditions. For Case B boundary, an increase and decrease in buckling load of about 15% and 19% was observed by increasing and decreasing the baseline thicknesses by 80%, respectively. For the Case A boundary conditions, increasing the baseline thicknesses by 20% increased the buckling load with about 2% and same reduction percentage of 2% was observed when the baseline thicknesses of the liners were reduced by 20%. Although the model used an approximated homogenised solid core, the present study altered the core baseline thickness of the control package by increasing and decreasing the thickness by 20%. The result of the buckling load was most sensitive to the alteration, as 20% decrease in core thickness reduced the buckling load by about 43%, while 20% increase in core thickness raised the buckling load by about 64%, for both the Case A and Case B boundary conditions (Figure 4.17a). It was observed that the two boundary conditions had less effect on the results when the core thickness was altered. Results obtained were similar to the study by Åslund et al. (2014) who investigated the influence of face (liner) and core sheet thicknesses

on corrugated board panel buckling and collapse strength. The authors indicated that added material in the face sheet of the board panels has an impact on the maximum load of the board, which may be due to elevated local buckling of the face sheet. In addition, corrugated paperboard combinations using various paper thickness and grammage have great effect on the buckling resistance and compression strength of a package (Park et al., 2011).

The relationship between the liner thicknesses (inner and outer) for the standard vent package is shown in Figures. 4.18a – d. The trend in the relationship between the liner thicknesses and the buckling loads for the standard vent was observed to be similar to the control package shown in Figures 4.16a – d. Increase in the baseline liner thicknesses by 80% increased the buckling load of the standard vent package by 28% and 30% for Case A and B boundary conditions, respectively. A reduction in buckling load of about 39% and 27% for Cases A and Case B boundary conditions, respectively when the baseline liner thicknesses were reduced by 80%. From our results, increasing and reducing the baseline liner thicknesses by 20% raised and decreased the buckling loads by about 7% and 6%, respectively for Case A boundary condition, while for the same alterations in the liner thicknesses for Case B boundary conditions, the buckling load was raised and decreased by 7%. Interestingly, it was also observed that the buckling load increased and decreased by equal percentage of about 21% when the thicknesses were increased and decreased by 60% for Case A boundary conditions. Similar to the results obtained for the control package, a linear relationship was observed between the liner thickness and the buckling load. The coefficient of determination (R^2) was high for all the relationships: 0.985 for outer and inner thicknesses with Case A boundary conditions, and 0.999 for outer and inner thicknesses with Case B boundary conditions. For the standard vent package, increasing the core baseline thickness by 20% while keeping the liner (outer and inner) thickness constant increased the buckling load by about 57% and 56% for Case A and Case B boundary conditions, respectively. About 67% decrease in buckling load was observed when the core thickness was reduced by 20% for Case A boundary condition while for Case B boundary condition a reduction of about 61% in buckling load was observed (Figure 4.17b).

4.4.5 Simulation of the effect of platen contact on the predicted strength of the package

A contact model was used to simulate and investigate the effect of platen on the package. Glued and touching contact options were used between the platens and the package. The top and bottom platens were modelled as rigid bodies while the meshed package was specified as deformable contact body. In the simulation, glue contact was applied between the bottom platen and the package while touching contact was applied between the top platen and the package. For the contact interaction, a deformable-to-rigid (meshed-to-geometric) contact table was defined. Figure 4.19 shows the positioning of the top and bottom platen for the contact simulation. The top platen was position controlled and was set to drive the package

downwards 4% of its height as suggested by Han and Park (2007), in this case 10.8 mm of 270 mm. Figures 4.20a – f show the fringe plot for the displacement, Von Mises stress and the global stress obtained from the simulation for the control and standard vent packages. For both control and standard vent packages, there was an outward bulge in the length (long) side of the packages while the width (short) side of the packages buckled inward. The equivalent Von Mises stress from the simulation showed that maximum concentration was produced at the corners of the packages and slightly towards the middle of the package in both length and width of the standard vent package (Figures 4.20c and d). The control package experienced lower stress levels compared to the standard vent package, indicating the structural stability of a package without vent holes. About 66% difference in maximum Von Mises stress was observed between the control and standard vent packages. The large difference observed may be attributed to the fact that the results of the model did not consider a friction coefficient between the top platen and the package.

Fringe plots from the equivalent global stress (Figures. 4.20e and f) showed maximum stress concentration at the corners of the package, towards the centre of the package and at the bottom of the package. Similar to the equivalent Von Mises stress, the control package had a lower equivalent global stress of about 122 MPa when compared with the equivalent global stress of the standard vent package, which was about 323 MPa. In line with our findings, similar stress concentration around the corners of the package was reported by Han and Park (2007). To account for the effect of friction coefficient in the model, three friction coefficient: 0.1, 0.2 and 0.3 were applied in the model between the top platen and the standard vent package. The inclusion of friction coefficient in the model had an effect on the equivalent Von Mises stress observed on the package. When the maximum Von Mises stress of the package obtained with 0 friction coefficient was compared with the maximum Von Mises stress of the package obtained with 0.1 friction coefficient, a reduction of about 25% was observed in the latter. This may be attributed to the resistance that occurred between the top platen and the package on pushing down the platen. Increasing the friction coefficient to 0.2 and 0.3 reduced the maximum Von Mises stress insignificantly by about 1% for both friction coefficient, respectively (Figure 4.21).

Figures 4.22a – i show the fringe plot for the displacement, Von Mises stress and the global stress obtained from the contact simulation with the three friction coefficients (0.1, 0.2 and 0.3) used in the model. Unlike the displacement fringe plot of the package with 0 friction coefficient, an inward bulge was observed in the length (long) side of the package while the width (short) buckled outward (Figures 4.22a, d and g). Similar to the stress distribution seen on the package with 0 coefficient, the packages with friction coefficients exhibited the same Von Mises stress and global stress distributions (Figures 4.22b, c, e, f, h and i). When the displacement of the Standard vent package from the experimental and simulation (with 0.1 friction coefficient) results were compared (Figures 4.23a and b), similar

displacement pattern was observed. Visual evaluation of the displacement from within the inside of the package showed that the long and short sides of the package appeared to be concave and convex, respectively. The evaluation of the displacement pattern can be adapted to understanding the likely damages when packages are subjected to compression load, thereby reducing the packaging costs (Böröcz, 2015). The path plot of the Von Mises stress distribution at the corner for the control package, standard vent package and standard vent package with friction coefficient (0.1) from the bottom to the top of the package is shown in Figure 4.24. An important observation was that the Von Mises stress was higher towards the middle of the corners with the high stresses at a distance of about100 mm to about 200 mm. The high stresses at these points may be due to the inward and outward buckling of the package. It is crucial to know the stress distribution on the package to aid in the design of an efficient structurally strong corrugated paperboard package.

4.5 Conclusions

This study presented a validated structural FEA model able to predict the compression strength of VCP package commonly used in the fresh fruit industry. The material properties of the packaging materials were evaluated and used as input parameters in the model. The model was in good agreement, within 10%, when compared with the experimental results. Corrugated paperboard liner thickness for both control and standard vent packages had a significant effect on the compression strength of the package ($R^2 = 0.999$). Maximum stress concentration was found at the corners of the packages. Friction coefficient was observed to affect the displacement shape of the package. Length and width sides of the package buckled outward and inward, respectively with zero friction coefficient applied in the contact model while the application of friction coefficient caused the length and width sides of the package to bulge inward and outward, respectively. Knowing the constitutive relationship between the corrugated materials and including detailed geometric nonlinearities will enhance the development of models with different configurations for better package design.

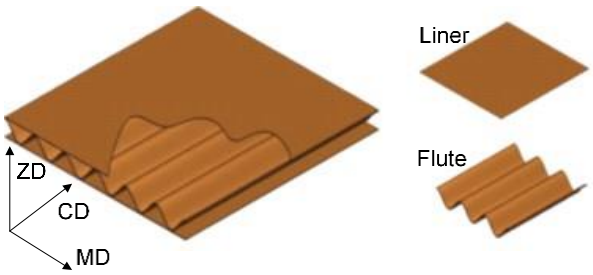

Figure 4.1: Basic geometry of a typical corrugated paperboard (MD is the machine direction, CD is the cross direction and ZD is the thickness direction).

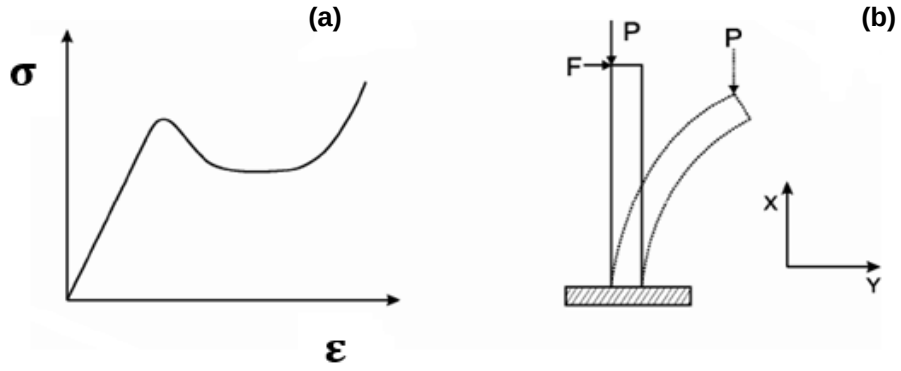

Figure 4.2: Diagram illustrating, (a) material nonlinearity and (b) geometric nonlinearity.

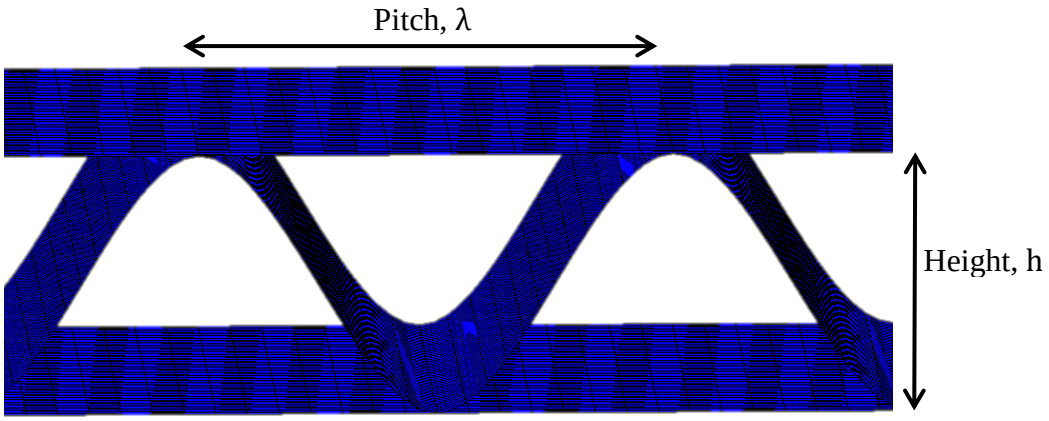

Figure 4.3: Geometry of the corrugated paperboard used in the FEA.

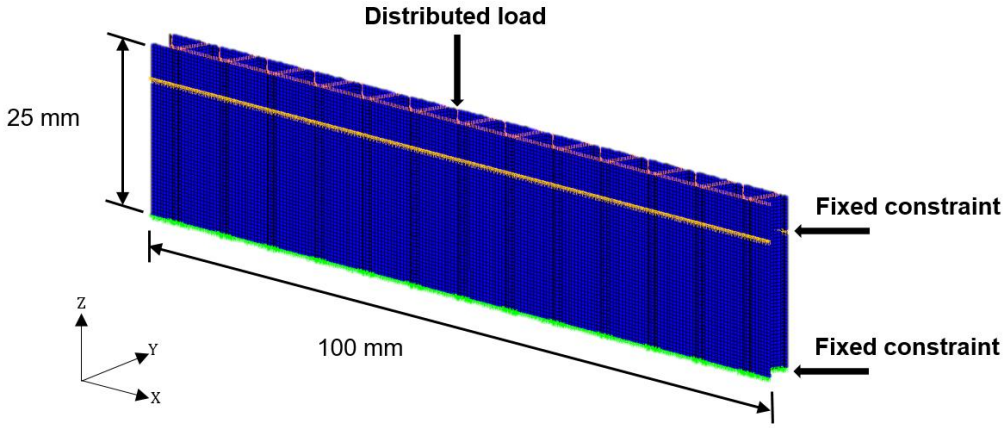

Figure 4.4: Finite element model setup for the edge compression test (ECT) indicating the boundary conditions.

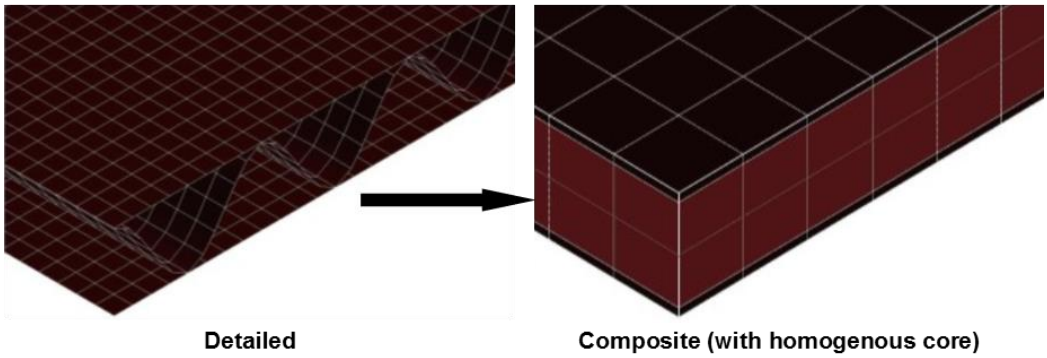

Figure 4.5: Modelling approach for the finite element simulation of the corrugated paperboard package.

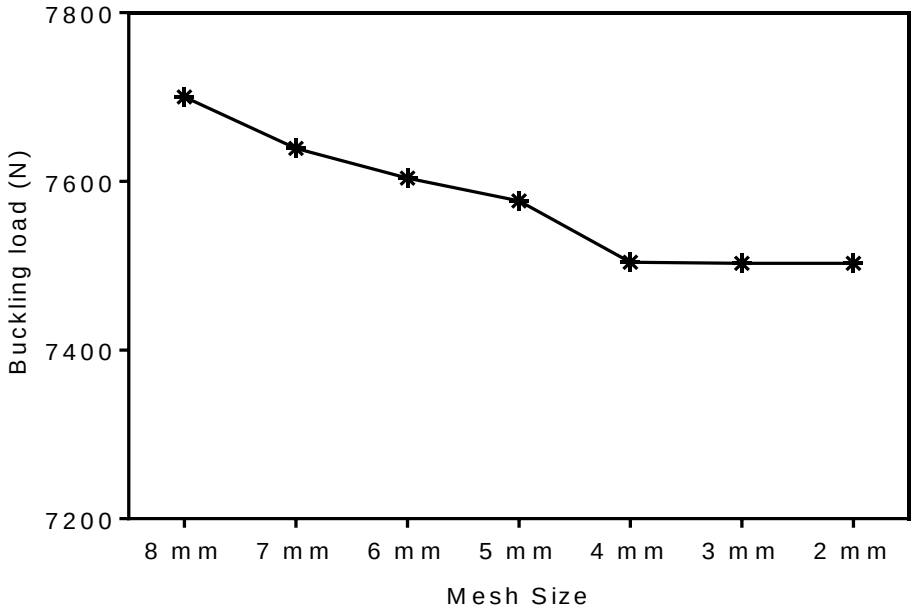

Figure 4.6: Typical mesh convergence study for the model.

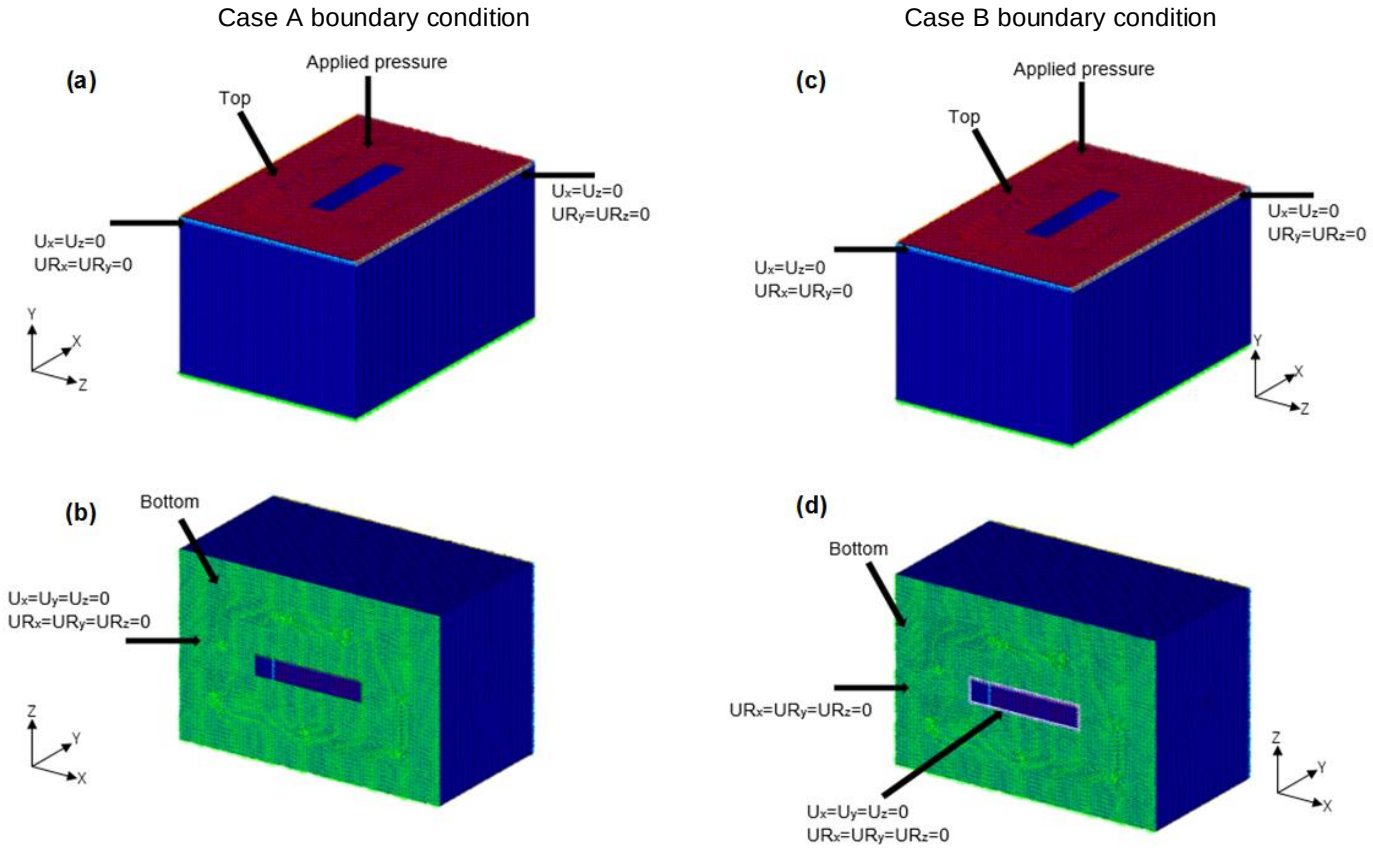

Figure 4.7: Boundary conditions used in the package simulation: a) Case A showing the constraints applied at the top of the package; b) Case A showing the constraints applied at the bottom of the package, c) Case B showing the constraints applied at the top of the package (same as Case A) and d) Case B showing the constraints applied at the bottom of the package.

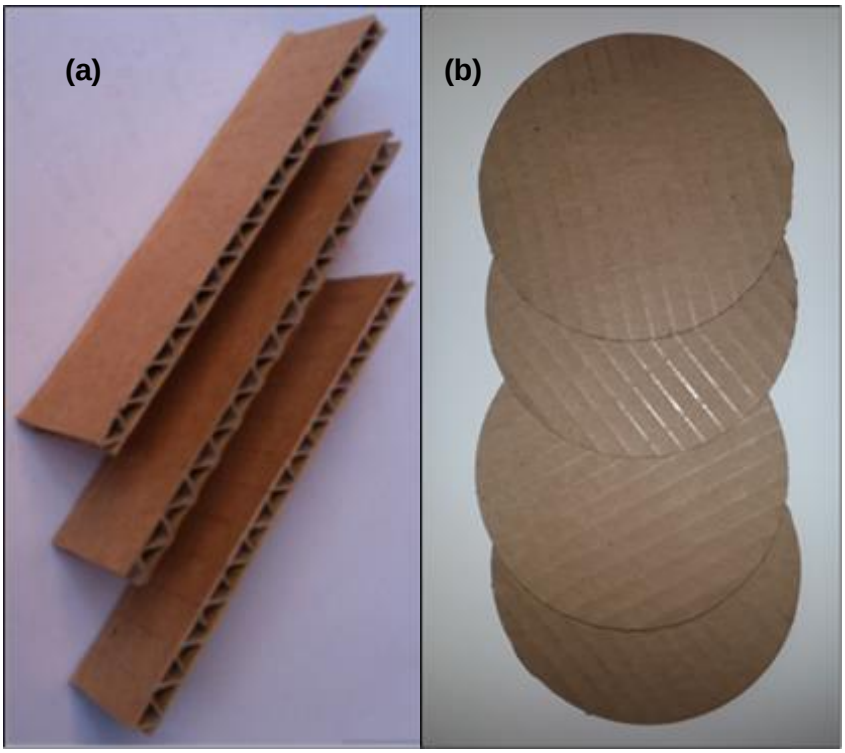

Figure 4.8: Corrugated paperboard samples for (a) edge compression test and (b) flat crush test.

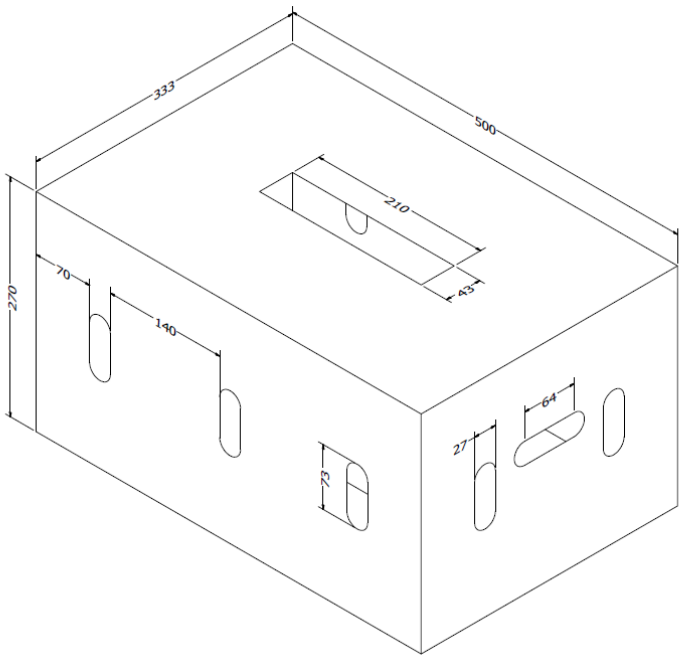

Figure 4.9: Geometry and dimension (mm) of the standard vent package

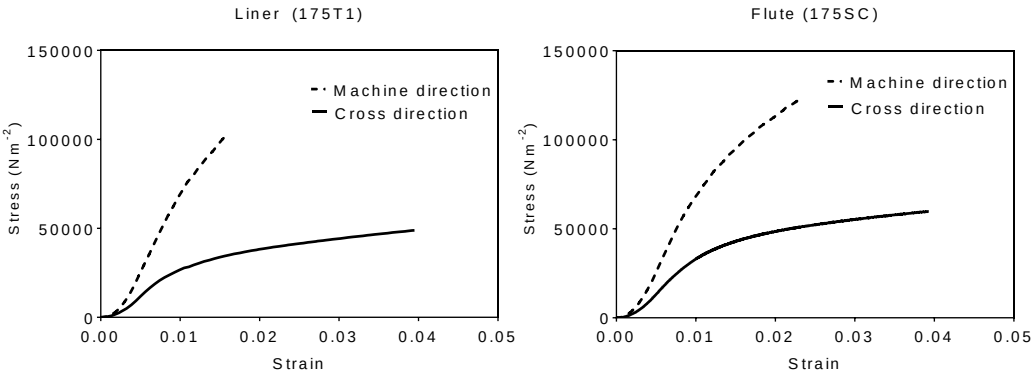

Figure 4.10: Typical stress-strain curve for the liner and the flute of the corrugated paperboard.

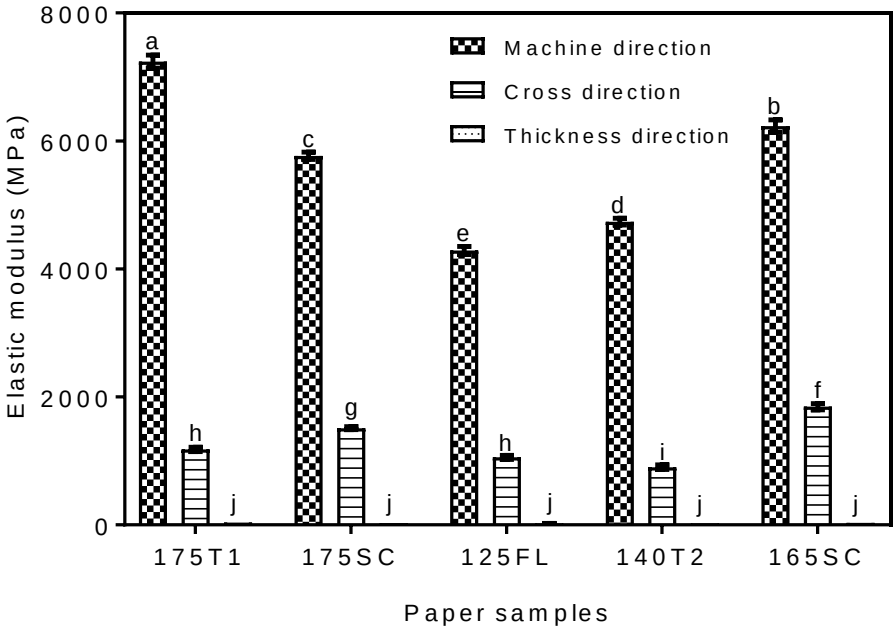

Figure 4.11: Elastic modulus of the paperboard grade at the three directions (machine, cross and thickness directions). Values show the mean and standard error. Different letters within a block show significant difference according to Duncan's Multiple Range tests.

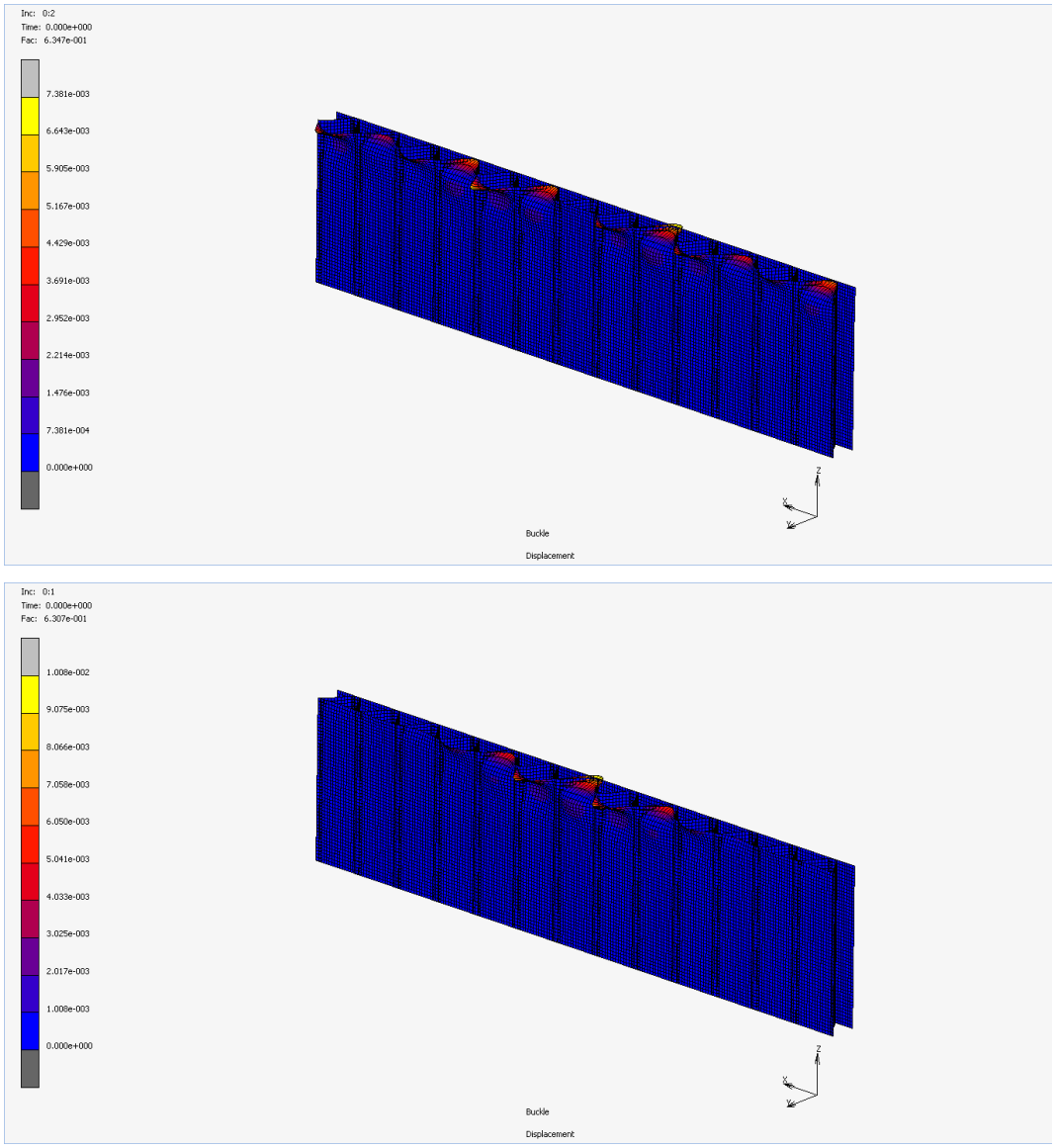

Figure 4.12: Plots of the first (top) and second (bottom) buckling modes for the small strain buckling analysis on C flute corrugated paperboard.

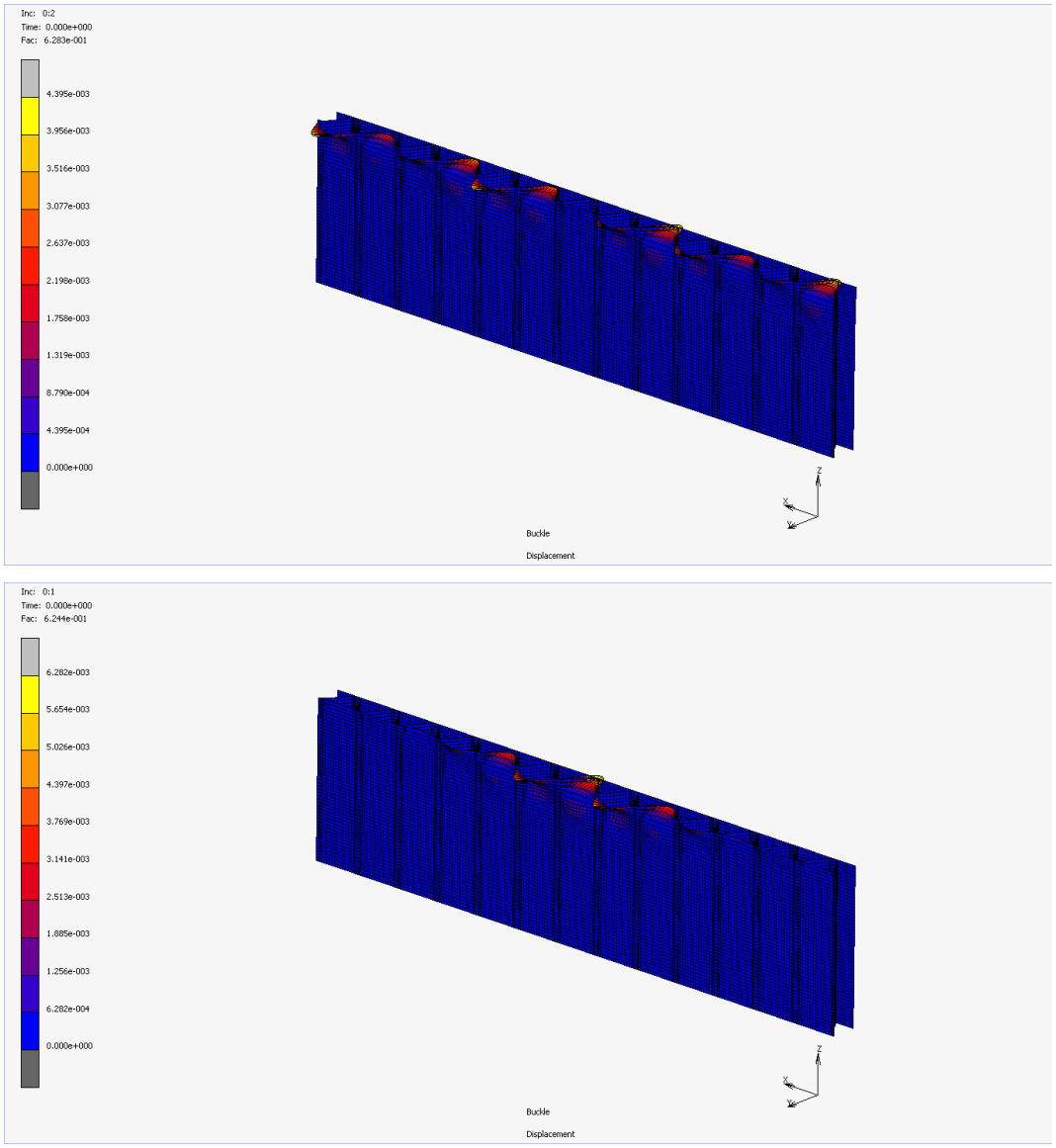

Figure 4.13: Plots of the first (top) and second (bottom) buckling modes for the large strain buckling analysis on C flute corrugated paperboard.

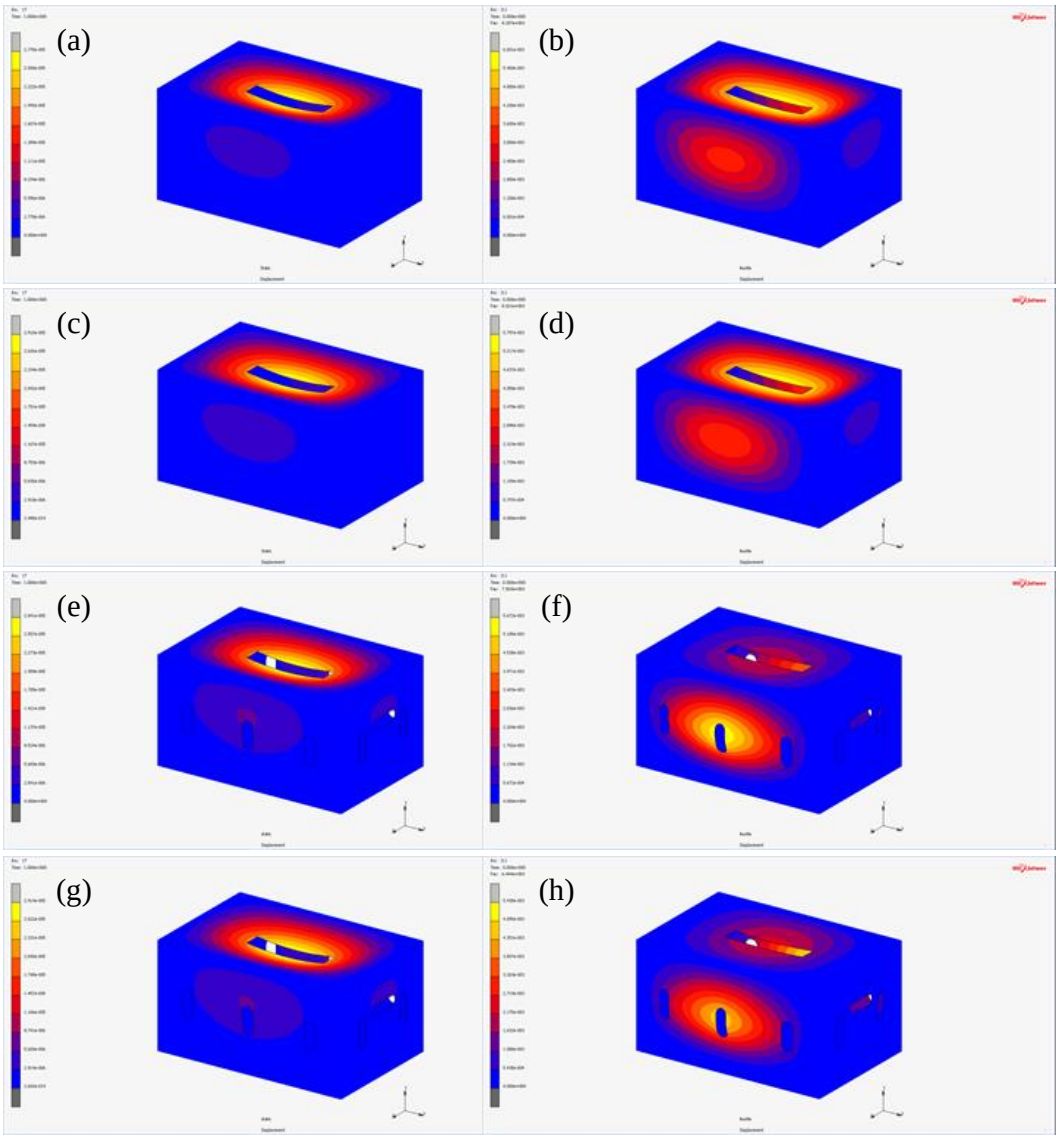

Figure 4.14: Fringe plot from the finite element simulation for (a) displacement of the control package with Case A boundary conditions, b) buckling mode of the control package with Case A boundary conditions, (c) displacement of the control package with Case B boundary conditions, (d) buckling mode of the control package with Case B boundary conditions, (e) displacement of the standard vent package with Case A boundary conditions (f) buckling mode of the standard vent package with Case A boundary conditions (g) displacement of the standard vent package with Case B boundary conditions and (h) buckling mode of the standard vent package with Case B boundary conditions.

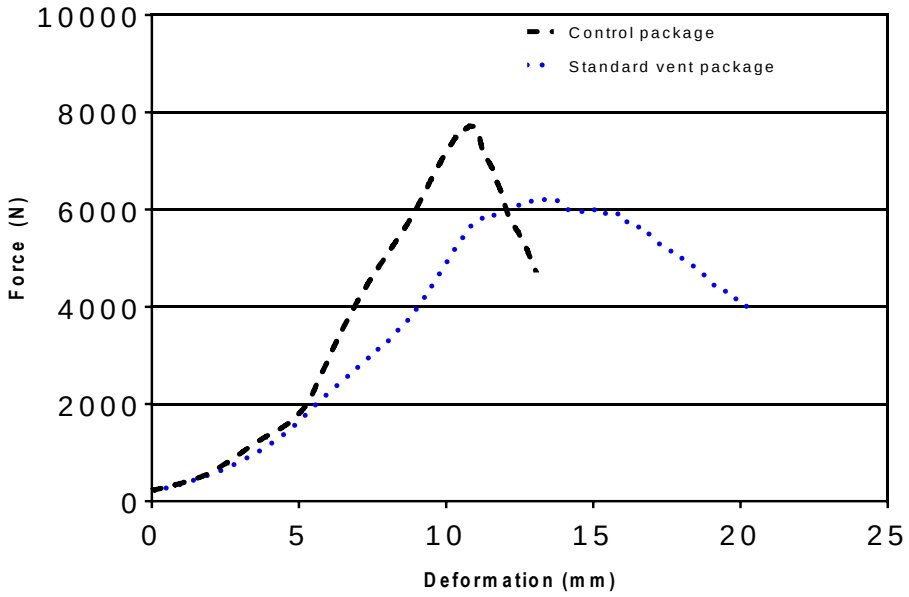

Figure 4.15: Typical force–deformation curve for the package obtained from the compression test for the control and standard vent packages.

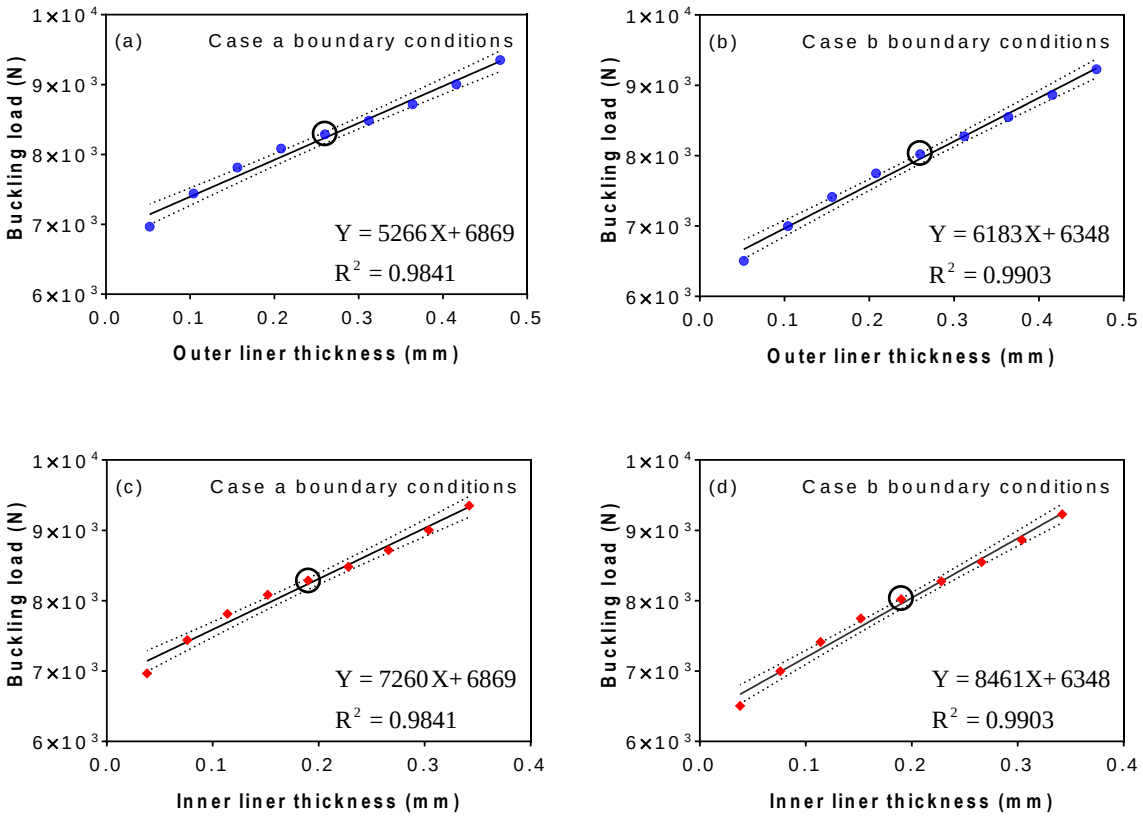

Figure 4.16: Relationship between the liner thickness (mm) and buckling load (N) for the control package with C flute (a) effect of outer liner thickness on buckling load with Case A boundary conditions, b) effect of outer liner thickness on buckling load with Case B boundary conditions, (c) effect of inner liner thickness on buckling load with Case A boundary conditions and (d) effect of inner liner thickness on buckling load with Case B boundary conditions. The black round circle represent the buckling load at the baseline thickness and the two dotted lines represent 95% confidence interval while the black line shows the curve fitting.

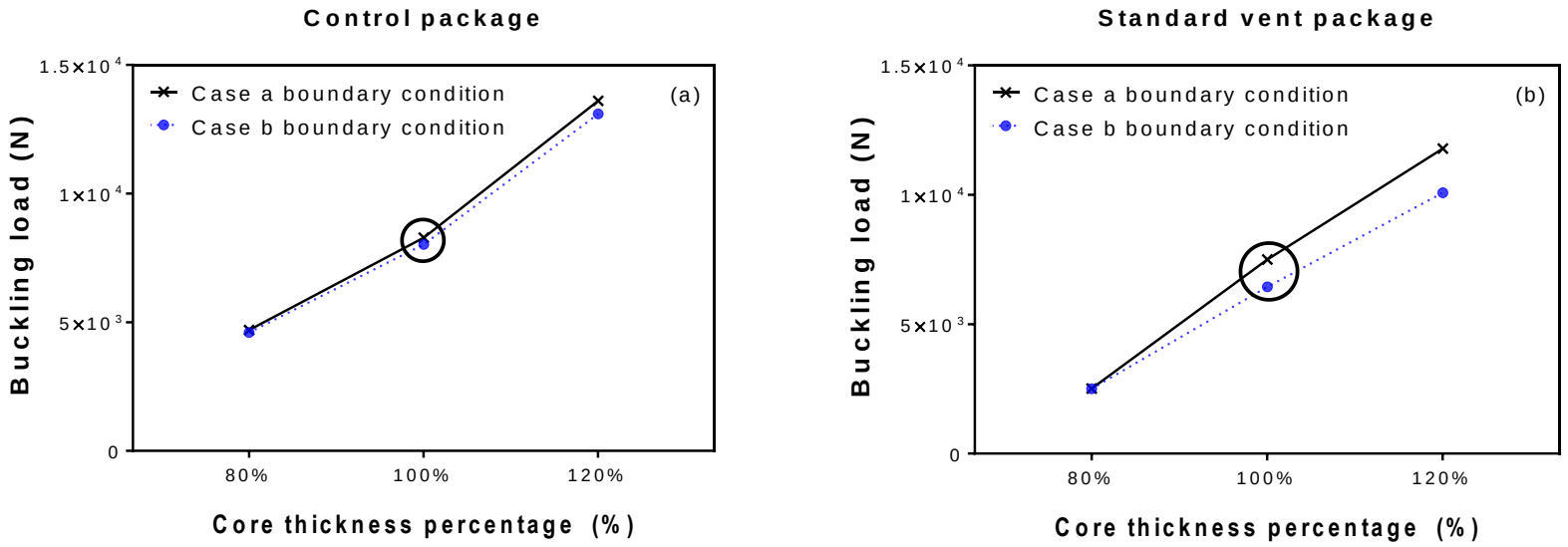

Figure 4.17: Relationship between the core thickness (mm) and buckling load (N) with Case A and Case B boundary conditions for (a) control package and (b) standard vent package. The black round circle represents the buckling load at the baseline thickness.

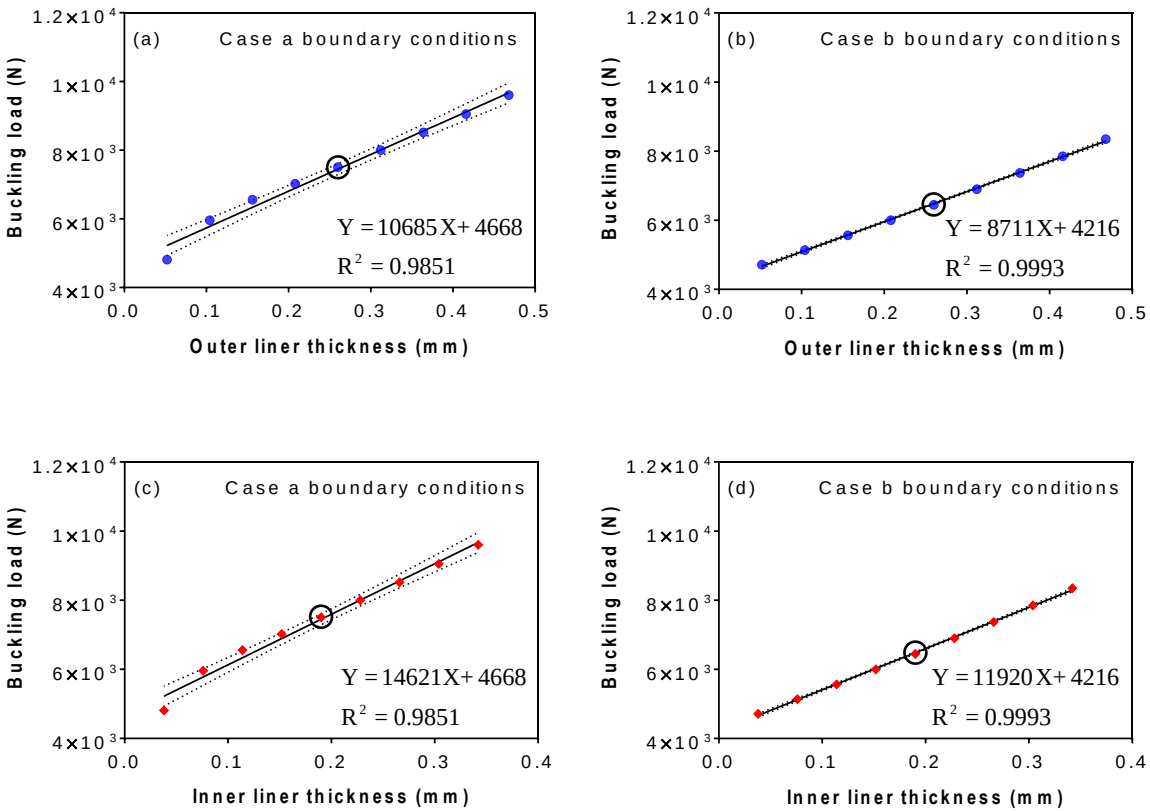

Figure 4.18: Relationship between the liner thickness (mm) and buckling load (N) for the standard vent package with C flute (a) effect of outer liner thickness on buckling load with Case A boundary conditions, b) effect of outer liner thickness on buckling load with Case B boundary conditions, (c) effect of inner liner thickness on buckling load with Case A boundary conditions and (d) effect of inner liner thickness on buckling load with Case B boundary conditions. The black round circle represent the buckling load at the baseline thickness and the two dotted lines represent 95% confidence interval while the black line shows the curve fitting.

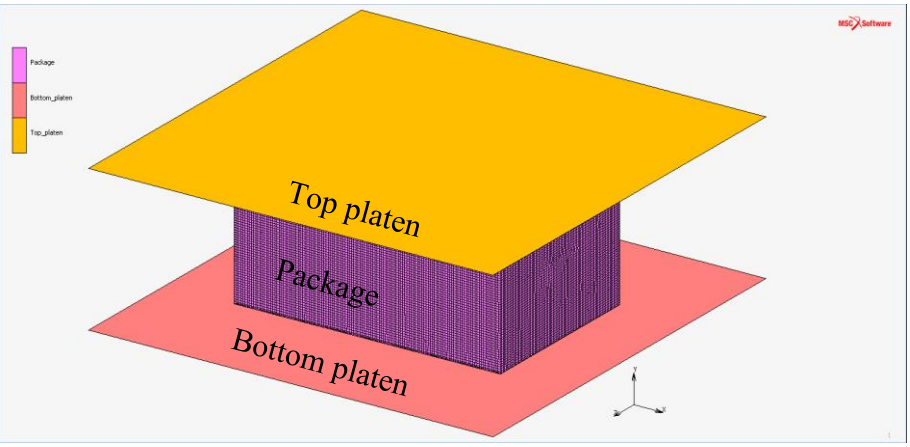

Figure 4.19: Modelling approach for the contact finite element simulation of the corrugated paperboard package showing the positions of the top and bottom platens.

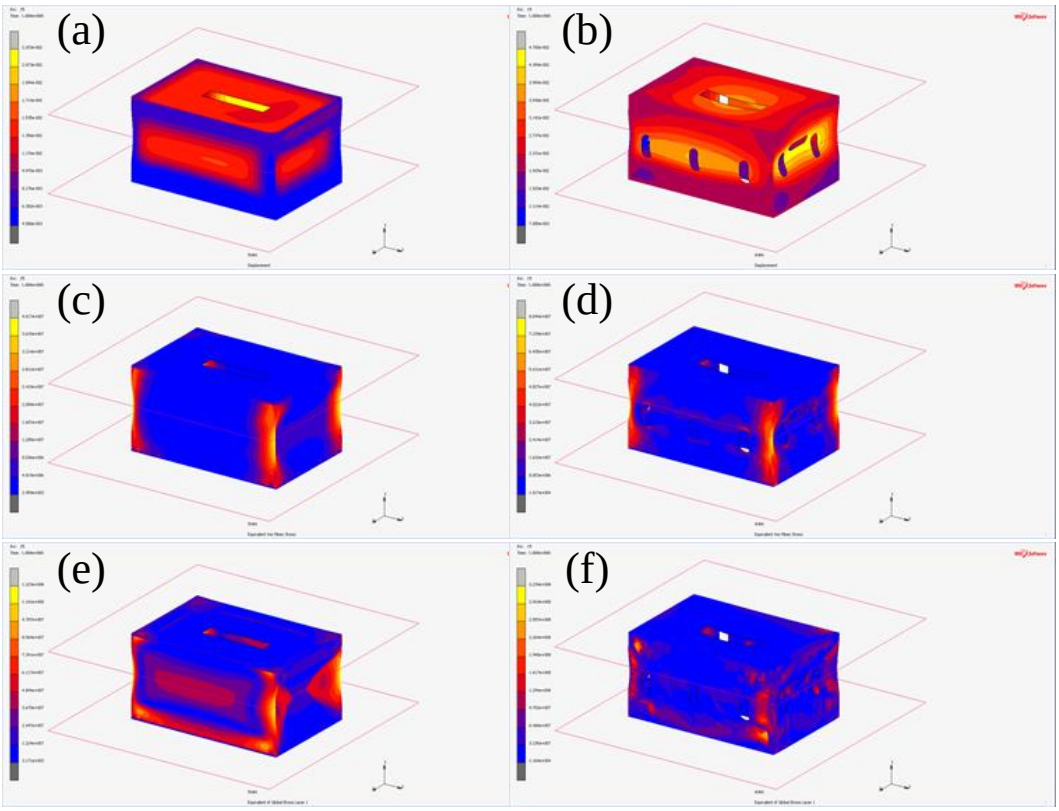

Figure 4.20: Fringe plot from the contact model simulation for (a) displacement of the control package, b) displacement of the standard vent package, (c) equivalent Von Mises stress of the control package, (d) equivalent Von Mises stress of the standard vent package (e) equivalent global stress of the control package and (f) equivalent global stress of the standard vent package.

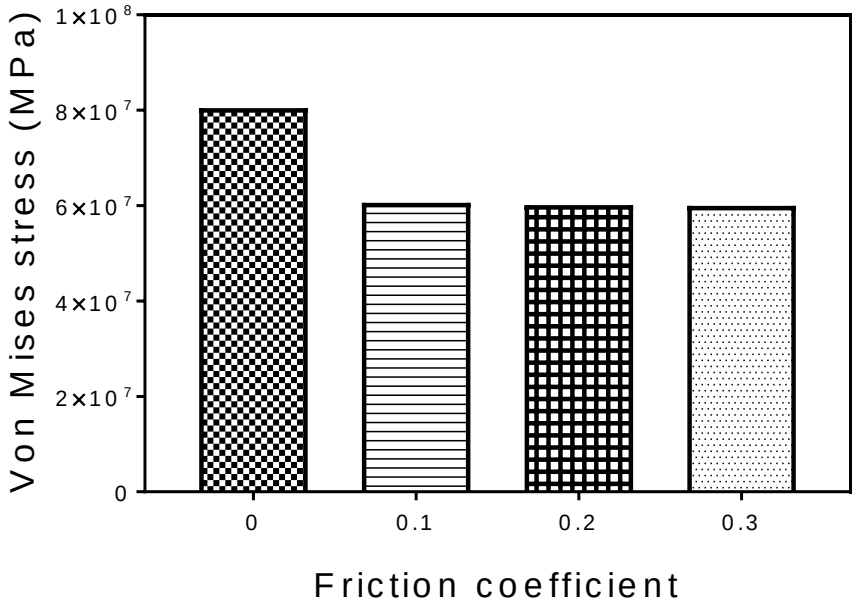

Figure 4.21: Effect of friction coefficient on maximum Von Mises stress.

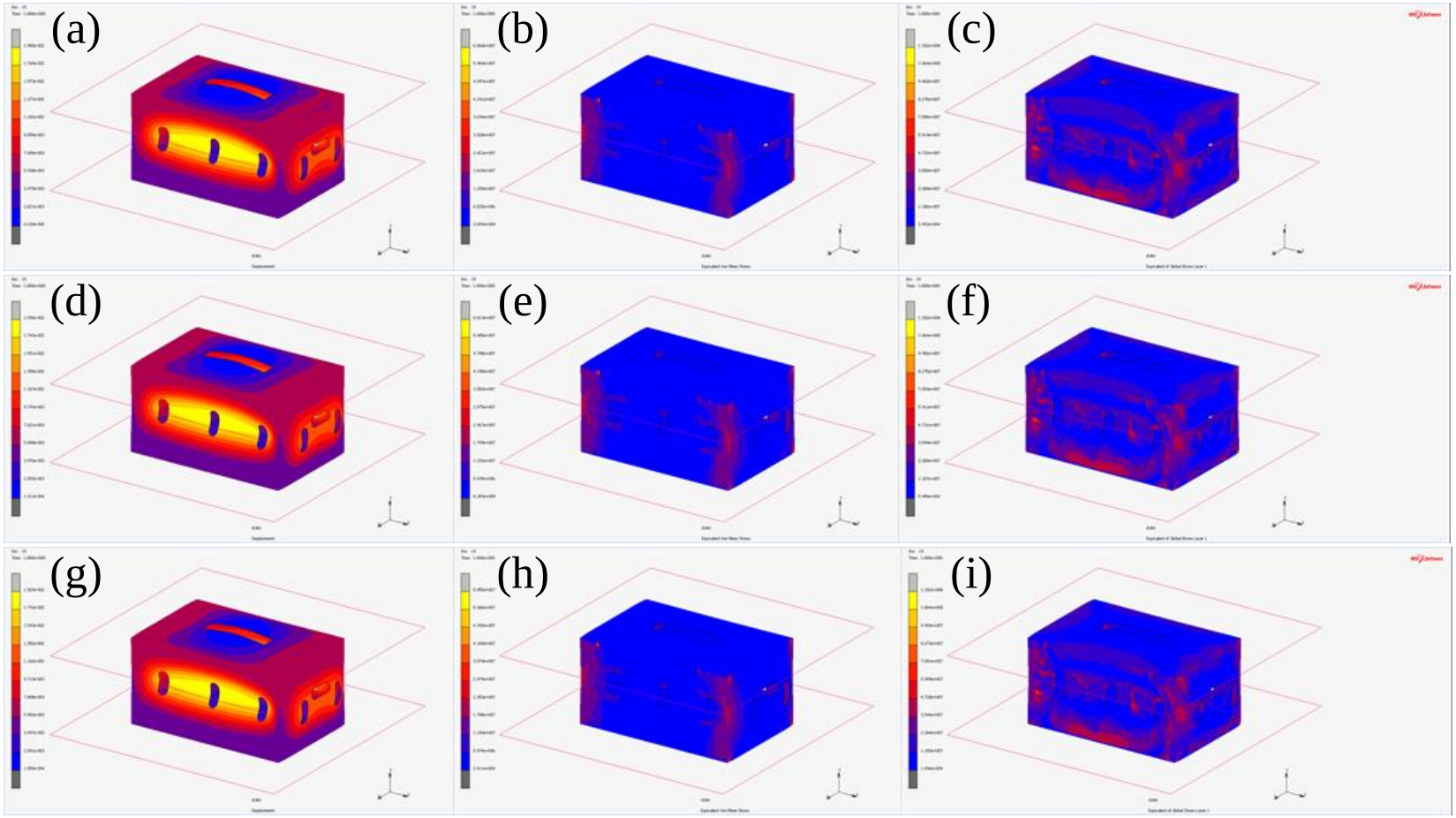

Figure 4.22: Fringe plot from the contact model simulation for (a) displacement of the standard vent package with 0.1 friction coefficient, b) equivalent Von Mises stress of the standard vent package with 0.1 friction coefficient, (c) equivalent global stress of the standard vent package with 0.1 friction coefficient, (d) displacement of the standard vent package with 0.2 friction coefficient, (e) equivalent Von Mises stress of the standard vent package with 0.2 friction coefficient,

(f) equivalent global stress of the standard vent package with 0.2 friction coefficient, (g) displacement of the standard vent package with 0.3 friction coefficient, (h) equivalent Von Mises stress of the standard vent package with 0.3 friction coefficient and (i) equivalent global stress of the standard vent package with 0.3 friction coefficient.

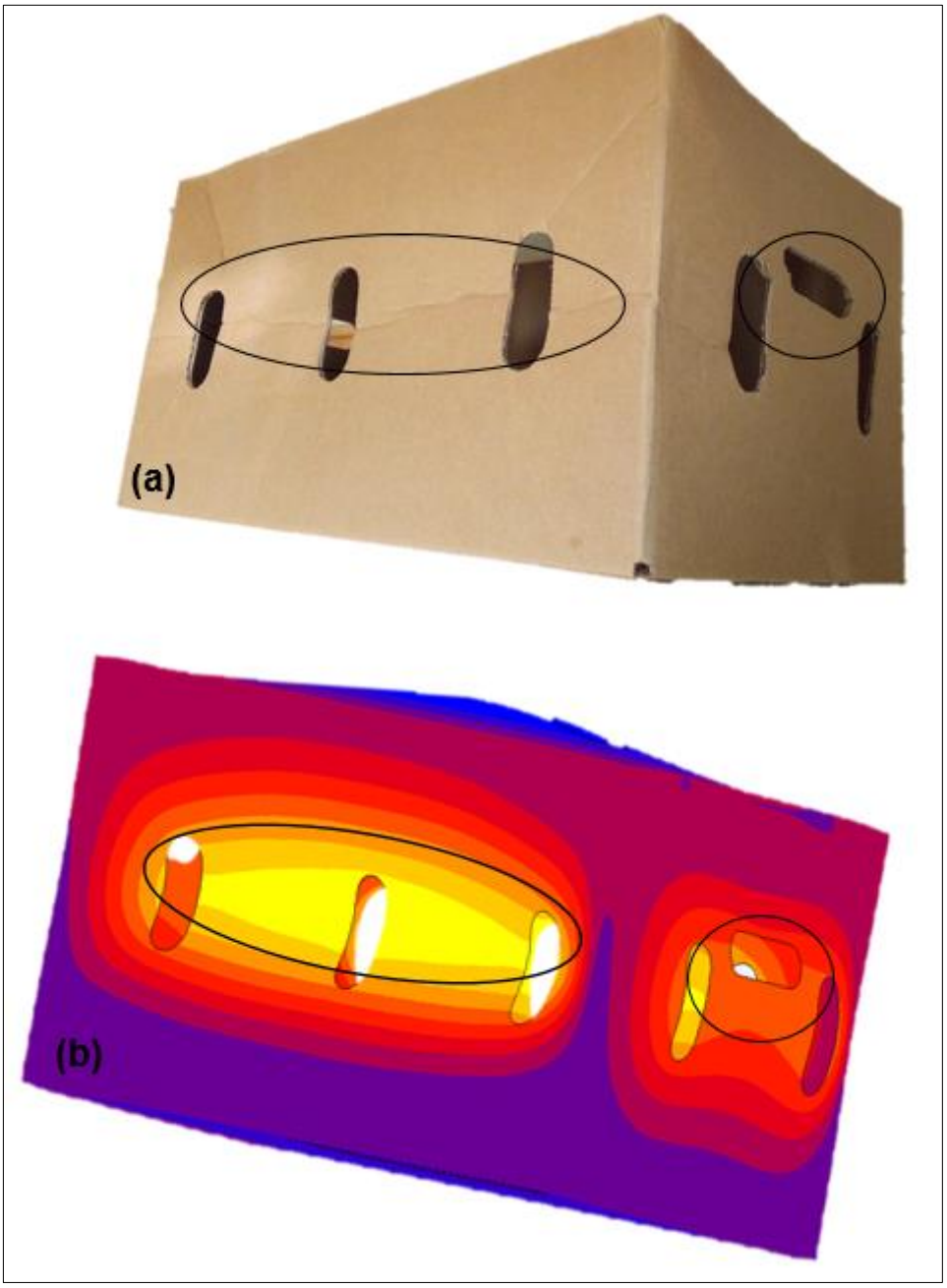

Figure 4.23: Example of the displacement pattern from the (a) experimental and (b) simulation (with 0.1 friction coefficient) results.

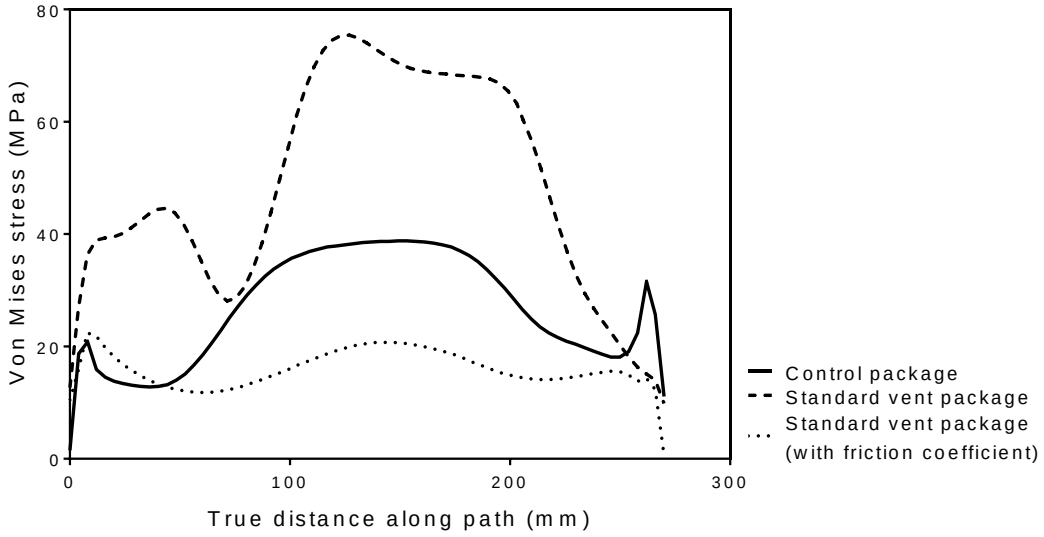

Figure 4.24: Path plot of the Von Mises stress along the corner of the package from the bottom to the top (height of the package).

Table 4.1: Thickness for the paper grade.

Paper grade	Thickness (mm)
125FL	0.1992±0.005
165SC	0.2174±0.001
175SC	0.2646±0.003
175T1	0.2604±0.004
140T2	0.2225±0.002

Table 4.2: Material properties for the B flute corrugated paperboard components and the homogenised core.

	Inner liner	Fluting	Outer liner	Homogenised core
E_x (MPa)	4739	5769	6232	1483
E_y (MPa)	901	1510	1847	2083
E_z (MPa)	24	29	31	7
ν_{xy}	0.34	0.33	0.34	0.23
ν_{xz}	0.01	0.01	0.01	0.01
ν_{yz}	0.01	0.01	0.01	0.01
G_{xy} (MPa)	800	1142	1313	680
G_{xz} (MPa)	86	105	113	27
G_{yz} (MPa)	26	43	52	59

Note: E_x, E_y, and E_y are the elastic constants (elasticity modulus) in the MD, CD and ZD, respectively; ν_{xy}, ν_{xz} and ν_{yz} are the Poisson's ratios which represent the coupling between axial and transverse strains; G_{xy}, G_{xz}, and G_{yz} are the shear moduli which represent the relationship between the three modes of shear stress and strain.

Table 4.3: Material properties for the C flute corrugated paperboard components and the homogenised core.

	Inner liner	Fluting	Outer liner	Homogenised core
E_x (MPa)	4287	5769	7240	1483
E_y (MPa)	1056	1510	1180	2083
E_z (MPa)	21	29	36	7
ν_{xy}	0.34	0.33	0.34	0.23
ν_{xz}	0.01	0.01	0.01	0.01
ν_{yz}	0.01	0.01	0.01	0.01
G_{xy} (MPa)	823	1142	1131	680
G_{xz} (MPa)	78	105	132	27
G_{yz} (MPa)	30	43	34	59

Note: Note: $\boldsymbol{E_x}$, $\boldsymbol{E_y}$, and $\boldsymbol{E_y}$ are the elastic constants (elasticity modulus) in the MD, CD and ZD, respectively; $\boldsymbol{\nu_{xy}}$, $\boldsymbol{\nu_{xz}}$ and $\boldsymbol{\nu_{yz}}$ are the Poisson's ratios which represent the coupling between axial and transverse strains; $\boldsymbol{G_{xy}}$, $\boldsymbol{G_{xz}}$, and $\boldsymbol{G_{yz}}$ are the shear moduli which represent the relationship between the three modes of shear stress and strain.

Table 4.4: Equivalent core stiffness calculations used in determining the equivalent core properties of the corrugated paperboard.

A	Theoretical value	D	Theoretical value
A_{11}	$\dfrac{E_x t}{1+6(1-\nu_{xy}\nu_{yx})\left(\dfrac{f^2}{t^2}\right)\left(\psi^2-\dfrac{\psi}{2\pi}\sin(2\pi\psi)\right)}$	D_{11}	$\dfrac{E_x t^3}{12\left(1-\nu_{xy}\nu_{yx}\right)}\psi$
A_{22}	$E_y t\psi$	D_{22}	$\dfrac{E_x t^3}{12\left(1-\nu_{xy}\nu_{yx}\right)}\psi+\dfrac{1}{2}E_y t f^2$
A_{12}	$\nu_{xy}A_{11}$	D_{12}	$\nu_{xy}D_{11}$
A_{33}	$G_{xy}\dfrac{t}{\psi}$	D_{33}	$G_{xy}\dfrac{t^3}{12\psi}$

where ψ is the wave number (flute length per liner length), t is the corrugated sheet thickness, f is the amplitude of the flute, E_x is the elastic modulus in the MD, E_y is the elastic modulus in the CD, ν_{xy} is the major Poisson's ration (transverse contraction due to an axial extension), ν_{yx} is the minor Poisson's ration (axial contraction due to a transverse extension), G_{xy} is the shear modulus.

Note: The corrugated paperboard was approximated by ignoring the bending extension-coupling matrix assuming a symmetric laminate. Hence, the matrix B is zero.

Table 4.5: Edge compression resistance and flat crush resistance of the studied C and B flutes corrugated paperboards.

Corrugated paperboard property	Flute profile	
	C flute	B flute
ECT (kN m^{-1})	6.40±0.07[c]	4.32±0.03[d]
FCT (kN m^{-2})	397.18±9.34[a]	256.04±4.33[b]

Note: Values show the mean and standard error. Values within a column followed by a different letter within a block are significantly different according to Duncan's Multiple Range tests. ECT and FCT means edge compression test and flat crust test, respectively.

Table 4.6: Buckling loads of the package.

Package type	Buckling load (N)				
	Case A boundary conditions	Case B boundary conditions	Experimental	Percentage difference (%) (Experimental and Case A boundary conditions)	Percentage difference (%) (Experimental and Case B boundary conditions)
Control	8287	8021	7268	13	10
Standard Vent	7503	6444	6797	10	5

Chapter 5. Investigating the role of geometrical configurations of ventilated fresh produce packaging to improve the mechanical strength – Experimental and numerical approach *

Abstract

Ventilated corrugated paperboard (VCP) packaging is widely utilised particularly in the fresh fruit industry to protect and preserve the packed fruit against damage and facilitate bulk handling during transportation and logistics. During handling, storage and distribution, these packages require venting to maintain uniform and adequate cooling within the package. However, the presence of ventilation openings compromises the strength of the packages. This study, therefore, aimed at evaluating the mechanical behaviour of ventilated packages by considering the influence of different geometrical configurations of vents. The compression strength of four package designs, each for three vent areas (2%, 4%, and 8%) and three corrugated paperboard grades (B-, C- and BC-flute boards) were quantified experimentally and results were compared with finite element simulations. A negative and almost linear relationship was found between compression strength and vent area. Packages with BC-flute board grade and B-flute board grades had the greatest and lowest compression strength, respectively, with percentage reduction as high as 72% for 2% vent area, 65% for 4% vent area and 67% for 8% vent area. The Edge and Standard vent package designs performed best compared to the Alt and Multi vent package designs. Numerical results and experimental results were in good agreement, within 10%. Irrespective of the package design, maximum stress was observed to be concentrated at the corners of the package. This study demonstrated the need for alternative package designs to improve the mechanical strength while still providing proper and adequate ventilation to the packed produce.

Keywords: Ventilated packaging, buckling load, vent area, finite element analysis, compression strength, package design.

---

*Sections of this work have been published in:

Berry, T.M., **Fadiji, T.S**., Defraeye, T., Opara, U.L., 2017. The role of horticultural carton vent hole design on cooling efficiency and compression strength: A multi-parameter approach. *Postharvest Biology and Technol*ogy, 124, 62–74.

5.1 Introduction

In the postharvest handling and distribution of fresh and processed food, packaging is very crucial (Opara & Fadiji, 2018; Fadiji et al., 2017; 2016a, b, c; Pathare & Opara, 2014; Pathare et al., 2012b). The function of packaging includes protecting the packed product, facilitating storage, handling and transportation of the products as well as advertising packed products to the end-users (Marsh & Bugusu, 2007). The use of corrugated paperboard packages has increased extensively and has remained an essential part of the growing food packaging industry (Han & Park, 2007; Beldie et al., 2001). However, in the supply chain journey and distribution of fresh horticultural produce, packages and produce are exposed to various loads, which could be static or dynamic (Singh et al., 2009). Stacking packages on one another results in an internal pressure of the package within a stack, and in combination with the pressure from the environment lead to static loads. The dynamic loads experienced by the package come from shock and vibration during transportation (Beldie et al., 2001). These loads can cause damage to the package and packed produce either singly or in combination (Opara & Fadiji, 2018; Pathare & Opara, 2014; Lu et al., 2012; 2010).

Corrugated paperboard has been prevalently used to manufacture produce containers, particularly in the fresh fruit industry. Its success is due to numerous advantages: efficient and economic material characteristics, good protection of the produce, low cost, recyclability and biodegradability (Fadiji et al., 2018a; Talbi et al., 2009; Han & Park, 2007). The structure of corrugated paperboard comprises of two liners separated by a corrugated core usually referred to as fluting (Figure 5.1). The orthotropic nature of corrugated paperboard is characterised mainly by three directions, which are the machine direction (MD), cross direction (CD) and the thickness direction (ZD). These directions define the properties of the paperboard and correspond to the direction parallel to rolling during manufacturing, in-plane direction normal to the MD (transverse) and out-of-plane through the thickness direction, respectively (Figure 5.1) (Bartolozzi et al., 2013; Allaoui et al., 2011; 2009a, b; Jiménez-Caballero et al., 2009; Talbi et al., 2009; Biancolini, 2005).

Horticultural produce such as fruit and vegetables remain alive after harvest, taking up oxygen and producing metabolic heat, water vapour and carbon dioxide (Opara, 2011). Due to the adverse effect of high temperature in promoting senescence and quality degradation of horticultural produce, rapid removal of heat build through cooling and maintaining continuous uniform airflow are crucial to increase the shelf life and assure the safety and quality of the produce (Defraeye et al., 2015; Opara, 2011). This led to the advent of ventilated corrugated paperboard packaging which has the ability to promote rapid cooling and maintain an efficient air distribution within the package with reduced internal packaging material (Defraeye et al., 2015; Pathare et al., 2012b; Thompson et al., 2010; De Castro et al., 2005). Although maintaining an efficient and adequate cold chain is important in postharvest handling of fresh produce, there is a need to balance this with the need to ensure the physical protection and resistance of the package and packed produce to mechanical

loads (impact, compression or vibration) that may arise during postharvest handling (Opara, 2011; Vigneault & De Castro, 2005; Vigneault & Goyette, 2002).

The ventilation openings in packages can be designed to meet various strength and cooling criteria (Han& Park, 2007; Jinkarn et al., 2006). A proper package must take into consideration different geometrical configurations of the vent such as total vent area, shape, size and location to enhance cooling while still providing sufficient mechanical strength (Pathare et al., 2012b; Biancolini & Brutti, 2003; Émond & Vigneault, 1998). Excessive or inadequate ventilation will jeopardise the quality of both the package and the packed produce through their effects in maintaining the cold chain (Opara, 2011). About 9–20% decrease in the strength of fruit packages was reported to be due to ventilation holes. Poorly designed ventilation openings forces package designers to use higher board grades, consequently increasing the production cost of the packages (Han& Park, 2007). The need to balance the requirements of both the packed produce and the package was highlighted by Singh et al. (2008).

During the distribution of fresh produce, excessive multi-layer stacking of packages is a primary concern for designers. The bottom package experiences the highest load and hence must possess adequate and sufficient compression strength to withstand the load without collapsing (Daxner et al., 2007). Jiménez-Caballero et al. (2009) described compression strength as the most important requirement common to all package types, particularly corrugated paperboard packages, since any package has to support the weight of the other packages stacked on top of it. Furthermore, to achieve an optimum between produce protection and efficient packaging design, the package compression strength is the primary property to balance package integrity and waste. Improving the package design continually have resulted in better packages, which in turn provides better protection to the packed produce. However, optimal package design remain a challenge in the packaging industry (Biancolini et al., 2005). A clear understanding of the detailed design factors is therefore crucial (Biancolini & Brutti, 2003).

Different models have been developed to predict the compression strength of corrugated packages. The most well-known semi-empirical formula is the McKee's equation (Pathare & Opara, 2014; McKee et al., 1963). This has been a lasting contribution to the design of corrugated paperboard packages, especially in the prediction of package compression strength (Dominic et al., 2015). The equation has been modified to fit in various conditions for example, Kawanishi (1989) adjusted the formula to predict the compression strength of regular slotted container (RSC) packages and based on the board ring crush strength, Kellicutt and Landt (1952) predicted the package compression strength. However, the need for a more accurate prediction of the compression strength of corrugated paperboard packages has led to the use of finite element analysis (FEA). FEA has the advantages to save time and cost compared to experimental analysis (Park et al., 2012; Delele et al., 2010; Haj-Ali et al., 2009). In addition, detailed analysis is possible by adjusting

several parameters (geometrical configurations) and extending the analysis to different package types (Jiménez-Caballero et al., 2009).

Using FEA, Pommier et al. (1991) predicted the top to bottom compression strength of a corrugated paperboard carton. Beldie et al. (2001) modelled the mechanical behaviour of paperboard packages subjected to static compression load. The paperboard was modelled as an orthotropic, linear elastic-plastic laminate. The initial stiffness (resistance to bending caused by a given applied force) of the package was reported to be due to the low stiffness of the lower and upper corners of the package. Numerical analysis was in agreement with experimental results. Biancolini and Brutti (2003) investigated the buckling behaviour of corrugated board packages by means of numerical and experimental analysis. The authors used a homogenisation procedure for the corrugated board and elastic material properties. Model results could accurately predict the incipient buckling observed during the experimental analysis.

The work by Han and Park (2007) used FEA to investigate the loss in package strength due to design parameters such as ventilation openings. The authors considered the stress distribution and stress levels on the package for the different styles of vent holes. Vertical oblong-shaped vents symmetrically placed within a certain distance to the left and right from the centre was reported to be the most appropriate shape. The FEA simulation results revealed a strong correlation with the experimental data. Although the experimental study by Singh et al. (2008) showed that circular vent holes performed poorly in retaining the strength of single walled corrugated boxes when compared with vertically oriented rectangular or parallelogram vent holes, the study by Jinkarn et al. (2006) conversely reported circular ventilation openings to have better mechanical strength retention of a package.

Among many factors such as paper stiffness, package shape, pre- and post-printing on the corrugated materials, and package and produce interactions that affect the strength of corrugated paperboard packaging, ventilation opening configurations and board grades play a crucial role. In addition, although there is scholarly evidence on the mechanical strength of packages and a few studies using FEA, there is a need for further research combining different package design configurations including ventilation openings and paperboard grades. Additionally, detailed understanding of FEA in order to improve its numerical accuracy by incorporating geometrical nonlinearity such as contact analysis is paramount. The aim of this research was to investigate the role of geometrical configurations of vents on corrugated paperboard package to improve the mechanical strength. The results of the FEA were validated with experimental studies.

5.2 Finite element analysis

5.2.1 Package design and properties

Telescopic cartons with four vent configurations were evaluated in this study: Standard vent, Altvent, Multivent and Edgevent package designs. All the package designs had the same geometrical dimensions (500 x 333 x 270 mm), with a length-to-height ratio of approximately 1.85. The Standard vent package (total vent area, TVA = 4%), usually with four internal pulp trays is extensively and commercially implemented for apple packaging in the export cold chain (Berry et al., 2016; 2015). In handling fruit commercially, the use of trays is a common practice (Berry et al., 2017). The Multivent and the Altvent designs were proposed as possible replacements to the Standard vent as they may improve ventilation and airflow distribution between the packed fruit, placed on the trays. Based on a similar design, which has been implemented for handling citrus fruit due to its successful application and high performance, the Edgevent design was proposed in this study (Berry et al., 2017; Defraeye et al., 2014; 2013; Delele et al., 2013a, b). For each of the package designs, three vent hole areas were evaluated (total vent area = 2%, 4% and 8%). A package without vent holes with the same geometrical dimensions (500 x 333 x 270 mm) was used as a benchmark for comparison purposes. The package designs were constructed to have maximum ventilation hole alignment during pallet stacking. Dimensions for the package designs are shown in Figure 5.2.

The cartons were made using a corrugated fibreboard-cutting machine (KM series 6, Kasemake House, Cheshire, United Kingdom), shown in Figure 5.3, and then assembled and glued by hand. The corrugated paperboard used for manufacturing the packages was made from Kraft paper. For the different package designs, three corrugated paperboard grades were evaluated: single wall corrugated paperboard with a B and C flute profile, and a double wall corrugated paperboard with a BC flute profile. The paper grammage (g m^{-2}) combination for B and C flutes was 140T2/175SC/165SC and 175T1/175SC/125FL, respectively. FL indicates fluting liner, SC indicates semi-chemical paperboard, T1 indicates fully recycled board and T2 indicates partly recycled linerboard. Based on ten replicates according to ISO 534 standard procedures (ISO, 2011), the thicknesses of the paper samples were 0.1992 mm, 0.2174 mm, 0.2646 mm, 0.2604 mm and 0.2225 mm for 125FL, 165SC, 175SC, 175T1 and 140T2, respectively. Based on ten measurements, the thicknesses of the corrugated paperboards used to manufacture the cartons were about 2.8 mm, 3.9 mm and 6.2 mm for the B, C and BC boards, respectively. The edge compression resistance measured according to FEFCO No. 8 recommendations for a rectangular corrugated paperboard (100 mm x 25 mm) was 4.32 kN m^{-1} for the B-flute board, .6.40 kN m^{-1} for the C-flute board and 6.63 kN m^{-1} for the BC-flute board.

5.2.2 FEA modelling and procedures

ANSYS® Design Modeller™ Release 18.1 (ANSYS, Canonsburg, PA, USA) was used to develop the geometry of the package designs. Mesh generation and

numerical analyses were done with MSC Patran (MSC Software Corporation, CA, USA) and Mentat/Marc (MSC Software Corporation, California, USA), respectively. The choice of the analysis software, Marc, was due to its robust capabilities for nonlinear problems such as contact, large deformation and multiphysics analyses. The material properties used in the simulation were linear elastic 3D orthotropic properties. As employed in the study by Fadiji et al. (2016c), the package was modelled as a composite structure, which comprises of three layers: the liners (outer and inner) and a solid core (Figure 5.4). The equivalent properties for the solid core were calculated based on methods reported by Biancolini et al. (2010) and Biancolini (2005). The method approximated the corrugated sandwiched structure as a homogenous material and the stiffness matrix was calculated based on the function that describes the fluting of the corrugated paperboard. In this study, a sine wave pattern was used to approximate the fluting (Figure 5.5).

The ABD matrix of the laminate was calculated using the equivalent plate bending stiffness formula for the corrugated core as shown in Table 5.1. The ABD matrix defines the elastic properties of the entire laminate and provides a relation between the applied loads and the associated strains in the laminate, hence it allows for determining the force and moment resultants given a set of imposed strains and curvature. Matrix A represents the extension in-plane stiffness matrix, matrix B represents the bending extension-coupling matrix and matrix D represents the bending stiffness matrix. In the approximation of the corrugated paperboard, the bending extension-coupling matrix was ignored, assuming a symmetric laminate. Hence, the matrix B was taken as zero.

In the FEA simulation, three mechanical properties were used as input parameters: Young's modulus, shear modulus and Poisson's ratio. Following the ISO 1924-2 recommendations (ISO, 2008), Young's modulus in the MD and CD were obtained by simple tensile tests while the Young's modulus in the ZD was estimated using Eq. (5.1) as given by Sirkett et al. (2007) and Beldie et al. (2001). Shear modulus values were derived from Young's modulus as given by Sirkett et al. (2007) in Eq. (5.2).

$$E_{ZD} = \frac{E_{MD}}{200} \tag{5.1}$$

$$\begin{aligned} G_{xy} &= 0.387\sqrt{E_{MD}E_{CD}} \\ G_{xz} &= \frac{E_{MD}}{55} \\ G_{yz} &= \frac{E_{CD}}{35} \end{aligned} \tag{5.2}$$

E_{MD} and E_{ZD} is the Young's modulus in the machine direction and thickness direction, respectively while $G_{xy}, G_{xz},$ and G_{yz} are the shear moduli. Owing to the difficulty involved in measuring the Poisson's ratio of paperboard, the values given by Biancolini and Brutti (2003) for similar materials (0.33 for the flute paper and 0.34 for the liners) were used for ν_{xy} in this study. ν_{xz} and ν_{yz} were set as 0.01 according to Nordstrand (1995). The properties used in the FEA simulation are summarised in Table 5.2.

To allow for proper tracking of buckling, quadrilateral shell elements were used in the simulation. A convergence study was carried out on the Standard vent package with 4% TVA and C-flute board profile, to find the proper mesh size to use in the simulation. The result of the convergence study is shown in Figure 5.6 and hence, a mesh size of 4 mm was used in all subsequent simulations. Table 5.3 shows the number of elements adopted in the FEA simulation needed to give satisfactory results for the different package configurations. Figures 5.7a and b show the boundary conditions applied in the FEA model. The top of the package was constrained along the lengthwise (long) side of the package to allow for translation in the *y* direction while the translation in the *x* and *z* directions was prevented. Rotation in the *y* and *z* direction was fixed while the rotation in the *x* direction was allowed. Along the width (short) side of the package, translation and rotation were allowed in the *y* and *z* directions respectively, while the other directions were fixed. At the bottom, the translation and rotation were fixed for the edge nodes of the bottom hole, while the rotation was fixed for the remaining nodes at the bottom. Face pressure was applied at the top of the package. Linear buckling analysis was carried out to determine the critical buckling load and estimate the most likely buckling shape of the package. The Lanczos buckle extraction technique available in Marc was used in the analysis. In addition, a contact boundary condition was applied to study the effect of platen contact on the package strength. Nonlinear static analysis was performed and the large strain nonlinear procedure available in the Mentat/Marc (MSC Software Corporation, California, USA) finite element solver, incorporating geometric nonlinearities into the formulation was also activated.

5.3 Experimental analysis

5.3.1 Box compression test

In accordance with ASTM D4332 standard practice for conditioning containers, packages and packaging components prior to testing (ASTM, 2006), the packages were first preconditioned at 30 ± 1°C and relative humidity (RH) of 20–30% for 24 h and then conditioned at 23 ± 1°C and 50% RH for 24 h. The package conditioning was done using a versatile environmental chamber. BCTs were evaluated in accordance with the ASTM D642 Standard (ASTM, 2010), using a box compression tester (M500-25CT, Testomatic, Rochdale, United Kingdom) (Figure 5.8). A BCT is a pure top-to-bottom compression load test between flat

parallel steel plates that is carried out on an empty sealed corrugated board box using a constant deformation speed (Pathare et al., 2017). BCT was done immediately after conditioning the cartons. The cartons were compressed by applying a continuous motion of the platen at a speed of 12.7 ± 2.5 mm min^{-1} until failure was reached. The fixed-platen method of the compression tester was used i.e. the platen was not allowed to rotate. A preload of 222 N was applied on the test cartons to remove the initial transient effects. For each package design, eight samples were tested.

5.3.2 Statistical analysis

The statistical evaluations were performed using Statistica (v. 13.0, Statsoft, USA). The experimental data were treated with factorial analysis of variance (ANOVA) at 95% confidence level. The independent variables were the vent sizes and the corrugated paperboard grades. Duncan's multiple posthoc tests were used for comparison between the means with the differences at $p<0.05$ considered statistically significant. Graphical representations were made using GraphicPad Prism 7 software (GraphicPad Software, Inc. San Diego, USA). The standard error of the mean is indicated by error bars on the figures. Statistical difference between the mean was shown using the letters on the error bars. Means with the same letters are not statistically different. A correlation index Eq. (5.3) suggested by Lu et al. (2016) was used to check the statistical correlation between the simulation and experimental results,

$$R^2 = \frac{\sum Exp^2 - \sum \left(Exp - Sim\right)^2}{\sum Exp^2} \tag{5.3}$$

where R^2 is the correlation index, Exp and Sim represents the experimental and simulation results, respectively.

5.4 Results and discussion

5.4.1 Compression strength of the control package

A typical force-deformation curve from the box compression test for the Control package with B-flute, C-flute and BC-flute is shown in Figure 5.9. From the plot, it can be seen that the package with BC-flute board had the highest peak force (indicated with blue circle) followed by the package with C-flute board while package with B-flute board had the lowest peak force. Three distinctive regions are indicated in the force-deformation curves: toe, linear and failure regions. In the first region (toe), the carton begins to align in the direction of the load and stiffness gradually increases. Although loading in this region results in deformation, it does not exceed the elastic limit of the carton, hence unloading could subsequently restore the carton to its initial height. In the linear region, the stiffness of the carton remains approximately constant as a function of deformation. At the end of this

region, the carton starts to fail resulting in the failure region as indicated in Figure 5.9. In addition, the stiffness begins to decrease and unloading does not restore the carton to its initial length. Figure 5.10 shows the stiffness of the Control package for B-flute, C-flute and BC-flute board grades. The stiffness with BC-flute was higher than the stiffness with C-flute and B-flute by 23% and 78%, respectively. For all the board grades, there was a significant difference in the stiffness of the packages (Figure 5.10). The highest stiffness observed in the package with BC-flute may be attributed to the higher thickness of the corrugated board compared to the thicknesses of the C-flute and B-flute boards (Ramnath et al., 2016; Eriksson et al., 2014; Hägglund & Carlsson, 2012).

5.4.2 Effect of vent area and package design on package strength

5.4.2.1 B flute

Figure 5.11a shows the effect of the vent area (TVA = 2%, 4% and 8%) and package design (Alt, Edge, Standard and Multi vent hole configurations) on the compression strength. The compression strength of the package designs was observed to be significantly different from that of the Control package for all the three TVAs. For the 2% vent area, the Edge vent design had the highest compression strength of 3799.95±99.72 N, a reduction of about 12% when compared with the strength of the Control package with B-flute board. The compression strength for the Multi vent, Standard vent and Alt vent package designs was approximately 14%, 16% and 18%, respectively lower than that of the Control package. Similar to the 2% vent area, the Alt vent package design had the lowest compression strength for the 4% vent area as shown in Figure 5.11a. Here, the Standard vent design had the highest strength, 7% higher than that of the Alt vent package. The strength of the Edge and Multi vent package designs remained relatively high with a reduction of about 4.6% and 5.1% when compared with the Standard vent design. Statistically, for both 2% and 4% vent areas, no significant difference was observed in the compression strength of the Edge, Multi and Standard vent designs. For the 8% vent area, the Multi vent design was the strongest, although no significant difference in the compression strength for the Alt, Edge and Multi vent package designs could be observed. The Standard vent package showed the lowest compression strength (3035.58±108.61 N), a difference of about 8%, when compared with the compression strength of the Multi vent package. The strength of the strongest package (Multi vent) was significantly different (p<0.05) from the strength of the weakest package at 8% vent area.

5.4.2.2 C flute

For the C-flute board, Standard vent package design was the strongest while Multi vent package design was the weakest in all the vent areas (Figure 5.11b). The difference between the strongest and weakest package (Standard and Multi vent designs) was about 14%, 10% and 10% for TVA = 2%, 4% and 8%, respectively. There was a significant difference (p<0.05) between the strongest and weakest package in all the vent areas. When the compression strength of the Control package

was compared with the strongest package (Standard vent design) for all TVAs, the compression strength reduced by about 7%, 8% and 18%, respectively. The compression strength for the Alt, Edge and Multi vent designs was observed to be statistically insignificant ($p<0.05$) for the 4% vent area. For the 8% vent area, the compression strength of the Alt vent design differed significantly from the strength of the Multi vent design, with a percentage of about 10%.

For all the package designs with C-flute board, the compression strength reduced with an increase in vent area. The compression strength of the strongest package (Standard vent design) for 2% vent area reduced by 1% at 4% vent area and by 12% at 8% vent area. For the weakest package (Multi vent design), a reduction of about 10% was observed in the compression strength when the vent area was increased from 2% to 8%. For the Alt and Edge vent design, the compression strength reduced by 5% and 14%, respectively at 8% vent area when compared with 2% vent area.

5.4.2.3 BC flute

For the BC-flute board, the Edge vent package design had the highest compression strength for all the vent areas while the lowest compression strength was observed for the Multi vent design (Figure 5.11c). Except for the 2% vent area, the strongest package (Edge vent design) differed significantly ($p<0.05$) when compared with the weakest package (Multi vent design) for both the 4% and 8% vent areas. Similar to the packages with C-flute board, an increase in vent area resulted in a reduction in the compression strength for all the designs. For the Edge vent design, the compression strength reduced by 6% on changing the vent area from 2% to 4%, while a 14% reduction was observed on changing the vent area from 2% to 8%. A reduction of about 3% and 15% in compression strength was observed when the vent area was changed from 2% to 4% and from 2% to 8%, respectively for the Standard vent design. For both the Alt and Multi vent designs, changing the vent area to 2% from 4% reduced the compression strength by about 10%. Changing the vent area from 2% to 8% reduced the compression strength by 23% for the Alt vent design and by 21% for the Multi vent design.

The compression strength for all the package designs were not significantly different for the 2% vent area. Furthermore, the compression strength for the Control package was not significantly different from the Edge and Alt vent package designs. For the 4% vent area, no significant difference in the compression strength of the Edge, Alt and Standard vent package designs could be observed. However, the compression strength of all the designs was significantly lower than that of the Control package. The compression strength for the Alt, Multi and Standard vent package designs was not significantly different for the 8% vent area. Furthermore, the Edge vent design differed in strength when compared to the Alt vent design. In the same trend as the 4% vent area, the compression strength of all the package designs was significantly lower than the Control package.

5.4.2.4 Summary

The result obtained for all the board grades showed an almost linear relationship between the vent area and the reduction in compression strength. Individual regression analysis for the various package designs was significant ($p<0.05$), with r-squared values ranging from 0.799 to 0.999, indicating a good fit. Our finding was similar to the study by Park (2000) who reported about 9%-20% decrease in compression strength of fruit cartons due to ventilation holes. Another study by Han and Park (2007) investigated the loss of compression strength due to 2% vent area in double-walled corrugated cartons. The authors reported the loss in compression strength to be within 10%. Singh et al. (2008) reported that the compression strength of single-walled corrugated cartons reduced in a linear fashion in correlation with the percentage of material removed for ventilation openings.

In this present study, the Standard and Edge vent designs performed in general better when compared to other designs. As shown in Figure 5.2, the Standard vent design had three oblong shaped vent holes oriented vertically on the lengthwise side of the package. Singh et al. (2008) emphasised the shape of the vent hole as a critical factor affecting the strength of packages. Similar to the studies by Han and Park (2007) and Singh et al. (2008), who reported vertically oriented oblong vent holes as the best choice when considering the mechanical strength of the package, the Standard vent design showed good mechanical performance for all the vent areas. However, Jinkarn et al. (2006) reported that packages with circularly shaped vent holes better retained and showed the smallest reduction in compressive strength. The Edge vent design shown in Figure 5.2 with half-circular vent holes, located at the top and bottom of each side also had a good resistance to compression loads and even slightly outperformed the Standard vent design when BC-flute was used (Figure 5.11c).

Thompson et al. (2002) emphasised the importance of vent holes for cooling. It is therefore crucial to design the vent holes to provide uniform cooling of the packed produce and maintain the structural integrity of the package. As proposed by Pathare et al. (2012b) and Thompson et al. (2002), vent holes >5% of the total area of the package wall requires careful design to provide sufficient package strength. A reasonable compromise between the cooling efficiency and the mechanical resistance for paperboard packages is about 5 to 6% vent area (Pathare et al., 2012b; Thompson, 2008; Thompson et al., 2008). In addition, the length of vent holes should be <25% of the height of the package to maintain the strength and stability of the package when stacked (Han & Park, 2007). In a recent study by Berry et al. (2017), the authors investigated the effect of vent holes on the cooling performance of identical package designs used in this present study. The authors reported that the seven-eighths cooling time (SECT) of the Multi vent design was the lowest when compared to the other designs. In comparison to the Multi vent package, the SECT for the Edge, Standard and Alt vent designs was about 127%, 11% and 6% longer, respectively.

Although the compression strength of the Multi vent package design was lower compared to the other designs studied, produce packed in the Multi vent design cooled fastest (Berry et al., 2017). The shorter cooling time as reported by the authors could be attributed to the multiple vent holes placed on the face of the package as shown in Figure 5.2. This allowed for evenly distributed and uniform airflow within the package. Although the Alt vent distributed air across all the layers within the package, the lower cooling performance could be attributed to the fewer vent holes. Other studies have shown a linear relationship between the number of vent holes and airflow uniformity (Delele et al., 2013a, b; Dehghannya et al., 2011; De Castro et al., 2005). However, increasing the number of vent holes on a package results in relatively small vent holes, which can be blocked by the packed produce (Delele et al., 2013b). Due to the placement of the vent holes for the Edge vent design at the top and bottom of the package, packed produce at the top and bottom of the package cooled faster and more uniformly compared to produce placed in the middle of the package (Berry et al., 2017).

Increasing the vent area from 2% to 8% improved the cooling performance of the Multi vent package significantly by about 34% while no significant (<5%) improvements were observed for the Alt, Standard and Multi vent package designs (Berry et a., 2017). In another study by Delele et al. (2013b), increasing the vent area from 7% to 11% had no significant effect on the cooling time. It was therefore concluded that the cooling rate of packed produce does not necessarily increase on increasing the vent area above a certain value. However, the increase in vent area would have an adverse effect on the package by compromising the mechanical integrity and stability, consequently leading to the damage of the packed produce. The design of a proper package is therefore crucial and must be such that it is able to provide sufficient mechanical support to minimise produce damage (Opara & Fadiji, 2018; Biancolini & Brutti, 2003; Émond & Vigneault, 1998) while still maintaining uniform airflow and enhancing the cooling performance (Berry et al., 2016; Pathare et al., 2012b).

5.4.3 Effect of board grade and package design on package strength

Figures 5.12a – c show the effect of board grade and package design for each vent area. For all the vent areas, packages with BC-flute board had the greatest compression strength while packages with B-flute board had the lowest compression strength. The percentage difference in compression strength between the packages with BC-flute board and the packages with B-flute board for all the designs ranged from 60% to 72% for the 2% vent area, 54% to 65% for the 4% vent area and 49% to 67% for the 8% vent area. For the 2% vent area (Figure 5.12a), no significant difference in the compression strength between the package designs for the B-flute could be observed. However, the compression strength of all the package designs was significantly different from the Control package.

As shown in Figure 5.12b for the 4% vent area, the Standard vent design was the strongest for both B-flute board and C-flute board while for the BC-flute board, the

Edge vent design was the strongest package. The Alt vent design was the weakest package for the B-flute board while the Multi vent package design was the weakest for both C-flute and BC-flute board grades. For the B-flute board, the compression strength of the weakest package (Alt vent) reduced by about 7% when compared to the strongest package (Standard vent). In comparison with the strongest package (Standard vent) for the C-flute board, the weakest package (Multi vent) reduced by about 9%. Whereas for the BC-flute board, a reduction in compression strength of about 12% was observed for the weakest package (Multi vent) when compared with the strongest package (Edge vent). For the B-flute board, no significant difference in the compression strength between the strongest package and the weakest package while for C-flute and BC-flute boards, there was a significant difference (p<0.05).

Figure 5.12c shows the effect of board grade and package design for the 8% vent area. For the B-flute board packages, Multi vent package had the greatest compression strength while the Standard vent package had the lowest compression strength with a 8% difference. No significant difference was observed in the compression strength between all the package designs. In contrast, for the C-flute board packages, the Standard vent package was the strongest while the Multi vent package was the weakest with a difference of about 10%. There was a significant difference (p<0.05) in the compression strength between the strongest package (Standard vent) and the weakest package (Multi vent). For the package designs with BC-flute board, the Edge vent package was the strongest. The compression strength for the Standard, Alt and Multi vent package designs reduced by 8%, 11% and 16%, respectively when compared with the strongest package (Edge vent). Furthermore, the compression strength of the strongest package (Edge vent) was significantly difference (p<0.05) from the compression strength of the weakest package (Multi vent). The results suggest the importance of characterising different boards as well as board components in the design of package vent configuration. Lightweight liners on corrugated boards were observed to displace localised buckling, consequently affected the strength of the board (Popil, 2012). Hence, vent design should be selected with the cognisance of board properties being used in order to improve the strength of the package (Berry et al., 2017).

5.4.4 Comparison between the experimental and numerical compression strength for the package designs

Figures 5.13a – c show the plot of the buckling mode for the Control package with B-flute, C-flute and BC-flute. The buckling load or compression strength for the Control package design with B-flute, C-flute and BC-flute are 4536 N, 8021 N and 8884 N, respectively. The Control package with B-flute corrugated board had the lowest compression strength while the compression strength C-flute board and BC-flute board increased the compression strength of the Control package by 77% and 96%, respectively. Comparing the numerical compression strength of the Control package with B-flute (4334.05±85.22 N) with the experimental compression strength showed a difference of about 5%. For the Control package with C-flute (7268.57±158.47 N) and BC-flute (7945.35±261.29 N), the difference between the

numerical compression strength and experimental results were about 10% and 11%, respectively.

The plots for the buckling shape of the various package design for all the vent areas (2%, 4% and 8%) evaluated for B-flute, C-flute and BC-flute board packages are shown in Figure 5.14, Figure 5.15 and Figure 5.16, respectively. From the plots, it was observed that buckling originated from the centre of the faces of the package, particularly the lengthwise (long) side of the package. Panyarjun and Burgess (2001) attributed failure of packages to localised crushing of the board on the faces of the package. In addition, it was observed that the width (short) side of the packages was more resistance to buckling. This may be attributed to the lower width-to-height ratio of the short side with compared to length-to-height ration of the long side. Wei et al. (2011) investigated the effect of aspect ratio on the compression strength of corrugated boxes and reported a decrease in compression strength with an increase in the aspect ratio.

Figure 5.17 shows the comparison between the experimental and simulation compression strength for all the package designs. Both experimental and simulation compression strength for all the package designs were shown to be significantly dependent on the percentage of vent area (Pathare et al., 2012b; Émond & Vigneault, 1998). Table 5.4 summarises the percentage difference and the correlation index between the numerical and experimental compression strength for all the package designs, for the different board grades and vent areas. The numerical predictions of the package strength agree reasonably well with the experimental results, although in most cases the model predictions were higher than the experimental results. For the B-flute, C-flute and BC-flute board packages, the range of the percentage difference between the numerical and experimental compression strength was within 8.6%, 9.8% and 11.2%, respectively. Furthermore, a high correlation index was obtained between the numerical and experimental results.

5.4.5 Effect of platen contact on the predicted package strength

In order to demonstrate the effect of applied boundary conditions on the predicted strength of the package, a contact model was applied between the platen and the package at the top and at the bottom. The positions of the platens are illustrated in Figure 5.18. In the simulation, the package was defined as a meshed deformable body while the platens (top and bottom) were defined as rigid surface bodies. The interaction between the package and the bottom platen was defined with a glued contact type to represent a fixed boundary condition at the bottom, while the interaction between the package and the top platen was defined as a touching contact type. The top platen was position controlled and was set to move downwards 4% of the package height as suggested by Han & Park (2007). A friction coefficient of 0.1 as suggested by Fadiji et al. (2018c) was applied between the top platen and the package. The Coulomb bilinear (displacement) friction model was used in the simulation. The simulation was performed for packages with C-flute

board grades at different vent area. The maximum equivalent Von Mises stress for all the package designs at different vent area is shown in Figure 5.19.

Generally, the Von Mises stress was observed to be dependent on vent area. Packages with 8% ventilation opening had the greatest stress while packages with 2% ventilation opening had the lowest stress. The percentage difference in the stress between the 8% and 2% vent area was 62%, 25%, 66% and 54% for Standard, Edge, Alt and Multi vent designs, respectively. The presence of ventilation openings on single-walled corrugated containers was reported to cause strength reduction of about 50%. Hence, the substantial difference observed in the stress observed in this study implies that material removal from the walls of the package would lead to a decrease in the package strength, consequently reducing the stacking strength of the package and its ability to protect the packed produce. In addition, a total vent area of 5–6% for corrugated paperboard cartons is a good compromise between the ventilation area and strength (Kader, 2002). The Standard and Edge vent package designs performed better in strength compared to the Alt and Multi vent package designs (Figure 5.19). For the Standard vent package design, the difference in stress when the vent area was changed from 4% to 8% was more than the when the vent area was changed from 2% to 4%. This may be attributed to the larger openings on the walls of the package at 8% TVA. However, minimal difference in stress was observed when the vent area was changed from 2% to 4% and from 4% to 8%, for the Edge vent package design. This may be due to the positioning of the vent holes for the Edge vent design, which is far from the centre of the package walls.

It was observed that the maximum stress is concentrated at the corners of the packages for all the package designs. Hence, the failure of the carton is dominated by the corners. This may be attributed to the short height of the packages (Hägglund & Carlsson, 2012). Similar observations were reported by Han and Park (2007). Typical fringe plots of the equivalent Von Mises stress distribution at the corner of the package for the smallest vent area (i.e. 2% TVA) are shown in Figure 5.20 for all the package designs. Typical qualitative visual comparison between the experimental and simulation displacements for the largest vent area (i.e. 8% TVA) for all the package designs are shown in Figure 5.21. Generally, an outward (convex) and inward (concave) bowing of the panels occurred for all the package designs. The long (indicated by the ellipse shape) and short (indicated by the circle shape) sides of the Multi vent package had an outward and inward bow, respective for both the experimental and simulation displacements. The Standard vent package had a bowed outward on both the long side and short side of the package while the Alt vent package bowed inward on the long side and outward on the short side. The simulation and experimental displacement shapes for both Standard and Alt vent package designs were similar. For the Edge vent package, the long side of both the simulation and experimental displacement shape were similar, with an outward bow. However, a contrast was observed for the short side as the experimental displacement shape had an outward bow while the simulation displacement shape had an inward bow. Although the displacement shape gives a prior knowledge of

how the package will bulge when a load is applied, it was observed that variation could occur. The amount of bulging is usually governed by the bending stiffness and the dimension of the package (Hägglund & Carlsson, 2012).

5.5 Conclusions

This study applied experimental and numerical approaches to evaluate the effect of vent hole design on the mechanical strength of paperboard packaging used in the horticultural industry. The packages were designed to have three total vent area (TVAs = 2%, 4% and 8%) and three corrugated paperboard grades: two single-walled (B- and C-boards) and one double-walled (BC-board). Box compression test was performed at standard conditions (23 °C and 50% RH) on the packages to assess the mechanical strength, and results were compared with numerical evaluations. The mechanical strength of the packages was significantly affected by the vent area and corrugated paperboard grades. Increasing the vent area linearly reduces the strength of the packages, with r-squared values ranging from 0.799 to 0.999. Packages with BC-flute board had the greatest compression strength while packages with B-flute board had the lowest compression strength. A significant contribution of this study is the use of different package designs with the results showing that the Edge and Standard vent designs had higher resistance to compression load compared to the Multi and Alt vent designs. In addition, there was a significant interaction between the corrugated paperboard grades and the different package designs as well as the total vent area. Therefore, it is worth noting that the efficacy of the package vent hole design is largely dependent on the properties of the chosen grade of paperboard. From the numerical results, buckling originated from the centre of the long side of the package while the short side was more resistant to buckling. Furthermore, maximum stress concentration was found at the corners of the packages from the contact FEA model. These findings were compared with numerical results and were found to be in good agreement. This study highlighted the importance of evaluating the effect of geometrical configurations on package strength, underlining the effects of vent area and corrugated paperboard types. This will assist package designers develop efficient packages that will balance the need for adequate mechanical strength and provide optimum airflow within the package. Furthermore, given the substantial effect of the paperboard grade on the strength of the packages at standard environmental conditions, further research on the performance of the packages in cold chain conditions should be carried out, as these conditions may influence the properties of the paperboard grade, which in turn could influence the strength of the packages significantly.

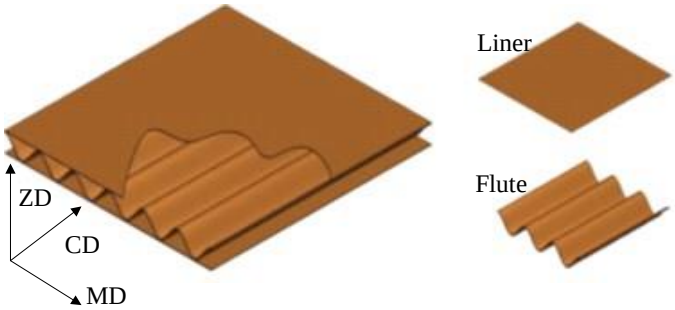

Figure 5.1: Basic geometry of a typical corrugated paperboard (MD is the machine direction, CD is the cross direction and ZD is the thickness direction).

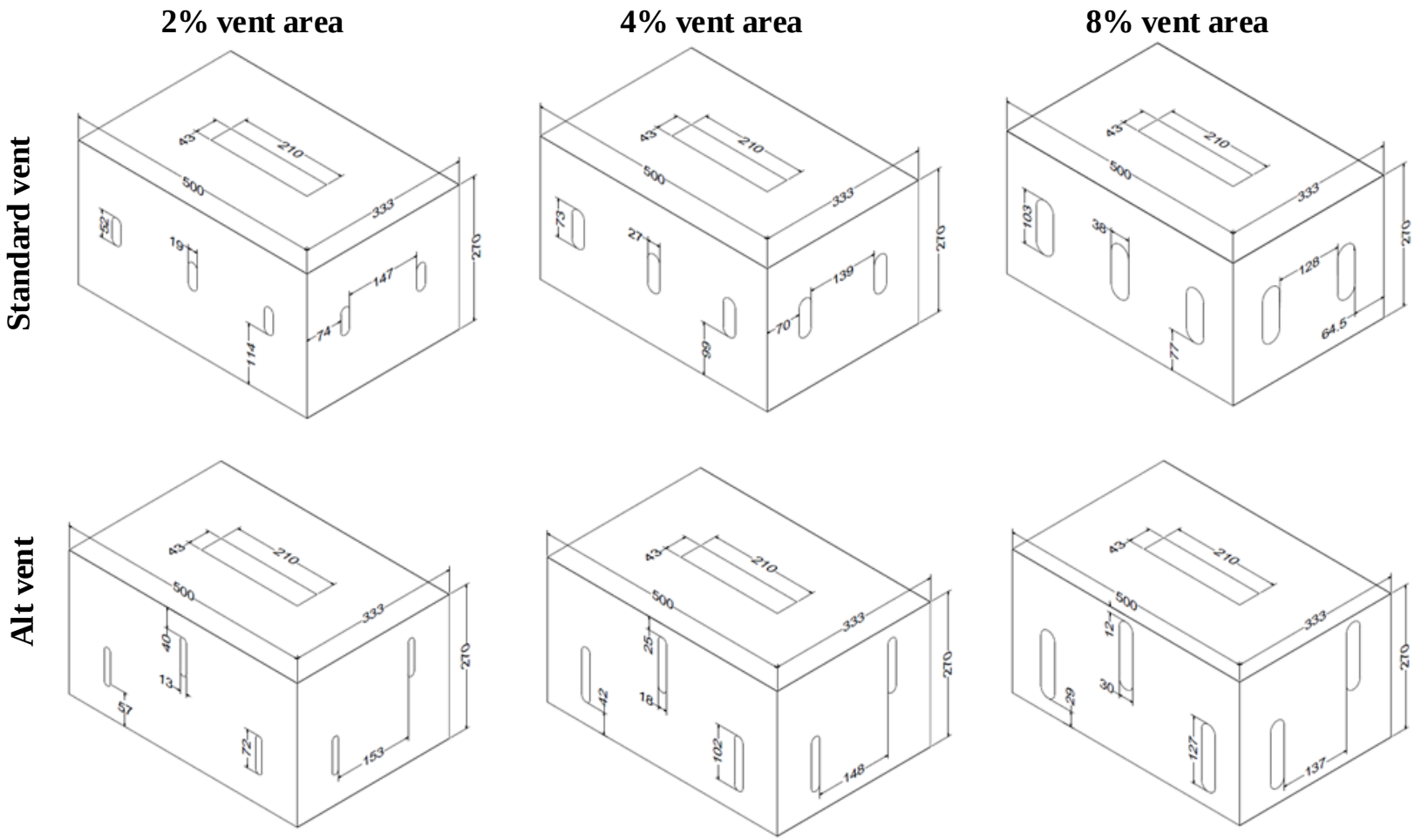

Figure 5.2: Geometry and dimension (in mm) of the corrugated paperboard packages.

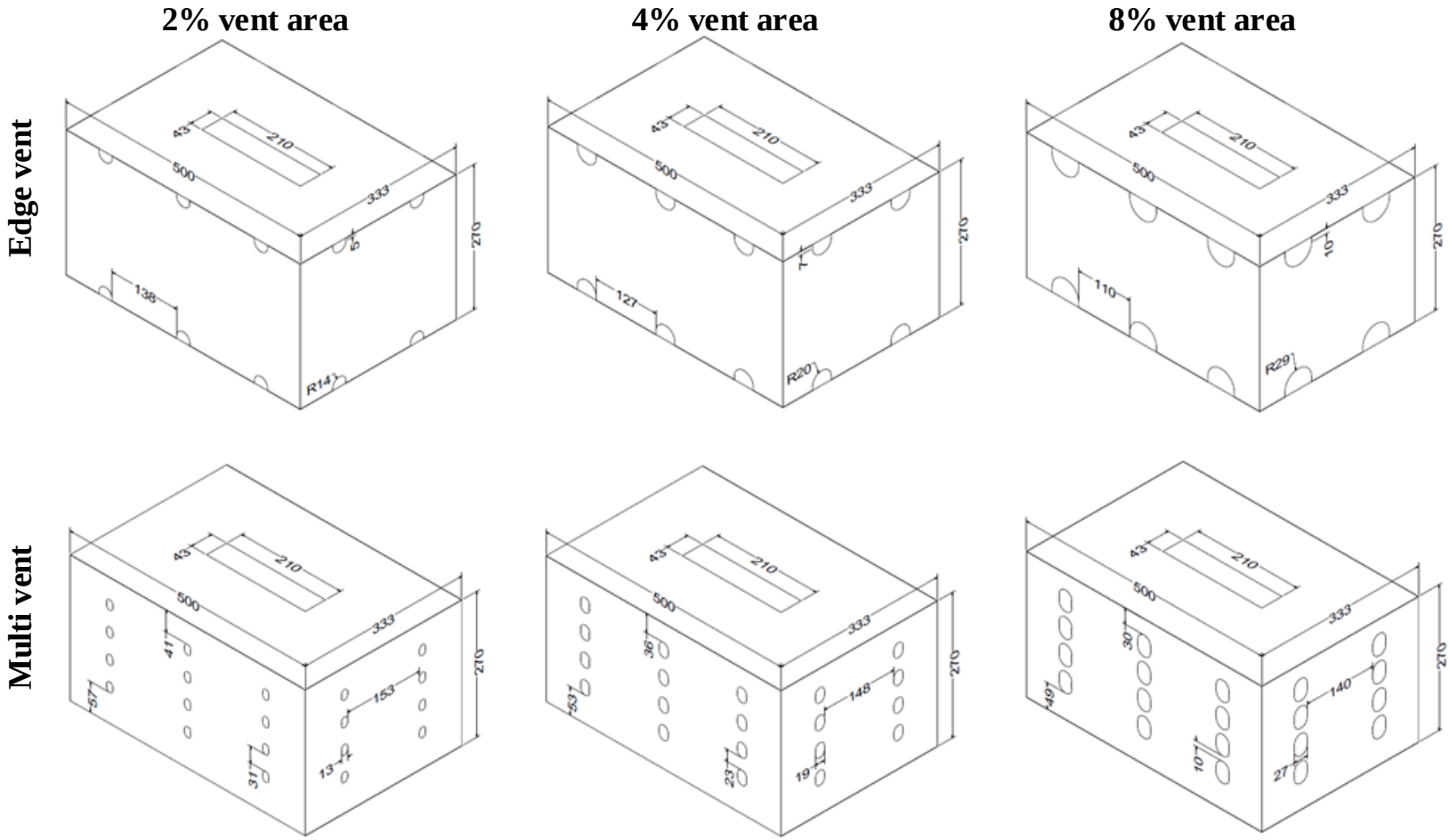

Figure 5.2: Geometry and dimension (in mm) of the corrugated paperboard packages (Continued).

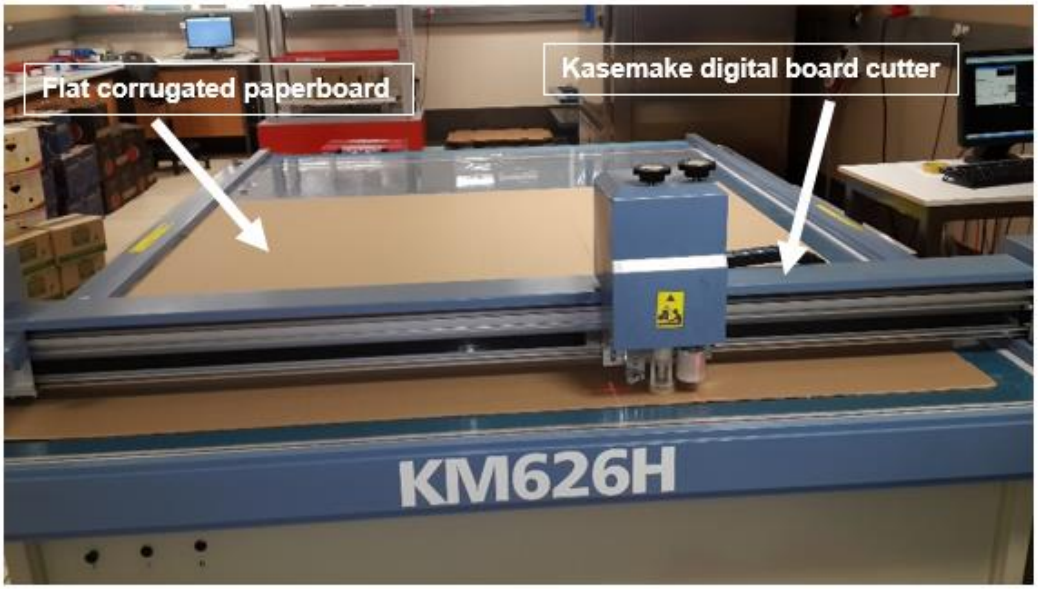

Figure 5.3: Carton manufacturing using the Kasemake digital board cutter (KM series 6, Kasemake House, Cheshire, United Kingdom).

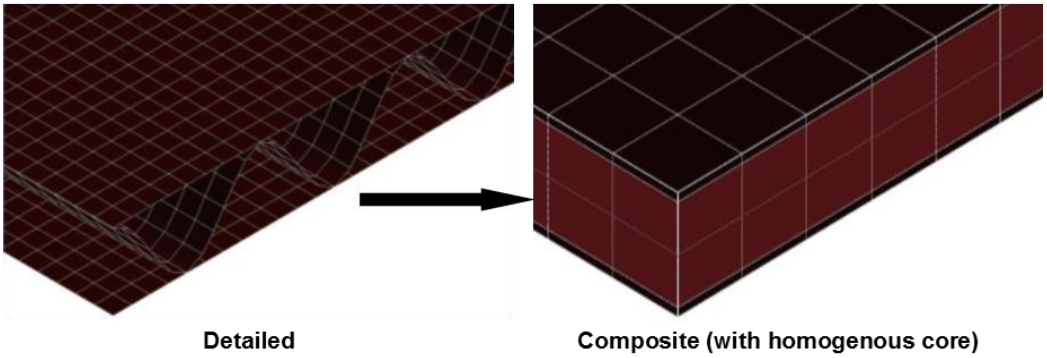

Figure 5.4: Modelling approach for the numerical simulation of the corrugated paperboard packages.

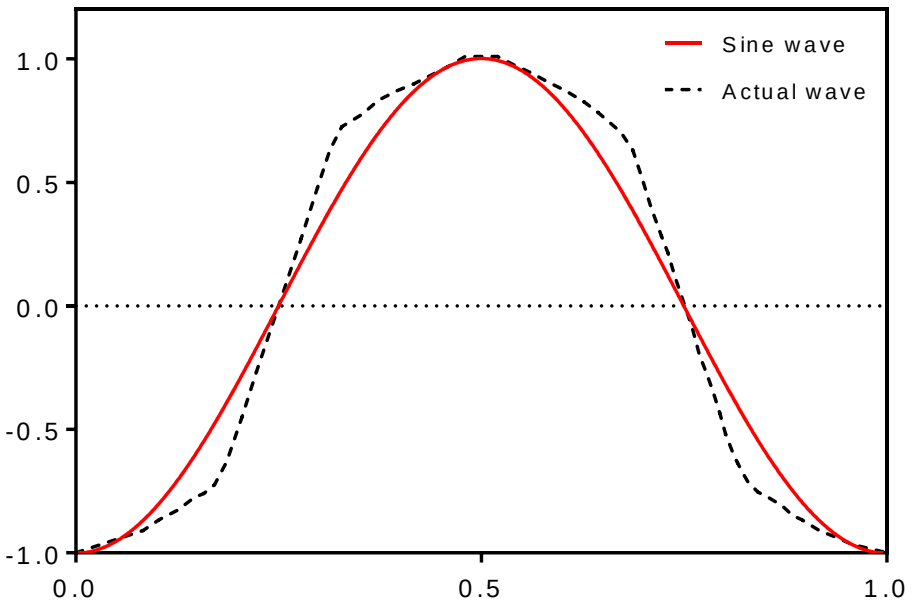

Figure 5.5: Geometry depicting the actual flute shape and the flute wave function used in calculating the solid core properties.

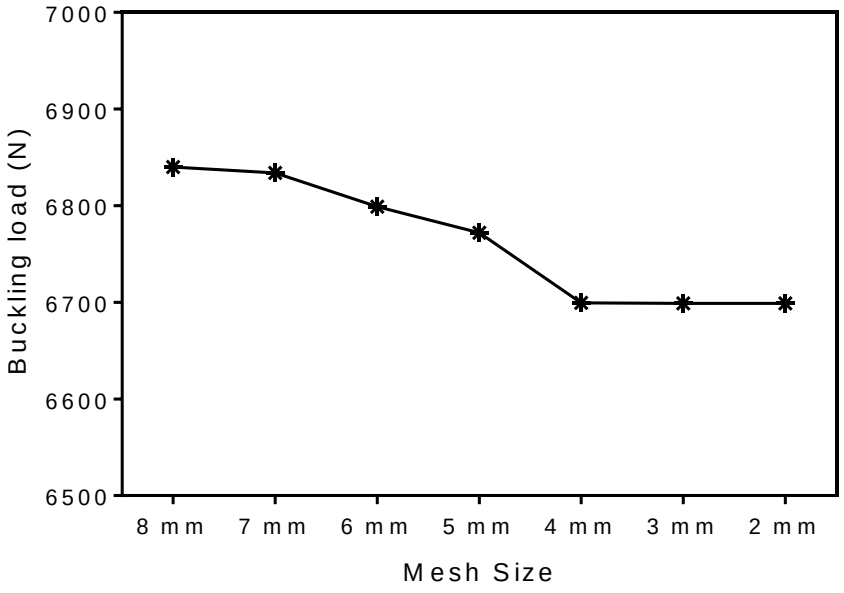

Figure 5.6: Convergence study for the simulation.

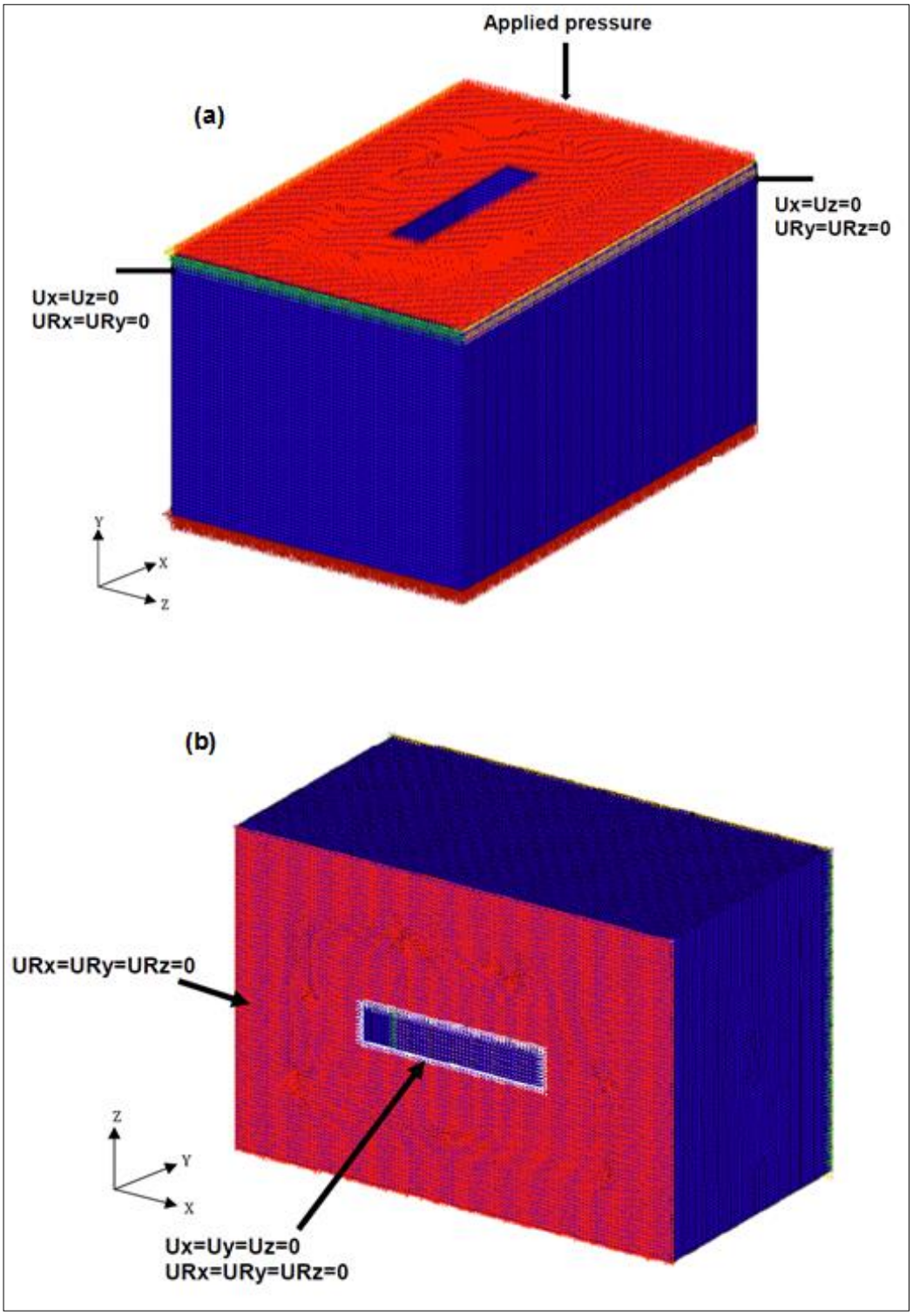

Figure 5.7: Boundary conditions used in the package simulation showing: (a) top of the package and (b) bottom of the package.

Figure 5.8: Testomatic box compression tester (M500-25CT, Testomatic, Rochdale, United Kingdom).

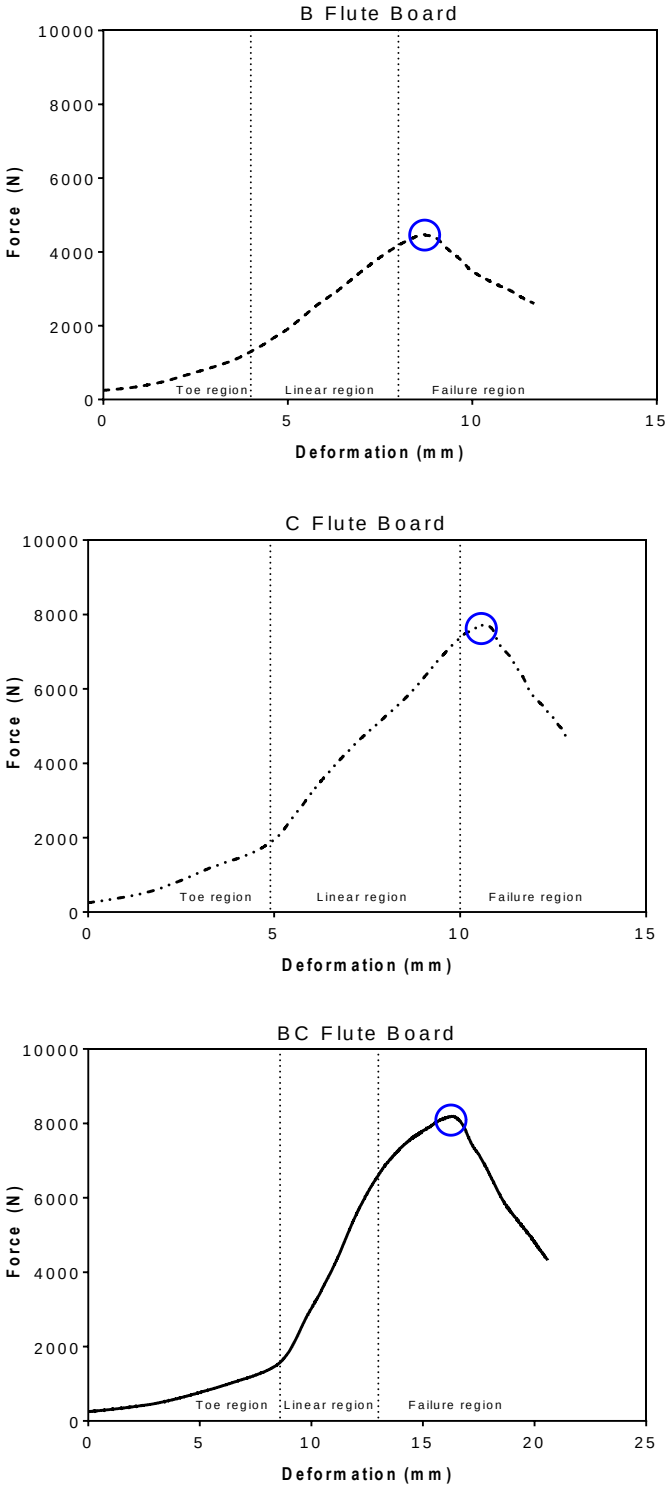

Figure 5.9: Typical force-deformation curve for the Control package with B-flute, C-flute and BC-flute board grades.

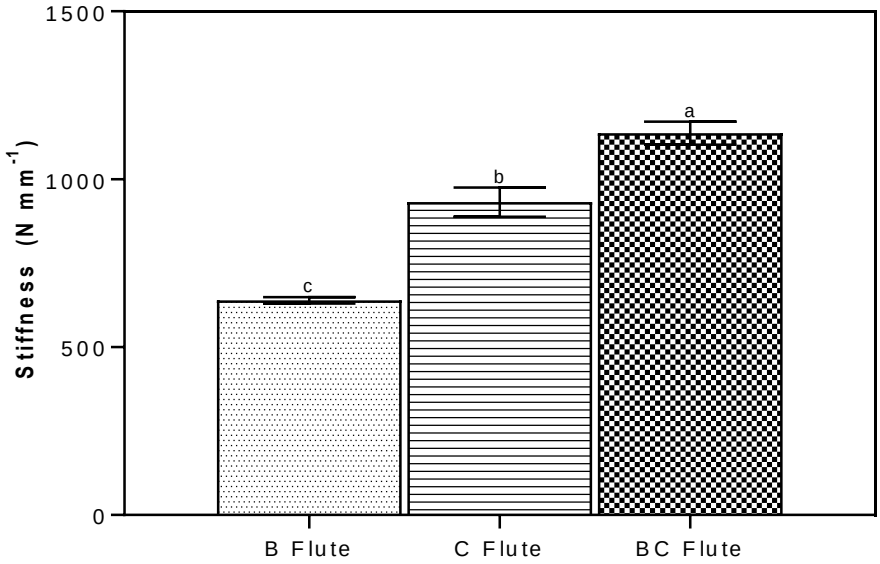

Figure 5.10: Stiffness of the Control package with B-flute, C-flute and BC-flute board grades.

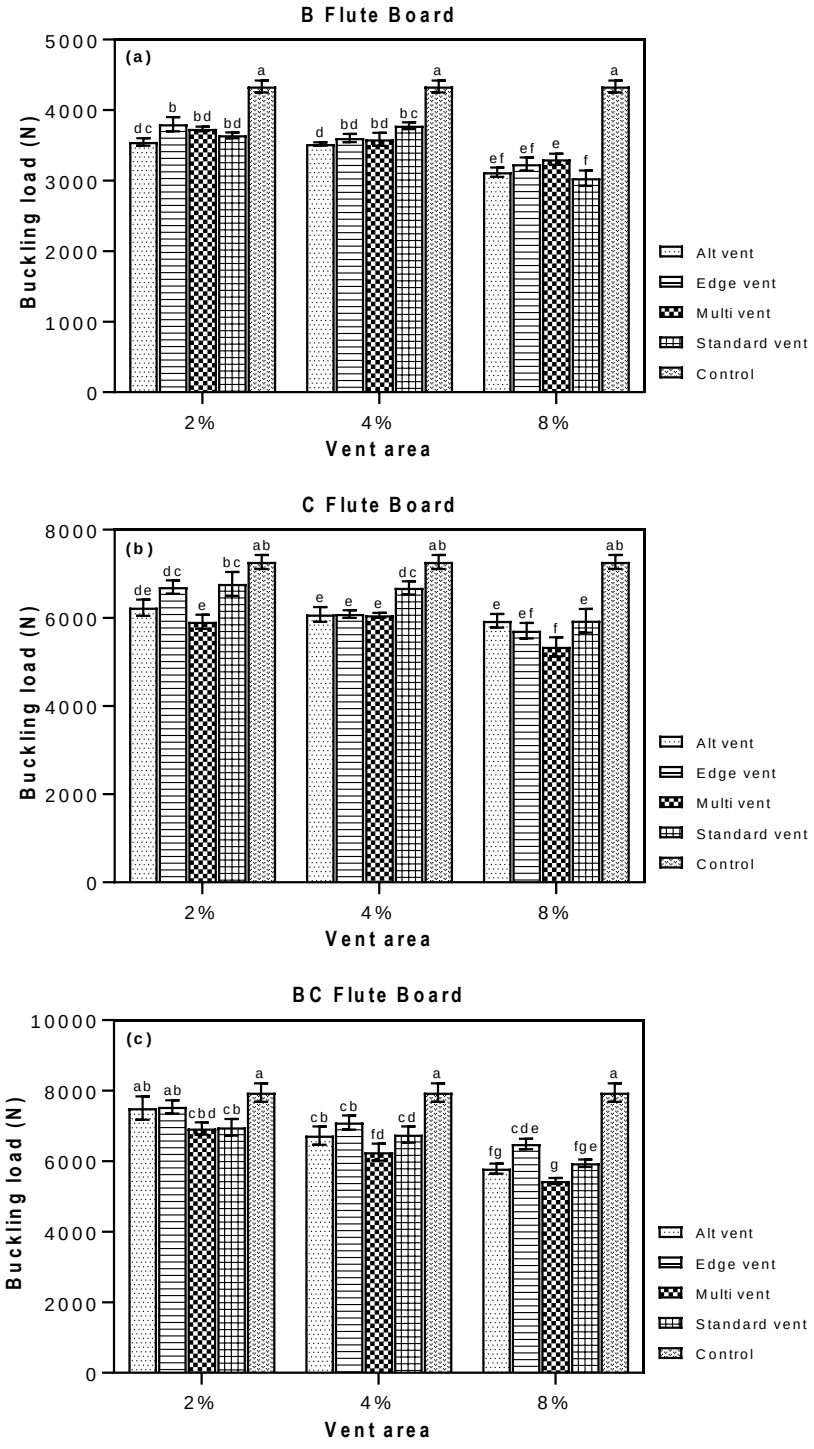

Figure 5.11: Effect of vent area and package design on buckling load for different flute board grade: (a) B-flute board, (b) C-flute board and (c) BC-flute board.

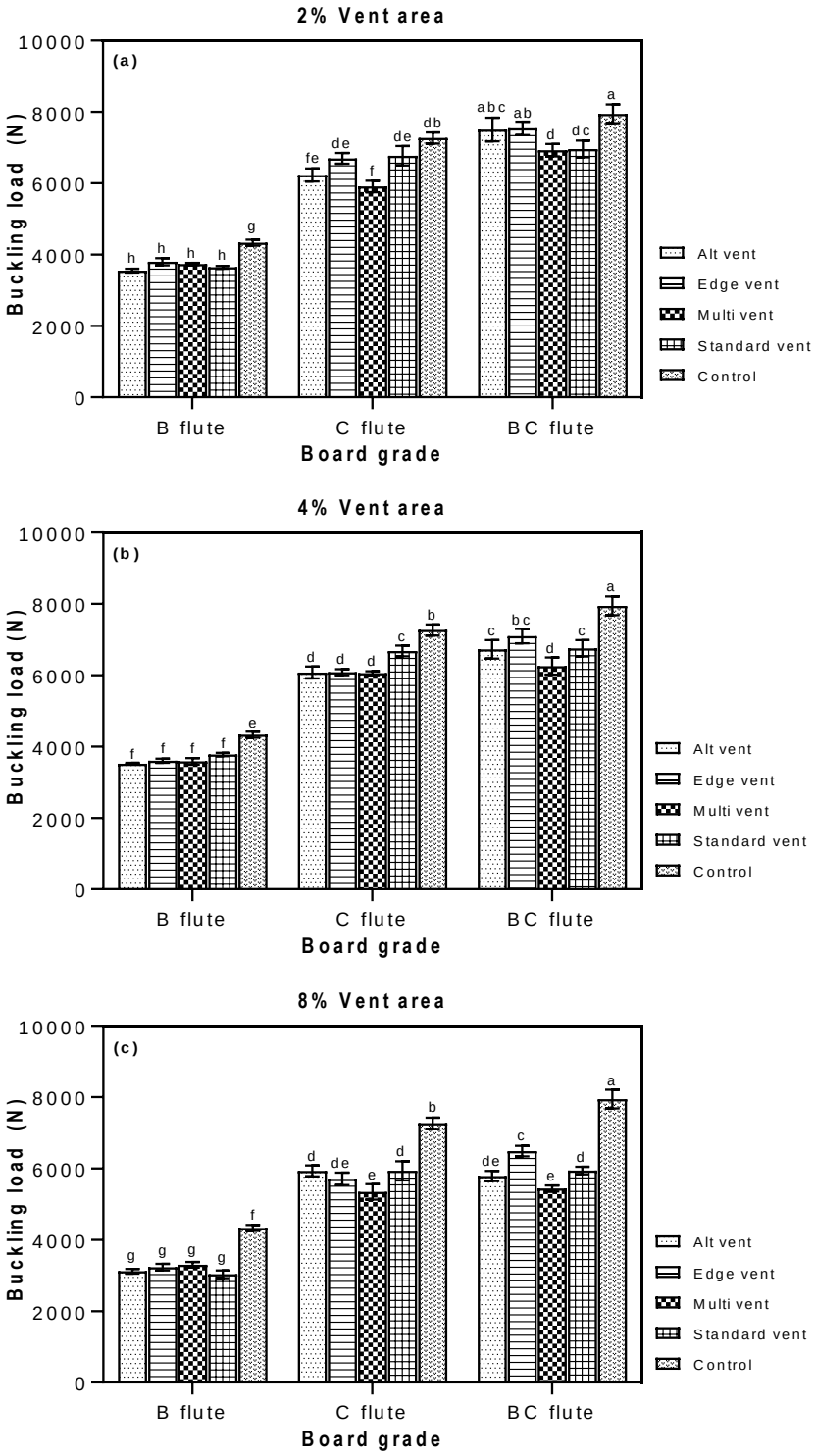

Figure 5.12: Effect of board grade and package design on buckling load for different vent area: (a) 2% vent area, (b) 4% vent area and (c) 8% vent area.

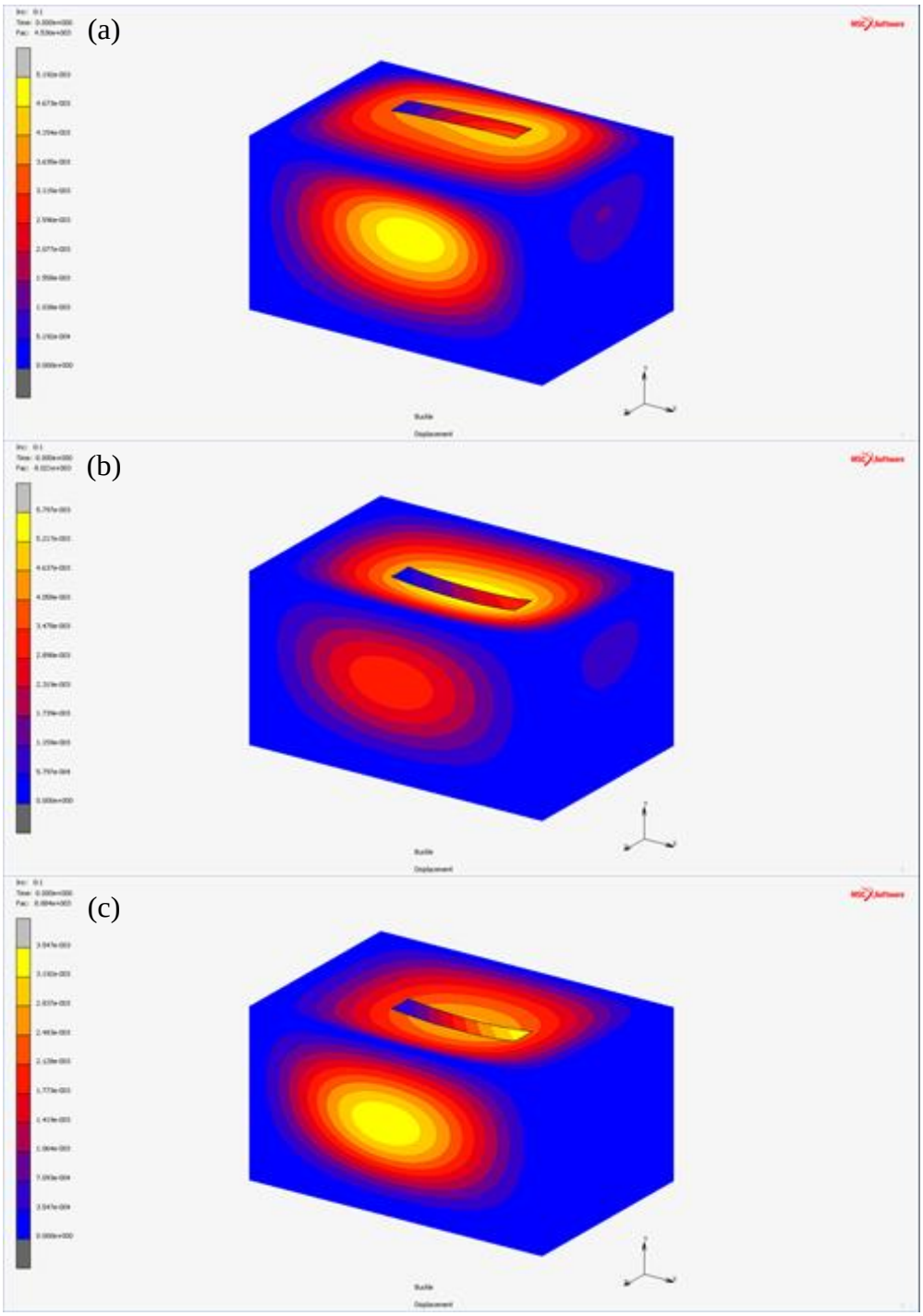

Figure 5.13: Plot of the buckling mode of the control package with (a) B-flute board, (b) C-flute board and (c) BC-flute board.

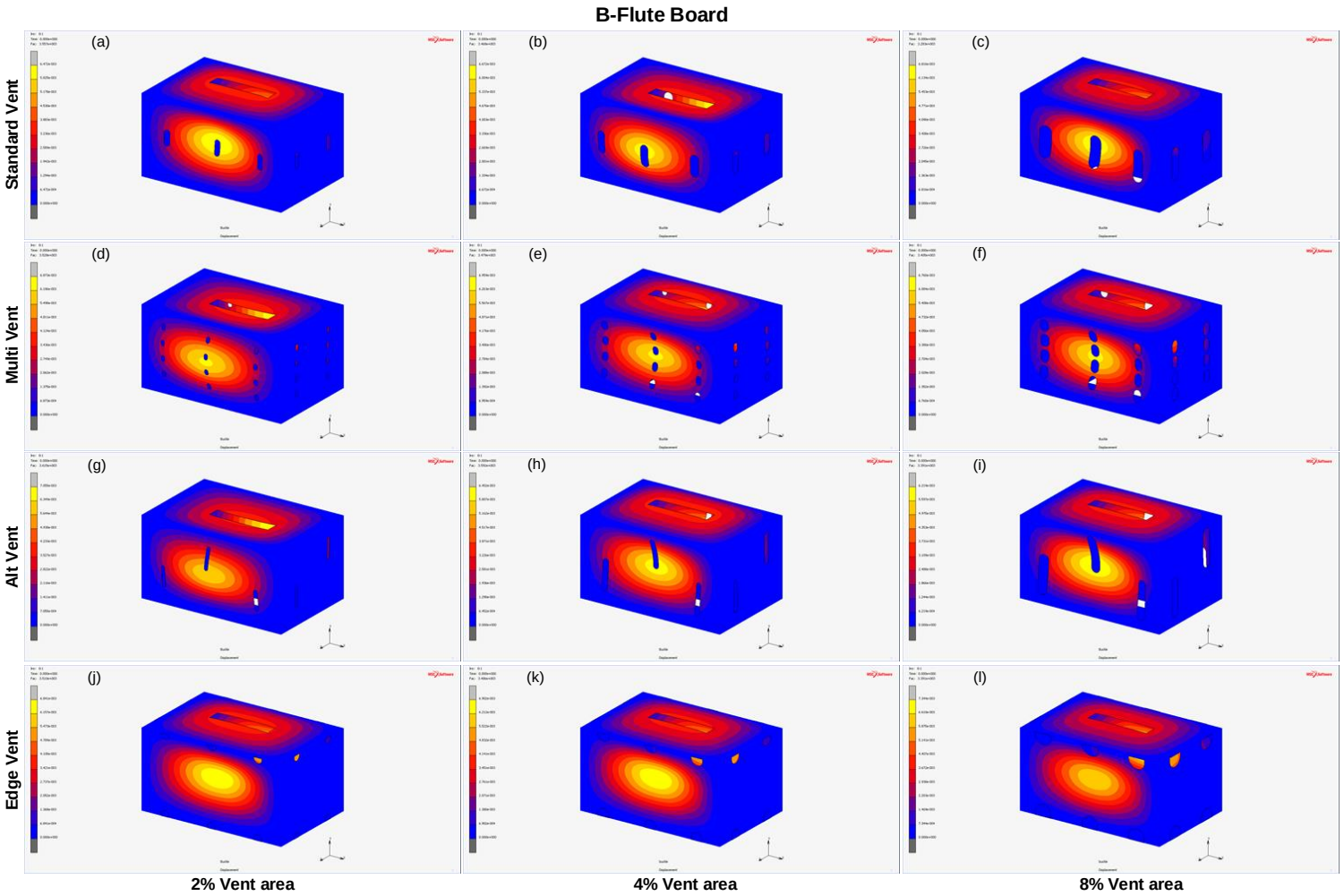

Figure 5.14:Plot showing the buckling mode for the different package designs and different vent areas with B-flute board: (a) Standard vent with 2% vent area, (b) Standard vent with 4% vent area, (c) Standard vent with 8% vent area, (d) Multi vent with 2% vent area, (e) Multi vent with 4% vent area, (f) Multi vent with 8% vent area, (g) Alt vent with 2% vent area, (h) Alt vent with 4% vent area, (i) Alt vent with 8% vent area, (j) Edge vent with 2% vent area, (k) Edge vent with 4% vent area and (l) Edge vent with 8% vent area.

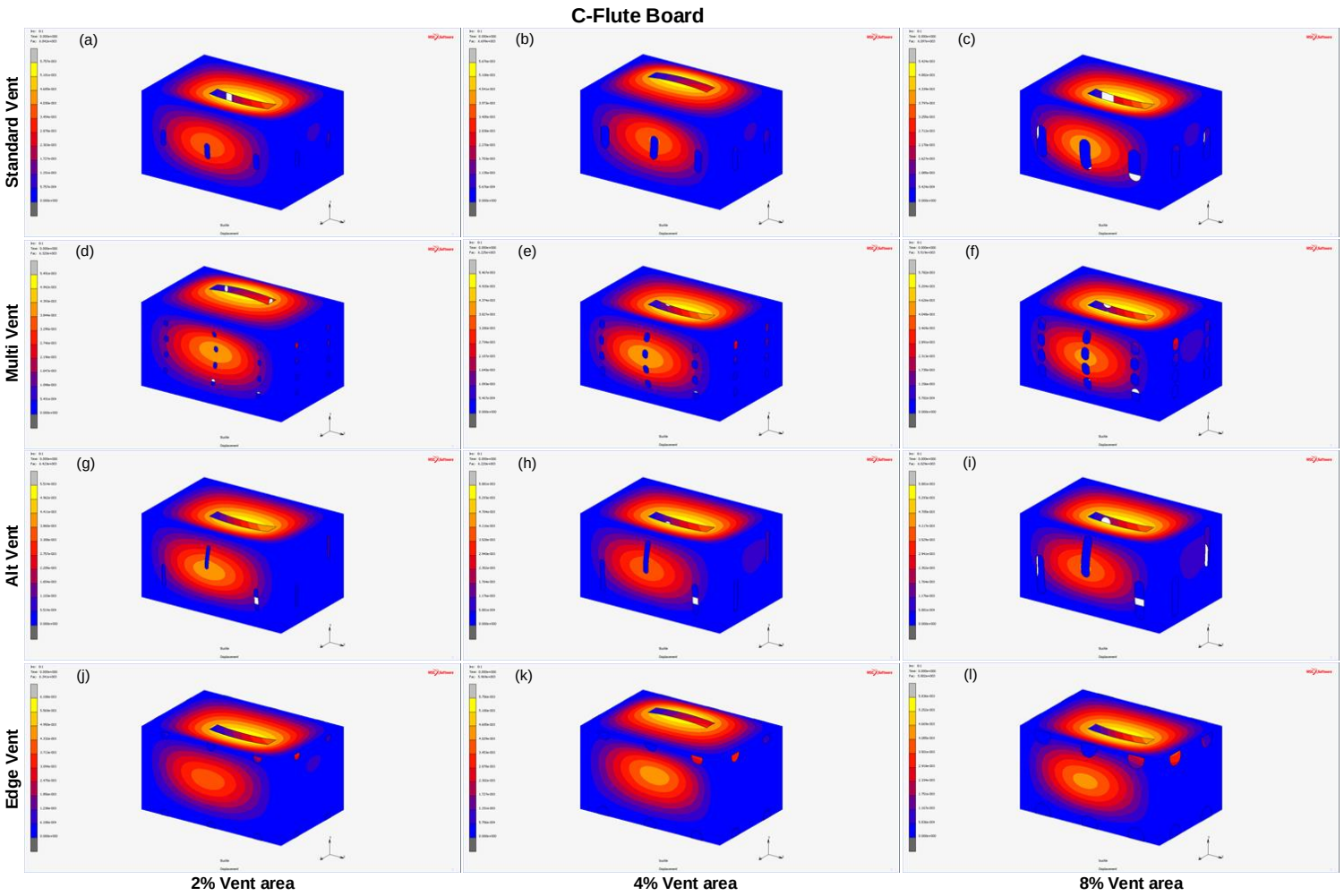

Figure 5.15: Plot showing the buckling mode for the different package designs and different vent areas with C-flute board: (a) Standard vent with 2% vent area, (b) Standard vent with 4% vent area, (c) Standard vent with 8% vent area, (d) Multi vent with 2% vent area, (e) Multi vent with 4% vent area, (f) Multi vent with 8% vent area, (g) Alt vent with 2% vent area, (h) Alt vent with 4% vent area, (i) Alt vent with 8% vent area, (j) Edge vent with 2% vent area, (k) Edge vent with 4% vent area and (l) Edge vent with 8% vent area.

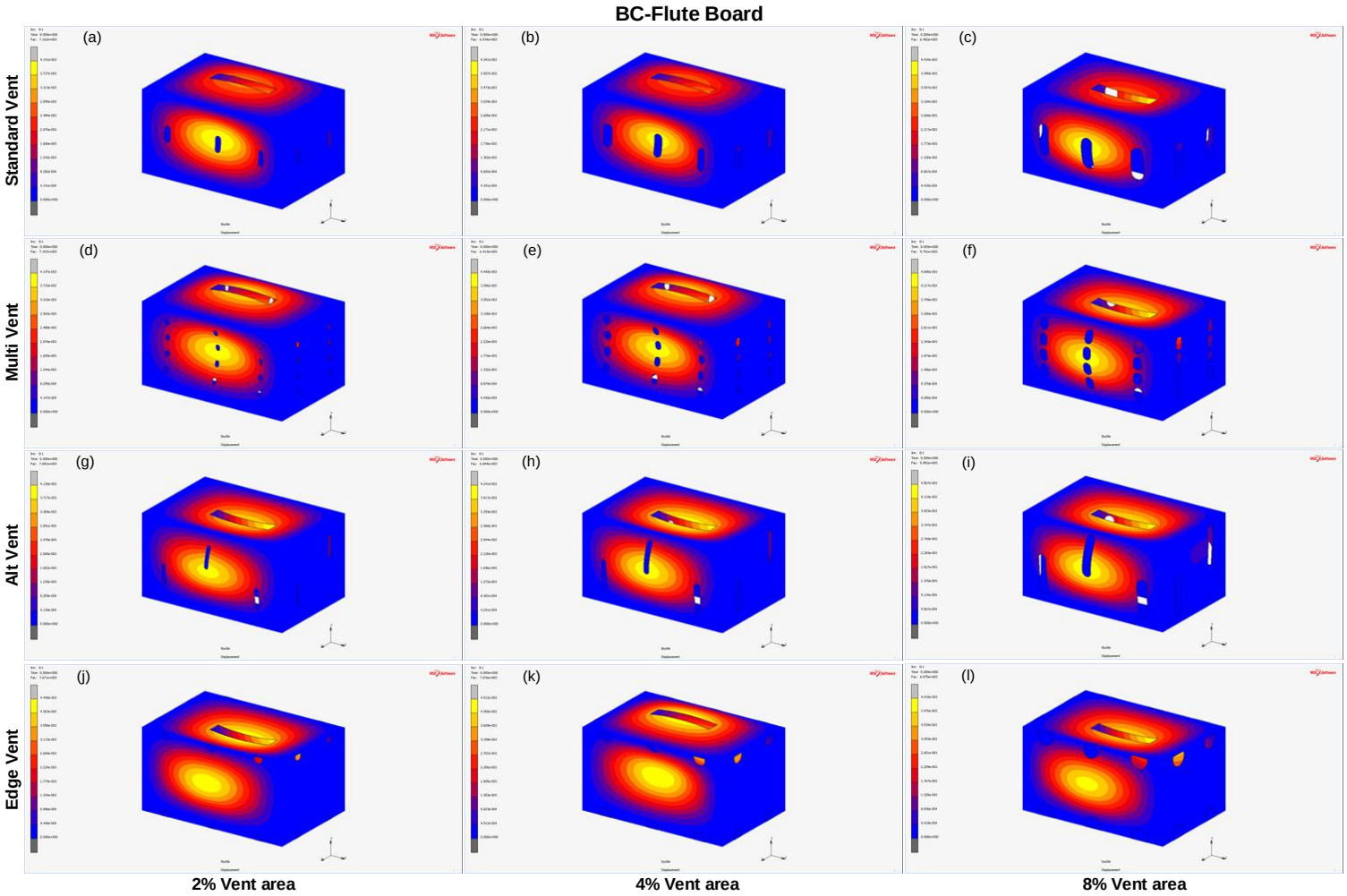

Figure 5.16: Plot showing the buckling mode for the different package designs and different vent areas with BC-flute board: (a) Standard vent with 2% vent area, (b) Standard vent with 4% vent area, (c) Standard vent with 8% vent area, (d) Multi vent with 2% vent area, (e) Multi vent with 4% vent area, (f) Multi vent with 8% vent area, (g) Alt vent with 2% vent area, (h) Alt vent with 4% vent area, (i) Alt vent with 8% vent area, (j) Edge vent with 2% vent area, (k) Edge vent with 4% vent area and (l) Edge vent with 8% vent area.

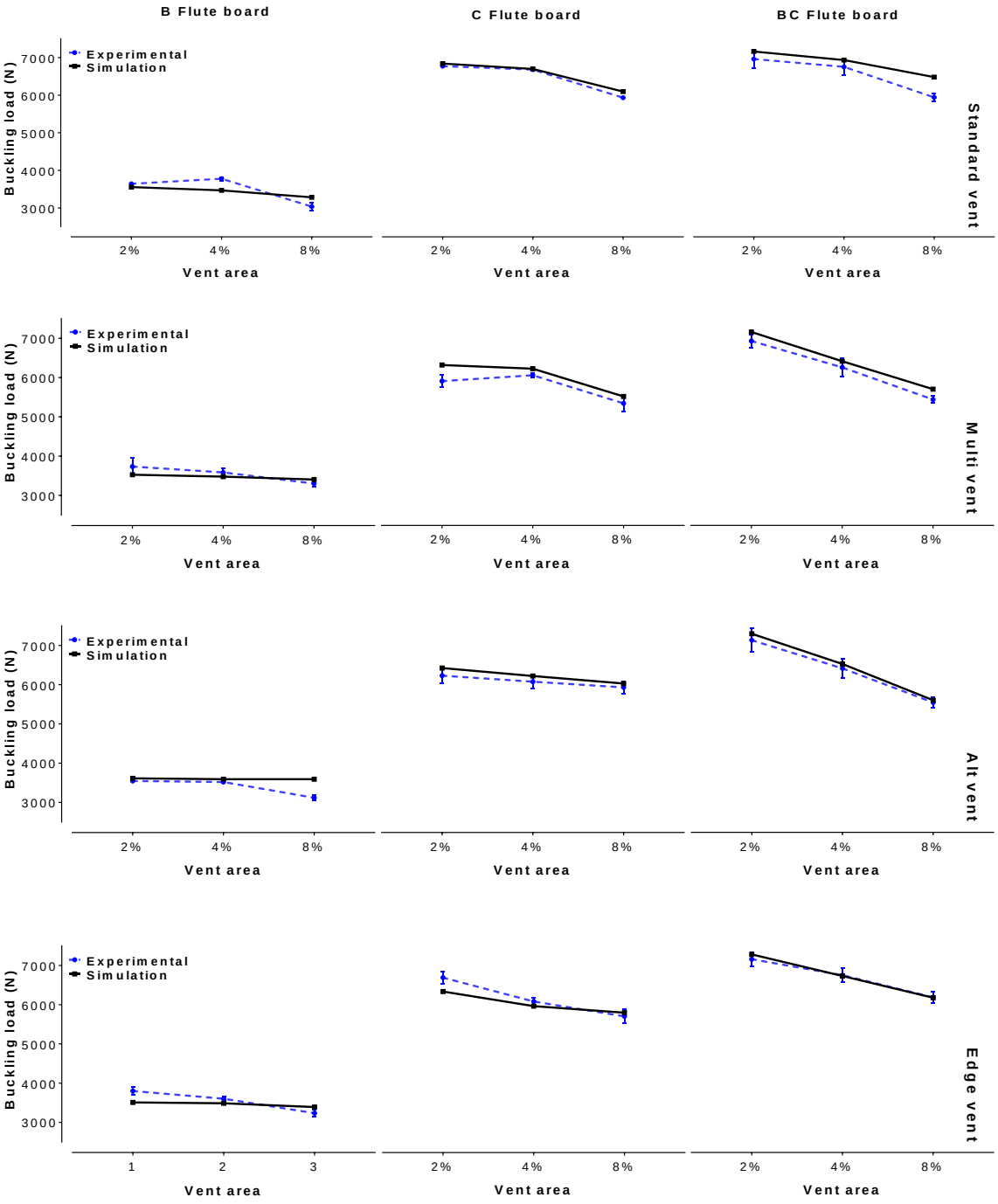

Figure 5.17: Comparison between the experimental and simulation buckling load for Standard, Multi, Alt and Edge vent packages at different vent areas.

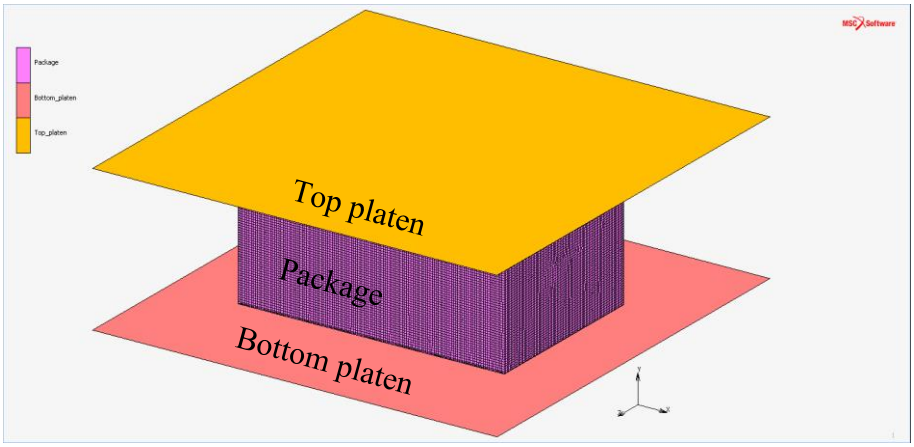

Figure 5.18: Illustration of the FEA contact modelling approach indicating the positioning of the package and the platens (top and bottom).

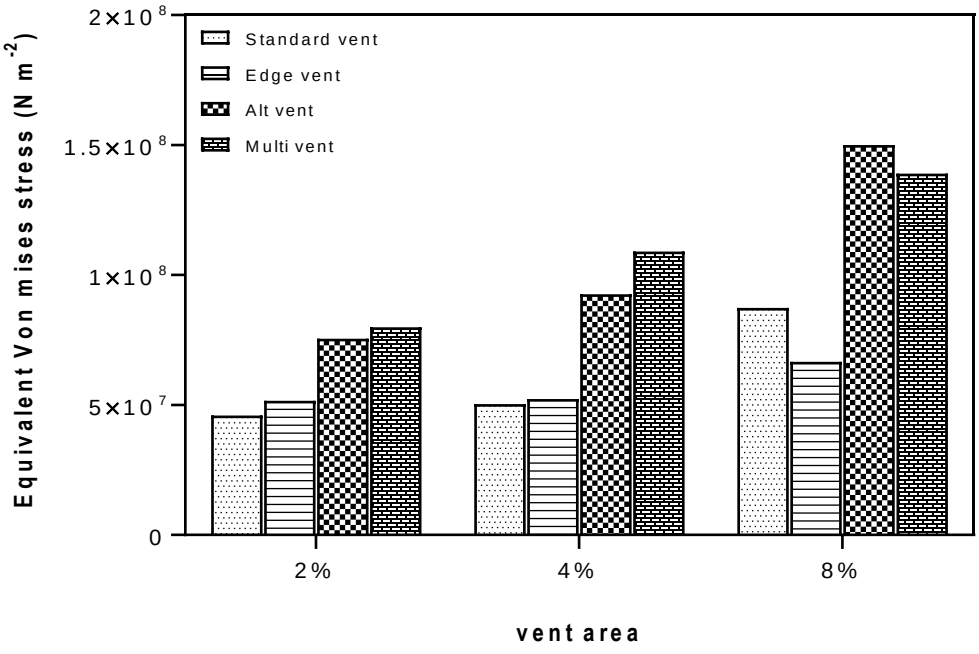

Figure 5.19: Maximum equivalent Von Mises stress at different vent area for all the package designs.

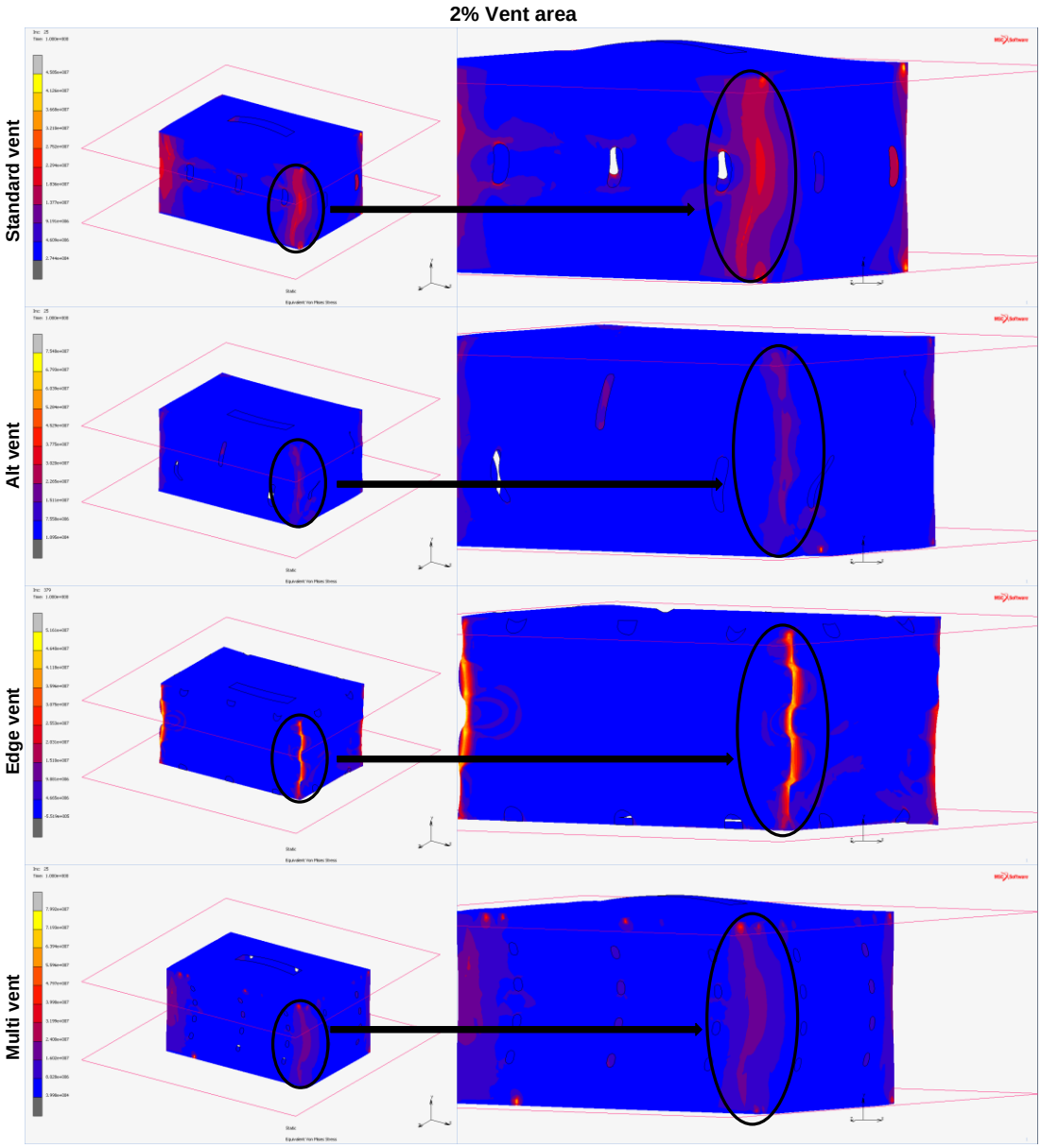

Figure 5.20: Typical fringe plots showing the distribution of the equivalent Von Mises stress from the contact model simulation for all the package designs with the 2% vent area.

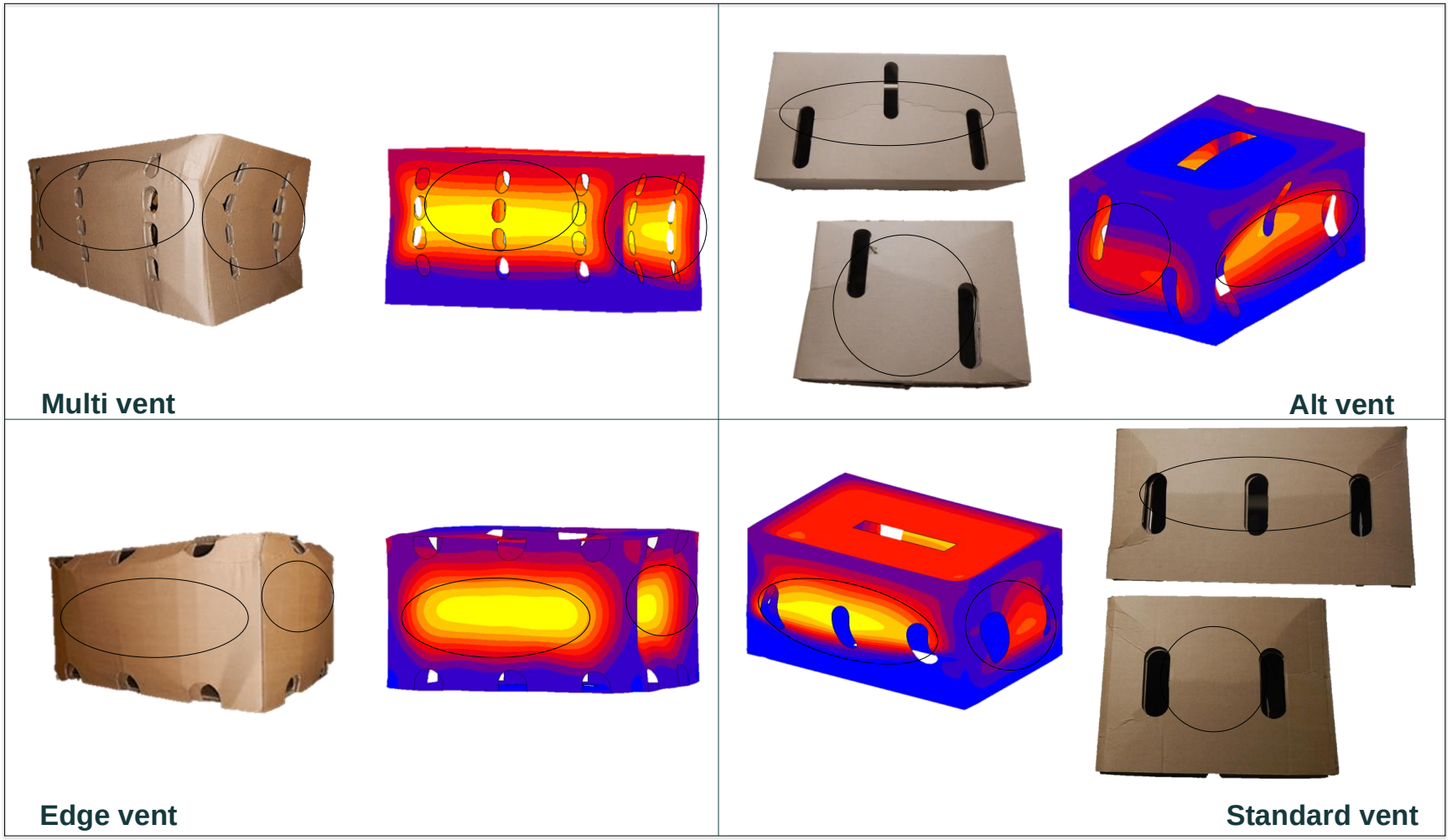

Figure 5.21: Qualitative visual comparison of the displacement shape between the experimental and simulation results for 8% vent area for all package designs. The ellipse shape is used to indicate the long side of the package while the circle shape is used to indicate the short side of the package.

Table 5.1: Equivalent core stiffness calculations used in determining the equivalent core properties of the corrugated paperboard.

A	Theoretical value	D	Theoretical value
A_{11}	$\frac{E_x t}{1+6(1-\nu_{xy}\nu_{yx})\left(\frac{f^2}{t^2}\right)\left(\psi^2-\frac{\psi}{2\pi}\sin(2\pi\psi)\right)}$	D_{11}	$\frac{E_x t^3}{12\left(1-\nu_{xy}\nu_{yx}\right)}\psi$
A_{22}	$E_y t\psi$	D_{22}	$\frac{E_x t^3}{12\left(1-\nu_{xy}\nu_{yx}\right)}\psi+\frac{1}{2}E_y t f^2$
A_{12}	$\nu_{xy}A_{11}$	D_{12}	$\nu_{xy}D_{11}$
A_{33}	$G_{xy}\frac{t}{\psi}$	D_{33}	$G_{xy}\frac{t^3}{12\psi}$

where ψ is the wave number (flute length per liner length), t is the corrugated sheet thickness, f is the amplitude of the flute, E_x is the elastic modulus in the MD, E_y is the elastic modulus in the CD, ν_{xy} is the major Poisson's ration (transverse contraction due to an axial extension), ν_{yx} is the minor Poisson's ration (axial contraction due to a transverse extension), G_{xy} is the shear modulus.

Note: The corrugated paperboard was approximated by ignoring the bending extension-coupling matrix assuming a symmetric laminate. Hence, the matrix B is zero.

Table 5.2: Material properties for the B and C flute corrugated paperboard components and the homogenised core.

Properties	B Flute			C Flute			Homogenised core
	Inner liner	Fluting	Outer liner	Inner liner	Fluting	Outer liner	
E_x (MPa)	4739	5769	6232	4287	5769	7240	1483
E_y (MPa)	901	1510	1847	1056	1510	1180	2083
E_z (MPa)	24	29	31	21	29	36	7
ν_{xy}	0.34	0.33	0.34	0.34	0.33	0.34	0.23
ν_{xz}	0.01	0.01	0.01	0.01	0.01	0.01	0.01
ν_{yz}	0.01	0.01	0.01	0.01	0.01	0.01	0.01
G_{xy} (MPa)	800	1142	1313	823	1142	1131	680
G_{xz} (MPa)	86	105	113	78	105	132	27
G_{yz} (MPa)	26	43	52	30	43	34	59

Table 5.3: Number of mesh elements used for the various FEA simulations.

Carton Configuration	Vent size	Number of element
Altvent	2%	46146
	4%	44745
	8%	43468
Edgevent	2%	44993
	4%	44233
	8%	42595
Multivent	2%	47366
	4%	46662
	8%	44181
Standard vent	2%	45930
	4%	44648
	8%	43260

Table 5.4: Percentage difference and correlation index between the numerical and experimental buckling loads.

Vent configuration	TVA	B flute corrugated board		C flute corrugated board		BC flute corrugated board	
		Percentage difference (%)	Correlation index	Percentage difference (%)	Correlation index	Percentage difference (%)	Correlation index
Control	0%	4.6	0.9978	9.8	0.9893	11.2	0.9860
	2%	2.4	0.9994	1.0	0.9999	2.8	0.9992
Standard Vent	4%	8.6	0.9932	0.3	0.9999	2.6	0.9993
	8%	7.8	0.9934	2.7	0.9992	8.7	0.9917
	2%	5.7	0.9970	6.7	0.9952	3.3	0.9989
Multi Vent	4%	3.0	0.9991	2.7	0.9992	2.5	0.9994
	8%	3.1	0.9990	3.2	0.9989	4.7	0.9977
	2%	1.9	0.9996	3.1	0.9990	2.3	0.9994
Alt Vent	4%	2.0	0.9996	2.3	0.9994	1.8	0.9997
	8%	8.4	0.9924	1.6	0.9997	1.1	0.9999
	2%	7.9	0.9942	5.4	0.9972	1.7	0.9997
Edge vent	4%	3.3	0.9989	1.9	0.9996	0.3	0.9999
	8%	4.7	0.9977	1.6	0.9997	0.2	0.9999

Chapter 6. Investigating the effects of package design and environmental conditions on the creep behaviour of ventilated packages

Abstract

During handling, storage and transportation of fresh horticultural produce such as pome fruit, packages are often stacked. The resistance of the package, particularly the bottom package to the weight on it is regarded as a measure of its compression strength. Over time, due to the load, the package losses its strength which results into collapse, consequently leading to damage of the packed produce. This time-dependent phenomenon is known as creep. A package should therefore be able to withstand the load on it over its life span. Hence, this study aimed to investigate the creep behaviour of three corrugated paperboard packages at two environmental conditions under constant load for a 12 h duration. The packages were two vented packages (Standard vent and Multi vent designs) and an unvented Control package. The environmental conditions used in the study were standard conditions (23 °C and 50% RH) and refrigerated conditions (2 °C and 85% RH). The Bailey-Norton creep law and Power law models showed a good correlation with the experimental creep strain. Load and environmental conditions affected the creep of the packages. High load resulted in an increased creep rate. Refrigerated conditions increased the creep rate of the packages in comparison with the standard conditions. Package configuration also had a significant effect on the creep rate. The unvented Control package had the lowest creep rate compared to the vented packages.

Keywords: Ventilated packaging, creep rate, moisture, compression strength, environmental conditions.

6.1 Introduction

Packaging plays a crucial role in the long and complicated journey of horticultural produce from the grower to the consumer (Fadiji et al., 2018a; Pathare et al., 2016). Over the years, the development of horticultural packages has become a rapidly growing industry (Fadiji et al., 2018a, b, Berry et al., 2017). Globally, corrugated paperboard packaging is commonly utilised to protect, store and transport products including food, electronics, and horticultural produce such as fresh fruit and vegetables. The popularity and usage of corrugated paperboard packaging has increased due to its low cost, being lightweight, low weight-to-strength ratio, high stiffness-to-weight ratio and environmentally acceptable attributes (Fadiji et al., 2018a, b; 2016; Giampieri et al., 2011; Talbi et al., 2009). The ability to deliver products to the end-users or export market in a satisfactory condition without loss in quality was reported to be directly linked to a country's economic growth (Navaranjan & Johnson, 2006). According to the report by SmithersPira (2014), the global consumption of corrugated paperboard will increase by about 56% by 2021 (140 million tonnes, worth $ US 269 billion) when compared to the consumption in 2013 which was about 90 million tonnes, worth $ US 140 billion. With the enormous increase in the usage of corrugated paperboard packaging, particularly in the food and horticultural industries, continual evaluation and improvement of the packages to meet performance requirements are paramount. In addition, in the development of corrugated paperboard packaging, design plays a vital role since optimised packaging will enhance the value of the packed products (SmithersPira, 2014). Due to the respiration of horticultural produce, packages are vented to allow for precooling of the packed produce and adequate air circulation within the package (Ngcobo et al., 2013; Pathare et al., 2012b; Thompson et al., 2010; De Castro et al., 2005; Émond & Vigneault, 1998). The presence of vents reduces the structural stability and strength of the packages (Fadiji et al., 2018b; Pathare & Opara, 2014; Singh et al., 2008; Han & Park, 2007). Hence, the package must have enough openings to provide uniform airflow through the produce, while providing suitable structural strength (Vigneault & de Castro, 2005; Vigneault & Goyette, 2002). During transportation and distribution, these packages are often stacked on a pallet resulting in a constant compression load for a long duration (Köstner et al., 2018). These loads lead to short-term buckling or long-term creep buckling (Hussain et al., 2017; Navaranjan & Johnson, 2006). Packages placed at the bottom of the stack experience the highest loads resulting in a significant out-of-plane deformation of the vertical walls before total collapse of the stacked packages. The box compression test (BCT) has been used to quantify and constitute a general measure of the performance potential of corrugated paperboard packages (Pathare et al., 2017; Markström, 1988). At constant rate of deformation, a compressive load is applied to the package in a BCT, until failure occurs. The load at failure is known as the maximum compression strength of the package.

Although the BCT gives an idea of the maximum load a package can withstand, it does not account for the long-term behaviour of the package, the creep deformation and package lifetime under constant applied load. Creep is a slow time dependent

phenomenon common to cellulosic materials, for example paper based materials (Paunonen & Gregersen, 2010; Considine et al., 1989). Despite the high stiffness-to-weight and low weight-to-strength ratios of corrugated paperboard packaging, its structural performance and mechanical behaviour tend to degrade over time, particularly with variations in the environmental conditions such as relative humidity (RH) and temperature. Changes in RH have great adverse effects on the mechanical properties, fibre network strength and the package lifetime due to an increase in the moisture content (Dongmei et al., 2013; Navaranjan & Johnson, 2006; Salmen, 1993). Furthermore, the hygrothermal effect could lead to high rate of compressive creep, particularly in stacked packages during long-term transportation and storage (Navaranjan et al., 2013). To minimise the damage incurred by the package and the packed produce, package designers often overdesign the packages, resulting in higher manufacturing costs. Thus, there is an utmost need to investigate and understand the performance of the packages for real supply or distribution chain conditions.

Some researchers have investigated the creep deformation of corrugated paperboard and its components (Köstner et al., 2018; Chen et al., 2017; Hiller, 2016; Mattsson & Uesaka, 2013; Uesaka & Juntunen, 2012; Guo et al., 2008; Rahman et al., 2007; Fellers & Panek, 2007; Pasco et al., 2006; Kim et al., 2006; Navaranjan & Johnson, 2006; Alfthan, 2004; Vorakunpinij et al., 2004; Morgan, 2004; Chalmers, 2001; Considine et al., 1994; Gunderson & Tobey, 1990; Byrd & Koning, 1978; Byrd, 1984, 1972a, b). Byrd (1972a, b) examined the tensile and compressive creep of paperboard in constant and cyclic humidity conditions. More periodic failures and higher creep rates were reported under cyclic humidity conditions than under constant humidity conditions, at equal creep loads. Furthermore, during the tensile creep of a single paper fibre, the fibril angle increased and decreased in cyclic and constant RH conditions, respectively. The study by Byrd and Koning (1978) compared the compressive creep performance of corrugated paperboard from recycled and virgin paperboards. Higher deformation was observed with the recycled paperboard compared to the virgin paperboard. These results were corroborated in the study by Byrd (1984), who reported poor performance with recycled paperboard compared to virgin paperboard. In addition, the deformation of the corrugated paperboard showed about two to five times larger deformation compared to the deformation of its components. Considine et al. (1989) examined the mechano-sorptive performance of two paperboards in a changing humidity environment under an edge compressive load. The study reported a direct relationship between the creep rate and stiffness loss, and they were able to successfully predict the failure of the paperboard.

DeMaio and Patterson (2006) studied the influence of bonding on the tensile creep behaviour of paper. Results from the study showed no difference in the creep behaviour of paper in cyclic RH and constant RH with regards to bonding. The bond structure and the changes in bonding did not contribute to accelerated creep. However, unloaded or inefficiently loaded sheet structures could lead to

redundancy in bonding, consequently affecting accelerated creep. The creep properties and recoverability of double-wall corrugated paperboard with A and B flutes was studied by Guo et al. (2008). The creep properties and recoverability were affected by both RH and constant compression load, and was more sensitive to RH. The authors reported a linear increase in the deformation rate during the initial stages of loading. However, during the creep stage of loading, the deformation rate was exponential. A residual strain was observed after the removal of the compression load.

With numerous studies available on the creep of paper and paperboard, very few focused on paper packages (Hussain et al., 2017; Bronkhorst, 1997; Leake & Wojcik, 1993; Leake & Wojcik, 1989; Leake, 1988; Koning & Stern, 1977; Moody & Skidmore, 1966; Dagel & Brynhildsen, 1959; Stott, 1959; Kellicutt & Landt, 1951). Although, the BCT is used to quantify the maximum compression load that the bottom package can withstand when stacked, it does not account for the creep deformation or the lifetime of the package (Hussain et al., 2017), which could lead to over or under-designed packages. Given that creep phenomenon is slow and no widely acceptable testing protocol has been established for paper packages (Hussain et al., 2017), understanding the behaviour of the packages in real life situation is very important, and will enhance optimum package designs. Moreover, determining the lifetime of a package is the most difficult and important parameter to measure or predict. Therefore, the aim of this study is investigate the effects of package design and environmental conditions on creep behaviour of ventilated packages for handling fresh horticultural produce under variable loads applied for a short duration.

6.2 Basic principle of creep

The design of paper packages must be such that they can sufficiently withstand loads over a long period of time. When paper materials are exposed to long-term loading, there is a continuous increase in deformation. This process is time-dependent, and is referred to as creep (Haslach, 2000). Creep can be defined as a progressive increase of strain in a material exposed to a constant load, observed over a long duration. Creep is a condition that occurs due to non-recoverable deformation in paper due to its viscoelastic nature. Usually for paper materials, accelerated creep occurs with varying relative humidity. This time-dependent behaviour adversely affects paperboard packaging and may lead to package failure/damage or shortening of life during handling, transport and in storage. An example of this is the compressive buckling or collapse of stacked cartons during transportation and storage with varying ambient relative humidity (Haslach, 2000). Creep phenomenon is usually characterised by three stages of deformation: primary, secondary and tertiary creep (Figure 6.1). The primary creep stage, otherwise known as transient creep, is characterised by relatively high strain rates that increase instantaneously with the application of the load. In relation to the total creep curve, the duration of this stage is typically short. In the secondary creep stage

(steady state creep), the strain rate reaches a minimum value and remains approximately constant over a long duration (Chen et al., 2011b; Arvidsson & Grönvall, 2004; Eagleton, 1995). This is the linear portion of the creep curve and is the most important stage in structural design, since a longer creep duration is observed than during the primary creep stage. The third stage, which is the tertiary stage, is characterised by a rapidly increasing strain rate. This occurs over a short period of time, and it continues until fracture or rupture occurs. The simplest form of creep case to investigate is uniaxial loading. Eq. (6.1) shows a general mathematical representation of a creep curve:

$$\varepsilon^c = F(\sigma, T, t) = f(\sigma) g(T) h(t) \tag{6.1}$$

where ε^c is the creep strain, σ is the uniaxial stress, T is the temperature and t is the time. Temperature and time play key roles in the creep behaviour. Eq. (6.1) shows the separability of the effects of stress, temperature and time

Often, the functional relationship between time and creep strain can be represented using the Power law model as shown in Eq. (6.2):

$$\varepsilon^c = at^b \tag{6.2}$$

However, for most structural designs, the primary and secondary stages of the creep curve is often used to determine the integrity of the structure utilising the Bailey-Norton law (sometimes called creep power law) (Ahmad et al., 2017):

$$\varepsilon^c = A\sigma^n t^m \tag{6.3}$$

where A, n and m are temperature dependent material constants, generally independent of the stress. Usually, $n > 1$ and $0 \leq m \leq 1$. While, the constants a, b, n and m are dimensionless, A is known as the creep strain-hardening coefficient, with units of $m^2 (N\ s)^{-1}$.

6.3 Materials and Methods

6.3.1 Packaging materials

Three types of packages were used in this study: a Control package without vent holes and two ventilated corrugated paperboard packages (VCP). The VCP package designs used were the Standard vent and Multi vent designs. The packages were fabricated using a corrugated paperboard die cutter and then assembled and glued. The Standard vent design is specifically used for handling pome fruit in international trade from South Africa (Berry et al., 2017, 2015) while the Multi vent design was proposed as an alternative to the Standard vent design (Berry et al., 2017). The packages are regular slotted cartons, which consist of inner and outer boxes (Figure 6.2). Both Standard and Multi vent designs have oblong-shaped vent holes oriented vertically on the long and short sides of the packages. The total vent

area of both packages was 4%. For all the package types, the paperboard grammage combination was 250K/175B/250K for the outer carton and 250K/175C/250K for the inner carton The numerical values indicate the paperboard grammages (g m^{-2}) for the fluting and liners respectively. K indicates Kraft linerboards while B and C indicate the fluting profile of the paperboard. The thickness of the liners was 0.349 ± 0.002 mm while the thickness of the flute was 0.249 ± 0.002 mm. The outer dimensions of the packages (in mm) are 500 x 333 x 270.

6.3.2 Box compression test (BCT)

BCT is a pure top-to-bottom compression load test between two flat steel platens using a constant deformation rate (Pathare et al., 2017). The Lansmont compression tester (Lansmont Corporation, Monterey CA, USA) was used for the BCT (Figure 6.3). Prior to the BCT, the packages were conditioned at 23 ± 1 °C and 50 ± 2% RH for 24 h in a versatile environmental chamber (model MLR − 352H) following the ASTM D4332 recommendations (ASTM, 2006). The recommended ASTM D642 standard was used for the compression test (ASTM, 2010); using a continuous motion of the top platen at a speed of 12.7 ± 2.5 mm min^{-1}, with a preload of 222 N applied to the package until failure was reached. The compression load and crosshead displacement were recorded. The compression test was done at two environmental conditions: standard conditions (23 °C and 50% RH) and refrigerated conditions for fresh horticultural produce (2 °C and 85% RH). To be able to mimic the refrigerated condition, an environmental chamber was constructed around the compression tester as shown in Figure 6.3. Five packages for each design were tested.

6.3.3 Compression creep tests

Before each creep test, the packages were conditioned as recommended by the ASTM D4332 standard. For the tests done at the refrigerated conditions, the packages were stored in a cold room at the same environmental conditions for 24 h. The weight of the package was monitored hourly using an electronic weighing balance (ML3002.E, Mettler Toledo, Switzerland) with a precision of 0.01 g. This was done to evaluate the increase in weight of the package as it absorbs moisture. The moisture absorption was calculated using Eq. (6.4) as described by Andrés et al. (2014):

$$M_A(\%) = {W_W - W_D}/{W_D} \times 100 \tag{6.4}$$

where M_A is the moisture absorption (%), W_W is the wet weight of the package (g) and W_D is the dry weight of the package (g) (measured before it was placed in the cold room).

At the end of the creep tests done at the refrigerated conditions, moisture content of the paperboard was determined as described by Hussain et al. (2017). The moisture

content was evaluated by cutting out a side panel from the package and weighing it to determine the wet weight. This was then dried in an oven dryer (Model nr. 072160, Prolab Instruments, Sep Sci., South Africa), at 105 °C for 72 h and then reweighed to determine the dry weight. Moisture content of the package at the end of the test was obtained as the percentage difference between the wet and dry weight relative to the wet weight.

Compression creep was performed using the Lansmont compression tester (Lansmont Corporation, Monterey CA, USA) following the recommendation of the ASTM D7030 standard (ASTM, 2017). The compression creep of the packages was studied at constant temperature and relative humidity. Two environmental conditions, similar to the BCT was used in the creep tests: standard conditions (23 ± 1 °C and 50% RH) and refrigerated conditions for fresh horticultural produce (2 °C and 85% RH). The constant compression loads applied for the creep test were chosen as 50% and 80% of the maximum compression strength obtained from the BCT for the standard conditions. For the refrigerated conditions, 50% of the maximum compression strength obtained from the BCT was applied. The load used during the creep test at the refrigerated conditions was due to the inability of the packages to withstand higher loads, as a result of the absorbed moisture. The packages were compressed with the applied constant load for 12 h. The parameters were combined together to form the experimental conditions for each of the package designs. For example, the combination of standard conditions (23 ± 1 °C and 50% RH), 50% of the maximum compression strength and 12 h duration is a form of experimental condition. Based on the displacements obtained as a function of time, the creep strain was calculated using Eq. (6.5):

$$\varepsilon_t^c = \frac{\delta_t}{h} \tag{6.5}$$

where ε_t^c is the creep strain at time t, δ_t is the displacement at time t and h is the undeformed/original height of the package.

6.3.4 Statistical analysis

The constant parameters of the creep model were obtained by fitting it to the experimental data using regression analysis and curve fitting tools in MATLAB (R2017a, MathWorks, Natick, Massachusetts). The models used were the Bailey Norton law and the Power law. The statistical analysis was carried out using Statistica software (version 13.0, StatSoft Inc., Tulsa, USA). The experimental data were treated with one-way analysis of variance (ANOVA) at 95% confidence level and with the differences at $p<0.05$ considered statistically significant. Error bars on the figures indicate the standard error of the mean. The letters on the error bars were used to show the statistical difference. Mean values with the same letters are not statistically different.

6.4 Results and discussions

6.4.1 Package moisture absorption

Figures 6.4a and 6.4b show the weight of the Control package when stored under the refrigerated conditions and the moisture uptake by the package for 24 h, respectively. From the plot, it was observed that the weight of the package, which is caused by moisture absorption, increases significantly (p<0.05) for the first five hours in storage. As the time increases, the rate of moisture absorption reduces. From about 10 h in storage, the rate of moisture absorption reduces to less than 1 percent every hour for the remaining time duration. This indicated that the package stored under the refrigerated conditions was practically in equilibrium. The hygroscopic nature of paper material allows it to absorb moisture from, and release moisture to its environment (Parker et al., 2006). The equilibrium state is achieved when the paper neither absorbs moisture nor releases moisture, and is a function of the surrounding environment (Pathare & Opara, 2014). Similar to our study, Allaoui et al. (2009a) stored corrugated paperboard and its constituents at 95% RH and showed that moisture equilibrium was achieved after 100 mins. In addition, moisture equilibrium for paperboards was reached within a day of storage at high RH of about 95% (Hung et al., 2010). Results obtained from the moisture absorption by the package stored in the refrigerated conditions formed the basis for the subsequent storage time for the experiments reported in this study.

6.4.2 Compression strength of the packages

The mean compression strength for all the package design is shown in Figure 6.5a. The Control package had the highest compression strength when compared to other designs at both standard and refrigerated conditions (Figure 6.5a). At the standard conditions, the compression strength of the Standard and Multi vent designs reduced by approximately 20% and 37%, respectively when compared to that of the Control package. The reduction in compression strength was observed to be statistically significant (p<0.05). Similarly, in comparison to the Control package, at the refrigerated conditions, the compression strength of the Standard vent design was approximately 15% lower while that of the Multi vent design was approximately 33% lower. No significant difference (p<0.05) was observed in the compression strength of the Control and Standard vent packages at refrigerated conditions. However, there was a significant difference (p<0.05) in the compression strength of the Control and Multi vent packages.

The change in environmental conditions had a significant effect (p<0.05) on each of the package designs. Changing the conditions from standard to refrigerated conditions, resulted in the compression strength to decrease by 31% for the Control package, 27% for the Standard vent and 26% for the Multi vent. Paper, a cellulosic material responds to RH differently and consequently absorb or desorb moisture at different rates. This characteristic property of paper material could be critical in the performance of a paperboard package (Fadiji et al., 2017; Eagleton, 1995; Allaoui et al., 2009b). The reduction in the compression strength at the refrigerated

conditions may be attributed to the moisture absorbed at the high RH and low temperature. About half the strength of corrugated box is lost when the RH is increased from 50 to 90% (Dimitrov, 2010; Whitsitt & McKee, 1972). Increase in the moisture absorbed by the package elevates the water content appreciably, thus breaking the bonds between the cellulose fibres. This can adversely affect the stacking strength of the package (Bronlund et al., 2013). In addition, the strength of paper packages can be reduced within hours during high RH storage conditions (Twede & Selke, 2005). The study by Bandyopadhyay et al. (2002) reported a substantial reduction in the mechanical properties (tensile strength, yield stress and elastic moduli) of paper at high RH. Paunonen and Gregersen (2010) reported the compression strength of transport boxes made from polyethylene coated solid paperboard to decrease linearly by 380 N for every one percent change in moisture content. The authors reported similar trends for uncoated corrugated boxes. About 19% decrease in the edge compression strength of corrugated paperboard was reported when the RH was increased from 30% to 90% (Zhang et al., 2011). In the packaging of fresh horticultural produce, rapid cooling is required to increase the shelf life of the packed produce, hence the packages must be designed to accommodate the handling and distribution environmental conditions throughout the postharvest journey of the produce.

Figure 6.6 shows the stiffness of the different package designs used in this study, at standard and refrigerated conditions. At standard conditions, package designs had significant effect on the stiffness (p<0.05). The Control package had the highest stiffness while a reduction in stiffness was approximately 30% and 56% for the Standard and Multi vent designs, respectively. Similarly, the highest stiffness was obtained for the Control package at refrigerated conditions. The stiffness of the Standard vent reduced by approximately 51% while that of the Multi vent reduced by approximately 64% when compared with the stiffness of the Control package.

Changing the environmental conditions from standard to refrigerated conditions adversely affected the stiffness of the package significantly (p<0.05) as can be seen in Figure 6.6. For the Control package, the stiffness reduced by approximately 45% while a reduction of approximately 61% and 55% was observed for the Standard and Multi vent designs, respectively. Stiffness and compressive strength are important properties for packages to perform well under stacking loads (Ellis & Rudie, 1991). High package stiffness reduces the tendency of buckling, improves its stacking strength and produce protection (Ellis & Rudie, 1991). Moisture content was reported by Twede and Selke (2005) to have a negative effect on the stiffness of paper packages. In addition, package stiffness was reported to increase on reducing humidity (Friedli et al., 2013).

6.4.3 Package displacement

The corresponding displacement at the maximum compression strength for all the package design is shown in Figure 6.5b. Package displacement is a measure of the extent a package will be compressed at the end of a BCT. It is also defined as the

difference in the package height at the beginning and at the end of the BCT (Pathare et al., 2017; Singh et al., 2007). As shown in Figure 6.5b, the Control package had a displacement of about 10.5 mm while the Standard and Multi vent designs had displacements of about 10.3 mm and 11.5 mm, respectively at standard conditions. There was no significant difference in the displacements of all the package designs. When compared with the standard conditions, the displacement of the Control package increased slightly by 3% at the refrigerated conditions. In comparison to the displacement at the standard conditions for the Standard vent design, an increase of about 23% was observed for the displacement at refrigerated conditions while for Multi vent design, the displacement at the refrigerated conditions reduced insignificantly by 6%. Generally, the displacement was not significantly (p<0.05) affected by the moisture absorbed at the refrigerated conditions. Our finding is in agreement with Hansson (2008) who reported the displacement of corrugated panels to be independent of moisture content. In addition, Hansson (2008) reported that the displacement of corrugated panel is only dependent on the geometry and boundary conditions of the panels. In another study by Paunonen and Gregersen (2010), the authors reported that displacement is independent of moisture content of boxes made of solid fibreboard with a polyethylene coating. A constant displacement of about 10 mm was observed with a range of 2–11% moisture content. Hence, the authors concluded that for corrugated packaging under compression load, failure criterion could be based on vertical displacement, which is not dependent on moisture content. Storage temperature and duration have also been shown not to have a significant effect on displacement of corrugated paper packages (Pathare et al., 2017, 2016).

6.4.4 Effect of package design and storage conditions on the creep behaviour

6.4.4.1 Impact of standard/ambient environmental conditions

Figures 6.7 and 6.8 show the creep strain plotted against time for the Control package when 50% and 80% of maximum compression strength obtained at the standard conditions were applied for 12 h, respectively. The creep strain vs time curve is a map of the displacement response of the package to a constant compressive load (Bronkhorst, 1997). Often, physical events that are connected to the way the package would respond to the applied load and environmental conditions influence the shape and behaviour of the curve. From the plot, the initial strain was observed to increase rapidly after the application of the load, and this represents the primary creep response (Navaranjan & Johnson, 2006). Beyond this, the creep strain rate was observed to be relatively constant, representing the secondary creep response of the package. The package at this stage gradually deformed under the applied sustained load. The Bailey-Norton creep law and the Power law were shown to predict the creep curve for the period of load application, with good correlation with the experimental creep strain. For the 50% load, the R^2 values were 0.9846 and 0.9980 for the Bailey-Norton creep law and the Power law, respectively, in comparison with the experimental creep strain obtained. For the 80% load, the R^2 values were 0.9850 and 0.9932 for the Bailey-Norton creep law

and the Power law, respectively. Higher load resulted in an increase in the creep rate of the package obtained from the secondary creep region of the displacement vs time curve. When 50% of the package compression strength was applied, the creep rate was (7 ± 2) x 10^{-6} mm s^{-1} while when 80% of the package compression strength was applied the creep rate was (2.9 ± 1.3) x 10^{-5} mm s^{-1}, a difference of about 122%. In addition, at the end of the 12 h creep of the package the height of the package had decreased by about 0.67 mm and 1.16 mm when 50% and 80% of the compression strength was applied, respectively.

For the Standard vent design, the creep rate when 50% and 80% constant load was applied was (7.6 ± 1) x 10^{-6} mm s^{-1} and (3.7 ± 2.6) x 10^{-5} mm s^{-1}, a difference of about 132%. The creep strain vs time curve for the Standard vent design at both loads applied was observed to be similar to that of the Control package. Similarly, the Bailey-Norton creep law and the Power law predictions of the creep strain correlated well with the experimental creep strain (Figures 6.9 and 6.10). At 50% load, the R^2 values were 0.9928 for the Bailey-Norton creep law and 0.9993 for the Power law. Likewise, correlation coefficient of 0.9976 and 0.9985 were obtained for the Bailey-Norton creep law and the Power law, respectively at 80% load. For the Standard vent design, at the end of the 12 h creep of the package the height of the package had decreased by about 0.84 mm and 0.99 mm when 50% and 80% of the compression strength was applied, respectively.

High correlation with experimental creep strain was observed for the Bailey-Norton creep law and the Power law predictions for the Multi vent package at both loads applied (50% and 80%), as shown in Figures 6.11 and 6.12. R^2 values were 0.9983 for the Bailey-Norton creep law and 0.9990 for the Power law at 50% load (Figure 6.11b) while the R^2 values were 0.9973 for the Bailey-Norton creep law and 0.9979 for the Power law at 80% load (Figure 6.12b). At the end of the duration with which the load was applied, the displacement of the Multi vent package was about 1.34 mm for the 50% load and 1.78 mm for the 80% load, a difference of about 26%. The creep rate obtained for the 50% was about 8.4 x 10^{-6} mm s^{-1} while the creep rate for the 80% load was about 4.8 x 10^{-5} mm s^{-1}, a difference of about 140%. Table 6.1 and Table 6.2 summarise the constant parameters obtained from the regression analysis using the Bailey-Norton creep law and the Power law models at 50% and 80% loads at standard conditions for all the package designs.

With the creep rate known after 12 h of loading, the failure time of the package can be predicted using the relationship given by Burgess et al. (2005). Often, a package would fail if it reaches its displacement obtained during the box compression test, hence the failure time is the time taken to cover the distance of its displacement at the average creep rate. Therefore, the failure time is given as,

$$T_f = \frac{\delta}{r} \tag{6.6}$$

where T_f is the time of failure (s), δ is the displacement obtained from the box compression test (mm) and r is the creep rate at a specific load level (mm s^{-1}). Since the creep rate for a duration of 12 h is known, the creep rate in the 12 h creep test can be obtained according to Burgess et al. (2005).

$$r = r_{12} \times F/100 - F \tag{6.7}$$

where r_{12} is the average creep rate in the 12 h creep test (mm s^{-1}) and F is the load level expressed as a percentage of the maximum compression strength.

The predicted time of failure for the Control package, Standard vent and Multi vent packages from Eqs. 6.6 and 6.7 were 17.4 days, 15.7 days and 15.8 days, respectively when the load applied was 50% of the package compression strength. When 80% of the package compression strength was applied for similar package designs, the predicted time of failure were 1.2 days, 0.8 days and 0.7 days, respectively.

6.4.4.2 Impact of refrigerated conditions

Paper product, which are hydrophilic materials exhibit great time-dependent behaviour when subjected to tensile or compressive load and are more susceptible to creep under high RH (Popil & Hojjatie, 2010). For the refrigerated condition, only the creep behaviour at 50% of the compressive strength was presented. This was due to the inconsistencies of the results at higher loads and the collapse of the packages on the application of loads greater than 50% of the compressive strength. This may be attributed to the absorbed moisture by the packages. Moisture absorption in paper material results in softening of the material and alters the stress-strain curve behaviour of the paper fibres (Vishtal & Retulainen, 2012). Furthermore, the moisture absorption due to high RH and low temperature raises the water content of the paper, thus breaking the bond of the cellulose fibre of the paper, hence adversely affecting the mechanical properties (Fadiji et al., 2017; Pathare & Opara, 2014; Zhang et al., 2011; Hung et al., 2010; Allaoui et al., 2009a). Figures 6.13–6.15 show the Bailey-Norton creep law and the Power law predictions of the creep strain for the 12 h duration for the Control package, Standard vent and Multi vent packages, respectively. Good correlation was observed between the experimental creep strain and the predicted creep strain from the two models. R^2 values were 0.9985 for the Bailey-Norton creep law and 0.9989 for the Power law for the Control package. For the Standard vent design, R^2 values were 0.9985 and 0.9986 for the Bailey-Norton creep law and the Power law, respectively. R^2 values were 0.9916 for the Bailey-Norton creep law and 0.9925 for the Power law for the Multi vent design. Table 6.3 summarises the constant parameters obtained from the regression analysis using the Bailey-Norton creep law and the Power law models at 50% load at refrigerated conditions for all the package designs.

The creep rate obtained for the Control package was about 2.4 x 10^{-5} mm s^{-1}, which according to Eqs. 6.6 and 6.7, the time of failure is about 5.2 days. For the Standard vent design, the creep rate was about 4.5 x 10^{-5} mm s^{-1}, resulting in a predicted 3.3 days for the package to fail. The Multi vent design failed within the 12 h period at about 8 h. Creep rate obtained for the Multi vent package within this duration was about 0.0002 mm s^{-1}, corresponding to a predicted time of failure of about 14 h. Comparing the predicted time of failure and the actual time of failure, a difference of about 54%. At the end of the duration with which the load was applied, the displacement of the Control package and Standard vent design was about 2.26 mm and 4.83 mm, respectively, a difference of about 72%. For the Multi vent design, the displacement at the time of failure was about 8.03 mm, which was about 25% lesser than the displacement obtained during the box compression strength. Although this present study focused on the creep behaviour of ventilated packages under constant environmental conditions, cyclic RH environments have been reported to result in higher creep rates for equal creep loads applied to paper and paperboard (Morgan, 2005; Bronkhorst, 1997; Söremark & Fellers, 1992; Byrd, 1972a, b). Average moisture content for all the package at the end of the creep test was about 9%.

6.5 Conclusions

To protect fresh horticultural produce from mechanical damage that may occur during transportation, storage and distribution, package must be strong enough to withstand the load exerted on it with time. This study aimed to study the creep behaviour of three corrugated paperboard packages at two environmental conditions under constant load for 12 h duration. The package design used were: a Control package without vent holes, Standard vented and Multi vented packages. A good fit of the Bailey-Norton creep law and Power law models on the creep strain vs time curve was obtained in the duration of the applied constant load for the all the packages, at both environmental conditions. R^2 values were in the range of 0.9846 to 0.9990. Load and RH was observed to have evident effects on the creep behaviour of the packages. The creep rate of the packages increased with an increase in the load applied and RH. For both standard and refrigerated conditions, the Multi vent design had the highest creep rate while the Control package had the lowest creep rate. This study provides basic data to package designers on the time-dependent property of paperboard packaging relevant to package design applications to protect fresh horticultural produce adequately during handling, storage and transportation. However, more test protocols is required, which incorporates quantifying the effects of cyclic environmental conditions (moisture accelerated creep) on the performance of the packages as well as the effects of longer duration. In addition, this study showed that vent holes affected the creep rate of the package. The Control package, without vent had the lowest creep rate compared with the vented packages, specifically the Multi vent package, with the highest creep rate. Therefore, package designers need to take in account the role of vent holes on the creep behaviour of the packages while still ensuring uniform cooling and proper airflow within the package. Furthermore, this research has

provided preliminary evidence for package lifetime under loads and humidity/temperature, which is the most critical performance parameter of a package.

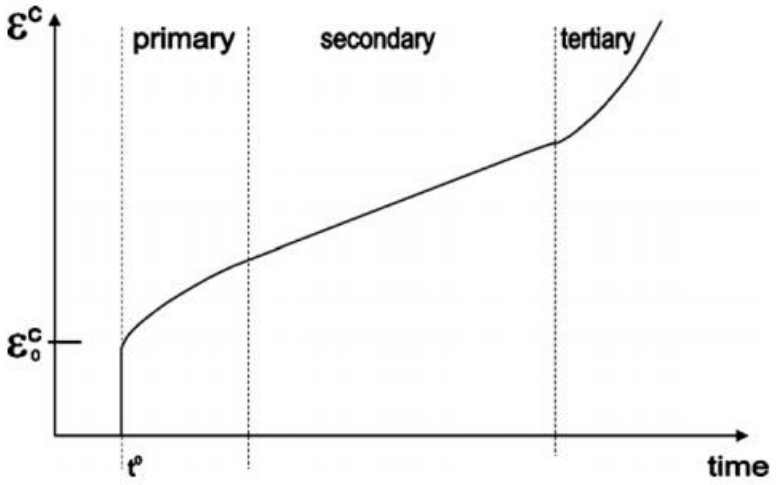

Figure 6.1: A typical creep curve for a viscoelastic material under constant stress over an extended duration. ε^c *and* ε_0^c *is the creep strain and the instantaneous elastic displacement when instantaneous load is applied, respectively.*

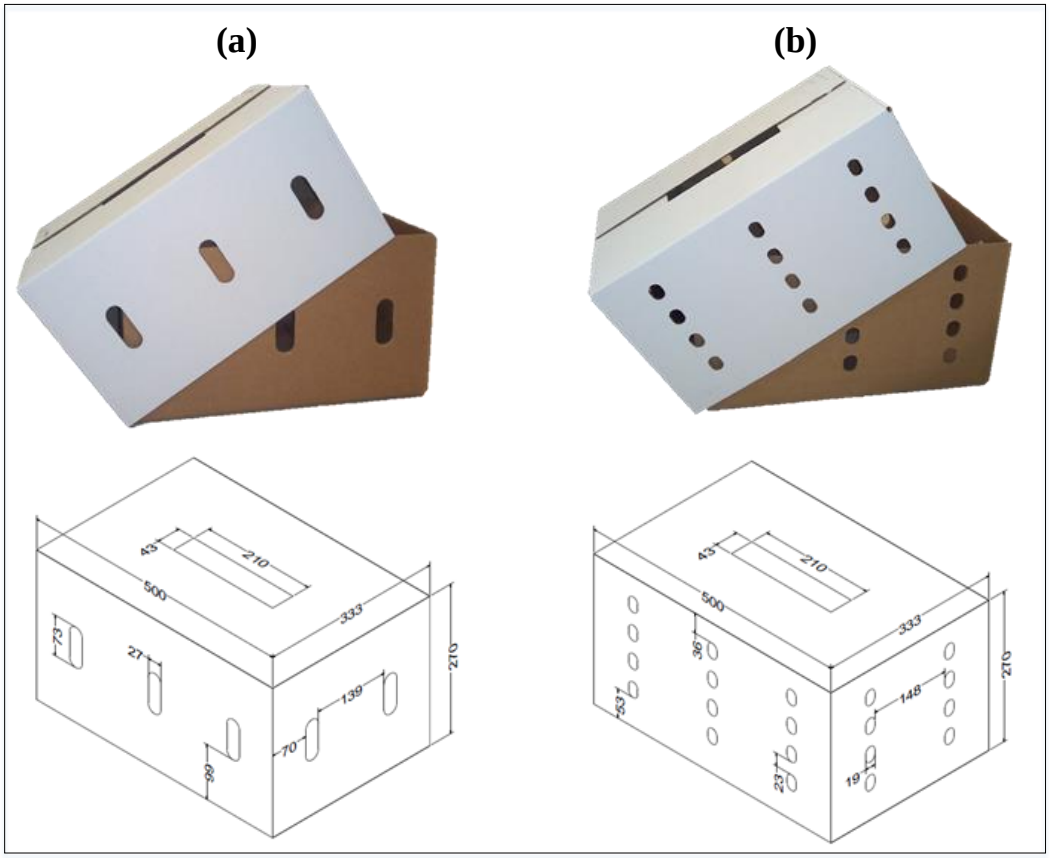

Figure 6.2: Geometry of the telescopic package (top) and dimensions in mm (bottom) of the (a) Standard vent and (b) Multi vent packages.

Figure 6.3: Diagram showing the (a) climate chamber around the box compression tester and (b) Lansmont compression tester (Lansmont Corporation, Monterey CA, USA).

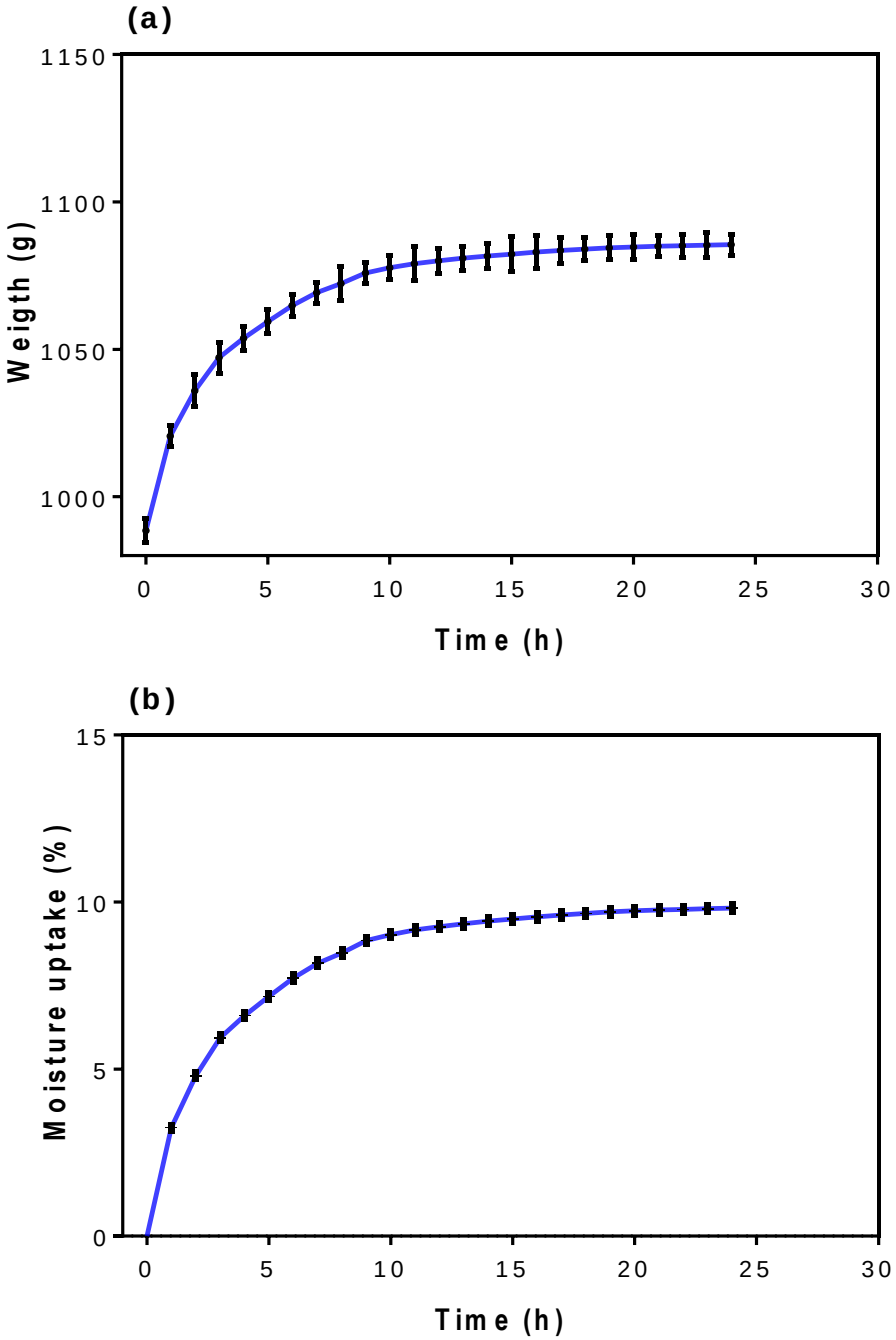

Figure 6.4: (a) Weight of the package during conditioning at refrigerated conditions and (b) moisture uptake (%) of the package during conditioning at refrigerated conditions. Black short lines represent the error bar.

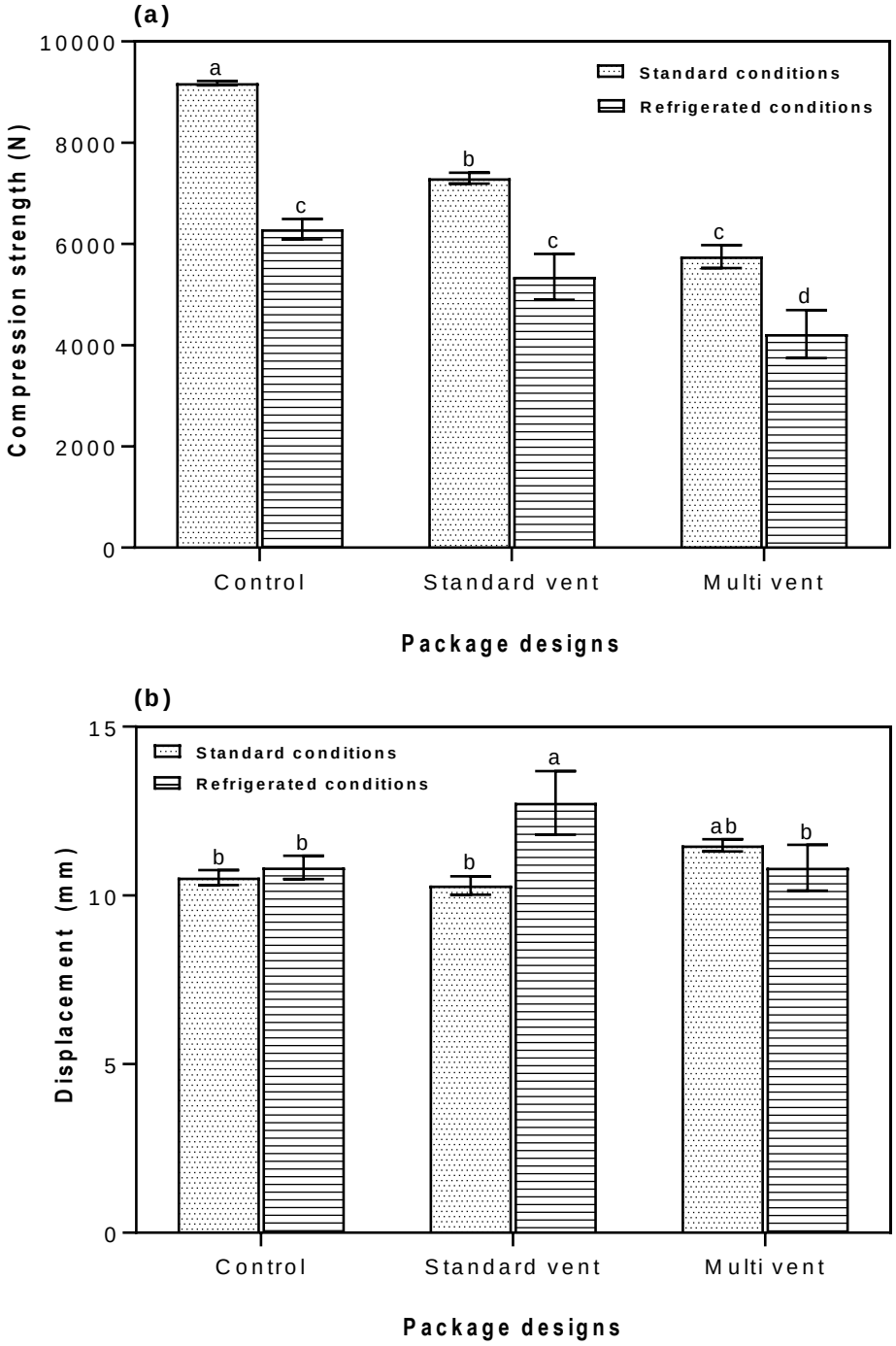

Figure 6.5: Bar chart showing (a) compression strength and (b) Displacements at maximum compression strength for all the package design at different environmental conditions. Error bars on the figures indicate the standard error of the mean. The letters on the error bars were used to show the statistical difference ($p<0.05$). Mean values with the same letters are not statistically different ($p<0.05$).

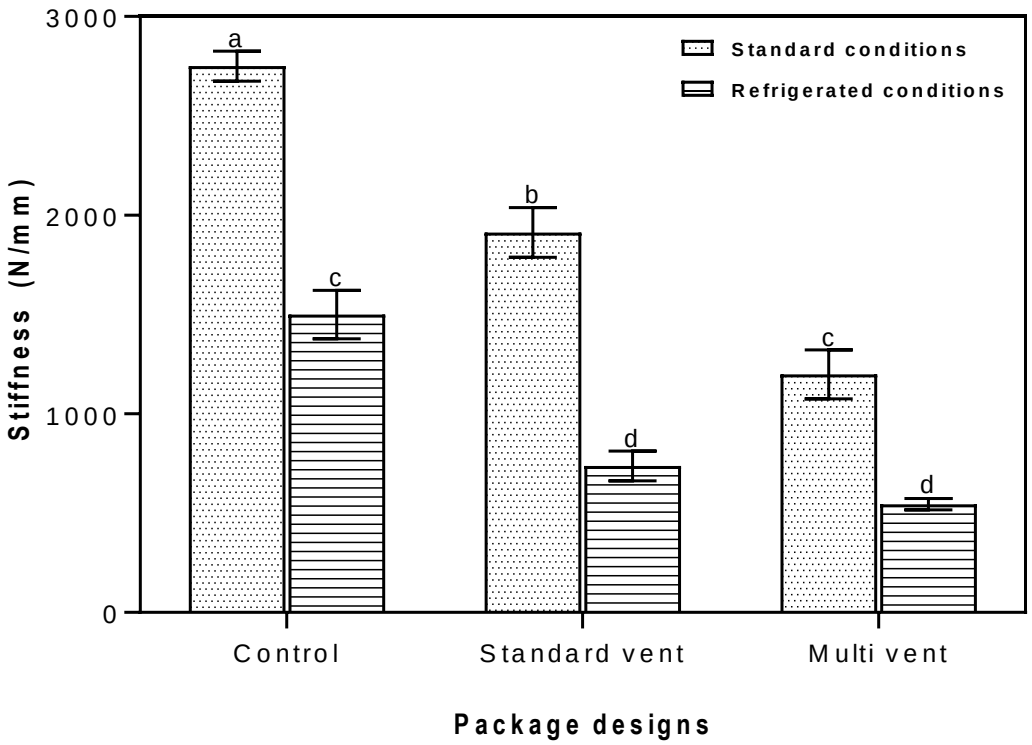

Figure 6.6: Stiffness of the difference package design at standard and refrigerated conditions. Error bars on the figures indicate the standard error of the mean. The letters on the error bars were used to show the statistical difference ($p<0.05$). Mean values with the same letters are not statistically different ($p<0.05$).

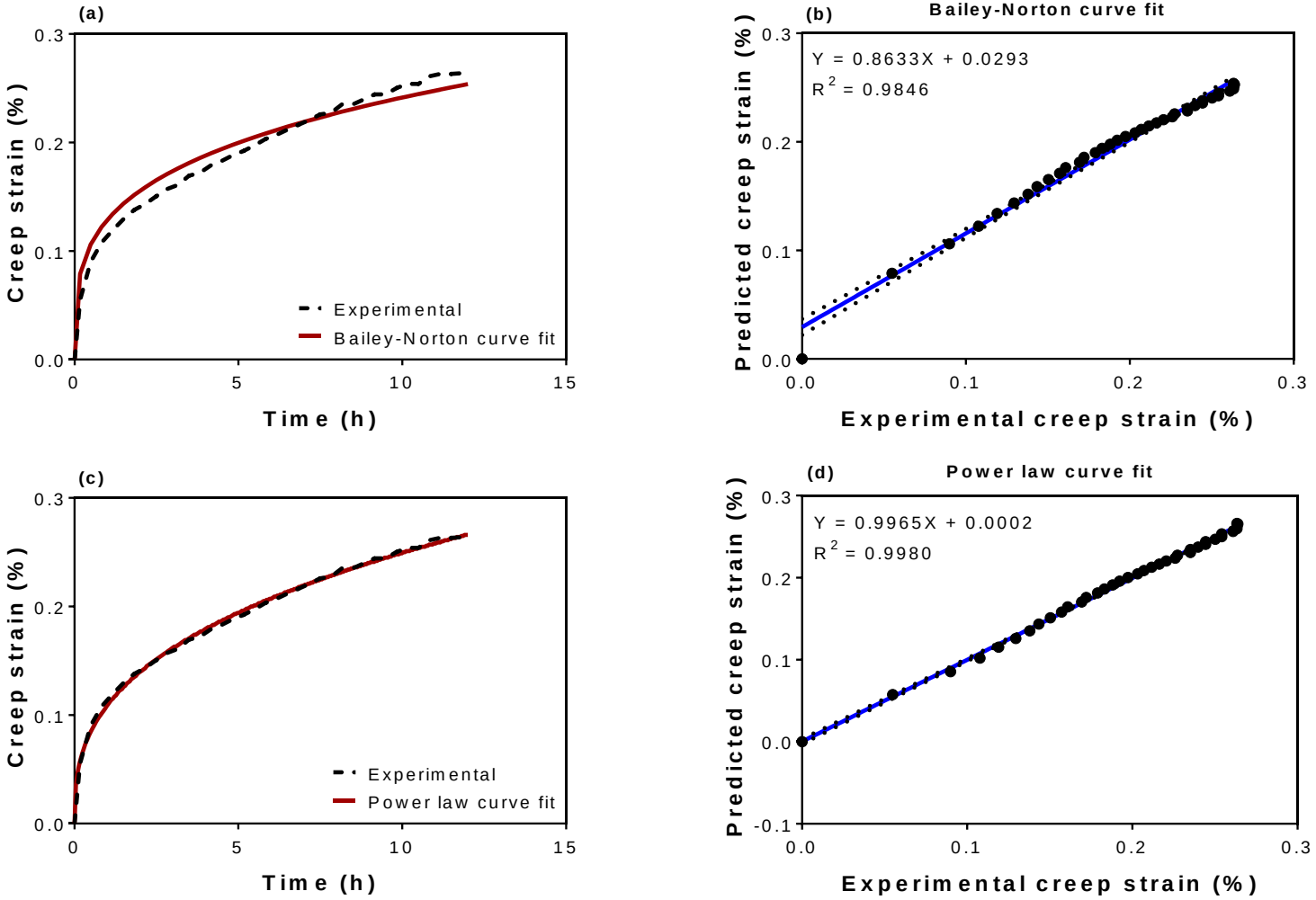

Figure 6.7: Creep strain vs time curve fitted with Bailey-Norton creep law and Power law models for the Control package with 50% load at standard conditions.

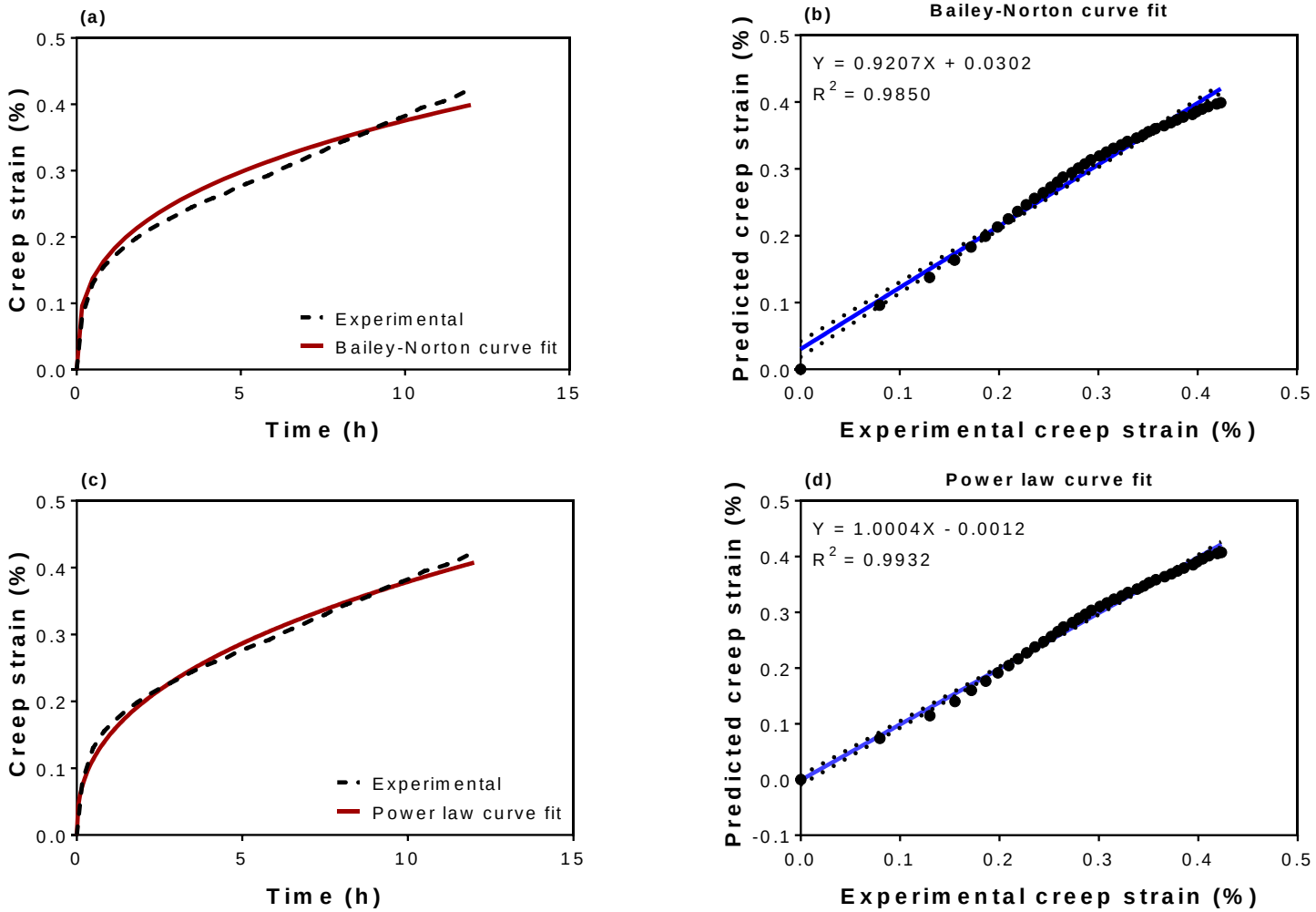

Figure 6.8: Creep strain vs time curve fitted with Bailey-Norton creep law and Power law models for the Control package with 80% load at standard conditions.

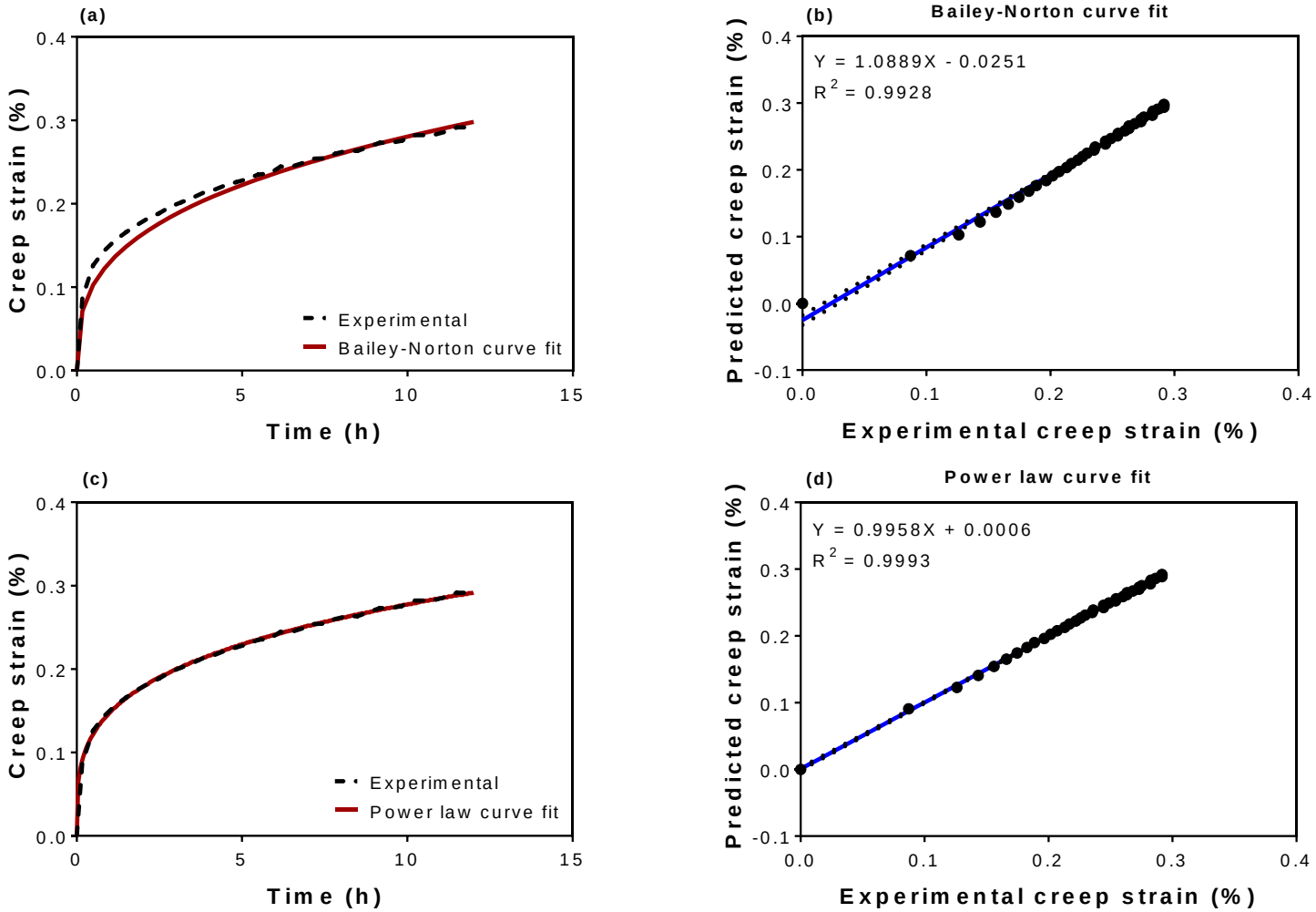

Figure 6.9: Creep strain vs time curve fitted with Bailey-Norton creep law and Power law models for the Standard vent package with 50% load at standard conditions.

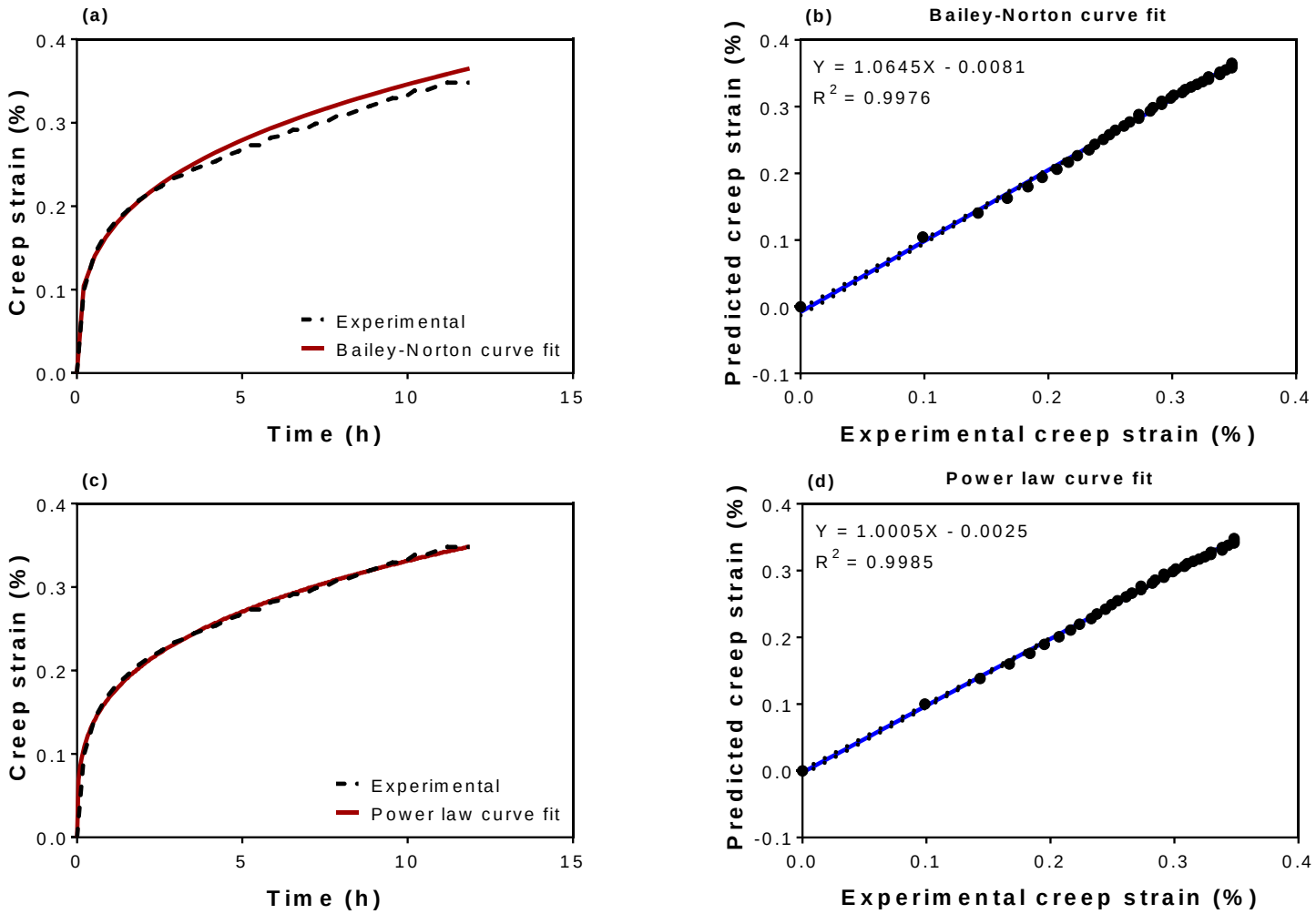

Figure 6.10: Creep strain vs time curve fitted with Bailey-Norton creep law and Power law models for the Standard vent package with 80% load at standard conditions.

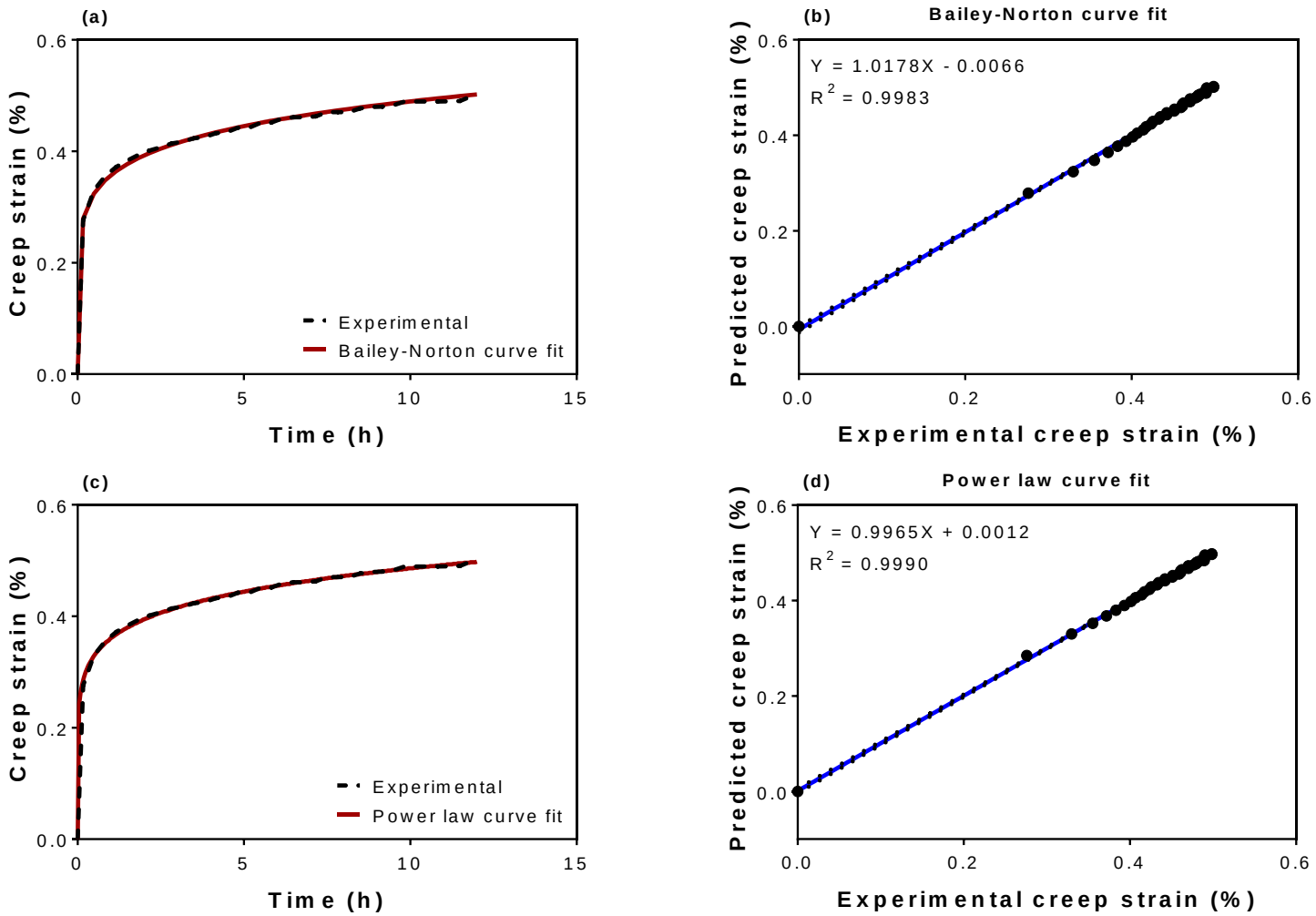

Figure 6.11: Creep strain vs time curve fitted with Bailey-Norton creep law and Power law models for the Multi vent package with 50% load at standard conditions.

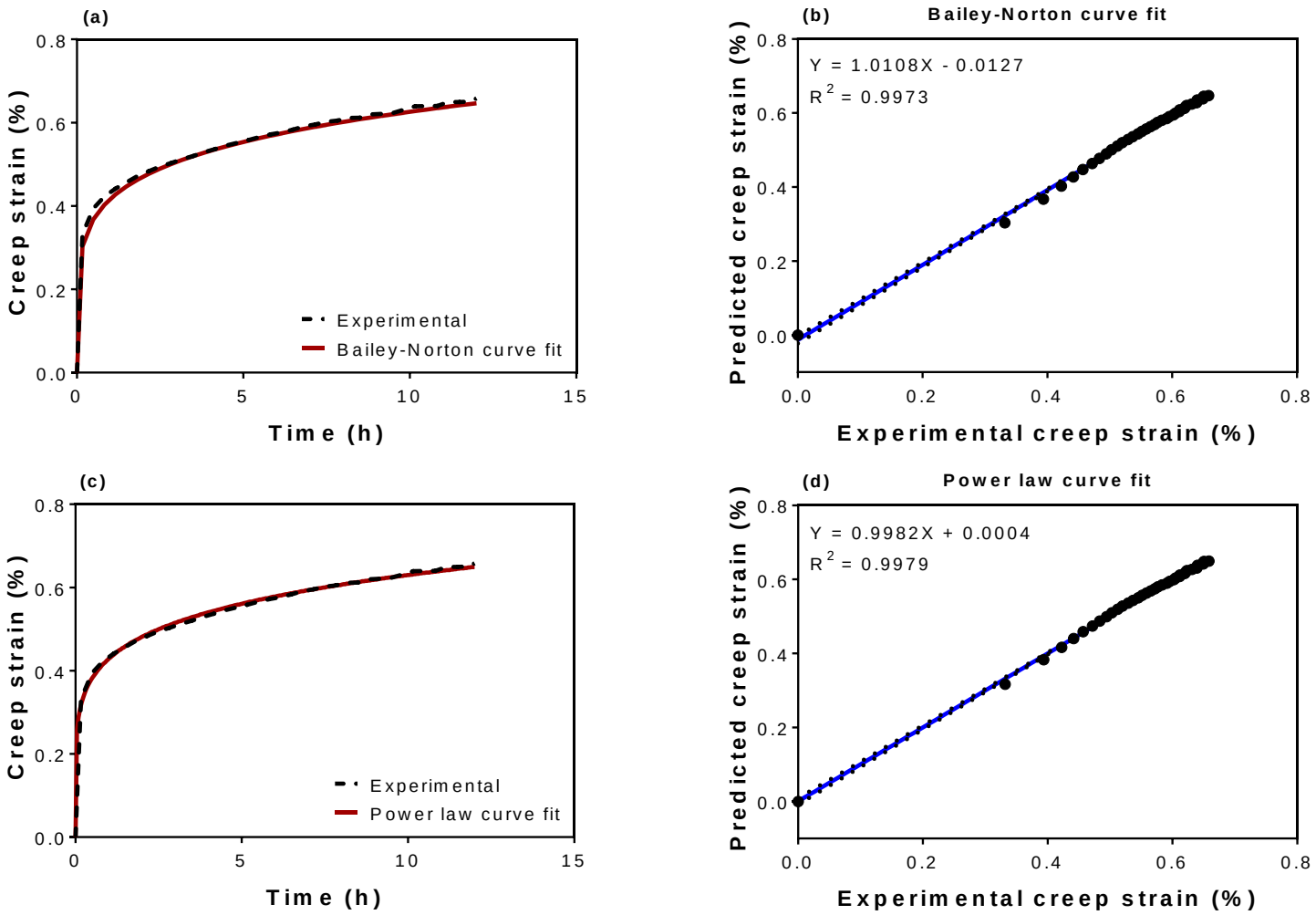

Figure 6.12: Creep strain vs time curve fitted with Bailey-Norton creep law and Power law models for the Multi vent package with 80% load at standard conditions.

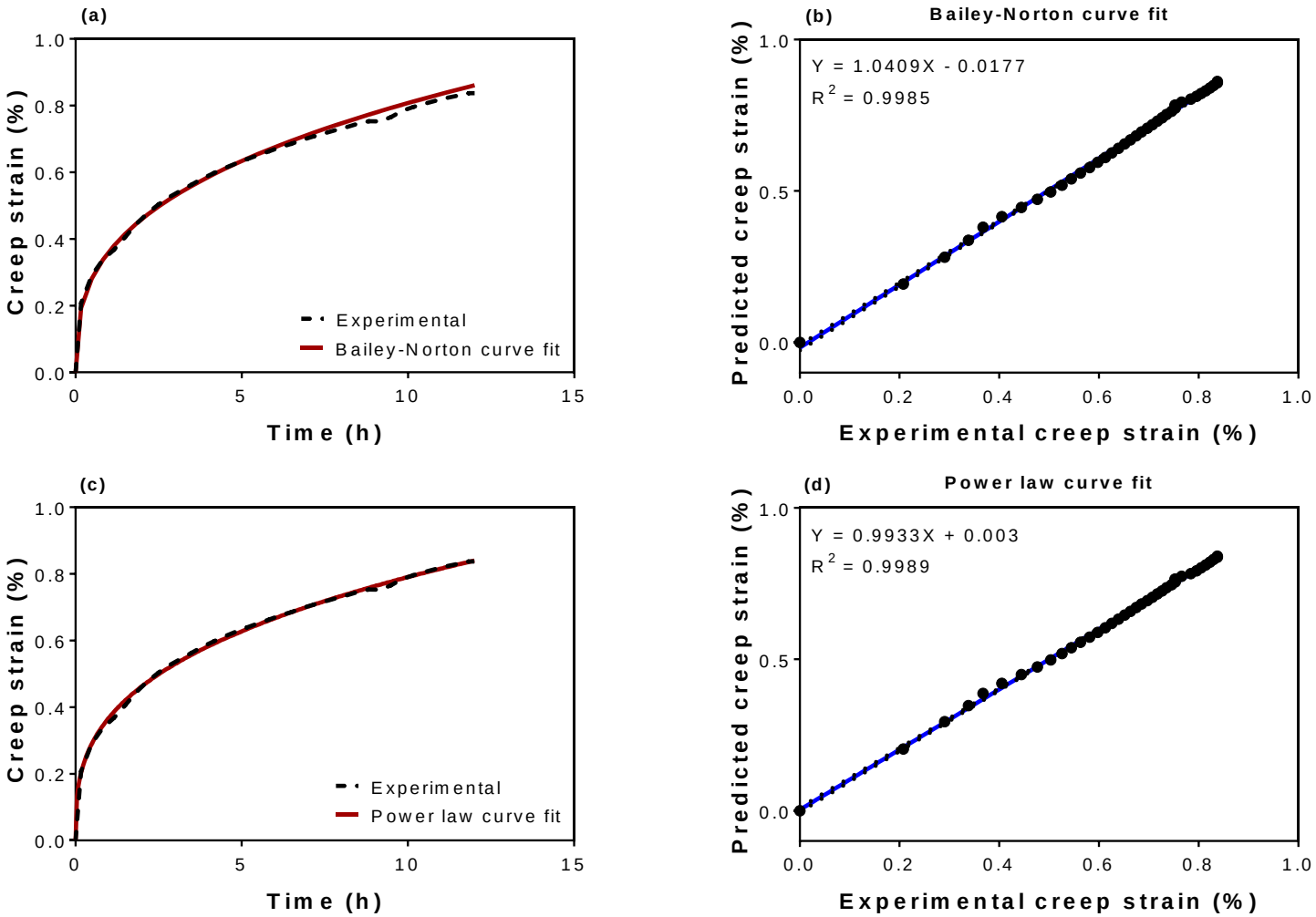

Figure 6.13: Creep strain vs time curve fitted with Bailey-Norton creep law and Power law models for the Control package with 50% load at refrigerated conditions.

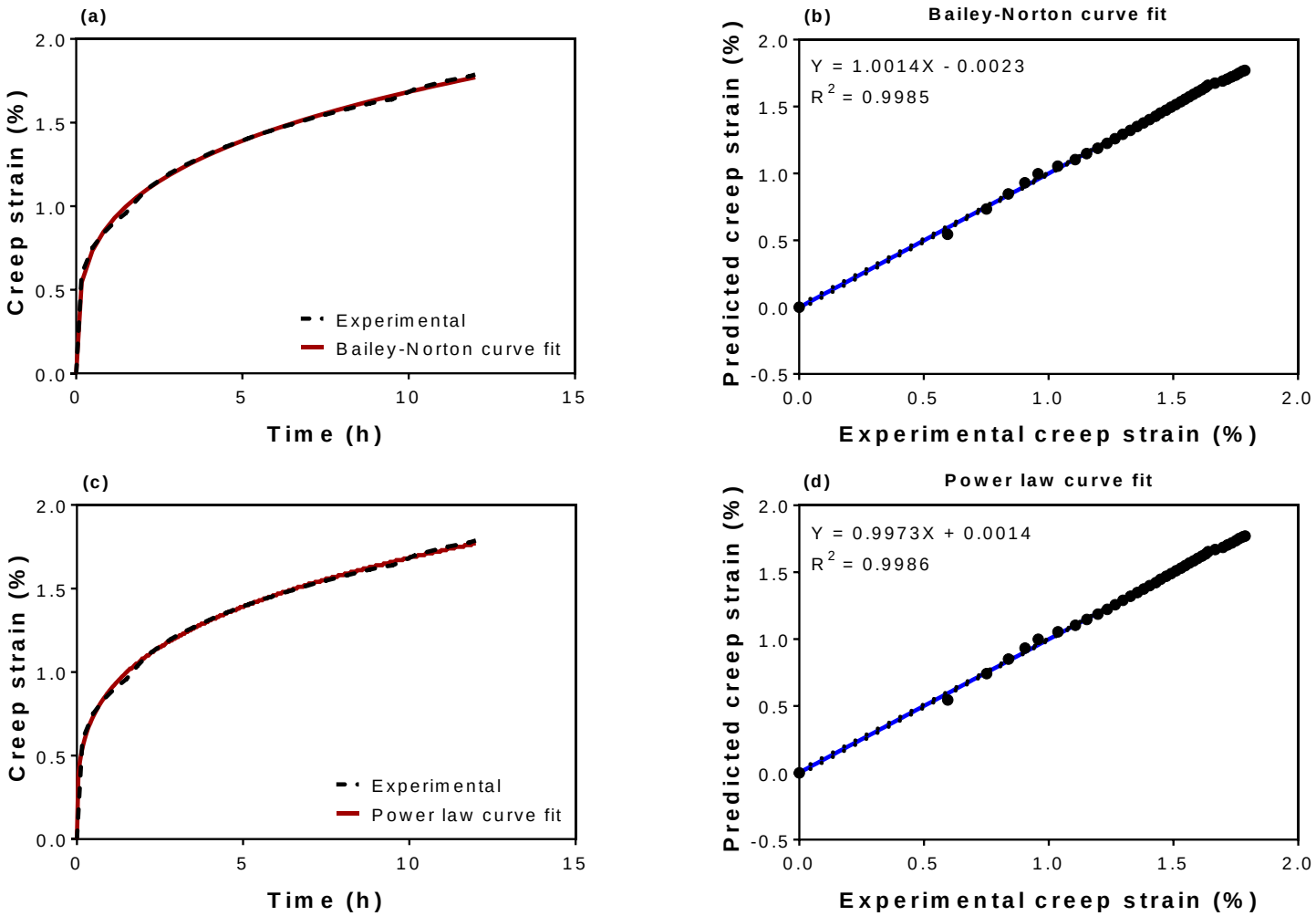

Figure 6.14: Creep strain vs time curve fitted with Bailey-Norton creep law and Power law models for the Standard vent package with 50% load at refrigerated conditions.

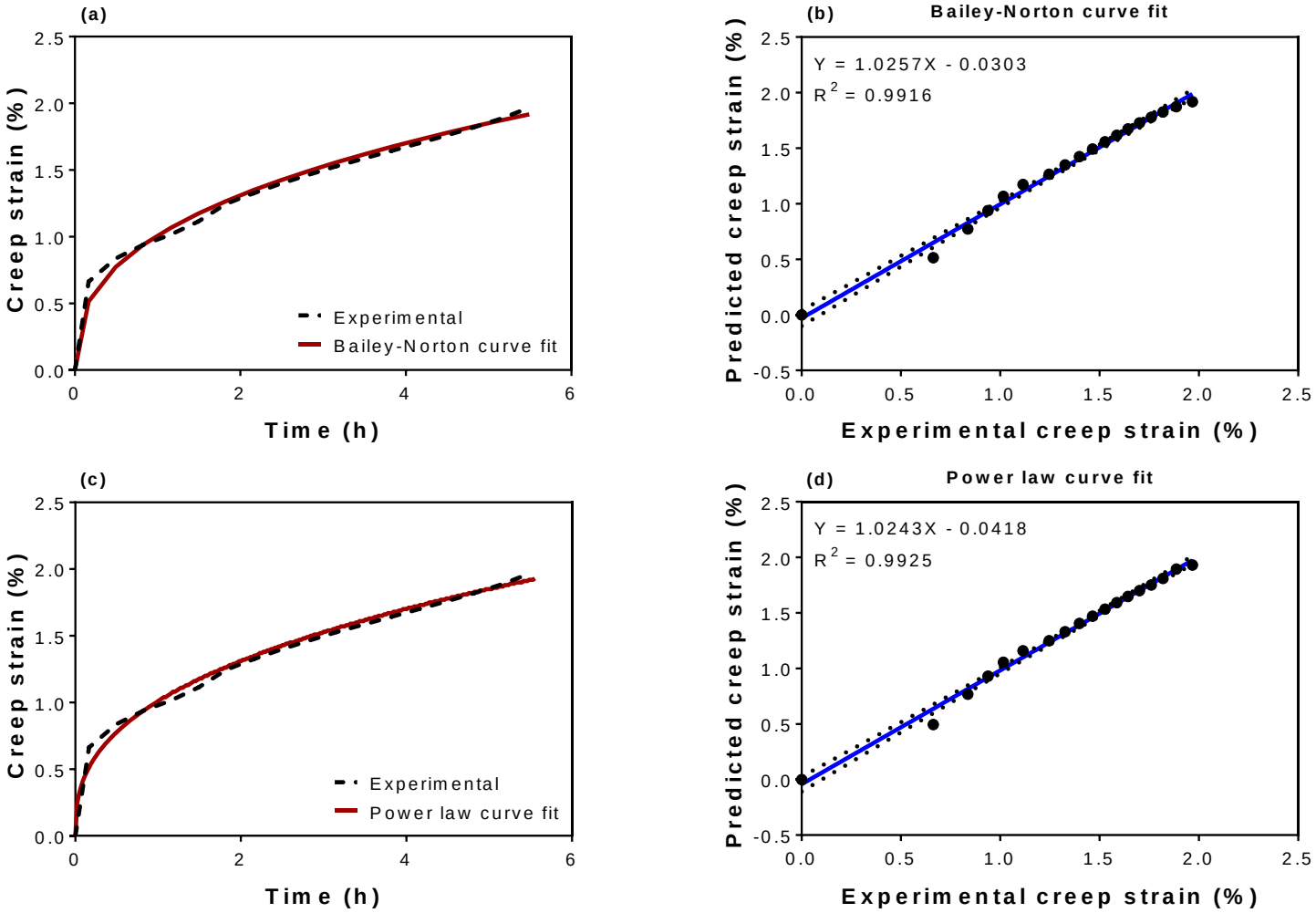

Figure 6.15: Creep strain vs time curve fitted with Bailey-Norton creep law and Power law models for the Multi vent package with 50% load at refrigerated conditions.

Table 6.1: Parameters obtained from the Bailey-Norton creep law and Power law models for the creep strain for 50% load applied at standard conditions.

50% of the compression strength				
Package type	parameter	Bailey-Norton creep law {Eq. (6.3)}	parameter	Power law {Eq. (6.2)}
Control	n	1.0192	a	5.6915×10^{-5}
	m	0.2732	b	0.3603
Standard vent	n	0.9939	a	0.0002
	m	0.3338	b	0.2734
Multi vent	n	1.2865	a	0.0012
	m	0.1373	b	0.1298

Note: The creep strain-hardening coefficient (A) obtained from the Bailey-Norton creep law was constant for all the package types with a value of 4.10×10^{-9} $N^{-1}m^2s^{-1}$. ε^c is the creep strain and t is the time (s).

Table 6.2: Parameters obtained from the Bailey-Norton creep law and Power law models for the creep strain for 80% load applied at standard conditions.

80% of the compression strength				
Package type	parameter	Bailey-Norton creep law {Eq. (6.3)}	parameter	Power law {Eq. (6.2)}
Control	n	0.9566	a	5.5921×10^{-5}
	m	0.3334	b	0.4018
Standard vent	n	0.9938	a	0.0002
	m	0.3094	b	0.2925
Multi vent	n	1.2690	a	0.0011
	m	0.1771	b	0.1673

Note: The creep strain-hardening coefficient (A) obtained from the Bailey-Norton creep law was constant for all the package types with a value of 4.10×10^{-9} $N^{-1}m^2s^{-1}$. ε^c is the creep strain and t is the time (s).

Table 6.3: Parameters obtained from the Bailey-Norton creep law and Power law models for the creep strain for 50% load applied at refrigerated cold chain conditions.

50% of the compression strength				
Package type	parameter	Bailey-Norton creep law {Eq. (6.3)}	parameter	Power law {Eq. (6.2)}
Control	n	1.0991	a	0.0002
	m	0.3499	b	0.3324
Standard vent	n	1.2741	a	0.0009
	m	0.2754	b	0.2754
Multi vent	n	1.2311	a	0.0005
	m	0.3769	b	0.3769

Note: The creep strain-hardening coefficient (A) obtained from the Bailey-Norton creep law was constant for all the package types with a value of 4.10 x 10^{-9} $N^{-1}m^2s^{-1}$. ε^c is the creep strain and t is the time (s).

Chapter 7. Evaluating the displacement field of paperboard packages subjected to compression loading using digital image correlation (DIC)

Abstract

Digital image correlation (DIC) is a full-field non-contact optical technique for measuring displacements in experimental testing based on correlating several digital images taken during the test, particularly images before and after deformation. Application of DIC cuts across several fields, particularly in experimental solid mechanics; however, its potential application to paperboard packaging has not been fully explored. To preserve fresh horticultural produce during postharvest handling, it is crucial to understand how the packages deform under mechanical loading. In this study, 3D digital image correlation with two cameras and stereovision was used to determine the full-field displacement of corrugated paperboard packaging subjected to compression loading. Strain fields were derived from the displacement fields. Results obtained from the displacement fields showed the initiation and development of the buckling behaviour of the carton panels. The displacement was observed to be largely heterogeneous. The displacement field in the horizontal direction was smaller compared to that of vertical and out-of-plane directions. In addition, the strain variation increased as load increased, which could be a precursor to material failure. The technique proved to be efficient in providing relevant information on the displacement and strain fields at the surface panels of corrugated paperboard packages used for handling horticultural produce. In addition, it offers prospects for improved mechanical design of fresh produce packaging.

Keywords: Digital image correlation (DIC), displacement, strain, corrugated paperboard packages, compression test, package design.

7.1 Introduction

Paper as a packaging material has been widely used for various products such as food, horticultural produce, medicine, clothing, electronics, among others (Zhou et al., 2013). This packaging material is adopted widely because it belongs to a group of flexible materials, low in cost and has an excellent lightweight performance, i.e., its low weight-to-strength ratio and high stiffness-to-weight ratio (Flatscher et al., 2011; Giampieri et al., 2011; Navaranjan & Johnson, 2006). For flexible materials, nonlinearity and viscoelasticity properties are apparent, and due to the softness of the materials, creep and stress relaxation are common (Zhou et al., 2013; Navaranjan & Johnson, 2006).

In experimental solid mechanics, measurement of the surface deformation of materials and structures is a crucial step (Pan et al., 2009). To obtain adequate measurements in the localised region, it is crucial to apply a robust full-field measurement method. Some optical measurement methods such as speckle photography, laser interferometry, and image correlation methods have provided promising alternatives and have been successful in different applications. According to Sutton et al. (2000), the use of digital image correlation (DIC) in particular has become predominant for full-field measurement in solid mechanics. Pan et al. (2009) described DIC as a non-interferometric optical technique. Non-interferometric techniques under experimental conditions have less precise requirements and to evaluate the surface strain/deformation on an object, the technique compares the gray intensity changes on the surface of an object before and after deformation. The DIC technique is a typical non-interferometric optical technique with very distinct advantages of simple experimental set-up, minimum requirement on experimental environment without the need of laser source and wide range of its application (Pan & Li, 2011), has been widely accepted for full-field motion measurement, it expands its use to deformation and shape measurement at various temporal and spatial scale, characterisation of mechanical parameters as well as numerical and theoretical experimental cross validation. Like every other optical measurement method, DIC has been successfully used in various fields, including science and engineering research (Orteu, 2009; Pan et al., 2009; Sutton et al., 2008; Sutton et al., 2000; Luo et al., 1994). Pan et al. (2012), Huang et al. (2009) and Yoneyama et al. (2007) reported DIC to be one of the most popular and active techniques used in experimental mechanics with successful application in various areas demonstrated through its effectiveness and practicality.

In measuring the mechanical properties of flexible materials, including paper, Zhou et al. (2013) highlighted three problems that could be encountered in general: (a) alteration in results due to extra reinforcement added by the instrument/equipment. For example, extensometers attached to the surface of a sample increases the local stiffness of the sample; (b) the deformation in flexible materials is relatively large and they are characterised by nonlinearity, therefore, during measurement, the instrument must have good stability and (c) real time monitoring of the packages during transportation through the supply chain is difficult. Although the DIC

technique has minimal requirements when it comes to the experimental environment, this technique is not trouble-free. The fact that DIC is an optical measurement method which is based on matching images or patterns, for instance before and after deformation, it implies that measurements rely strongly on the quality of the acquired images.

Several authors have used digital image correlation in various ways including observing the local mechanical behaviour of materials like metals, polymers and ceramics (Hild & Roux, 2006; Wattrisse et al., 2001; Sutton et al., 1986). Strain measurements and the elastic properties of materials like silicon, steel, polycrystalline, and brittle materials have also been determined using DIC (Godara et al., 2009; Chasiotis & Knauss, 2002; Wattrisse et al., 2001; Sutton et al., 1986). Although there is a limited application of full-field optical techniques like DIC on paper and paperboards, there are some evidence that the mechanical behaviour when subjected to various load can be determined using these techniques for strain measurement (Viguié & Dumont, 2013; Considine et al., 2005; Wong et al., 1996; Thorpe & Choi, 1992). For example, the local grammage and local strain was reported by Wong et al. (1996) to be inversely proportional in uncalendared paper sheets. In the study by Thorpe and Choi (1992), the authors measured the strains on the surface of a box panel subjected to compression with a two-dimensional (2D) DIC by considering both the convex and concave buckling modes. The information obtained by the authors was incomplete and particularly not sufficient when dealing with buckling problems because the contribution of the out-of-plane displacement to the strain components was not considered. The authors showed that the corner regions of the box panel are more significantly affected by the in-plane shear strains. Allansson and Svärd (2001) measured the displacement field of a board panel under compression with a supporting frame in the out of plane direction using a digital speckle photography technique. The study by Considine et al. (2005) used direct observation to evaluate the local deformation of paperboard and hand sheets. The authors used DIC to capture and analyse images under increasing tension and found the variation in strain to increase with an increase in load. The strain became more erratic near failure, indicating many local failures.

During the last decades, the use of DIC techniques, particularly in displacement and strain measurements have been greatly developed. For example, measuring a three-dimensional (3D) displacement field and surface strain field of any 3D object is now possible (Viguié et al., 2011). However, the use of DIC to measure the displacement field of ventilated paperboard packages subjected to mechanical loads has not yet been reported in detail. Since the nature of paper is highly heterogeneous, it is of importance to know the fibre distribution, pattern and localised straining of the paper. Therefore, the aim of this study was to deepen the knowledge of the displacement field of corrugated paperboard cartons under compressive load.

7.2 Basic principles of digital image correlation (DIC)

The concept of using DIC for determining surface deformation was proposed in the beginning of the 1980s by a group of researchers at the University of Carolina, when it was applied to solid mechanics (Pan et al., 2009; Schreier, 2003; Sutton et al., 1986). Its development over the years has made DIC technique powerful and popular in areas such as; fracture mechanics, full field motion, high temperature deformation measurements, biomaterials, inverse stress analysis and wood products etc. (Pan & Li, 2011). In recent years, the technique of DIC has been applied to deformation measurements of images acquired from X-ray micro tomography, scanning electron microscopy (SEM) and atomic force microscopy (AFM).

DIC is an application based on the comparison of two images acquired at different states, one before deformation and the other one after (Hung et al., 2003). These images are referred to as reference and deformed images, respectively. In another definition by Pan et al. (2010), the author defined DIC as non-contact, full field optical metrology used to measure deformation accurately, which could be two-dimensional (2D) or three-dimensional (3D) and shape obtained from digital images of the test object surface, which are recorded at different configurations. The basic principle of digital image correlation involves tracking or matching of the same points (pixels) between the image captured before deformation and a series of deformed images captured after deformation as shown in Figure 7.1 (Tekieli et al., 2017; Pan et al., 2012, 2010, 2009; Zhou et al., 2012). To be able to compute the displacement at point p, a square reference subset of $(2M + 1)$ x $(2M + 1)$ pixels, centralised at $p(x, y)$ from the reference image is chosen and used as a tracking means of its corresponding position in the deformed image.

The test samples must be covered with a random speckle pattern, serving as a deformation information carrier (Pan et al., 2010). These pictures are converted to greyscale from a RGB colour model and treated as a matrix. Each matrix element equals a pixel that represents a specific point on the sample surface, with its value based on its intensity from black to white (Tekieli et al., 2017).

To determine the displacement, a ROI (Region of Interest) which is a computational grid is defined on the sample's surface. The position of the speckles in the ROI taken before and after deformation is correlated. Based on the correlation criteria used, the displacement field can be computed. To evaluate the correspondence between the reference and deformed subsets, the cross-correlation (CC) criterion or the sum of squared difference (SSD) criterion are used (Tang et al., 2012; Pan et al., 2010). Common cross-correlation criterion and sum of squared difference criterion used are summarised in Tables 7.1 and 7.2, respectively.

7.3 Materials and methods

7.3.1 Packaging materials and their properties

Three package types were used in this study: unvented Control package and two ventilated corrugated paperboard packages (VCP) referred to as the Standard and the Multi vent designs. The packages were fabricated using a corrugated paperboard die cutter and then assembled and glued. The Standard vent design is specifically used for handling pome fruit in international trade from South Africa (Berry et al., 2017, 2015) while the Multi vent design was proposed as an alternative to the Standard vent design (Berry et al., 2017). The packages are regular slotted cartons, which consist of inner and outer boxes. Both Standard and Multi vent designs have oblong-shaped vent holes oriented vertically on the long and short sides of the packages. The total vent area of both the VCP packages was 4%. For all the package types, the paperboard grammage combination was 250K/175B/250K for the outer carton and 250K/175C/250K for the inner carton The numerical values indicate the paperboard combinations (fluting and liners) grammages (g m^{-2}). K indicates Kraft linerboards while B and C indicate the fluting profile of the paperboard. The thickness of the liners was 0.349 ± 0.002 mm while the thickness of the flute was 0.249 ± 0.002 mm. The outer dimensions of the packages are 500 mm x 333 mm x 270 mm. Figure 7.2 shows the geometry of the control package, Standard vent and Multi vent designs while Figure 7.3 shows the dimensions of the Standard and Multi vent designs.

7.3.2 Package compression test

The Lansmont compression tester (Lansmont Corporation, Monterey CA, USA) was used to determine the compressive strength of the packages. The test was done following the recommendations of the ASTM D642 standard (ASTM, 2010). A preload of 222 N was applied to remove the initial transient effects, prior to obtaining the compression strength values. The fixed platen mode of the compression tester was used to conduct the compression test at a continuous speed of 12.7 ± 2.5 mm min^{-1} until failure was observed. Prior to the compression test, the packages were preconditioned at 30 ± 1 °C and RH of 20–30% for 24 h and then conditioned at 23 ± 1 °C and 50% RH for 24 h according to ASTM D4332 standard (ASTM, 2006). Three replicates for the different package designs were used for the compression test. During the compression test, as the load is applied progressively, a level of the load is reached where the panels of the package become unstable and bend laterally. This unstable behaviour causes the central region of the panel to decrease significantly in its ability to withstand further increase in load. The compressive load and crosshead displacement are recorded continuously until collapse occurs.

7.3.3 DIC technique for displacement field of the package

Figure 7.4 shows a schematic experimental set-up of a 3D DIC method used in this study. The DIC full field measurements were made during compression testing with

the LaVision® camera and software (LaVision Inc., Ypsilanti, MI, USA). The LaVision® 3D system consists of : two charge-coupled device (CCD) cameras with a 5-megapixel resolution, with the lenses having a focal length of 35 mm, LED light sources for illumination, and a computer with installed DaVis DIC software. The DIC system has the capability to measure in-plane and out-of-plane deformation with an accuracy of up to 0.01 pixels and 0.02 pixels, respectively. For the package preparation, a speckle pattern consisting of black dots was randomly applied on the white surface of the package (Figure 7.5). The accuracy of the results may be affected by the size of the dots in the speckle pattern (Tekieli et al., 2017), hence a suitable balance was ensured based on the experimental setup. For this study, the black dots were larger than three pixels to avoid poor correlation due to noise from the test (Crammond et al., 2013; Lecompte et al., 2006). The test was done within a short time after the spray painting to avoid aged speckle patterns, which could cause the paint to flake off leading to inaccurate measurements.

The concept of simple binocular vision is used in 3D image correlation and it applies a detailed calibration procedure to model the cameras (Kolanu et al., 2016; Toubal et al., 2005). An accurate approximation of the same specimen location can be determined for the 3D position with the sensor plane locations in both views for the same specimen point, once the two cameras are calibrated. Synchronisation of the image acquisition process is possible after the calibration to allow the two cameras to capture images simultaneously during the test. To assign the physical dimensions to the images, calibration of the image is required. The calibration plates on the ROI are shown in Figure 7.5. Using the co-ordinate system of the calibration plate, a co-ordinate system was defined.

As the objective of this study is to understand the displacement field of paperboard packages under compression, the images were acquired during the compression test at a frequency of 2 Hz. The exposure time for all the imaging was 3000 µs. In addition, the LED light was set to flash at the frequency of the imaging. The method of subset matching from the acquired images was used to determine the displacements. In this study, square pixel x pixel subsets sizes were used in the analyses. The subset used was 121 x 121 pixel, and the correlation was performed with a step size of 8 pixels. The small step size used was chosen to ensure a dense displacement fields. In order to match subsets from the reference image to the deformed image, the ZNSSD correlation method was employed (Huchzermeyer, 2017; Conradie, 2015). The correlation was done using the DaVis DIC software, after which the displacement fields was exported from and imported into Matlab for further operations. Strain fields are obtained by using the ′Gradient′ function in Matlab. This function uses a central and a single-sided differencing schemes for internal points in the displacement field and along the edges of the displacement field, respectively (Huchzermeyer, 2017; Conradie, 2015; Brynk et al., 2012).

7.4 Results and discussions

7.4.1 Package compression strength and displacement

A typical load-displacement curve for all the package designs is shown in Figure 7.6. From the curve, a linear part precedes the nonlinear part; this is often dependent on the hydrogen bond, moisture content and cellulose fibre in the paper (Allaoui et al., 2009a). In addition, the results showed that the Control package was stiffer than the Standard vent and the Multi vent designs. Figure 7.7a and 7.7b show the compression strength and its corresponding displacements, respectively for all the package designs. From Figure 7.7a, the compression strength of the unvented Control package was the highest. When the compression strength of the Standard vent and Multi vent design was compared with that of the Control package, a reduction in strength of approximately 20% and 37% was observed, respectively. Furthermore, there was a significant difference (p<0.05) between the compression strength of all the package designs. These results show the crucial role of the ventilation openings on the package strength (Dimitrov & Heydenrych, 2009; Singh et al., 2008). In addition, the lower compression strength observed for the Multi vent package may be attributed to the number of vent holes. For instance, the Multi vent design had 12 vent holes along the length of the package compared to the 3 vent holes of the Standard vent and the unvented Control package, which had no vent holes.

The average crosshead displacement obtained at the maximum compression strength for all the package designs is shown in Figure 7.7b. From Figure 7.7b, the Multi vent design had the highest displacement of about 11.5 ± 0.2 mm, while the displacement of the Standard vent design and the Control package was approximately 10.3 ± 0.3 mm and 10.5 ± 0.2 mm. No significant difference (p<0.05) in the displacement of the Control package and the Standard vent design was observed. However, the displacement obtained for the Multi vent design was significantly different (p<0.05) from the displacement of the Control package and the Standard vent design. In horticultural packaging, the maximum displacement where a package fails is important since it indicates whether the produce would be damaged or not if the package deforms but does not collapse completely (Defraeye et al., 2015; Frank, 2014; Campbell, 2010).

7.4.2 Evolution of the displacement field during compression

Typically, the output from the 3D DIC is u, v and w displacement maps and the shape of the measured image (Malesa et al., 2013). These represent displacements in the x-, y- and z-directions, respectively. It is worth mentioning that the displacement in the x- and y-directions are the in-plane displacements while the displacement in the z-direction is the out-of-plane displacement. Results of the displacement field in the x-, y- and z-directions for the reference image taken before the compression test for all the package designs is shown in Figure 7.8. Figure 7.9 shows the displacement field in the three directions that occurred mid-way through the compression test while Figure 7.10 shows the displacement field that occurred

when the package reached its maximum compression strength. From Figure 7.8, it can be seen that the initial displacement before the start of the compression test, for all the package designs was approximately zero.

The displacement for all the package designs has a largely heterogeneous distribution. The fibre heterogeneity of paper material has been explained in detail in the study by De Oliveira et al. (1990). It was observed that the displacement field behaviour mid-way through the compression test was different from that of the maximum deformed image. The displacement field taken mid-way through the test (Figure 7.9), was highly heterogeneous. Furthermore, the behaviour of the displacement field was influenced by the package design. It was observed that the displacement in the x-direction was highest at the bottom for the Control package while for the Standard vent and Multi vent packages, the displacement at the top of the package was highest. The same phenomenon of displacement fields was observed in the y-direction for all the package designs. Unlike the displacement fields in the x- and y-directions, the displacement field in the z-direction was highest at the top right corner for the Control package while for the Standard and Multi vent designs, the displacement was highest at the bottom left corner. Furthermore, the displacement in the x-, y- and z-direction mid-way through the compression test was observed to be of the same order. However, the displacement in the y-direction was highest for all the package types and the direction was in the negative y-direction indicating the effect of the compressive load (i.e. downward movement). The maximum displacement for the Control package, Standard vent and Multi vent designs was approximately 5.8 mm, 5.3 mm and 6.8 mm, respectively.

Similar to the displacement field mid-way through the compression test, the displacement field of the maximum deformed image was also highly heterogeneous and was influenced by the package design (Figure 7.10). Comparatively, for all the package designs, the displacement field in the x-direction is smaller than the displacement field in the y- and z-directions. Similar observations were reported in the study by Viguié et al. (2011). In addition, the displacement field in the x-direction for all the package designs behaved differently. For the Control package, the displacement in the x-direction at the top of the package panel was nearly zero, with the highest displacement located towards the bottom of the package panel and mostly negative. Highest displacement was located at the right edges of the panel for the Standard vent, with the displacement at the surface being homogenous and approximately zero. For the Multi vent, the displacement in the x-direction was highest towards the centre of the package panel. Also, the displacement in the y-direction was observed to be nearly homogenous over the surface of the package panel for all the package designs. In addition, the displacement in the y-direction was negative, indicating the downward movement of the panel as a result of the compressive load. Highest displacement in the y-direction was located at the top of the package panels. This can be attributed to the vertical translatory movement exhibited during the BCT. In addition, this may also be due to the crushing that occurs at the junction score of the package during the BCT. The maximum

displacement for the Control package, Standard vent and Multi vent designs was approximately 11.5 mm, 10.5 mm and 12.5 mm, respectively. The displacement in the z-direction i.e. the out-of-plane displacement was highest and was located towards the centre of the package panels. This indicated the predominance of buckling at the centre of the package panels.

The distribution of the out-of-plane displacement field for all the package designs was in the range of about 10 – 30 mm. The maximum displacement for the Control package, Standard vent and Multi vent designs was approximately 24 mm, 30 mm and 25 mm, respectively. The buckling shape of the out-of-plane displacement field for all the packages is shown in Figure 7.11. It can be seen that there was an outward buckling of the package panel of the deformed image. During stacking on a pallet, the packages placed at the bottom of the stack tend to experience the highest loads resulting in a significant out-of-plane deformation of the vertical walls before total collapse (Viguié et al. 2011; Navaranjan & Johnson, 2006). In addition, the out-of-plane displacement is usually small when the load level is below the maximum strength of the package (Figure 7.9), however, on reaching the maximum load, the package deforms rapidly hence decreasing the in-plane stiffness and increasing the out-of-plane displacement as can be seen in Figure 7.10 (Allansson & Svärd, 2001).

The components ε_{xx}, ε_{yy} and ε_{xy} of the strain field for the deformed image are shown in Figure 7.12. The strain behaviour for all the components was different for all the package designs. This shows that the deformation mechanisms can be significantly affected by the configuration of the package. However, it was observed that the variation in strain was more prominent along the edges of the ROI. Contrary to this observation, strain values were approximately zero for most of the components of the strain field at the centre of the ROI. The strain variation for the ε_{xx} component was more pronounced along the vertical edges of the ROI while that of the ε_{yy} component was more pronounced along the horizontal edges of the ROI. It is interesting to note that the strain was more localised in the ε_{xx} component for the Standard and Multi vent design, particularly around the vent holes. The characterisation of the mechanical heterogeneity of paperboard packages will help provide package designers with relevant information for control during manufacturing.

7.5 Conclusion

The DIC technique is a full-field non-contact optical technique for measuring displacements in experimental testing. A 3D DIC technique was applied to measure the full-field displacement and strain at the surface of three corrugated paperboard packages during compression loading. The packages used were unvented Control package and two VCP packages (Standard and the Multi vent). The results showed the development and behaviour of buckling on the surface of the package. The displacements of the packages were observed to be largely heterogeneous in its distribution. The displacement field in the x-direction was smaller compared to that in the y- and z-direction. Furthermore, for the maximum deformed image, the out-

of-plane displacement (i.e. z-direction) had the highest displacement values, with maximum value of approximately 24 mm for the Control package, 30 mm for the Standard vent and 25 mm for the Multi vent. In addition, the displacement was highest in the z-direction at the centre of the ROI and an outward buckling was observed for all the package designs. Package designs affected the strain variation, although strain values were approximately zero at the centre of the ROI. The strain components ε_{xx} and ε_{yy} were observed to be more prominent along the vertical and horizontal edges respectively irrespective of the package design. The obtained results show the applicability of DIC in displacement and strain measurements, particularly for paperboard packages. Furthermore, the results will help to foster better understanding of the failure mechanisms of the packages under compression load, offering prospects for the improvement of fresh produce packaging.

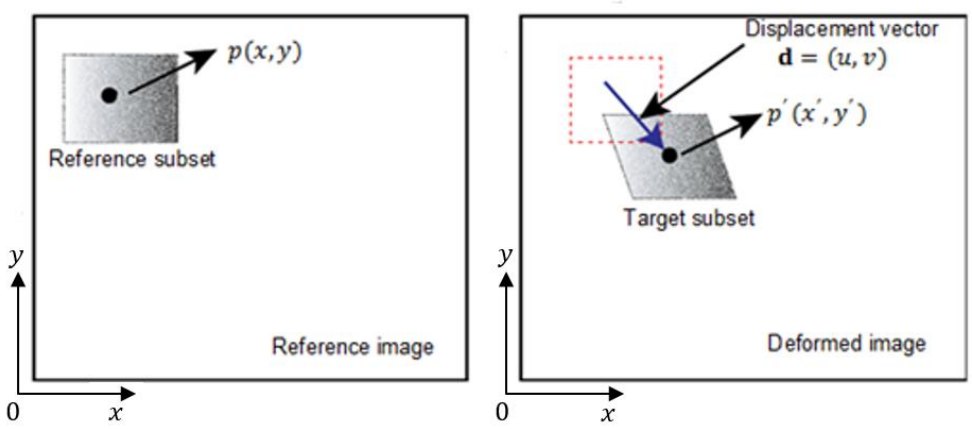

Figure 7.1: Schematic diagram of the reference subset (left) and deformed subset (right) before and after deformation, respectively.

Figure 7.2: Geometry of the different packages used.

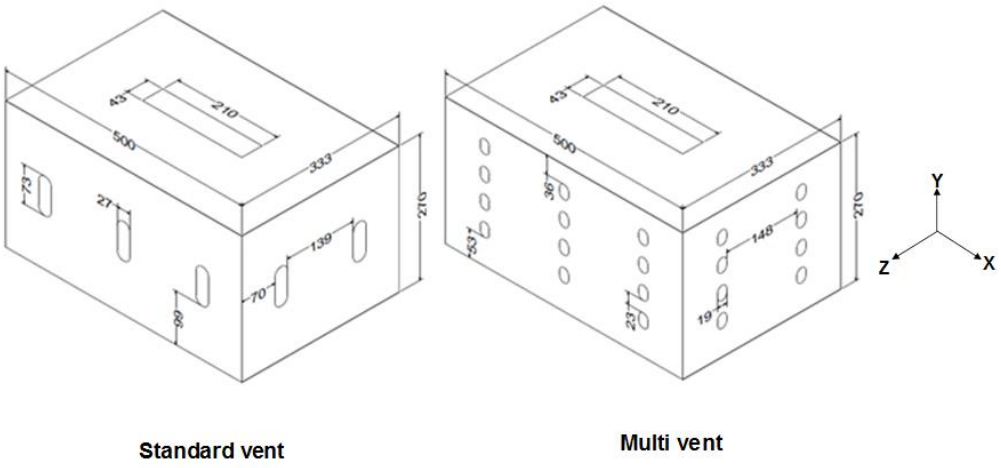

Figure 7.3: Geometry showing the dimensions (in mm) of the Standard and Multi vent designs.

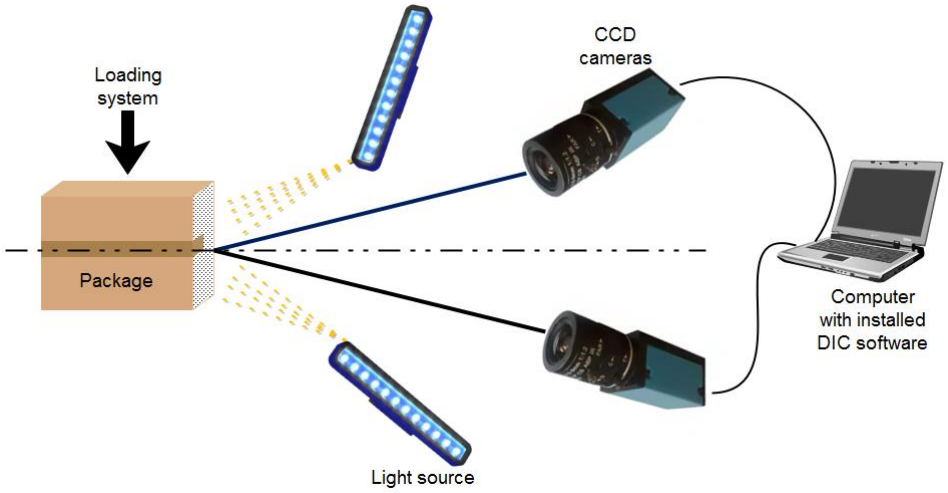

Figure 7.4: Schematic diagram illustrating the 3D digital image correlation (DIC) setup.

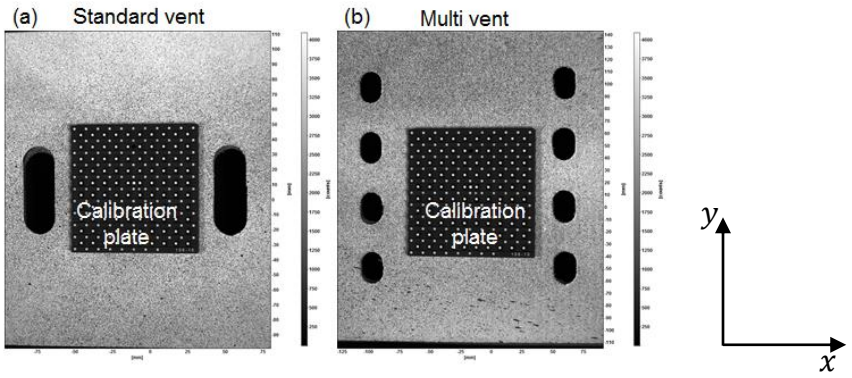

Figure 7.5: Typical speckle pattern used in the measurement a) Standard vent and b) Multi vent. The region of interest is also shown.

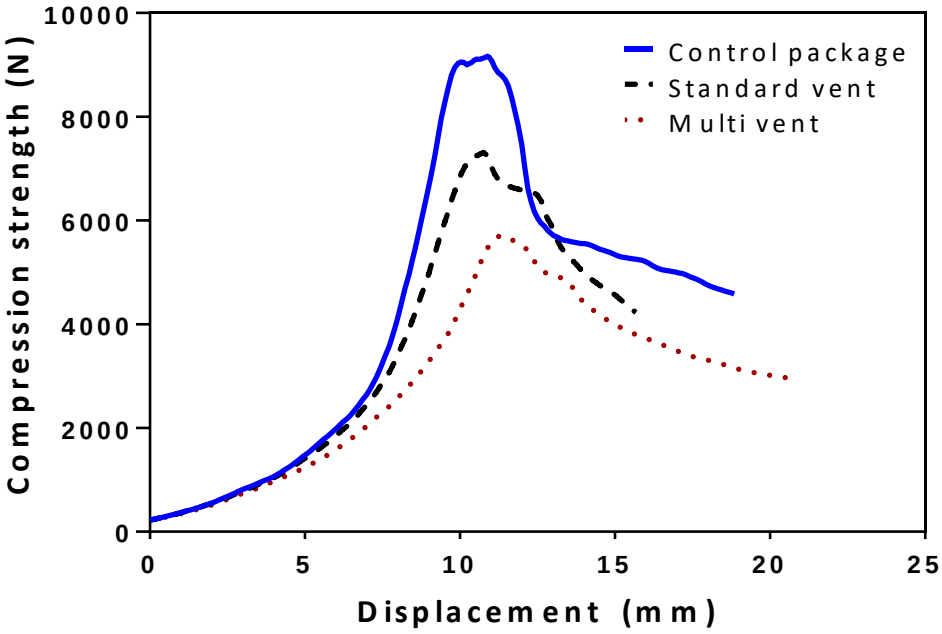

Figure 7.6: Load-displacement curve from the compression test for all the package design.

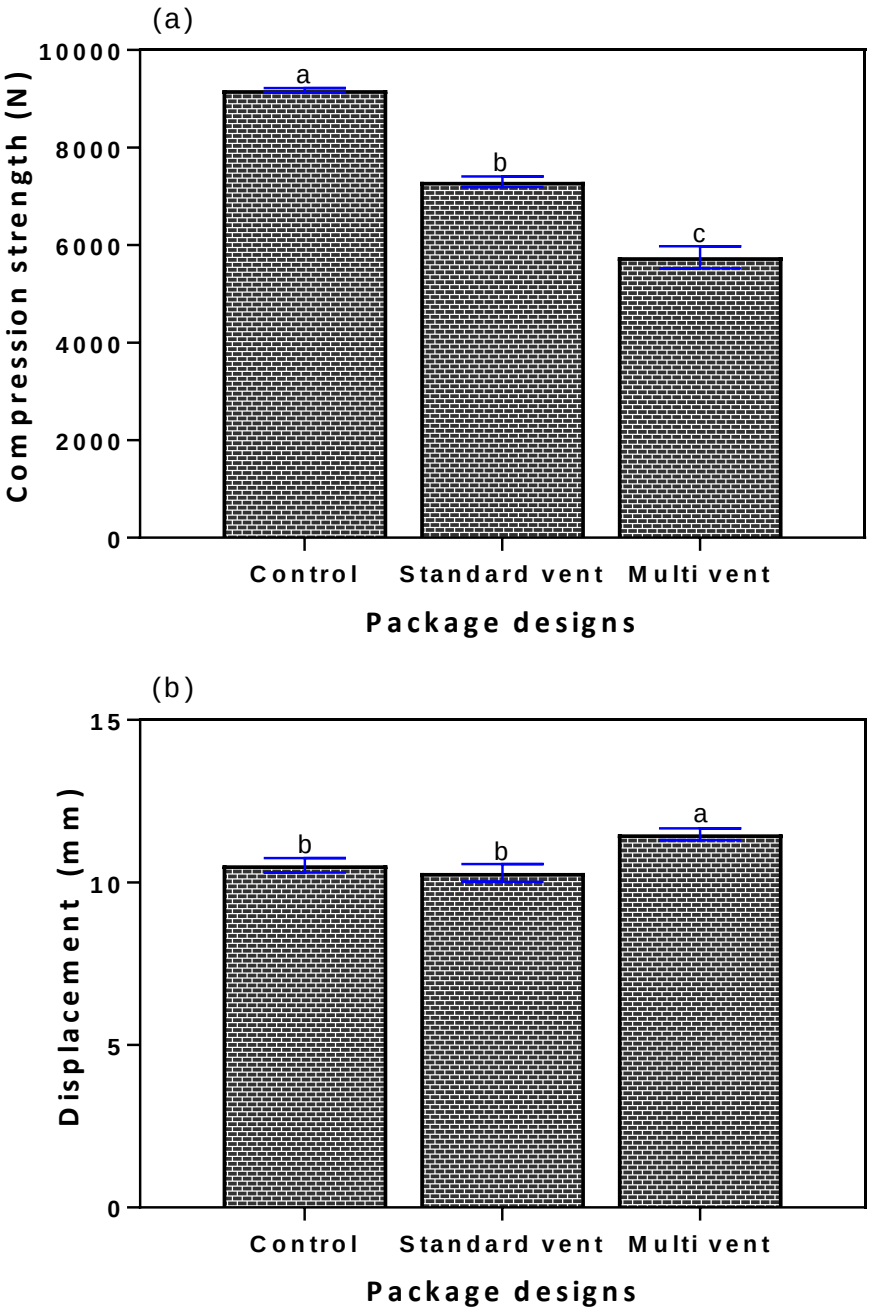

Figure 7.7: Bar chart showing (a) average compression strength (N) and (b) corresponding displacements for all the package designs. The letters on the error bars are used to show the statistical difference. Mean values with the same letters are not statistically different at $p<0.05$.

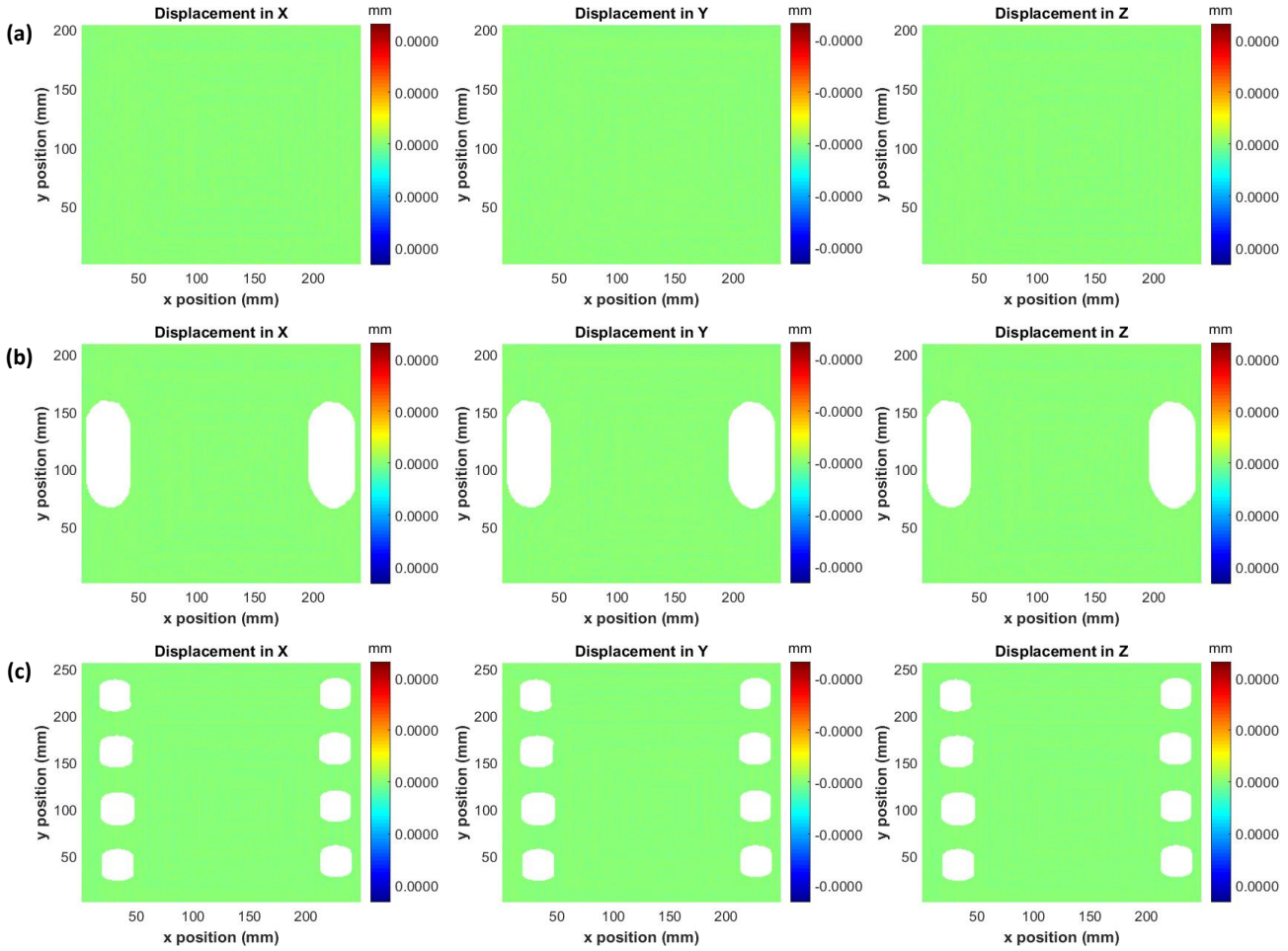

Figure 7.8: Displacement field of the reference image taken before the compression test for (a) Control package, (b) Standard vent and (c) Multi vent.

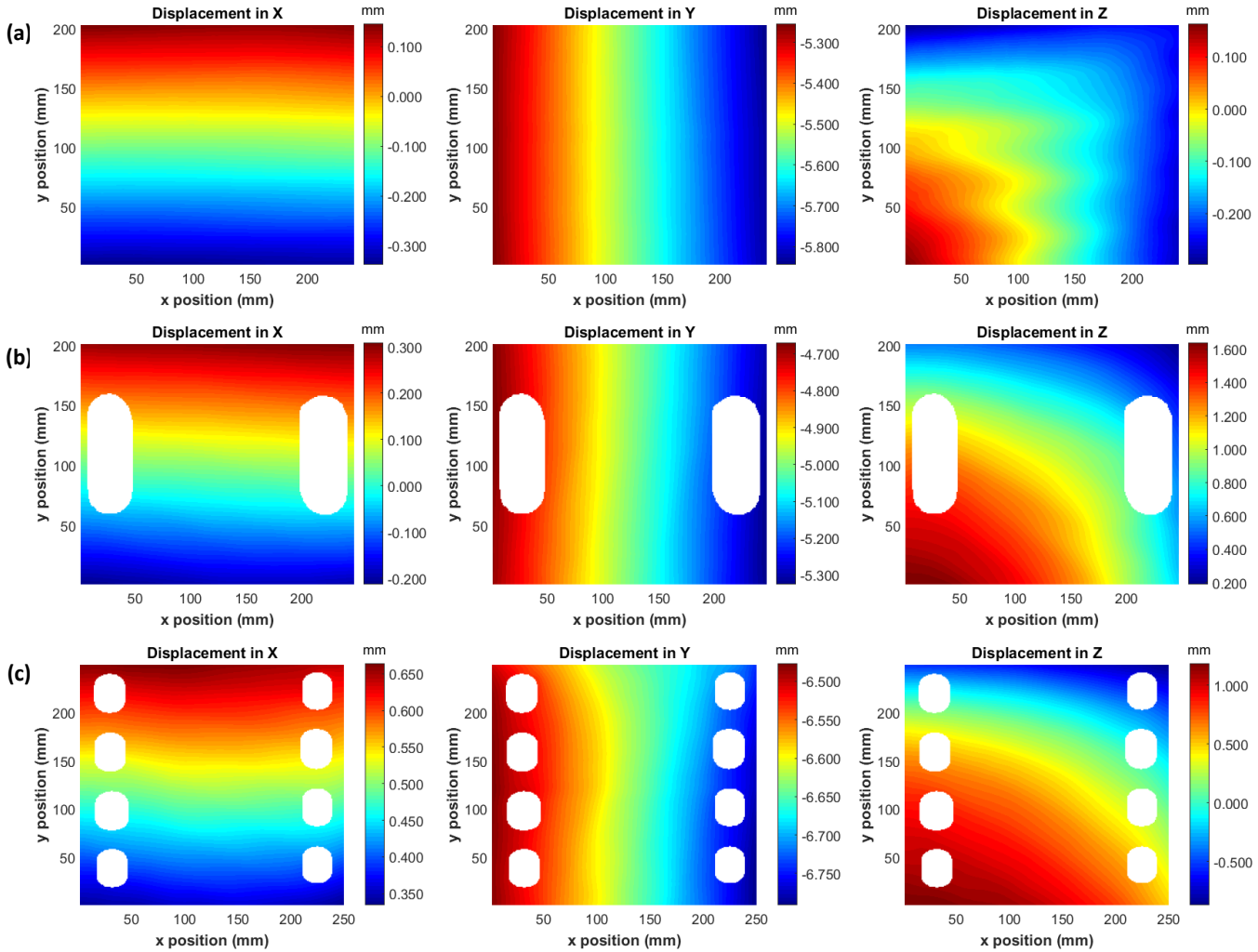

Figure 7.9: Displacement field of the image taken mid-way through the compression test for (a) Control package, (b) Standard vent and (c) Multi vent.

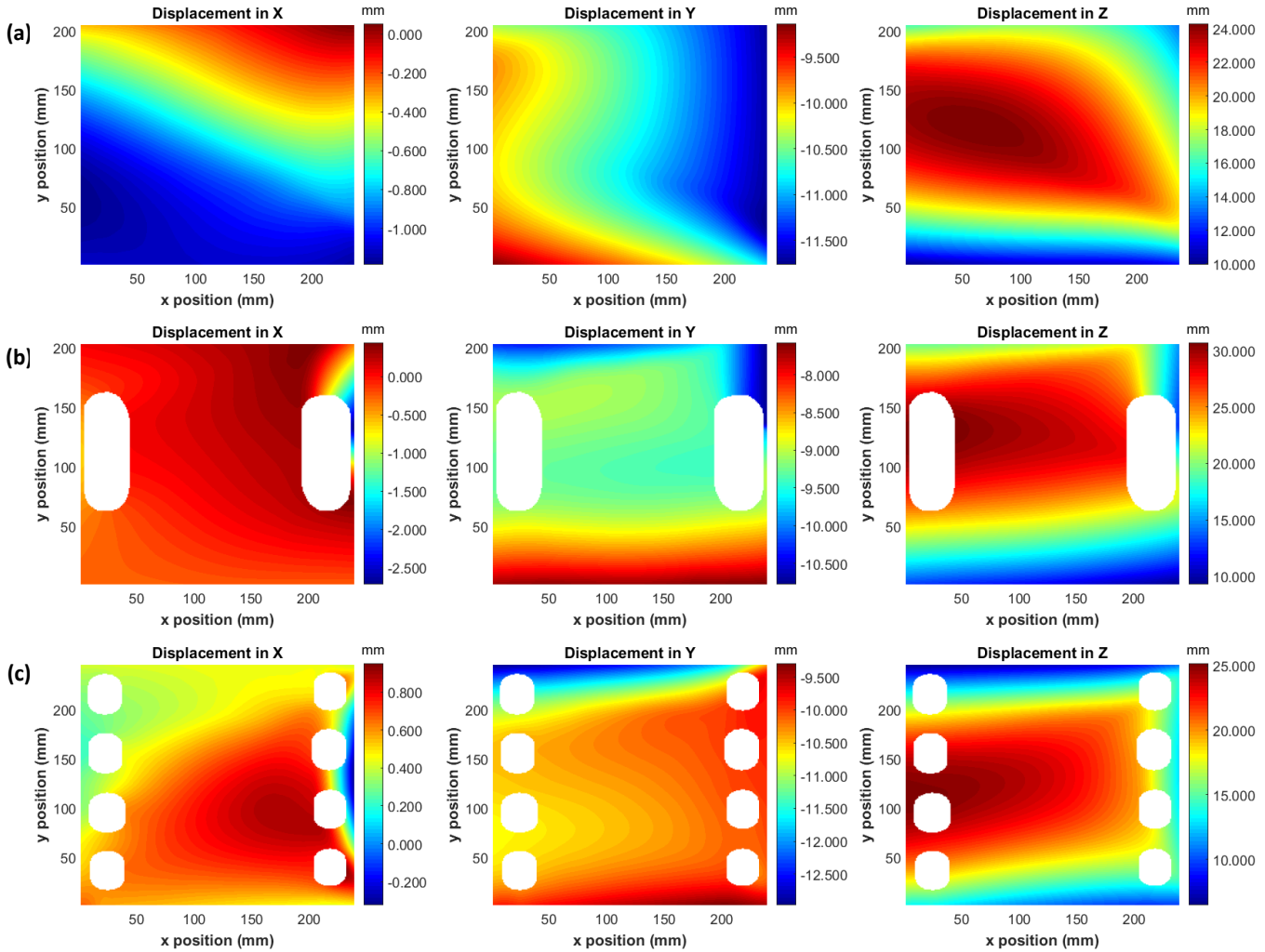

Figure 7.10: Displacement field of the maximum deformed image for (a) Control package, (b) Standard vent and (c) Multi vent.

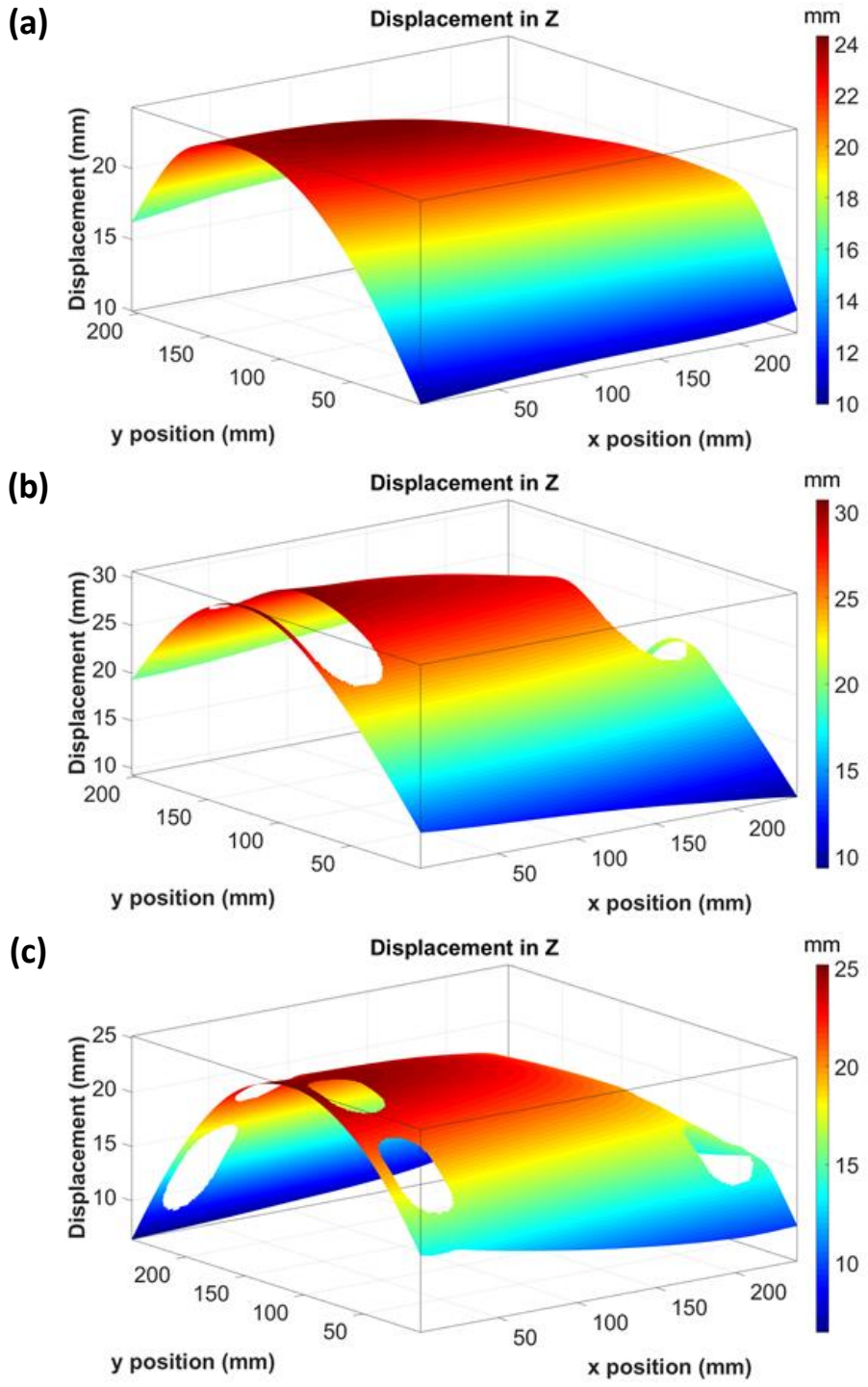

Figure 7.11: The out-of-plane displacement field of the maximum deformed image showing the buckling shape for (a) Control package, (b) Standard vent and (c) Multi vent.

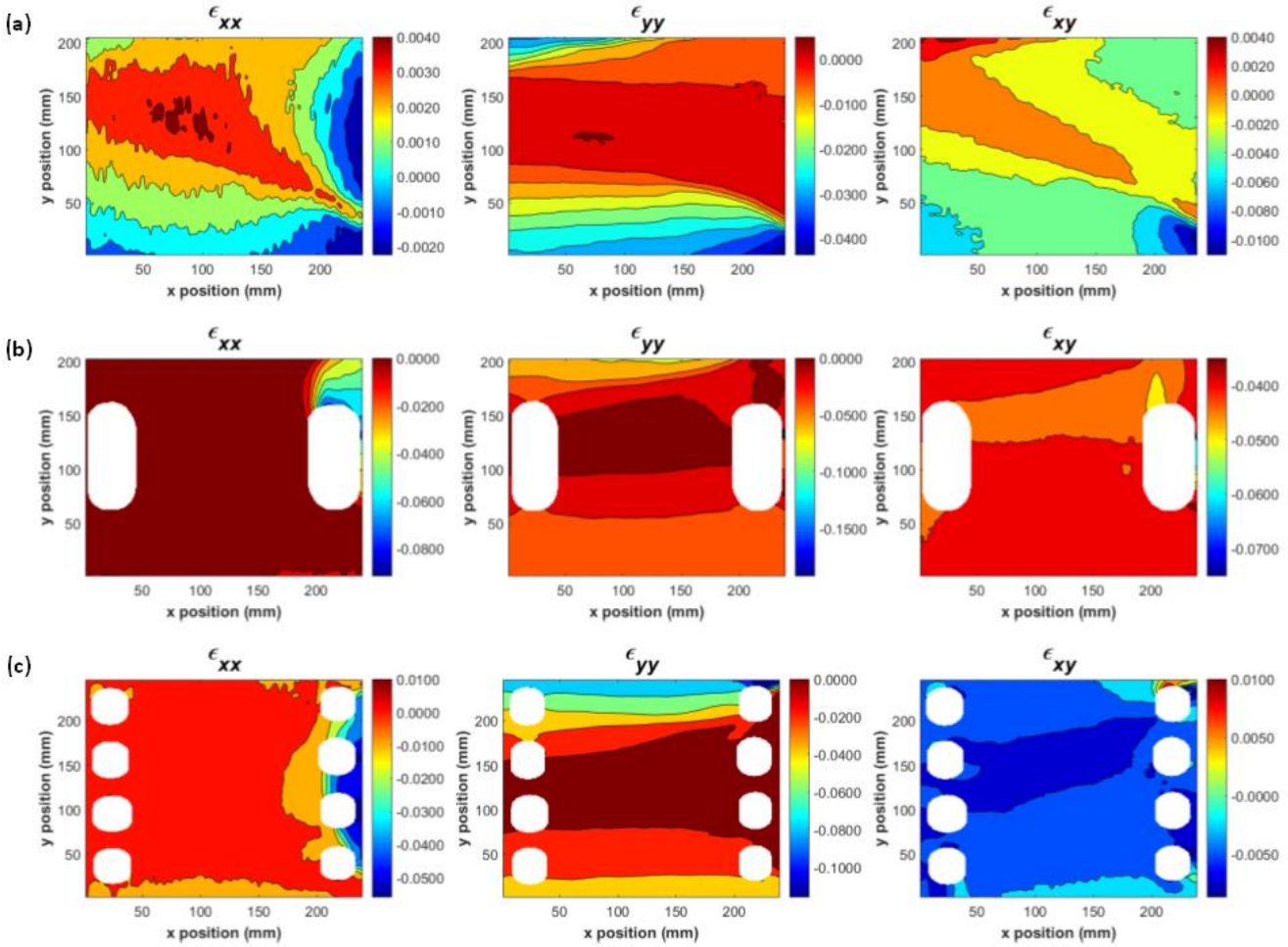

Figure 7.12: Strain field components of the maximum deformed image for (a) Control package, (b) Standard vent and (c) Multi vent.

Table 7.1: Cross-correlation (CC) criterion commonly used.

Cross-correlation criterion	**Definition**
Cross-correlation (CC)	$C_{CC} = \sum_{i=-M}^{M} \sum_{j=-M}^{M} \left[f\left(x_i, y_j\right) g\left(x_i^{'}, y_j^{'}\right) \right]$
Normalised cross-correlation (NCC)	$C_{NCC} = \sum_{i=-M}^{M} \sum_{j=-M}^{M} \left[\frac{f\left(x_i, y_j\right) g\left(x_i^{'}, y_j^{'}\right)}{\overline{f}\,\overline{g}} \right]$
Zero-normalised cross-correlation (ZNCC)	$C_{ZNCC} = \sum_{i=-M}^{M} \sum_{j=-M}^{M} \left\{ \frac{\left[f\left(x_i, y_j\right) - f_m \right] \times \left[g\left(x_i^{'}, y_j^{'}\right) - g_m \right]}{\Delta f \, \Delta g} \right\}$

$f\left(x_i, y_j\right)$ is the gray value of point $\left(x_i, y_j\right)$ in the reference subset of the reference image, $g\left(x_i^{'}, y_j^{'}\right)$ is the gray value of point $\left(x_i^{'}, y_j^{'}\right)$ in the corresponding subset of the deformed image, f_m and g_m are the mean intensity of the reference and target subsets, respectively.

Table 7.2: Sum of squared difference (SSD) correlation commonly used.

SSD correlation criterion	**Definition**
Sum of squared differences (SSD)	$C_{SSD} = \sum_{i=-M}^{M}\sum_{j=-M}^{M}\left[f\left(x_i, y_j\right) - g\left(x_i^{'}, y_j^{'}\right)\right]^2$
Normalised sum of squared differences (NSSD)	$C_{NSSD} = \sum_{i=-M}^{M}\sum_{j=-M}^{M}\left[\frac{f\left(x_i, y_j\right)}{\overline{f}} - \frac{g\left(x_i^{'}, y_j^{'}\right)}{\overline{g}}\right]^2$
Zero-normalised sum of squared differences (ZNSSD)	$C_{ZNSSD} = \sum_{i=-M}^{M}\sum_{j=-M}^{M}\left[\frac{f\left(x_i, y_j\right) - f_m}{\Delta f} - \frac{g\left(x_i^{'}, y_j^{'}\right) - g_m}{\Delta g}\right]^2$

$f\left(x_i, y_j\right)$ is the gray value of point $\left(x_i, y_j\right)$ in the reference subset of the reference image, $g\left(x_i^{'}, y_j^{'}\right)$ is the gray value of point $\left(x_i^{'}, y_j^{'}\right)$ in the corresponding subset of the deformed image, f_m and g_m are the mean intensity of the reference and target subsets, respectively.

Note: The correspondence location of the subsets involves searching the maximum and minimum correlation criterion in a specified area. Defining the terms in Tables 7.1 and 7.2:

$$f_m = \frac{1}{\left(2M+1\right)^2}\sum_{i=-M}^{M}\sum_{j=-M}^{M} f\left(x_i, y_j\right)$$

$$g_m = \frac{1}{\left(2M+1\right)^2}\sum_{i=-M}^{M}\sum_{j=-M}^{M} g\left(x_i^{'}, y_j^{'}\right)$$

$$\overline{f} = \sqrt{\sum_{i=-M}^{M}\sum_{j=-M}^{M}\left[f\left(x_i, y_j\right)\right]^2}$$

$$\overline{g} = \sqrt{\sum_{i=-M}^{M}\sum_{j=-M}^{M}\left[g\left(x_i^{'}, y_j^{'}\right)\right]^2}$$

$$\Delta f = \sqrt{\sum_{i=-M}^{M}\sum_{j=-M}^{M}\left[f\left(x_i, y_j\right) - f_m\right]^2}$$

$$\Delta g = \sqrt{\sum_{i=-M}^{M}\sum_{j=-M}^{M}\left[g\left(x_i^{'}, y_j^{'}\right) - g_m\right]^2}$$

Chapter 8. General conclusions

8.1 A synopsis of the research contributions

In the postharvest handling and distribution of fresh horticultural produce, processed food and other biomaterials, the role of packaging is very crucial (Pathare et al., 2012b). According to Pathare and Opara (2014), packaging helps to facilitate the storage and transportation of produce and most importantly, protects packed produce against hazards that may occur during the distribution cycle, i.e. from production to the final consumer. Mechanical hazards to package/produce can be categorised as compression, impact or vibration. These could result in damage to the produce and is often evident as bruising (Opara &Pathare, 2014; Harker, 2009). Some of the consequences of produce damage are postharvest losses or waste, reduction in quality, rejection by the consumers, decrease in purchasing price and reduction in income generated from produce export. Among many packaging types such as glass, paper, metals, and plastics that exist, paperboard packaging has been commonly used for fresh produce, particularly fruit and vegetables. These produces respire, hence need to be cooled and, also require continuous removal of heat build-up within the package to avoid spoilage. This has consequently led to the advent of ventilated corrugated paperboard (VCP) packages, which have been used extensively for handling fresh produce due to its potential in promoting uniform and rapid cooling (Thompson et al., 2010). The continual improvement of the package is therefore paramount to ensure safe delivery of the produce to the end-users. Therefore, the aim of this research was to gain a better understanding of the structural performance of VCP packaging to enhance the development of better and improved package designs.

To achieve the aim of this research, an extensive literature review was undertaken in chapters 2 and 3. Chapter 2 elucidated the performance of corrugated paperboard packaging towards reducing mechanical damage to horticultural produce. Additionally, different factors such as manufacturing processes and environmental conditions affecting the performance of paperboard packaging were presented. Numerical modelling such as FEA has proven to be successful in predicting the structural integrity of various products subjected to mechanical loadings. Hence, chapter 3 provided recent application of FEA in food packaging, with emphasis on corrugated paperboard packaging. Following these reviews, four stand-alone research chapters are presented to address the objectives of this research.

FEA was applied to predict the compression strength of corrugated paperboard packages used for handling fresh produce in chapter 4. This study considered the geometrical nonlinearities of the package in the modelling approach. The FEA model was validated with experimental studies and a good agreement was found, within 10%. The strength of the package was shown to be linearly related to the liner thickness of the corrugated paperboard. Although, an approximated homogenised core was used to represent the fluting of the corrugated paperboard, the thickness of the core had significant influence on the compression strength of

the package. From the contact model result, maximum stress was concentrated at the corner of the packages. Additionally, the paper materials and the paperboard used for manufacturing the package were characterised to determine the tensile properties, edge compression resistance and flat crush resistance. An important contribution of this study is the provision of the constitutive link between the corrugated paperboard materials, including the geometrical nonlinearities (contact boundary conditions) of the package, and their effects on the strength of the package. This led to the development of models of different package configurations to improve its structural integrity. Although the thickness of the liners of the package has a linear relationship with the package strength, changing the liner thickness has an insignificant and minimal effect on the strength of the package. As a result, there was a need to test the different paperboard grades. Furthermore, in the contact model, increasing the friction coefficient between the top platen of the compression tester and the top of the package above 0.1 resulted in insignificant change in stress on the package.

Various factors such as ventilation openings and configurations can affect or compromise the strength of VCP packages. Based on this, the functionality of VCP packages was studied with respect to different geometrical configuration of vent in chapter 5. The study used four package designs, three vent areas and three corrugated paperboard grades. The strength of the packages was quantified using FEA and validated with experimental studies. Vent area had a negative linear effect on the package strength. Double-walled paperboard grade resulted in the greatest compression strength compared to single-walled paperboard grade. Although, double-walled paperboard grade would increase the strength of the package, there should be a trade-off to avoid utilising more materials which can increase the manufacturing cost of the package. From the model results, the corner of the package incurred the maximum stress regardless of the package design. Experimental and simulation results correlated well and were within 10%. A major contribution of this study is the demonstration of the need for alternative package design in improving package strength, hence, minimising damage to packed produce, while still maintaining adequate ventilation within the package. Furthermore, this study showed the possibility of screening plausible package designs and discarding packages that will fail in an early manufacturing stage. In addition, there was a significant interaction between the corrugated paperboard grade and the different package design as well as the total vent area. Therefore, it is worth noting that the efficacy of the package vent hole design is largely dependent on the properties of the chosen grade of paperboard. From the numerical results, buckling originated from the centre of the long side of the package while the short side was more resistant to buckling. Furthermore, maximum stress concentration was found at the corners of the packages from the contact FEA model.

To protect packed fresh produce, a package must be able to withstand the exerted load for a long period of time at varying environmental conditions. This time-dependent phenomenon is known as creep. To understand this phenomenon, in

chapter 6, the creep behaviour of different package designs under applied constant load for a 12 h period, was studied at two environmental conditions: standard (23 °C and 50% RH) and refrigerated (2 °C and 85% RH) conditions. The creep rate of the packages increased with an increase in the applied load, and refrigerated conditions also accelerated the creep rate. In addition, the creep rate was significantly affected by the package configurations. Large inconsistencies in the creep behaviour of the package was observed at refrigerated conditions which indicated the influence of the absorbed moisture because of the high RH and low temperature. Furthermore, the study showed the applicability of Bailey-Norton creep law and Power law models in predicting the creep strain of the package for the duration of the applied load (i.e. 12 h), with good correlation with the experimental results. A contribution of this study is the provision of basic information to package designers on the time-dependent property of paperboard packaging relevant to package design applications to protect fresh horticultural produce. Additionally, package designers need to take cognisance of the role of package configuration on the creep behaviour of the packages. Also, this study provides evidence for package lifetime under different loads and humidity/temperature, which is the most critical performance parameter of a package. It was also found that varying environmental conditions had different effects on package designs. Moreover, low temperature and high humidity decreases the strength of the packages substantially, irrespective of the package designs.

Lastly, for more in-depth knowledge on the deformation phenomenon of packages under mechanical loading, the digital image correlation (DIC) technique was used to determine the displacement field of corrugated paperboard packages subjected to compression load in chapter 7. Findings showed the distribution of displacement field to be largely heterogeneous. The out-of-plane (z-direction) displacement was highest compared to the in-plane (x- and y- directions) displacements, which is an indication of buckling being a predominant phenomenon that occurs during package compression and it was observed to be concentrated at the centre of the package panels. Additionally, findings from this study showed that the packages exhibit vertical translatory motion during compression. This work contributes to the understanding of heterogeneous material behaviour of paperboard packages, which will help provide package designers with relevant information for control during manufacturing. As a result, the package strength will be enhanced and consequently foster the preservation of fresh horticultural produce against damage during postharvest handling. These findings presents preliminary evidence of the potential use of DIC in investigating the deformation phenomenon in paperboard packages under compression load.

8.2 Future research prospects

Based on the homogenised core approximation that was used in the FEA models for this study, an improvement could be a full detailed model of the package that takes account of the liners and the flute connection without approximation of the fluting. In addition, material nonlinearities that incorporates plasticity and creep

could be introduced to the model. Additionally, future research direction could be the evaluation of packaging systems at a larger scale using FEA by considering the influence of factors such as stack of packages and environmental conditions. This will contribute to the improvement of the packages for better performance.

It is worth mentioning that creep deformation process is very slow and requires several tests, incorporating several factors to establish widely accepted protocol. This work presented the creep behaviour of VCP packages under loads applied for a short duration. Future research directions could be to increase the duration of the applied load, probably till collapse or failure of the package. Furthermore, in the creep study of this research, constant environmental conditions were used, however, during transportation of fresh produce, the cold chain conditions could be very erratic. Therefore, test protocols that include cyclic environmental conditions and time-varying loadings would enhance a better understanding of package failure mechanism due to creep.

The application of DIC technique could also be utilised further to analyse the effects of various factors such as creep and pallet stacking on the deformation behaviour of the packages This is important because of the discrepancies in the behaviour of paper materials under different phenomena.

References

Aboura, Z., Talbi, N., Allaoui, S., & Benzeggagh, M. L. (2004). Elastic behaviour of corrugated cardboard: Experiments and modelling. *Composite Structures*, *63*(1), 53–62.

Ahmadi, E. (2012). Bruise susceptibilities of kiwifruit as affected by impact and fruit properties. *Research in Agricultural Engineering-UZEI*, *58*(3), 107–113.

Ahmadi, E., Barikloo, H., & Kashfi, M. (2016). Viscoelastic finite element analysis of the dynamic behaviour of apple under impact loading with regard to its different layers. *Computers and Electronics in Agriculture*, *121*, 1–11.

Ahmed, J., & Alam, T. (2012). An overview of food packaging: material selection and the future of packaging. *Handbook of Food Process Design*, (pp. 1237–1283). Wiley-Blackwell.

Ahmed, M. I. M., Curiel-Sosa, J. L., & Rongong, J. (2017). Charaterisation of creep behaviour using power law model in copper alloy. *Journal of Mechanical Engineering and Science*, *11*(1), 2503–2510.

Ahmed, S. I., & Bhoomkar, M. M. (2013). Comparative analysis of effect of fluting papers on ECT and FCT in single wall corrugated fibreboards. *Journal of Engineering Research and Studies*, *4*(4), 07–09.

Alava, M., & Niskanen, K. (2006). The physics of paper. *Reports on Progress in Physics*, *69*(3), 669–723.

Alfthan, J. (2004). The effect of humidity cycle amplitude on accelerated tensile creep of paper. *Mechanics of Time-Dependent Materials*, *8*(4), 289–302.

Allansson, A., & Svärd, B. (2001). *Stability and collapse of corrugated board–numerical and experimental analysis*. Master's Thesis. Lund University.

Allaoui, S., Aboura, Z., & Benzeggagh, M. L. (2009a). Effects of the environmental conditions on the mechanical behaviour of the corrugated cardboard. *Composites Science and Technology*, *69*(1), 104–110.

Allaoui, S., Aboura, Z., & Benzeggagh, M. L. (2009b). Phenomena governing uni-axial tensile behaviour of paperboard and corrugated cardboard. *Composite Structures*, *87*(1), 80–92.

Allaoui, S., Aboura, Z., & Benzeggagh, M. L. (2011). Contribution to the modelling of the corrugated cardboard behaviour. arXiv preprint arXiv: 1110.5417.

Ambaw, A., Delele, M. A., Defraeye, T., Ho, Q. T., Opara, L. U., Nicolai, B. M., & Verboven, P. (2013). The use of CFD to characterize and design post-harvest storage facilities: Past, present and future. *Computers and Electronics in Agriculture*, *93*, 184–194.

Andrés, A. I., Timón, M. L., Molina, G., González, N., & Petrón, M. J. (2014). Effect of MAP storage on chemical, physical and sensory characteristics of "níscalos"(Lactarius deliciosus). *Food Packaging and Shelf Life*, *1*(2), 179–189.

Aprajeeta, J., Gopirajah, R., & Anandharamakrishnan, C. (2015). Shrinkage and porosity effects on heat and mass transfer during potato drying. *Journal of Food Engineering*, *144*, 119–128.

Ari, I., & Muhtaroglu, N. (2013). Design and implementation of a cloud computing service for finite element analysis. *Advances in Engineering Software*, *60*, 122–135.

Armentani, E., Caputo, F., & Esposito, R. (2006). FE analyses of stability of single and double corrugated boards. In *Proceedings of the Fourth International Conference on Axiomatic Design, Firenze, Italy*. pp. 1–7.

Armstrong, P. A., Timm, E. J., Schulte, N. L., & Brown, G. K. (1991). Apple bruising in bulk bins during road transport. *American Society of Agricultural Engineers (USA)*. Paper No. 91-1020, St. Joseph, Michigan.

Arvidsson, J., & Grönvall, J. (2004). *Analysis of creep in paperboard packages with plastic tops*. Master's Thesis. Lund University.

Åslund, P. E., Hägglund, R., Carlsson, L. A., & Isaksson, P. (2014). Modelling of global and local buckling of corrugated board panels loaded in edge-to-edge compression. *Journal of Sandwich Structures & Materials*, *16*(3), 272–292.

ASTM (2017), D7030-04: Standard Test Method for Short Term Creep Performance of Corrugated Fiberboard Containers Under Constant Load Using a Compression Test Machine, American Society of Testing and Materials International, West Conshohocken, PA.

ASTM (2010). ASTM D642: Standard Test Method for Determining Compressive Resistance of Shipping Containers, Components, and Unit Loads. American Society of Testing and Materials International, West Conshohocken, PA.

ASTM, (2006). D4332-01: Standard Practice for Conditioning Containers, Packages, or Packaging Components for Testing. American Society of Testing and Materials International, West Conshohocken, PA.

Babini, A., Borsari, R., Fontanini, A., Dughiero, F., & Forzan, M. (2003). 3D FEM models for numerical simulation of induction sealing of packaging material. *COMPEL-The International Journal for Computation and Mathematics in Electrical and Electronic Engineering*, *22*(1), 170–180.

Bajema, R. W., & Hyde, G. M. (1998). Instrumented pendulum for impact characterization of whole fruit and vegetable specimens. *Transactions of the ASAE*, *41*(5), 1399–1405.

Bakker, A., Haidari, A. H., & Oshinowo, L. M. (2001). Realize greater benefits from CFD. *Chemical Engineering Progress*, *97*(3), 45–53.

Bandyopadhyay, A., Radhakrishnan, H., Ramarao, B. V., & Chatterjee, S. G. (2000). Moisture sorption response of paper subjected to ramp humidity changes: Modelling and experiments. *Industrial & Engineering Chemistry Research*, *39*(1), 219–226.

Bandyopadhyay, A., Ramarao, B. V., & Ramaswamy, S. (2002). Transient moisture diffusion through paperboard materials. *Colloids and Surfaces A: Physicochemical and Engineering Aspects*, *206*(1-3), 455–467.

Barbier, C., Larsson, P. L., & Östlund, S. (2005). Numerical investigation of folding of coated papers. *Composite Structures*, *67*(4), 383–394.

Barchi, G. L., Berardinelli, A., Guarnieri, A., Ragni, L., & Totaro Fila C. (2002). *Damage to loquasts by vibration-simulating intra state transport*. *Biosystems Engineering*, *82*, 305–312.

Bartolozzi, G., Pierini, M., Orrenius, U. L. F., & Baldanzini, N. (2013). An equivalent material formulation for sinusoidal corrugated cores of structural sandwich panels. *Composite Structures*, *100*, 173-185.

Batelka, J. J. (1994a). Corrugating medium reference: its influence on box plant operations and combined board properties and package performance. Project 3808: *Report to the technical division of the containerboard and Kraft paper group of the American forest and paper association.* Institute of Paper Science and Technology, Atlanta, Georgia.

Batelka, J. J. (1994b). The effect of boxplant operations on corrugated board edge crush test. *Tappi Journal*. 77(4), 193–198.

Beex, L. A. A., & Peerlings, R. H. J. (2009). An experimental and computational study of laminated paperboard creasing and folding. *International Journal of Solids and Structures*, *46*(24), 4192–4207.

Beldie, L. (2001). *Mechanics of paperboard packages: performance at short term static loading*. Doctoral dissertation, Lund University.

Beldie, L., Sandberg, G., & Sandberg, L. (2001). Paperboard packages exposed to static loads–finite element modelling and experiments. *Packaging Technology and Science*, *14*(4), 171–178.

Bennett, P. G., McKinlay, P. R., Shaw, N. W., & Stott, R. A. (1989). *Methods of making corrugated paper board.* U.S. Patent No. 4,886,563. Washington, DC: U.S. Patent and Trademark Office.

Berardinelli, A., Donati, V., Giunchi, A., Guarnieri, A., & Ragni, L. (2005). Damage to pears caused by simulated transport. *Journal of Food Engineering*, *66*(2), 219–226.

Berardinelli, A., Donati, V., Giunchi, A., Guarnieri, A., & Ragni, L. (2003a). Effects of sinusoidal vibrations on quality indices of shell eggs. *Biosystems Engineering*, *86*(3), 347–353.

Berardinelli, A., Donati, V., Giunchi, A., Guarnieri, A., & Ragni, L. (2003b). Effects of transport vibrations on quality indices of shell eggs. *Biosystems Engineering*, *86*(4), 495–502.

Berry, T. M. (2017). *Optimisation of multi-scale ventilated package design for next-generation cold chain strategies of horticulture produce*. Doctoral dissertation, Stellenbosch University.

Berry, T. M., Fadiji, T. S., Defraeye, T., & Opara, U. L. (2017). The role of horticultural carton vent hole design on cooling efficiency and compression strength: A multi-parameter approach. *Postharvest Biology and Technology*, *124*, 62–74.

Berry, T. M., Defraeye, T., Nicolaï, B. M., & Opara, U. L. (2016). Multiparameter analysis of cooling efficiency of ventilated fruit cartons using CFD: Impact of vent hole design and internal packaging. *Food and Bioprocess Technology*, *9*(9), 1481–1493.

Berry, T. M., Delele, M. A., Griessel, H., & Opara, U. L. (2015). Geometric design characterisation of ventilated multi-scale packaging used in the South African pome fruit industry. *Agricultural Mechanization in Asia, Africa, and Latin America*, *46*(3), 34–42.

Betancur-Muñoz, P., Osorio-Gómez, G., Martínez-Cadavid, J. F., & Duque-Lombana, J. F. (2014). Integrating design for assembly guidelines in packaging design with a context-based approach. *Procedia CIRP*, *21*, 342–347.

Biancolini, B. M. E., & Brutti, C. (2003). Numerical and experimental investigation of the strength of corrugated board packages. *Packaging Technology and Science*, *16*(2), 47–60.

Biancolini, M. E. (2005). Evaluation of equivalent stiffness properties of corrugated board. *Composite Structures*, *69*(3), 322–328.

Biancolini, M. E., Brutti, C., & Porziani, S. (2009). Analysis of corrugated board panels under compression load. *Steel and Composite Structures*, *9*(1), 1–17.

Biancolini, M. E., Brutti, C., & Porziani, S. (2010). Corrugated board containers design methods. *International Journal of Computational Materials Science and Surface Engineering*, *3*(2-3), 143–163.

Biancolini, M. E., Brutti, C., Mottola, E., & Porziani, S. (2005). *Numerical evaluation of buckling and post-buckling behaviour of corrugated board containers*. Paper presented at the XXXIV Convegno Nazionale Associazione Italiana per l'Analisi delle Sollecitazioni.

Bivainis, V., & Jankauskas, V. (2015). Impact of Corrugated Paperboard Structure on Puncture Resistance. *Materials Science*, *21*(1), 37–61.

Bollen, A. F., Cox, N. R., Dela Rue, B. T., & Painter, D. J. (2001). A descriptor for damage susceptibility of a population of produce. *Journal of Agricultural Engineering Research*, *78*(4), 391–395.

Bollen, A. F., Nguyen, H. X., & Dela Rue, B. T. (1999). Comparison of methods for estimating the bruise volume of apples. *Journal of Agricultural Engineering Research*, *74*(4), 325–330.

Borgqvist, E., Wallin, M., Ristinmaa, M., & Tryding, J. (2015). An anisotropic in-plane and out-of-plane elasto-plastic continuum model for paperboard. *Composite Structures*, *126*, 184–195.

Borgqvist, E., Wallin, M., Tryding, J., Ristinmaa, M., & Tudisco, E. (2016). Localized deformation in compression and folding of paperboard. *Packaging Technology and Science*, *29*, 397–414.

Böröcz, P. (2015). Measurement and analysis of deformation shapes on corrugated cardboard logistical boxes under static and dynamic compression. A*cta Technica Jaurinensis*, *8*(4), 320–329.

Borodulina, S., Kulachenko, A., Galland, S., and Nygårds, M. (2012). Stress-strain curve of paper revisited. *Nordic Pulp and Paper Research Journal*, *27*(2), 318–328.

Boyette, M., Sanders, D., & Rutledge, G. (1996). *Package requirements for fresh fruits and vegetables*. Ralley, NC.USA: The North Carolina Agricultural Extension service. North Carolina State University. Publication, (9/96).

Brandenburg, R. K., & Lee, J. J. L. (1993). *Fundamentals of Packaging Dynamics*. M T S Systems Corporation, Michigan.

Brynk, T., Molak, R. M., Janiszewska, M., & Pakiela, Z. (2012). Digital Image Correlation measurements as a tool of composites deformation description. *Computational Materials Science*, *64*, 157–161.

Bronkhorst, C. A. (1997). Towards a more mechanistic understanding of corrugated container creep deformation behaviour. *Journal of Pulp and Paper Science*, *23*(4), J174–J181.

Bronlund, J. E., Redding, G. P., & Robertson, T. R. (2013). Modelling steady-state moisture transport through corrugated fibreboard packaging. *Packaging Technology and Science*, *27*(3), 193–201.

Brusewitz, G. H., McCollum, T. G., & Zhang, X. (1991). Impact bruise resistance of peaches. *Transactions of the ASAE*, *34*, 962–965.

Budimir, I., Lajić, B., & Pasanec Preprotić, S. (2012). Evaluation of mechanical strength of five layer corrugated cardboard depending on waveform types. *Acta Graphica*, *23*(3-4), 111–120.

Burgess, G., Singh, S. P., & Srinangyam, M. (2005). Predicting collapse times for corrugated boxes under constant top load using short-term creep tests. *Journal of Testing and Evaluation*, *33*(4), 283–286.

Byrd, V. L. (1972a). Effect of relative humidity changes during creep on handsheet paper properties. *Tappi Journal*, *55*(2), 247–252.

Byrd, V. L. (1972b). Effect of relative humidity changes on compressive creep response of paper. *Tappi Journal*, *55*(11), 1612–1613.

Byrd, V. L. (1984). Edgewise compression creep of fiberboard components in a cyclic-relative-humidity environment. *Tappi Journal*. *67*(7), 86–90.

Byrd, V. L., & Koning, J. W. (1978). Corrugated fibreboards edgewise compression creep in cyclic relative humidity environments. *Tappi Journal*, *61*(6), 35–37.

Caldicott, P. J. (1991). Distribution testing—sine or random?. *Packaging Technology and Science*, *4*(5), 287–291.

Campanone, L. A., & Zaritzky, N. E. (2005). Mathematical analysis of microwave heating process. *Journal of Food Engineering*, *69*(3), 359–368.

Campbell, A. (2010). *The use of A-flute, B-flute, AC-flute, and BC-flute corrugated paperboard as a cushioning material*. Master's Thesis. Clemson University.

Cannella, F., & Dai, J. S. (2006). Crease stiffness and panel compliance of carton folds and their integration in modelling. *Proceedings of the Institution of Mechanical Engineers, Part C: Journal of Mechanical Engineering Science*, *220*(6), 847–855.

Celik, H. K. (2017). Determination of bruise susceptibility of pears (Ankara variety) to impact load by means of FEM-based explicit dynamics simulation. *Postharvest Biology and Technology*, *128*, 83–97.

Celik, H. K., Rennie, A. E., & Akinci, I. (2011). Deformation behaviour simulation of an apple under drop case by finite element method. *Journal of Food Engineering*, *104*(2), 293–298.

Chalmers, I. R. (2001). A comparison between static and cyclic humidity compression creep performance of linerboard. *Appita Journal*, *54*(5), 435–438.

Chamberlain, D., & Kirwan, M. J. (2013). Paper and paperboard–raw materials, processing and properties. In: *Handbook of Paper and Paperboard Packaging Technology*. New York: John Wiley & Sons, Ltd.

Chandrupatla, T. R., Belegundu, A. D., Ramesh, T., & Ray, C. (2002). *Introduction to finite elements in engineering* (Vol. 2). Upper Saddle River, NJ: Prentice Hall.

Chasiotis, I., & Knauss, W. G. (2002). A new micro-tensile tester for the study of MEMS materials with the aid of atomic force microscopy. *Experimental*

Mechanics, *42*(1), 51-57.

Chen, D. S. D., Singh, R. K., Haghighi, K., & Nelson, P. E. (1993a). Finite element analysis of temperature distribution in microwaved cylindrical potato tissue. *Journal of Food Engineering*, *18*(4), 351–368.

Chen, H., & De Baerdemaeker, J. (1993b). Modal analysis of the dynamic behavior of pineapples and its relation to fruit firmness. *Transactions of the ASAE*, *36*(5), 1439–1444.

Chen, J., Zhang, Y. L., & Sun, J. (2011a). An overview of the reducing principle of design of corrugated box used in goods packaging. *Procedia Environmental Sciences*, *10*, 992–998.

Chen, Z., Yan, N., Deng, J., & Smith, G. (2011). Flexural creep behavior of sandwich panels containing Kraft paper honeycomb core and wood composite skins. *Materials Science and Engineering: A*, *528*(16-17), 5621-5626.

Chen, Z., Yan, N., Deng, J., Semple, K. E., Sam-Brew, S., & Smith, G. D. (2017). Influence of environmental humidity and temperature on the creep behavior of sandwich panel. *International Journal of Mechanical Sciences*, *134*, 216–223.

Cheon, Y. J., & Kim, H. G. (2015). An equivalent plate model for corrugated-core sandwich panels. *Journal of Mechanical Science and Technology*, *29*(3), 1217–1223.

Chonhenchob, V., & Singh, S. P. (2003). A comparison of corrugated boxes and reusable plastic containers for mango distribution. *Packaging Technology and Science*, *16*(6), 231–237.

Chonhenchob, V., Sittipod, S., Swasdee, D., Rachtanapun, P., Singh, S. P., & Singh, J. A. (2009). Effect of truck vibration during transport on damage to fresh produce shipments in Thailand. *Journal of Applied Packaging Research*, *3*(6). 27–38.

Chuntranuluck, S., Wells, C. M., & Cleland, A. C. (1998). Prediction of chilling times of foods in situations where evaporative cooling is significant—Part 1. Method development. *Journal of Food Engineering*, *37*(2), 111–125.

Conradie, J. H. (2015). *Characterising failure of structural materials using digital images*. Masters Thesis. Stellenbosch University.

Considine, J. M., Gunderson, D. E., Thelin, P., & Fellers, C. (1989). Compressive creep behavior of paperboard in a cyclic humidity environment-exploratory experiment. *Tappi Journal*, *72*(11), 131–136.

Considine, J. M., Scott, C. T., Gleisner, R., & Zhu, J. Y. (2005, September). Use of digital image correlation to study the local deformation field of paper and paperboard. In *13th fundamental research symposium conference* (pp. 613-630).

Considine, J. M., Stoker, D. L., Laufenberg, T. L., & Evens, J. W. (1994). Compressive creep behaviour of corrugating components affected by humid environment. *Tappi Journal*, *77*, 87–95.

Cook, R., Malkus, D., Plesha, M., & Witt, R. (2002). *Concepts and applications of finite element analysis* (4th ed.). New York: Wiley.

Courant, R. (1943). Variational methods for the solution of problems of equilibrium and vibrations. *Bulletin of the American Mathematical Society*, *49*(1), 1–23.

Crammond, G., Boyd, S. W., & Dulieu-Barton, J. M. (2013). Speckle pattern quality assessment for digital image correlation. *Optics and Lasers in Engineering*, *51*(12), 1368–1378.

Csavajda, P., Böröcz, P., Mojzes, Á., & Molnár, B. (2017). The effect of creasing lines on the compression strength of adjustable height corrugated boxes. J*ournal of Applied Packaging Research*, *9*(1),15–22.

Curcio, S., Aversa, M., Calabrò, V., & Iorio, G. (2008). Simulation of food drying: FEM analysis and experimental validation. *Journal of Food Engineering*, *87*(4), 541–553.

Dagel, A. V., & Brynhildsen, H. O. (1959). Tidens Inverkan pa pappladors belastingsformaga. *Svensk Pappperstidning*, *62*(3), 77–82.

Dano, M. L., & Bourque, J. P. (2009). Deformation behaviour of paper and board subjected to moisture diffusion. *International Journal of Solids and Structures*, *46*(6), 1305–1316.

Daub, E., & Gottsching, L. (1988). Gluing and gluability of corrugating medium and linerboard-Part 1. *Papier*, *42*(6), 274–285.

Daxner, T., Flatscher, T., & Rammerstorfer, F. G. (2007). Optimum design of corrugated board under buckling constraints. In *7th World congress on structural and multidisciplinary optimization, COEX Seoul, Korea*, 349–358.

De Alwis, A. A. P., & Fryer, P. J. (1990). A finite-element analysis of heat generation and transfer during ohmic heating of food. *Chemical Engineering Science*, *45*(6), 1547–1559.

De Borst, R., Crisfield, M. A., Remmers, J. J., & Verhoosel, C. V. (2012). *Nonlinear finite element analysis of solids and structures*. John Wiley & Sons.

De Castro, L.R., Vigneault, C., & Cortez, L.A.B. (2005). Effect of container openings and airflow on energy required for forced air cooling of horticultural produce. *Canadian Biosystems Engineering*, *47*(3), 1–9.

De Oliveira, R. C., Mark, R. E., & Perkins, R. W. (1990). Evaluation of the effects of heterogeneous structure on strain distribution in low density papers. *Mechanics of Wood and Paper Materials, AMD*, *112*, 37–61.

Defraeye, T., Cronjé, P., Berry, T., Opara, U. L., East, A., Hertog, M., Verboven, P., & Nicolai, B. (2015). Towards integrated performance evaluation of future packaging for fresh produce in the cold chain. *Trends in Food Science & Technology*, *44*, 201–225.

Defraeye, T., Lambrecht, R., Delele, M. A., Tsige, A. A., Opara, U. L., Cronjé, P., Verboven, P., & Nicolai, B. (2014). Forced-convective cooling of citrus fruit: cooling conditions and energy consumption in relation to package design. *Journal of Food Engineering*, *121*, 118–127.

Defraeye, T., Lambrecht, R., Delele, M. A., Tsige, A. A., Opara, U. L., Cronjé, P., Verboven, P., & Nicolai, B. (2013). Forced-convective cooling of citrus fruit: Package design. *Journal of Food Engineering*, *118*(1), 8–18.

Defraeye, T., Wu, W., Prawiranto, K., Fortunato, G., Kemp, S., Hartmann, S., Cronje, P., Verboven, P., & Nicolai, B. (2017). Artificial fruit for monitoring the thermal history of horticultural produce in the cold chain. *Journal of Food Engineering*, *215*, 51–60.

Dehghannya, J., Ngadi, M., & Vigneault, C. (2010). Mathematical modelling procedures for airflow, heat and mass transfer during forced convection cooling of produce: A review. *Food Engineering Reviews*, *2*(4), 227–243.

Dehghannya, J., Ngadi, M., & Vigneault, C. (2011). Mathematical modeling of airflow and heat transfer during forced convection cooling of produce considering various package vent areas. *Food Control*, *22*(8), 1393–1399.

Delele, M. A., Ngcobo, M. E. K., Getahun, S. T., Chen, L., Mellmann, J., & Opara, U. L. (2013a). Studying airflow and heat transfer characteristics of a horticultural produce packaging system using a 3-D CFD model. Part I: Model development and validation. *Postharvest Biology and Technology*, *86*, 536–545.

Delele, M. A., Ngcobo, M. E. K., Getahun, S. T., Chen, L., Mellmann, J., & Opara, U. L. (2013b). Studying airflow and heat transfer characteristics of a horticultural produce packaging system using a 3-D CFD model. Part II: Effect of package design. *Postharvest Biology and Technology*, *86*, 546–555.

Delele, M. A., Verboven, P., Ho, Q. T., & Nicolaï, B. M. (2010). Advances in mathematical modelling of postharvest refrigeration processes. *Stewart Postharvest Review*, *6*(2), 1–8.

DeMaio, A., & Patterson, T. (2006). Influence of bonding on the tensile creep behavior of paper in a cyclic humidity environment. *Mechanics of Time-Dependent Materials*, *10*(1), 17–33.

Dimitrov, K. O. (2010). *Relationship between the ECT-strength of corrugated board and the compression strength of liner and fluting medium papers*. Master's Thesis. University of Pretoria, South Africa.

Dimitrov, K., & Heydenrych, M. (2009). Relationship between the edgewise compression strength of corrugated board and the compression strength of liner and fluting medium papers. *Southern Forests*, *71*(3), 227–233.

Dintwa, E., Jancsók, P., Mebatsion, H. K., Verlinden, B., Verboven, P., Wang, C. X., Thomas, C. R., Tijskens, E., Ramon, H., & Nicolai, B. (2011). A finite element model for mechanical deformation of single tomato suspension cells. *Journal of Food Engineering*, *103*(3), 265–272.

Dintwa, E., Van Zeebroeck, M., Ramon, H., & Tijskens, E. (2008). Finite element analysis of the dynamic collision of apple fruit. *Postharvest Biology and Technology*, *49*(2), 260–276.

Domaneschi, M., Perego, U., Borgqvist, E., & Borsari, R. (2017). An industry-oriented strategy for the finite element simulation of paperboard creasing and folding. *Packaging Technology and Science*, *30*(6), 269–294.

Dominic, C. A., Östlund, S., Buffington, J., & Masoud, M. M. (2015). Towards a conceptual sustainable packaging development model: A corrugated box case study. *Packaging Technology and Science*, *28*(5), 397–413.

Dongmei, W. (2009). Cushioning properties of multi-layer corrugated sandwich structures. *Journal of Sandwich Structures and Materials*, *11*(1), 57–66.

Dongmei, W., Huxiang, G., & Ziyou, B. (2013). Effect investigation of relative humidity and temperature on multi-layer corrugated sandwich structures. *Journal of Sandwich Structures and Materials*, *15*(2), 156–167.

Dunn, D. J. (2003). *Adhesives and sealants: technology, applications and markets*. Smithers Rapra Publishing.

Dunn, H. M. (2000). *Micromechanisms of paperboard deformation*. Doctoral dissertation, Massachusetts Institute of Technology.

Eagleton, D. G. (1995). *Creep properties of corrugated fibreboard containers for produce in simulated road transport environment*. Doctoral dissertation, Victoria University of Technology.

Ellis, R. L. & Rudie, A. W. (1991). Ideal fibres for Pulp and Paper Products, *21st Southern Forest Tree improvement Conference*, June 17-20, 1991, Knoxville Tennessee.

El-Ramady, H. R., Domokos-Szabolcsy, É., Abdalla, N. A., Taha, H. S., & Fári, M. (2015). Postharvest management of fruits and vegetables storage. In *Sustainable agriculture reviews* (pp. 65-152). Springer International Publishing.

Emblem, A. (Ed.). (2012). *Packaging technology: Fundamentals, materials and processes*. Elsevier.

Emblem, A., & Emblem, H. (2012). *Packaging technology: Fundamentals, materials and processes*. Woodhead Publishing Limited.

Émond, J. P., & Vigneault, C. (1998). Reusable containers for the preservation of fresh fruits and vegetables. *U.S. Patent No. 5,727,711*. Washington, DC: U.S. Patent and Trademark Office.

EPA Environmental Protection Agency (U.S.) (2006).Plastics. Washington, D. C.: EPA. Available from: http://www.epa.gov/epaoswer/non-hw/muncpl/plastic.htm (Accessed 10.10.17).

Erbay, Z., & Icier, F. (2010). A review of thin layer drying of foods: Theory, modelling, and experimental results. *Critical Reviews in Food Science and Nutrition*, *50*(5), 441–464.

Erdogan, E. S., & Eksi, O. (2014). Prediction of wall thickness distribution in simple thermoforming moulds. *Strojniški vestnik-Journal of Mechanical Engineering*, *60*(3), 195–202.

Eriksson, D., Korin, C., & Thuvander, F. (2014). Damage to carton board packages subjected to concentrated loads. In *19th IAPRI World Conference on Packaging, Melbourne, Australia, June 15-18, 2014* (pp. 172–182). Victoria University.

Fadiji, T. (2015). *Mechanical design and performance evaluation of ventilated packages*. Master's Thesis. Stellenbosch University.

Fadiji, T., Berry, T. M., Coetzee, C. J., & Opara, U. L. (2018a). Mechanical design and performance testing of corrugated paperboard packaging for the postharvest handling of horticultural produce. *Biosystems Engineering*, *171*, 220-244.

Fadiji, T., Coetzee, C. J., Berry, T. M., Ambaw, A., & Opara, U. L. (2018b). The efficacy of finite element analysis (FEA) as a design tool for food packaging: A review. *Biosystems Engineering*, *174*, 20–40.

Fadiji, T., Ambaw, A., Coetzee, C. J., Berry, T. M., & Opara, U. L. (2018c). Application of finite element analysis to predict the mechanical strength of ventilated corrugated paperboard packaging for handling fresh produce. *Biosystems Engineering*, *174C*, 260–281.

Fadiji, T., Berry, T., Coetzee, C. J., & Opara, L. (2017). Investigating the mechanical properties of paperboard packaging material for handling fresh produce under different environmental conditions: Experimental analysis and finite element modelling. *Journal of Applied Packaging Research*, *9*(2), 20–34.

Fadiji, T., Coetzee, C., Pathare, P., & Opara, U. L. (2016a). Susceptibility to impact damage of apples inside ventilated corrugated paperboard packages: Effects of package design. *Postharvest Biology and Technology*, *111*, 286–296.

Fadiji, T., Coetzee, C., Chen, L., Chukwu, O., & Opara, U. L. (2016b). Susceptibility of apples to bruising inside ventilated corrugated paperboard packages during simulated transport damage. *Postharvest Biology and Technology*, *118*, 111–119.

Fadiji, T., Coetzee, C., & Opara, U. L. (2016c). Compression strength of ventilated corrugated paperboard packages: Numerical modelling, experimental validation and effects of vent geometric design. *Biosystems Engineering*, *151*, 231–247.

FAO, 2009. *How to Feed the World in 2050*. Food and Agriculture Organization, Rome.

Faoro, V., Khatchatourian, O., & Toniazzo, N. A. (2013). Simulation of airflow in grain storage bins. *Proceeding Series of the Brazilian Society of Computational and Applied Mathematics*, *1*(1). 1–4.

Farber, J. M. (1991). Microbiological aspects of modified-atmosphere packaging technology: a review. *Journal of Food Protection*, *54*(1), 58–70.

Fasina, O. O., & Fleming, H. P. (2001). Heat transfer characteristics of cucumbers during blanching. *Journal of Food Engineering*, *47*(3), 203–210.

Fellers, C. R., & Carlsson, L. A. (1983). *Handbook of Physical and Mechanical Testing of Paper and Paperboard* (R. E. Mark, Ed.), Marcel Dekker Inc., New York.

Fellers, C., & Panek, J. (2007). Effect of relative humidity cycle start point and amplitude on the mechano-sorptive creep of containerboard. In *61st Appita Annual Conference and Exhibition, Gold Coast, Australia 6-9 May 2007*: Proceedings(p. 291). Appita Inc..

Fellows, P. J. (2009). *Food processing technology: Principles and practice*. Elsevier.

Ferrua, M. J., & Singh, R. P. (2011). Improved airflow method and packaging system for forced-air cooling of strawberries. *International Journal of Refrigeration*, *34*(4), 1162–1173.

Flatscher, T., Daxner, T., Pahr, D. H., & Rammerstorfer, F. G. (2011). Optimization of corrugated paperboard under local and global buckling constraints. *Multiscale Methods in Computational Mechanics*, *55*, 329–346.

Fox, T., & Fimeche, C., 2013. *Global food: Waste not, want not*. Institute of Mechanical Engineers, London, UK.

Franca, A. S., & Haghighi, K. (1995). Adaptive finite element analysis of air flow inside grain dryers. *Drying Technology*, *13*(1-2), 125–146.

Frank, B. (2014). Corrugated box compression—A literature survey. *Packaging Technology and Science*, *27*(2), 105–128.

Friedli, T., Basu, P., Bellm, D., & Werani, J. (2013). Leading pharmaceutical operational excellence. *Leading Pharmaceutical Operational Excellence Outstanding Practices and Cases*, 411-418.

Gällstedt, M., & Hedenqvist, M. S. (2006). Packaging-related mechanical and barrier properties of pulp fibre chitosan sheets. *Carbohydrate polymers*, *63*(1), 46–53.

Gällstedt, M., Brottman, A., & Hedenqvist, M. S. (2005). Packaging-related properties of protein-and chitosan-coated paper. *Packaging Technology and Science*, *18*(4), 161–170.

Gan, R. Z., Feng, B., & Sun, Q. (2004). Three-dimensional finite element modelling of human ear for sound transmission. *Annals of Biomedical Engineering*, *32*(6), 847–859.

Gander, J. W., McKee, R. C., & Whitsitt, W. J. (1969). Study of the fundamental properties of corrugating medium which govern bonding and method of measurement. *Project 2696-3, report one: a summary report to Fourdrinier Kraft Board Institute, Inc.*

Garcia-Romeu-Martinez, M. A., Singh, S. P., Cloquell-Ballester, V. A., & Saha, K. (2007). Measurement and analysis of international air parcel shipping environment for DHL and FedEx between Europe and United States. *Packaging Technology and Science*, *20*(6), 421–429.

Garg, S. K., Gupta, V., & Jangra, V. (2016). Effect of moisture content on printability of corrugated board. *International Journal of Scientific Engineering and Applied Science*. *2*(5), 269–275.

Gartaganis, P. A. (1976). Cobalt tracer method for direct measurement of starch consumption on corrugator. *Pulp and Paper-Canada*, *77*(7), 69–72.

Geng, J. P., Tan, K. B., & Liu, G. R. (2001). Application of finite element analysis in implant dentistry: A review of the literature. *The Journal of Prosthetic Dentistry*, *85*(6), 585–598.

Getahun, S., Ambaw, A., Delele, M., Meyer, C. J., & Opara, U. L. (2017a). Analysis of airflow and heat transfer inside fruit packed refrigerated shipping container: Part I–Model development and validation. *Journal of Food Engineering*, *203*, 58–68.

Getahun, S., Ambaw, A., Delele, M., Meyer, C. J., & Opara, U. L. (2017b). Analysis of airflow and heat transfer inside fruit packed refrigerated shipping container: Part II–Evaluation of apple packaging design and vertical flow resistance. *Journal of Food Engineering*, *203*, 83–94.

Getahun, S., Ambaw, A., Delele, M., Meyer, C. J., & Opara, U. L. (2018). Experimental and numerical investigation of airflow inside refrigerated shipping containers. *Food and Bioprocess Technology*, *11*(6), 1164–1176.

Giampieri, A., Perego, U., & Borsari, R. (2011). A constitutive model for the mechanical response of the folding of creased paperboard. *International Journal of Solids and Structures*, *48*(16-17), 2275–2287.

Gilchrist, A. C., Suhling, J. C., & Urbanik, T. J. (1998). Nonlinear finite element modelling of corrugated board. *ASME Applied Mechanics Division-Publications-AMD*, *231*, 101–106.

Gilland, B. (2002). World population and food supply: can food production keep pace with population growth in the next half-century?. *Food Policy*, *27*(1), 47–63.

Godara, A., Raabe, D., Bergmann, I., Putz, R., & Müller, U. (2009). Influence of additives on the global mechanical behaviour and the microscopic strain localization in wood reinforced polypropylene composites during tensile deformation investigated using digital image correlation. *Composites Science and Technology*, *69*(2), 139–146.

Godshall, W. D., & Koning, J. W. (1972). *Method for measuring and controlling web tension of corrugating medium during singlefacing process* (Vol. 219). US Dept. of Agriculture, Forest Service Forest Products Laboratory.

Gołacki, K., Bobin, G., Stropek, Z. (2009). Bruise resistance of apples (Melrose variety). *Teka Komisji Motoryzacji i Energetyki Rolnictwa-OLPAN*, *9*, 40–47.

Gooren, L. G. J. (2006). *Creasing behaviour of corrugated board*. Master's Thesis. Eindhoven University of Technology.

Gospodinov, D., Stefanov, S., & Hadjiiski, V. (2011). Use of the finite element method in studying the influence of different layers on mechanical characteristics of corrugated paperboard. *Tehnički vjesnik*, *18*(3), 357–361.

Gunderson, D. E., & Tobey, W. E. (1990). Tensile creep of paperboard—effect of humidity change rates. In: Caulfield, D.F., Passaretti, J.D., Sobczynski, S.F. (Eds.), Materials interaction relevant to the pulp, paper, and wood industries. *Materials Research Society symposium proceedings*, vol. 197, San Francisco, California, pp. 213–226.

Guo, Y., & Zhang, J. (2004). Shock absorbing characteristics and vibration transmissibility of honeycomb paperboard. *Shock and Vibration*, *11*(5-6), 521–531.

Guo, Y., Fu, Y., & Zhang, W. (2008). Creep properties and recoverability of double-wall corrugated paperboard. *Experimental Mechanics*, *48*(3), 327–333.

Guo, Y., Hou, J., Xu, W., & Cao, G. (2010) Comparison studies on strength properties of corrugated and honeycomb composite paperboards. *Proceedings of the 17th IAPRI World Conference on Packaging.*

Gupta, K. K., & Meek, J. L. (1996). A brief history of the beginning of the finite element method. *International Journal for Numerical Methods in Engineering*, *39*, 3761–3774.

Gustavsson, J., & Stage, J. (2011). Retail waste of horticultural products in Sweden. *Resources, Conservation and Recycling*, *55*(5), 554–556.

Hägglund, R., & Carlsson, L. (2012). Packaging performance. In K. Niskanen (Ed.), *Mechanics of paper products*. Berlin: De Gruyter.

Haghighi, K., Irudayaraj, J., & Stroshine, R. L. (1990). Grain kernel drying simulation using the finite element method. *Transactions of the ASAE*, *33*(6), 1957–1965.

Hagman, A. (2013). *Investigations of In-plane Properties of Paperboard*. Licentiate dissertation, KTH Royal Institute of Technology.

Haj-Ali, R., Choi, J., Wei, B. S., Popil, R., & Schaepe, M. (2009). Refined nonlinear finite element models for corrugated fibreboards. *Composite Structures*, *87*(4), 321–333.

Hallbäck, N., Girlanda, O., & Tryding, J. (2006). Finite element analysis of ink-tack delamination of paperboard. *International Journal of Solids and Structures*, *43*(5), 899–912.

Hämäläinen, P., Hallbäck, N., Gåård, A., & Lestelius, M. (2017). On the determination of transverse shear properties of paper using the short span compression test. *Mechanics of Materials*, *107*, 22–30.

Hammou, A. D., Duong, P. T. M., Abbès, B., Makhlouf, M., & Guo, Y. Q. (2012). Finite-element simulation with a homogenization model and experimental study of free drop tests of corrugated cardboard packaging. *Mechanics & Industry*, *13*(3), 175–184.

Han, J. & Park, J. M. (2007). Finite element analysis of vent/hand hole designs for corrugated fibreboard boxes. *Packaging Technology and Science*, *20*(1), 39–47.

Han, J. H., & Krochta, J. M. (2001). Physical properties and oil absorption of whey-protein-coated paper. *Journal of Food Science*, *66*(2), 294–299.

Han, J. W., Zhao, C. J., Yang, X. T., Qian, J. P., & Fan, B. L. (2015). Computational modelling of airflow and heat transfer in a vented box during cooling: Optimal package design. *Applied Thermal Engineering*, *91*, 883–893.

Hansson, T. (2008). *Deformation based failure criterion for corrugated board panels*. KTH, Solid Mechanics, Stockholm.

Hao, F., Lu, L., & Wang, J. (2016). Finite element analysis of moisture migration of multicomponent foods during storage. *Journal of Food Process Engineering*, *40*(1), 1–10.

Harker, R. (2009). Consumer preferences and choice of fruit: the role of avocado quality. In *4th Australian and New Zealand Avocado Growers Conference.*

Harrysson, A., & Ristinmaa, M. (2008). Large strain elasto-plastic model of paper and corrugated board. *International Journal of Solids and Structures*, *45*(11), 3334–3352.

Hashem, I. A. T., Yaqoob, I., Anuar, N. B., Mokhtar, S., Gani, A., & Khan, S. U. (2015). The rise of "big data" on cloud computing: Review and open research issues. *Information Systems*, *47*, 98–115.

Haslach, H. W. (2000). The moisture and rate-dependent mechanical properties of paper: A review. *Mechanics of Time-Dependent Materials*, *4*(3), 169–210.

Haslach, H. W. (2009). Time-dependent mechanisms in fracture of paper. *Mechanics of Time-Dependent Materials*, *13*(1), 11–35.

Havimo, M., Jalomäki, J., Granström, M., Rissanen, A., Iivanainen, T., Kemell, M., Heikkilä, M., Sipi, M., & Kilpeläinen, I. (2011). Mechanical strength and water resistance of paperboard coated with long chain cellulose esters. *Packaging Technology and Science*, *24*(4), 249–258.

Hayakawa, K. I., & Succar, J. (1982). Heat transfer and moisture loss of spherical fresh produce. *Journal of Food Science*, *47*(2), 596–605.

Henriod, R. E. (2006). Postharvest characteristics of navel oranges following high humidity and low temperature storage and transport. *Postharvest Biology and Technology*, *42*(1), 57–64.

Hernández-Pérez, A., Hägglund, R., Carlsson, L. A., & Avilés, F. (2014). Analysis of twist stiffness of single and double-wall corrugated boards. *Composite Structures*, *110*, 7–15.

Hicks, B. J., Mullineux, G., & Sirkett, D. (2009). A finite element-based approach for whole-system simulation of packaging systems for their improved design and operation. *Packaging Technology and Science*, *22*(4), 209–227.

Hild, F., & Roux, S. (2006). Digital image correlation: from displacement measurement to identification of elastic properties–a review. *Strain*, *42*(2), 69–80.

Hiller, B. (2016). Predicting the long-term mechanical behaviour of corrugated cardboard packaging based on speed rate controlled short term tests. In *Proceedings of Progress in Paper Physics Seminar Conference* (pp. 65-70).

Hinsch, R. T., Slaughter, D. C., Craig, W. L., & Thompson, J. F. (1993). Vibration of fresh fruits and vegetables during refrigerated truck transport. *Transactions of the ASAE*, *36*(4), 1039–1042.

Holt, J. E., & Schoorl, D. (1984). Package protection and energy dissipation in apple packs. *Scientia Horticulturae*, *24*(2), 165–176.

Hotchkiss, J. H. (1997). Food-packaging interactions influencing quality and safety. *Food Additives & Contaminants*, *14*(6-7), 601–607.

Hrennikoff, A. (1941). Solution of problems of elasticity by the framework method. *Journal of Applied Mechanics*, *8*(4), 169–175.

Hua, G. J., Shen, Y., Zhao, D., & Xie, Y. (2017). Experimental and numerical analysis of the edge effect for corrugated and honeycomb fibreboard. *Strength of Materials*, *49*(1), 188–197.

Huang, H., & Nygårds, M. (2010). A simplified material model for finite element analysis of paperboard creasing. *Nordic Pulp & Paper Research Journal*, *25*(4), 505–512.

Huang, H., & Nygårds, M. (2011). Numerical and experimental investigation of paperboard folding. *Nordic Pulp & Paper Research Journal*, *26*(4), 452–467.

Huang, H., & Nygårds, M. (2012). Numerical investigation of paperboard forming. *Nordic Pulp and Paper Research Journal*, *27*(2), 211–225.

Huang, H., Hagman, A., & Nygårds, M. (2014). Quasi static analysis of creasing and folding for three paperboards. *Mechanics of Materials*, *69*(1), 11–34.

Huang, Y. H., Liu, L., Yeung, T. W., & Hung, Y. Y. (2009). Real-time monitoring of clamping force of a bolted joint by use of automatic digital image correlation. *Optics & Laser Technology*, *41*(4), 408–414.

Hubbe, M. A. (2013). Prospects for maintaining strength of paper and paperboard products while using less forest resources: A review. *BioResources*, *9*(1), 1634–1763.

Huchzermeyer, R. L. (2017). *Measuring mechanical properties using digital image correlation: Extracting tensile and fracture properties from a single sample*. Master's Thesis. Stellenbosch University.

Huebner, K. H., Dewhirst, D. L., Smith, D. E., & Byrom, T. G. (2001). *The finite element method for engineers*. New York: John Wiley & Sons.

Hughes, T. J. (2012). *The finite element method: linear static and dynamic finite element analysis*. Courier Corporation.

Hui, Y. H., Legarretta, I. G., Lim, M. H., Murrell, K. D., & Nip, W. K. (Eds.). (2004). *Handbook of Frozen Foods.* (Vol. 133). CRC Press. pp. 499–519.

Hung, D. V., Nakano, Y., Tanaka, F., Hamanaka, D., & Uchino, T. (2010). Preserving the strength of corrugated cardboard under high humidity condition using nano-sized mists. *Composites Science and Technology*, *70*(14), 2123–2127.

Hung, P. C., & Voloshin, A. S. (2003). In-plane strain measurement by digital image correlation. *Journal of the Brazilian Society of Mechanical Sciences and Engineering*, *25*(3), 215–221.

Hussain, S., Coffin, D. W., & Todoroki, C. (2017). Investigating Creep in Corrugated Packaging. *Packaging Technology and Science*, *30*(12), 757–770.

Hutton, D. (2004). *Fundamentals of finite element analysis*. McGraw-Hill.

Ibrahim, A. M., & Mahmood, M. S. (2009). Finite element modelling of reinforced concrete beams strengthened with FRP laminates. *European Journal of Scientific Research*, *30*(4), 526–541.

Idah, P.A., Gana, Y. M., Ogbonnaya, C., & Morenikeji, O. O. (2012). Simulated transport damage study on fresh tomato (Lycopersicon esculentum) fruits. *Agricultural Engineering International: CIGR Journal*, *14*(2), 119–126.

Irudayaraj, J., Haghighi, K., & Stroshine, R. L. (1992). Finite element analysis of drying with application to cereal grains. *Journal of Agricultural Engineering Research*, *53*, 209–229.

ISO (2008). ISO 1924-2, "Paper and board - determination of tensile properties - part 2: constant rate of elongation method. International Organization for Standardization, Geneva, Switzerland.

ISO (2011). ISO 534: Paper and board — Determination of thickness, density and specific volume. International Organization for Standardization, Geneva, Switzerland.

Jackson, T., & Parker, I. (1998). The shape of the ring crush curve. *Appita Journal*, *51*(5), 349–355.

Jamialahmadi, A., Trost, T., & Östlund, S. (2008). Dynamic performance of corrugated boxes. In *16th IAPRI World Conference on Packaging*, Bangkok, Thailand.

Jamialahmadi, A., Trost, T., & Östlund, S. (2011). A proposed tool to determine dynamic load distribution between corrugated boxes. *Packaging Technology and Science*, *24*(6), 317–329.

Janjai, S., Lamlert, N., Intawee, P., Mahayothee, B., Haewsungcharern, M., Bala, B. K., & Müller, J. (2008). Finite element simulation of drying of mango. *Biosystems Engineering*, *99*(4), 523–531.

Jarimopas, B. B., Singh, S. P., & Saengnil, W. (2005). Measurement and analysis of truck transport vibration levels and damage to packaged tangerines during transit. *Packaging Technology and Science*, *18*(4), 179–188.

Jarimopas, B. B., Singh, S. P., Sayasoonthorn, S., & Singh, J. (2007). Comparison of package cushioning materials to protect post-harvest impact damage. *Packaging Technology and Science*, *20*(5), 315–324.

Jiménez-Caballero, M. A., Conde, I., García, B., & Liarte, E. (2009). Design of different types of corrugated board packages using finite element tools. In *SIMULIA Customer Conference*.

Jinkarn, T., Boonchu, P., & Bao-Ban, S. (2006). Effect of carrying slots on the compressive strength of corrugated board panels. *Kasetsart Journal*, *40*, 154–161.

Jo, J. Y., Min, C. K., & Shin, J. S. (2012). Manufacture of water-resistant corrugated board boxes for agricultural products in the cold chain system. *Journal of Korea Technical Association of the Pulp and Paper Industry*, *44*(2), 29–34.

Johnson, S., & Popil, R. (2015). Corrugated board bonding defect visualization and characterization. *International Journal of Adhesion and Adhesives*, *59*, 105–114.

Kabas, O., & Vladut, V. (2015). Determination of drop-test behavior of a sample peach using finite element method. *International Journal of Food Properties*, *18*(11), 2584–2592.

Kabas, O., Celik, H. K., Ozmerzi, A., & Akinci, I. (2008). Drop test simulation of a sample tomato with finite element method. *Journal of the Science of Food and Agriculture*, *88*(9), 1537–1541.

Kader, A. A. (2002). *Postharvest Technology of Horticultural Crops* (3rd ed., p. 353). Davis, California: University of California Department of Agriculture and Natural Resources.

Kannan, A., & Sandaka, P. C. G. (2008). Heat transfer analysis of canned food sterilization in a still retort. *Journal of Food Engineering*, *88*(2), 213–228.

Kaushal, M. C., Sirohiya, V. K., & Rathore, R. K. (2015). Corrugated board structure: A Review. *International Journal of Application of Engineering and Technology*, *2*(3). 228–234.

Kawanishi, K. (1989). Estimation of the compression strength of corrugated fibreboard boxes and its application to box design using a personal computer. *Packaging Technology and Science*, *2*(1), 29–39.

Kayabaşı, O., Yüzbasıoğlu, E., & Erzincanlı, F. (2006). Static, dynamic and fatigue behaviours of dental implant using finite element method. *Advances in Engineering Software*, *37*(10), 649–658.

Kellicutt, K. Q., & Landt, E. F. (1951). Safe stacking life of corrugated boxes. *Fibre Containers*, *36*(9), 28–38.

Kellicutt, K. Q., & Landt, E. F. (1952). Development of design data for corrugated fiberboard shipping containers. *Tappi Journal*, *35*(9), 398–402.

Khatchatourian, O. A., Toniazzo, N. A., & Gortyshov, Y. F. (2009). Simulation of airflow in grain bulks under anisotropic conditions. *Biosystems Engineering*, *104*(2), 205–215.

Kheyr, A. A., & Mortezaei, A. (2007). Nonlinear finite element analysis of reinforced concrete bridges. *Journal of Transportation Research*, *3*(4), 315–320.

Khwaldia, K., Basta, A. H., Aloui, H., & El-Saied, H. (2014). Chitosan–caseinate bilayer coatings for paper packaging materials. *Carbohydrate Polymers*, *99*, 508–516.

Kibirkštis, E., Lebedys, A., Kabelkaitė, A., & Havenko, S. (2007). Experimental study of paperboard package resistance to compression. *Mechanics*, *63*(1), 27–33.

Kim, H. J., Choi, W. Y., & Um, G. J. (2006). The effect of atmospheric conditions on the physical and mechanical properties of linerboard. *Journal of Korea Technical Association of the Pulp and Paper Industry*, *38*(5), 60–65.

Kirwan M.J. (2003). *Paper and paperboard packaging*. In: Coles R, McDowell D, Kirwan MJ, editors. *Food packaging technology*. London, U.K.: Blackwell Publishing, CRC Press. 241–281.

Kirwan, M. J. (Ed.). (2008). *Paper and paperboard packaging technology*. John Wiley & Sons.

Kirwan, M.J. & Strawbridge, J.W. (2003). *Plastics in food packaging*. In: Coles R, McDowell D, Kirwan MJ, editors. *Food Packaging Technology*. London, U.K.: Blackwell Publishing, CRC Press. 174–240.

Koichiro, O. (1972). *Method for manufacturing a composite corrugated paper board.* U.S. Patent No. 3,700,518. Washington, DC: U.S. Patent and Trademark Office.

Kołakowski, Z., Szewczyk, W., & Głowacki, K. (2015). Calculation of corrugated board flat crush resistance. *Wood Research*, *60*(5), 747–754.

Kolanu, N. R., Prakash, S. S., & Ramji, M. (2016). Experimental study on compressive behavior of GFRP stiffened panels using digital image correlation. *Ocean Engineering*, *114*, 290–302.

Koning Jr, J. W., & Stern, R. K. (1977). Long-term creep in corrugated fiberboard containers. *Tappi Journal*, *60*(12), 128–131.

Köstner, V., Ressel, J. B., Sadlowsky, B., & Böröcz, P. (2018). Measuring the creep behaviour of corrugated board by cascade and individual test rig. *Journal of Applied Packaging Research*, *10*(1), 46–61.

Koutsimanis, G., Getter, K., Behe, B., Harte, J., & Almenar, E. (2012). Influences of packaging attributes on consumer purchase decisions for fresh produce. *Appetite*, *59*(2), 270–280.

Kroeschell, W. O. (1990). Bonding on the corrugator: the myth of penetration-brittle bonds. *Tappi Journal*, *73*(2), 62–74.

Kroeschell, W. O. (1992). The edge crust test. *Tappi Journal*, *6*, 79–82.

Kruger, L., & Lacourse, N. (1990). Starch based adhesives. In *Handbook of Adhesives* (pp. 153–166). Springer US.

Krusper, A., Isaksson, P., & Gradin, P. (2007). Modelling of out-of-plane compression loading of corrugated paper board structures. *Journal of Engineering Mechanics*, *133*(11), 1171–1177.

Kueh, C. S. L. (2012). *Modelling buckling and post-buckling behaviours of corrugated paperboard structures*. Doctoral dissertation, University of Waikato.

Kulachenko, A., & Uesaka, T. (2012). Direct simulations of fibre network deformation and failure. *Mechanics of Materials*, *51*, 1–14.

Kulachenko, A., Gradin, P., and Koivurova, H. (2007). Modelling the dynamical behaviour of a paper web. Part II. *Computers and Structures*, *85*(3), 148–157.

Kumar, A., & Bhattacharya, M. (1991). Transient temperature and velocity profiles in a canned non-Newtonian liquid food during sterilization in a still-cook retort. *International Journal of Heat and Mass Transfer*, *34*(4-5), 1083–1096.

Kumar, A., Bhattacharya, M., & Blaylock, J. (1990). Numerical simulation of natural convection heating of canned thick viscous liquid food products. *Journal of Food Science*, *55*(5), 1403–1411.

Lakshmininarayana, H. (2004). *Finite elements analysis: Procedures in engineering*. Universities Press.

Leake, C. H. (1988). Measuring corrugated box performance. *Tappi Journal*, *71*(10), 71–75.

Leake, C. H., & Wojcik, R. (1989). Influence of the combining adhesive on box performance. *Tappi Journal*, *72*(8), 61–65.

Leake, C. H., & Wojcik, R. (1993). Humidity cycling rates: How they influence container life spans: Corrugated containers. *Tappi Journal*, *76*(10), 26–30.

Lecompte, D., Smits, A., Bossuyt, S., Sol, H., Vantomme, J., Van Hemelrijck, D., & Habraken, A. M. (2006). Quality assessment of speckle patterns for digital image correlation. *Optics and Lasers in Engineering*, *44*(11), 1132–1145.

Lee, H. J., Kim, T. C., Kim, S. J., & Park, S. J. (2005). Bruising injury of persimmon (Diospyros kaki cv. Fuyu) fruits. *Scientia Horticulturae*, *103*(2), 179–185.

Lertkittikul, J. (2017). Packaging waste reduction by design of experiments. *Asia-Pacific Journal of Science and Technology*, *19*(6), 886–890.

Li, Y., Stapleton, S. E., Simon, J. W., & Reese, S. (2016). Experimental and numerical study of paperboard interface properties. *Experimental Mechanics*, *56*(8), 1477–1488.

Li, Z., & Thomas, C. (2014). Quantitative evaluation of mechanical damage to fresh fruits. *Trends in Food Science & Technology*, *35*(2), 138–150.

Li, Z., Li, P., Yang, H., & Liu, J. (2013). Internal mechanical damage prediction in tomato compression using multiscale finite element models. *Journal of Food Engineering*, *116*(3), 639–647.

Lin, S. Y., & Krochta, J. M. (2003). Plasticizer effect on grease barrier and colour properties of whey-protein coatings on paperboard. *Journal of Food Science*, *68*(1), 229–233.

Lin, Y. E., Anantheswaran, R. C., & Puri, V. M. (1995). Finite element analysis of microwave heating of solid foods. *Journal of Food Engineering*, *25*(1), 85–112.

Linvill, E., & Östlund, S. (2014). The combined effects of moisture and temperature on the mechanical response of paper. *Experimental Mechanics*, *54*(8), 1329–1341.

Linvill, E., & Östlund, S. (2016). Parametric study of hydroforming of paper materials using the explicit finite element method with a moisture-dependent and temperature-dependent constitutive model. *Packaging Technology and Science*, *29*(3), 145–160.

Little, C. R., & Holmes, R. J. (2000). *Storage technology for apples and pears* (p. 528). Knoxfield: Highway Press Pty Ltd.

Lu, F., Ishikawa, Y., Kitazawa, H., & Satake, T. (2010). Measurement of impact pressure and bruising of apple fruit using pressure-sensitive film technique. *Journal of Food Engineering*, *96*(4), 614–620.

Lu, F., Ishikawa, Y., Kitazawa, H., & Satake, T. (2012). Assessment and prediction of repetitive impact damage to apple fruit using pressure-sensitive film technique. *Journal of Food, Agriculture & Environment*, *10*(2), 156–160.

Lu, L. X., Chen, X. Q., & Wang, J. (2016). Modelling and thermal analysis of tray-layered fruits inside ventilated packages during forced-air precooling. *Packaging Technology and Science*, *29*(2), 105–119.

Lu, T. J., Chen, C., & Zhu, G. (2001). Compressive behaviour of corrugated board panels. *Journal of Composite Materials*, *35*(23), 2098–2126.

Luo, P. F., Chao, Y. J., & Sutton, M. A. (1994). Application of stereo vision to three-dimensional deformation analyses in fracture experiments. *Optical Engineering*, *33*(3), 981–990.

Luo, P., Liu, Y. H., Zhao, X. Q., Song, P. P., Tan, N. S., & Sun, M. Y. (2011). Development of a starch adhesive for corrugated board under room temperature. In *Advanced Materials Research* (Vol. 179, pp. 812–817). Trans Tech Publications.

Luong, V. D., Abbès, F., Abbès, B., Duong, P. M., Nolot, J. B., Erre, D., & Guo, Y. Q. (2017, August). Finite Element Simulation of the Strength of Corrugated Board Boxes under Impact Dynamics. In *International Conference on Advances in Computational Mechanics* (pp. 369-380). Springer, Singapore.

Lyngå, H., & Sikö, G. (2003). *Moisture dynamics in corrugated board boxes*. Master's Thesis. Lund University.

Ma, Y., Gong, Z., Zhao, L., Han, Y., & Wang, Y. (2014). Finite element analysis of buckling of corrugated fiberboard. *Open Mechanical Engineering Journal*, *8*, 257–263.

Mahalik, N. P., & Nambiar, A. N. (2010). Trends in food packaging and manufacturing systems and technology. *Trends in Food Science & Technology*, *21*(3), 117–128.

Mäkelä, P., & Östlund, S. (2003). Orthotropic elastic–plastic material model for paper materials. *International Journal of Solids and Structures*, *40*(21), 5599–5620.

Malesa, M., Malowany, K., Tomczak, U., Siwek, B., Kujawińska, M., & Siemińska-Lewandowska, A. (2013). Application of 3D digital image correlation in maintenance and process control in industry. *Computers in Industry*, *64*(9), 1301–1315.

Maltenfort, G. G. (1980). Compression load distribution on corrugated boxes. *Paperboard Packaging*, *65*(9), 71–72.

Mangaraj, S., Goswami, T. K., & Mahajan, P. V. (2009). Applications of plastic films for modified atmosphere packaging of fruits and vegetables: A review. *Food Engineering Reviews*, *1*(2), 133–158.

Mann, R. W., Baum, G. A., & Habeger Jr, C. C. (1979). Determination of all nine orthotropic elastic constants for machine-made paper. *Tappi Journal*, *63*, 163–166.

Marcille-Lorenz, M., & Whitsitt, W. J. (1990). Double-backer bonding technology. *Tappi Journal*, *73*(5), 137–142.

Marcondes, J. (1992). Cushioning properties of corrugated fiberboard and the effects of moisture content. *Transactions of the ASAE*, *35*(6), 1949–1953.

Marcondes, J. A. (1994). *An introduction to fibreboard packaging*. Victoria University of Technology, Centre for Packaging, Transportation and Storage.

Marín, F., Sánchez, J. L., Arauzo, J., Fuertes, R., & Gonzalo, A. (2009). Semichemical pulping of Miscanthus giganteus. Effect of pulping conditions on some pulp and paper properties. *Bioresource Technology*, *100*(17), 3933–3940.

Mark, R. E., & Borch, J. (2001). *Handbook of physical testing of paper* (Vol. 1). Crc Press.

Markström, H. (1988). *Testing methods and instruments for corrugated board*. Lorentzen & Wettre.

Markström, H. (1999). *Testing methods and instruments for corrugated board: A handbook*. Lorentzen & Wettre.

Marsh, K., & Bugusu, B. (2007). Food packaging—roles, materials, and environmental issues. *Journal of Food Science*, *72*(3), R39–R55.

Mascarenhas, W. J., Akay, H. U., & Pikal, M. J. (1997). A computational model for finite element analysis of the freeze-drying process. *Computer Methods in Applied Mechanics and Engineering*, *148*(1-2), 105–124.

MATLAB (version 8.5.0) [computer software]. (2017). Natick, Massachusetts: The MathWorks Inc.

Mattsson, A., & Uesaka, T. (2013). Time-dependent, statistical failure of paperboard in compression. In *The 15th Pulp and Paper Fundamental Research Symposium, 8-13 September 2013; Cambridge, UK*. Pulp and Paper Fundamental Research Society.

Matzinger, B., & Tong, C. (1993). *Commercial Postharvest Handling of Fresh Market Apples (Malus sp.)*. Minnesota Extension Service, University of Minnesota, Agriculture.

McKee, R. C., & Gander, J. W. (1967). Properties of corrugating medium which influence runnability. *Tappi Journal*, *50*(7), A35.

McKee, R. C., Gander, J. W., & Wachuta, J. R. (1963). Compression strength formula for corrugated boxes. *Paperboard Packaging*, *48*(8), 149–159.

McPherson, C. J., Mullineux, G., Berry, C., Hicks, B. J., & Medland, A. J. (2004). The performance envelope of forming shoulders and implications for design and manufacture. *Proceedings of the Institution of Mechanical Engineers, Part B: Journal of Engineering Manufacture*, *218*(8), 925–934.

Meng, G., Trost, T., & Östlund, S. (2007). Stacking misalignment of corrugated boxes-a preliminary study. In *23rd IAPRI Symposium on Packaging, September 3-5, Windsor, UK*.

Moaveni, S. (2008). *Finite element analysis theory and application with ANSYS*, 3/e. Pearson Education India

Montanuci, F. D., Perussello, C. A., de Matos Jorge, L. M., & Jorge, R. M. M. (2014). Experimental analysis and finite element simulation of the hydration process of barley grains. *Journal of Food Engineering*, *131*, 44–49.

Moody, R. C., & Skidmore, K. E. (1966). How dead load, downward creep influence corrugated box design. *Package Engineering*, *11*(8), 75–81.

Morgan, D. G. (2004). A mechanistic creep model and test procedure. *Appita Journal: Journal of the Technical Association of the Australian and New Zealand Pulp and Paper Industry*, *57*(4), 299–304.

Morgan, D. G. (2005). Analysis of creep failure of corrugated board in changing or cyclic humidity regimes. In *59th Appita Annual Conference and Exhibition: Incorporating the 13th ISWFPC (International Symposium on Wood, Fibre and Pulping Chemistry), Auckland, New Zealand, 16-19 May 2005: Proceedings* (p. 393). Appita Inc.

Mulkoglu, O., Guler, M. A., & Demirbag, H. (2015). Drop test simulation and verification of a dishwasher mechanical structure. In *10th European LS-DYNA Conference*.

Nagasawa, S., Fukuzawa, Y., Yamaguchi, T., Tsukatani, S., & Katayama, I. (2003). Effect of crease depth and crease deviation on folding deformation characteristics of coated paperboard. *Journal of Materials Processing Technology*, *140*(1), 157–162.

Nagasawa, S., Yamagata, D., Fukuzawa, Y., & Murayama, M. (2006). Stress analysis of wedged rupture in surface layer of coated paperboard. *Journal of Materials Processing Technology*, *178*(1), 358–368.

Natarajan, S., Govindarajan, M., & Kumar, B. (2014). *Fundamentals of packaging technology*. PHI Learning Pvt. Ltd.

Navaranjan, N., & Johnson, B. (2006). Modelling and experimental study of creep behaviour of corrugated paperboard. In *60th appita annual conference and exhibition. Melbourne, Australia*. pp. 43–50.

Navaranjan, N., Dickson, A., Paltakari, J., & Ilmonen, K. (2013). Humidity effect on compressive deformation and failure of recycled and virgin layered corrugated paperboard structures. *Composites Part B: Engineering*, *45*(1), 965–971.

Netz, E. (1998). Washboarding and print quality of corrugated board. *Packaging Technology and Science*, *11*(4), 145–167.

Neumayer, D., Chatiri, M., & Höermann, M. (2006). Drop test simulation of a cooker including foam packaging and pre-stressed plastic foil wrapping. In *9th International LSDYNA Users Conference.* pp. 18–33.

Nevins, A. L. (2008). *Significant factors affecting horticultural corrugated fibreboard strength*. Doctoral dissertation. Massey University.

Ngcobo, M. E. K. (2012). *Resistance to airflow and moisture loss of table grapes inside multi-scale packaging*. Doctoral dissertation, Stellenbosch University.

Ngcobo, M. E., Delele, M. A., Opara, U. L., & Meyer, C. J. (2013). Performance of multi-packaging for table grapes based on airflow, cooling rates and fruit quality. *Journal of Food Engineering*, *116*(2), 613–621.

Ngcobo, M. E., Delele, M. A., Opara, U. L., Zietsman, C. J., & Meyer, C. J. (2012). Resistance to airflow and cooling patterns through multi-scale packaging of table grapes. *International Journal of Refrigeration*, *35*(2), 445–452.

Nguyen, T. A., Dresselaers, T., Verboven, P., D'hallewin, G., Culeddu, N., Van Hecke, P., & Nicolaï, B. M. (2006). Finite element modelling and MRI validation of 3D transient water profiles in pears during postharvest storage. *Journal of the Science of Food and Agriculture*, *86*(5), 745–756.

Nikishkov, G. P. (2004). *Introduction to the finite element method*. Technical report. University of Aizu.

Niskanen, K. (Ed.). (2012). *Mechanics of paper products*. Walter de Gruyter Incorporated.

Nordstrand, T. (2003). *Basic testing and strength design of corrugated board and containers*. Doctoral dissertation, Lund University.

Nordstrand, T. M. (1995). Parametric study of the post-buckling strength of structural core sandwich panels. *Composite Structures*, *30*(4), 441–451.

Nordstrand, T. M., & Carlsson, L.A. (1997). Evaluation of transverse shear stiffness of structural core sandwich plates. *Composite Structure*. *37*(2), 145–153.

Nordstrand, T., Blackenfeldt, M., & Renman, M. (2003). A strength prediction method for corrugated board containers. *Report TVSM-3065, Div. of Structural Mechanics, Lund University: Sweden*, *13*.

Norfariza, A. (2012). *Estimation of corrugated cardboard strength with a new tensile or shear test method*. Master's Thesis. Nagaoka University of Technology.

Norton, T., & Sun, D. W. (2006). Computational fluid dynamics (CFD)–an effective and efficient design and analysis tool for the food industry: A review. *Trends in Food Science & Technology*, *17*(11), 600–620.

Nygårds, M., Hallbäck, N., Just, M., & Tryding, J. (2005). A finite element model for simulations of creasing and folding of paperboard. In *ABAQUS Users' Conference*. pp. 1–15.

Nygårds, M., Just, M., & Tryding, J. (2009). Experimental and numerical studies of creasing of paperboard. *International Journal of Solids and Structures*, *46*(11-12), 2493–2505.

Öchsner, A., & Öchsner, M. (2016). *The Finite Element Analysis Program MSC Marc/Mentat: A First Introduction*. Springer.

Oelofse, S. H., & Nahman, A. (2013). Estimating the magnitude of food waste generated in South Africa. *Waste Management & Research*, *31*(1), 80–86.

Oliveira, M. E., & Franca, A. S. (2000). Finite element analysis of microwave heating of solid products. *International Communications in Heat and Mass Transfer*, *27*(4), 527–536.

Opara, U. L. (February 2011). *From hand holes to vent holes: What's next in innovative horticultural packaging?* Inaugural Lecture (p. 24). South Africa: Stellenbosch University.

Opara, U. L., & Fadiji, T. (2018). Compression damage susceptibility of apple fruit packed inside ventilated corrugated paperboard package. *Scientia Horticulturae*, *227*, 154–161.

Opara, U. L., & Mditshwa, A. (2013). A review on the role of packaging in securing food system: Adding value to food products and reducing losses and waste. *African Journal of Agricultural Research*, *8*(22), 2621–2630.

Opara, U. L., & Pathare, P. B. (2014). Bruise damage measurement and analysis of fresh horticultural produce—A review. *Postharvest Biology and Technology*, *91*, 9–24.

Orteu, J. J. (2009). 3-D computer vision in experimental mechanics. *Optics and Lasers in Engineering*, *47*(3), 282-291.

Ortiz, M., & Pandolfi, A. (1999). Finite-deformation irreversible cohesive elements for three-dimensional crack-propagation analysis. *International Journal for Numerical Methods in Engineering*, *44*(9), 1267–1282.

Östlund, S., & Nygårds, M. (2009). Through-thickness mechanical testing and computational modelling of paper and board for efficient materials design. In *Hannu Paulapuro Symposium, Esbo, Finland*. pp. 69–82.

Paine, F. A. (2012). *The packaging user's handbook*. Springer Science & Business Media.

Paine, F. A., & Paine, H. Y. (1992). *A handbook of food packaging*. Glasgow: Blackie Academic & Professional.

Pan, B., & Li, K. (2011). A fast digital image correlation method for deformation measurement. *Optics and Lasers in Engineering*, *49*(7), 841–847.

Pan, B., Qian, K., Xie, H., & Asundi, A. (2009). Two-dimensional digital image correlation for in-plane displacement and strain measurement: A review. *Measurement Science and Technology*, *20*(6), 062001.

Pan, B., Wu, D., & Xia, Y. (2012). An active imaging digital image correlation method for deformation measurement insensitive to ambient light. *Optics & Laser Technology*, *44*(1), 204–209.

Pan, B., Xie, H., & Wang, Z. (2010). Equivalence of digital image correlation criteria for pattern matching. *Applied Optics*, *49*(28), 5501–5509.

Pan, Z., Singh, R. P., & Rumsey, T. R. (2000). Predictive modelling of contact-heating process for cooking a hamburger patty. *Journal of Food Engineering*, *46*(1), 9–19.

Pandit, R. B., & Prasad, S. (2003). Finite element analysis of microwave heating of potato—transient temperature profiles. *Journal of Food Engineering*, *60*(2), 193–202.

Panyarjun, O., & Burgess, G. (2001). Prediction of bending strength of long corrugated boxes. *Packaging Technology and Science*, *14*(2), 49–53.

Park J. M. (2000). Design of corrugated fibreboard boxes with ventilation holes for cold storage. *Ministry of Industrial Resources/Korea Institute of Packaging Development and Research*, Seoul.

Park J.M., & Lee, M.H. (1999). Theoretical and finite element analysis for structural strength of paperboard stacked structure. *Journal of Korean Society of Packaging Science and Technology*, *5*(1), 13–20.

Park, H. J., Kim, S. H., Lim, S. T., Shin, D. H., Choi, S. Y., & Hwang, K. T. (2000). Grease resistance and mechanical properties of isolated soy protein-coated paper. *Journal of the American Oil Chemists' Society*, *77*(3), 269–273.

Park, J. M., Kim, G. S., Kwon, S. H., Chung, S. W., Kwon, S. G., Choi, W. S., & Kim, J. S. (2016). Modelling and analysis of cushioning performance for multi-layered corrugated structures. *Journal of Biosystems Engineering*, *41*(3), 221–231.

Park, J., Kim, G., Kim, H., Kwon, S., Mitusoka, M., Inoue, E., & Okayasu, T. (2011). Characteristics of vibration transmissibility for corrugated paperboard. *Journal of the Faculty of Agriculture, Kyushu University*, *56*(2), 327–333.

Park, J., Kim, G., Kwon, S., Chung, S., Kwon, S., Choi, W., Mitsuoka, M., Inoue, E., Okayasu, T., & Choe, J. (2012). Finite element analysis of corrugated board under bending stress. *Journal of the Faculty of Agriculture, Kyushu University*, *57*, 181–188.

Parker, I. H., Conn, A., & Jackson, T. (2005). The effect of network variables on the ring crush strength of handsheets. *Appita Journal: Journal of the Technical Association of the Australian and New Zealand Pulp and Paper Industry*, *58*(6), 448–454.

Parker, M. E., Bronlund, J. E., & Mawson, A. J. (2006). Moisture sorption isotherms for paper and paperboard in food chain conditions. *Packaging Technology and Science*, *19*(4), 193–209.

Pascall, M. A. (2010). Packaging for fresh vegetables and vegetable products. In N. Sinha (Ed.), *Handbook of vegetables and vegetable processing*. Oxford: Wiley-Blackwell.

Pasco, M. F., Suckling, I. D., & Morgan, D. G. (2006). Improved compressive creep performance of corrugated board using a covalent crosslinking agent. In *60th Appita Annual Conference and Exhibition, Melbourne, Australia 3-5 April 2006: Proceedings* (p. 51). Appita Inc..

Patel, P., Nordstrand, T., & Carlsson, L. A. (1997). Local buckling and collapse of corrugated board under biaxial stress. *Composite Structures*, *39*(1), 93–110.

Pathare, P. B., & Opara, U. L. (2014). Structural design of corrugated boxes for horticultural produce: A review. *Biosystems engineering*, *125*, 128–140.

Pathare, P. B., Berry, T. M., & Opara, U. L. (2016). Changes in moisture content and compression strength during storage of ventilated corrugated packaging used for handling apples. *Packaging Research*, *1*(1), 1–6.

Pathare, P. B., Berry, T. M., & Opara, U. L. (2017). Experimental investigation of compression strength of ventilated corrugated citrus packaging. *Packaging Research*, *2*(1), 22–27.

Pathare, P. B., Opara, U. L., & Delele, M. A. (2012a). Analysis of mechanical properties of vented corrugated container for fresh horticultural produce by finite element method. In *Silos and granular materials (SIGMA). International Conference of Agricultural Engineering-CIGR-AgEng: Agriculture and Engineering for a Healthier Life, Valencia, Spain*, CIGR-EurAgEng.

Pathare, P. B., Opara, U. L., Vigneault, C., Delele, M. A., & Al-Said, F. A. J. (2012b). Design of packaging vents for cooling fresh horticultural produce. *Food and Bioprocess Technology*, *5*(6), 2031–2045.

Paunonen, S., & Gregersen, Ø. (2010). The effect of moisture content on compression strength of boxes made of solid fibreboard with polyethylene coating. *Journal of Applied Packaging Research*, *4*(4). 223–242.

Peleg, K. (1985). Biomechanics of fruits and vegetables. *Journal of Biomechanics*, *18*(11), 843-862.

Perkins, S., Schnell, P., Kling, F., & Brittian, J. (2000). *The corrugated containers manufacturing process*. Tappi Press.

Persson, K. (1991). *Material model for paper: Experimental and theoretical aspects*. Diploma Report. Lund University.

Peterson, W. S. (1983). Flute/liner interaction for bending of combined board beams. *Paperboard Packaging*, *68*(8), 37–41.

Petrů, M., Novák, O., Herák, D., & Simanjuntak, S. (2012). Finite element method model of the mechanical behaviour of Jatropha curcas L. seed under compression loading. *Biosystems Engineering*, *111*(4), 412–421.

Petrů, M., Novák, O., Herák, D., Mašín, I., Lepšík, P., & Hrabě, P. (2014). Finite element method model of the mechanical behaviour of Jatropha curcas L. bulk seeds under compression loading: Study and 2D modelling of the damage to seeds. *Biosystems Engineering*, *127*, 50–66.

Phongphinittana, E., & Jearanaisilawong, P. (2013). A microstructurally-based orthotropic elasto-plastic model for paper and paperboard. *International Journal of Applied Science and Technology*, *5*(1), 19–25.

Pommier, J. C., & Poustis, J. (1990). Bending stiffness of corrugated board prediction using the finite element method. *Mechanics of Wood and Paper Materials*, *112*, 67–70.

Pommier, J. C., Poustis, J., Fourcade, E., & Morlier, P. (1991). Determination of the critical load of a corrugated box subjected to vertical compression by finite element methods. In *Proceedings of the 1991 International Paper Physics Conference, Kona, HI* (pp. 437–447).

Pommier, J., & Poustis, J. (1989). Box stacking strength prediction: Today McKee, tomorrow?. In *Proceedings of the 3rd Joint ASCE/ASME Mechanics Conference. CA, USA: San Diego*.

Popil, R. (2012). Overview of recent studies at IPST on corrugated board edge compression strength: Testing methods and effects of interflute buckling. *BioResources*, *7*(2), 2553–2581.

Popil, R. E. (2010). A new model for converting short span compression with other measurements to ring crush. *TAPPI PaperCon 2010, May 2-5, Proceedings*.

Popil, R. E., & Hojjatie, B. (2010). Effects of component properties and orientation on corrugated container endurance. *Packaging Technology and Science*, *23*(4), 189–202.

Popil, R. E., Coffin, D. W., & Kaewmanee, P. (2004). The role of liner buckling on the edgewise compressive strength of corrugated board. In *Abstract for paper presented at the 2004 Progress in Paper Physics Seminar, Trondheim, Norway*, (pp. 21-24).

Popil, R. E., Schaepe, M. K., Haj-Ali, R., Wei, B. S., & Choi, J. (2006). Adhesive level effect on corrugated board strength–experiment and FE modelling. In *2006 International Progress in Paper Physics Seminar, Miami University, Oxford Ohio*.

Poustis, J. (2005). *Corrugated fibreboard packaging*. In M. J. Kirwan (Ed.), *Paper and paperboard packaging technology* (pp. 317 – 372). Oxford: Wiley-Blackwell.

PPECB, (2013). PPECB - Annual Report 2012/2013. Cape Town.

Pradier, C., Cavoret, J., Dureisseix, D., Jean-Mistral, C., & Ville, F. (2016). An experimental study and model determination of the mechanical stiffness of paper folds. *Journal of Mechanical Design*, *138*(4), 041401.

Pré, G. (1992). Trends in food processing and packaging technologies. *Packaging Technology and Science*, *5*(5), 265–269.

Prusky, D. (2011). Reduction of the incidence of postharvest quality losses, and future prospects. *Food Security*, *3*(4), 463–474.

Puri, V. M., & Anantheswaran, R. C. (1993). The finite-element method in food processing: A review. *Journal of Food Engineering*, *19*(3), 247–274.

Ragni, L., & Berardinelli, A. (2001).Mechanical behaviour of apples, and damage during sorting and packaging. *Journal of Agricultural Engineering Research*, *78*(3), 273–279.

Ragulskis, K., Gegeckienė, L., Kibirkštis, E., Miliūnas, V., Zubrickaitė, L., Pauliukas, A., & Ragulskis, L. (2012). Dynamic study of transportation containers with packages. *Journal of Vibroengineering*, *14*(4), 1876–1884.

Raheem, D. (2012). Application of plastics and paper as food packaging materials–an overview. *Emirates Journal of Food and Agriculture*, *25*(3), 177–188.

Rahman, A. A., & Abubakr, S. (2007). A finite element investigation of the role of adhesive in the buckling failure of corrugated fibreboard. *Wood and Fibre Science*, *36*(2), 260–268.

Rahman, A. A., Urbanik, T. J., & Mahamid, M. (2007). FE analysis of creep and hygroexpansion response of a corrugated fiberboarad to a moisture flow: a transient nonlinear analysis. Wood and Fiber Science, 38(2), 268–277.

Ramasubramanian, M. K., & Muthuraman, K. (1999). Computational mechanics model for the brim forming process in paperboard container manufacturing. *Journal of Manufacturing Science and Engineering. Transaction of the ASME*, *125*(3), 476–483.

Ramasubramanian, M. K., & Wang, Y. (2007). A computational micromechanics constitutive model for the unloading behaviour of paper. *International Journal of Solids and Structures*, *44*(22), 7615–7632.

Ramnath Shenoy, C. M., Kumar, V., & Maheshwari, T. (2016) Determining the relationship between e flute corrugated board properties and its box compression strength. *International Journal of Research and Innovation in Applied Science*. *1*(9). 1–4.

Ramos-gonzalez, M., Connelly, W., & Pain, D. J. (2015). U.S. Patent No. 20,150,140,250. Washington, DC: U.S. Patent and Trademark Office.

Ranjan, R., Irudayaraj, J., Reddy, J. N., & Mujumdar, A. S. (2004). Finite-element simulation and validation of stepwise drying of bananas. *Numerical Heat Transfer, Part A*, *45*(10), 997–1012.

Rao, S. S. (2010). *The finite element method in engineering*. Elsevier.

Rayfield, E. J. 2007. Finite element analysis and understanding the biomechanics and evolution of living and fossil organisms. *Annual Review of Earth and Planetary Science*, *35*, 541–576.

Reddy, J. N. (2014). *An Introduction to Nonlinear Finite Element Analysis: with applications to heat transfer, fluid mechanics, and solid mechanics*. OUP Oxford.

Reh, S., Beley, J. D., Mukherjee, S., & Khor, E. H. (2006). Probabilistic finite element analysis using ANSYS. *Structural Safety*, *28*(1), 17–43.

Reis, A. B., Yoshida, C. M., Reis, A. P. C., & Franco, T. T. (2011). Application of chitosan emulsion as a coating on Kraft paper. *Polymer International*, *60*(6), 963–969.

Rennie, G. S. (1995). Quantifying the relationship between the short span compression and ring crush tests. *Tappi Journal*. *78*(7), 183–184.

Rhim, J. W. (2010). Effect of moisture content on tensile properties of paper-based food packaging materials. *Food Science and Biotechnology*, *19*(1), 243–247.

Rhim, J. W., Lee, J. H., & Hong, S. I. (2006). Water resistance and mechanical properties of biopolymer (alginate and soy protein) coated paperboards. *LWT-Food Science and Technology*, *39*(7), 806–813.

Rhim, J. W., Lee, J. H., & Hong, S. I. (2007). Increase in water resistance of paperboard by coating with poly (lactide). *Packaging Technology and Science*, *20*(6), 393–402.

Rigdahl, M., Andersson, H., Salmén, L., & Hollmark, H. (1984). The influence of moisture on the stiffness of paper in terms of network mechanics. *Fibre Science and Technology*, *20*(1), 1–11.

Ristinmaa, M., Saabye Ottosen, N., & Korin, C. (2012). Analytical prediction of package collapse loads-basic considerations. *Nordic Pulp and Paper Research Journal*, *27*(4), 806–813.

Robertson, G. L. (1993). *Food Packaging, Principles and Practice*, Marcel Dekker Inc.

Robertson, G. L. (2005). *Food Packaging, Principles and Practices* (2nd ed.). FL: CRC Press: Boca Raton.

Robertson, G. L. (2012). *Food Packaging, Principles and Practices* (3rd ed.). FL: CRC Press: Boca Raton.

Roduit, B., Borgeat, C. H., Cavin, S., Fragniere, C., & Dudler, V. (2005). Application of finite element analysis (FEA) for the simulation of release of additives from multilayer polymeric packaging structures. *Food Additives and Contaminants*, *22*(10), 945–955.

Romano, V. R., Marra, F., & Tammaro, U. (2005). Modelling of microwave heating of foodstuff: study on the influence of sample dimensions with a FEM approach. *Journal of Food Engineering*, *71*(3), 233–241.

Ruiz Altisent, M. (1991). Damage mechanisms in the handling of fruits: Progress in agricultural physics and engineering. *Commonwealth Agricultural Bureaux (CAB) International, Willingford, UK*, 231–255.

Sablani, S. S., Opara, L. U., & Al-Balushi, K. (2006). Influence of bruising and storage temperature on vitamin C content of tomato fruit. *Journal of Food Agriculture and Environment*, *4*(1), 54–56.

Sadrnia, H., Rajabipour, A., Jafari, A., Javadi, A., Mostofi, Y., Kafashan, J., Dintwa, E., & De Baerdemaeker, J. (2008). Internal bruising prediction in watermelon compression using nonlinear models. *Journal of Food Engineering*, *86*(2), 272–280.

Salarikia, A., Ashtiani, S. H. M., Golzarian, M. R., & Mohammadinezhad, H. (2017). Finite element analysis of the dynamic behavior of pear under impact loading. *Information Processing in Agriculture*, *4*(1), 64–77.

Salisbury, F.B., Ross, C.W., 1991. *Plant Physiology*, 4th ed. Belmont, CA.

Salmen, L. (1993). Responses of paper properties to changes in moisture content and temperature. *Presented at the tenth fundamental research symposium, Oxford* (pp. 369–430). Pira International.

Salminen, L. (2003). *Aspects of fracture processes in paper*. Doctoral dissertation, Helsinki University of Technology.

Samanta, K. K., Basak, S., & Chattopadhyay, S. K. (2016). Potentials of fibrous and nonfibrous materials in biodegradable packaging. In *Environmental Footprints of Packaging* (pp. 75-113). Springer Singapore.

Sangchai, P. (1997). *The Effect of cyclic environment on the compression strength of curtain coated corrugated containers.* Master's Thesis. Rochester Institute of Technology.

Šarčević, I., Banić, D., & Milčić, D. (2016). Evaluation of compressive test methods for paper using a mathematical model, based on compressive test for corrugated board. *Acta Graphica*, *27*(1), 47–50.

Satterthwaite, D., McGranahan, G., & Tacoli, C. (2010). Urbanization and its implications for food and farming. *Philosophical Transactions of the Royal Society of London B: Biological Sciences*, *365*(1554), 2809–2820.

Schaepe, M. (2000). The influence of pin adhesion strength on edge crush and box compression strength. *Corrugating International*, *2*(2), 35–39.

Schaldach, G., Berger, L., Razilov, I., & Berndt, H. (2000). Computer simulation for fundamental studies and optimisation of ICP spray chambers. *ISAS (Institute of Spectrochemistry and Applied Spectroscopy) Current Research Reports, Berlin, Germany*.

chlue, J. W. (1968). *The dynamic environment of spacecraft surface transportation*. Jet Propulsion Laboratory Technical Report 32.

Schreier, H. W. (2003). *Investigation of two and three-dimensional image correlation techniques with applications in experimental mechanics*. Doctoral dissertation. University of South Carolina.

Sek, M., Rouillard, V., Tarash, H., & Crawford, S. (2005). Enhancement of cushioning performance with paperboard crumple inserts. *Packaging Technology and Science*, *18*(5), 273–278.

Seyedabadi, E., Khojastehpour, M., & Sadrnia, H. (2015). Predicting cantaloupe bruising Using non-linear finite element method. *International Journal of Food Properties*, *18*(9), 2015–2025.

Shallhorn, P., Ju, S. H., & Gurnagul, N. (2004). A model for short-span compressive strength of paperboard. *Nordic Pulp & Paper Research Journal*, *19*(2), 130–134.

Shallhorn, P., Ju, S., & Gurnagul, N. (2005). A model for the ring crush test of paperboard. *Journal of Pulp and Paper Science*, *31*(3), 143–147.

Sharma, S. K., & Nautiyal, M. C. (2009). *Postharvest technology of horticultural crop* (Vol. 2). New India Publishing.

Siddiqui, M. W., & Ali, A. (Eds.). (2017). *Postharvest management of horticultural crops: practices for quality preservation*. CRC Press.

Side, C. (2008). *Food product development: based on experience*. John Wiley & Sons.

Singh, A., & Singh, Y. (1992). Effect of vibration during transportation on the quality of tomatoes. *Agricultural Mechanization in Asia, Africa and Latin America*, *23*(2), 70–72.

Singh, J. A., Bainbridge, P., Singh, S. P., & Olsen, E. (2007). Variability in compression strength and deflection of corrugated containers as a function of positioning, operators, and climatic conditions. *Journal of Applied Packaging Research*, *2*(2), 89–102.

Singh, J., Olsen, E., Singh, S. P., Manley, J., & Wallace, F. (2008). The effect of ventilation and hand holes on loss of compression strength in corrugated boxes. *Journal of Applied Packaging Research*, *2*(4), 227–238.

Singh, S. P., Burgess, G., & Xu, M. (1992). Bruising of apples in four different packages using simulated truck vibration. *Packaging Technology and Science*, *5*(3), 145–150.

Singh, S. P., Singh, J., & Paek, Y. (2009). New pressure sensitive device to measure and predict package drops. *Journal of Applied Packaging Research*, *3*(3), 149–160.

Singha, P., & Muthukumarappan, K. (2016). Quality changes and freezing time prediction during freezing and thawing of ginger. *Food Science & Nutrition*, *4*(4), 521–533.

Sirkett, D. M., Hicks, B. J., Berry, C., Mullineux, G., & Medland, A. J. (2007). Finite element simulation of folding carton erection failure. *Proceedings of the Institution of Mechanical Engineers, Part C: Journal of Mechanical Engineering Science*, *221*(7), 753–767.

Sirkett, D. M., Hicks, B. J., Berry, C., Mullineux, G., & Medland, A. J. (2006). Simulating the behaviour of folded cartons during complex packing operations. *Proceedings of the Institution of Mechanical Engineers, Part C: Journal of Mechanical Engineering Science*, *220*(12), 1797–1811.

Sittipod, S., Swasdee, D., Singh, S. P., & Singh, J. (2009). Effect of Truck Vibration during Shipments in Thailand. *Journal of Applied Packaging Research*, *3*(1), 27–38.

Skogman, R. T., & Scheie, C. E. (1969). The effect of temperature on moisture adsorption of Kraft paper. *Tappi Journal*. *52*(3), 489–490.

Slaughter, D. C., Hinsch, R. T., & Thompson, J. F. (1993). Assessment of vibration injury to Bartlett pears. *Transactions of the ASAE (USA)*, *36*(14), 1043–1047

Smith, J. P., Ramaswamy, H. S., & Simpson, B. K. (1990). Developments in food packaging technology. Part II. Storage aspects. *Trends in Food Science & Technology*, *1*, 111–118.

SmithersPira, (2016). *The future of corrugated board packaging*. SmithersPira.

Söremark, C., & Fellers, C. (1993). Mechano-sorptive creep and hygroexpansion of corrugated board in bending. *Journal of Pulp and Paper Science*, *19*(1), J19–J26.

Sørensen, G., & Hoffmann, J. (2003). Moisture sorption in moulded fibre trays and effect on static compression strength. *Packaging Technology and Science*, *16*(4), 159-169.

Soroka, W. (2002). *Fundamentals of packaging technology*. Institute of Packaging Professionals.

South African Department of Agriculture, Forestry and Fishery annual report (SADAFF), 2014.

SPI (1980). *Stacking performance of plastic bottles in corrugated boxes*. New York: The Society of Plastics Industry, Inc.

Sprague, C. H. (1982). Achieving adequate bonds on a consistent basis-precision in starch application. *Tappi Journal*, *65*(4), 137–139.

Sprague, C. H., & Whitsitt, W. J. (1982). Medium fracture and strength losses in fluting. *Tappi Journal*, *65*(10), 133–134.

Srirekha, A., & Bashetty, K. (2010). Infinite to finite: an overview of finite element analysis. *Indian Journal of Dental Research*, *21*(3), 425–432.

Stenberg, N. (2003). A model for the through-thickness elastic–plastic behaviour of paper. International *Journal of Solids and Structures*, *40*(26), 7483–7498.

Stenberg, N., Fellers, C., & Östlund, S. (2001). Measuring the stress-strain properties of paperboard in the thickness direction. *Journal of Pulp and Paper Science*, *27*(6), 213–221.

Stopa, R., Komarnicki, P., Szyjewicz, D., & Kuta, Ł. (2017). Modelling of carrot root radial press process for different shapes of loading elements using the finite element method. *International Journal of Food Properties*, 1–13.

Stott, R. A. (1959). Compression and stacking strength of corrugated fibreboard containers. *Appita Journal: Journal of the Technical Association of the Australian and New Zealand Pulp and Paper Industry*, *13*(2), 84–88.

Sukumaran, M. (2015). Performance and appearance of packaging grades of paper – study on quality measurement methods. *Indian Pulp and Paper Technical Association*. *27*(4). 20–39.

Sun, D. W. (Ed.). (2016). *Handbook of frozen food processing and packaging*. CRC Press.

Sutton, M. A., McNeill, S. R., Helm, J. D., & Chao, Y. J. (2000). Advances in two-dimensional and three-dimensional computer vision. *Photomechanics*. 323–372.

Sutton, M. A., Mingqi, C., Peters, W. H., Chao, Y. J., & McNeill, S. R. (1986). Application of an optimized digital correlation method to planar deformation analysis. *Image and Vision Computing*, *4*(3), 143-150.

Sutton, M. A., Yan, J. H., Tiwari, V., Schreier, H. W., & Orteu, J. J. (2008). The effect of out-of-plane motion on 2D and 3D digital image correlation measurements. *Optics and Lasers in Engineering*, *46*(10), 746-757.

Syed, I. A., & Bhoomkar, M. M. (2013). Comparative analysis of effect of fluting papers on ECT and FCT in single wall corrugated fibre boards. *Journal of Engineering Research and Studies*. *4*(4), 7–9.

Taher, B. J., & Farid, M. M. (2001). Cyclic microwave thawing of frozen meat: Experimental and theoretical investigation. *Chemical Engineering and Processing: Process Intensification*, *40*(4), 379–389.

Talbi, N., Batti, A., Ayad, R., & Guo, Y. Q. (2009). An analytical homogenization model for finite element modelling of corrugated cardboard. *Composite Structures*, *88*(2), 280–289.

Tang, Z., Liang, J., Xiao, Z., & Guo, C. (2012). Large deformation measurement scheme for 3D digital image correlation method. *Optics and Lasers in Engineering*, *50*(2), 122–130.

Tappi, (2006). T 494: Tensile properties of paper and paperboard (using constant rate of elongation apparatus). Technical Association of the Pulp and Paper Industry, Peachtree Corners, Georgia.

Tattiyakul, J., Rao, M. A., & Datta, A. K. (2001). Simulation of heat transfer to a canned corn starch dispersion subjected to axial rotation. *Chemical Engineering and Processing: Process Intensification*, *40*(4), 391–399.

Tekieli, M., De Santis, S., de Felice, G., Kwiecień, A., & Roscini, F. (2017). Application of digital image correlation to composite reinforcements testing. *Composite Structures*, *160*, 670-688.

Tevelow, F. L. (1983). The military logistical transportation vibration environment: Its characterization and relevance to MIL-STD fuse vibration testing. *US Army Electronics Research and Development Command, Harry Diamond Laboratories, Adelphi, Md*. 24–54.

Thakkar, B. K., Gooren, L. G., Peerlings, R. H. J., & Geers, M. G. D. (2008). Experimental and numerical investigation of creasing in corrugated paperboard. *Philosophical Magazine*, *88*(28-29), 3299–3310.

Thompson, J. (2004). Pre-cooling and storage facilities. In *The Commercial Storage of Fruits, Vegetables, and Florist and Nursery Stocks*; Agriculture Handbook 66; USDA: Washington, DC.

Thompson, J. F. (2008). *Commercial cooling of fruits, vegetables, and flowers*. UCANR Publications.

Thompson, J. F., Mejia, D. C., & Singh, R. P. (2010). Energy use of commercial forced-air coolers for fruit. *Applied Engineering in Agriculture*, *26*(5), 919–924.

Thompson, J. F., Mitchell, F. G., & Kasmire, R. F. (2002). Cooling horticultural commodities. In A. A. Kader (Ed.), *Postharvest Technology of Horticultural Crops* (3rd ed., p. 101). Davis, California: University of California Department of Agriculture and Natural Resources.

Thompson, J. F., Mitchell, F. G., Rumsey, T. R., Kasmire, R. F., & Crisosto, C. H. (2008). *Commercial cooling of fruits, vegetables, and flowers*. Oakland, California: University of California Department of Agriculture and Natural Resources.

Thorpe, J. L., & Choi, D. (1992). Corrugated container failure part 2 – strain measurements in laboratory compression tests. *Tappi Journal*, *75*(7), 155–161.

Timm, E. J., Brown, G. K., & R, A. P. (1996). Apple damage in bulk bins during semi - trailer transport. *Applied Engineering in Agriculture*, *12*, 367–377.

Timoshenko, S. P., & Gere, J. M. (1961). *Theory of elastic stability*. McGrawHill-Kogakusha Ltd, Tokyo.

Toubal, L., Karama, M., & Lorrain, B. (2005). Stress concentration in a circular hole in composite plate. *Composite Structures*, *68*(1), 31-36.

Touzinsky, G. F., Sprague, C. H., & Kloth, G. R. (1982). Fundamentals of the cold corrugating process-adhesives and bonding. *Tappi Journal*, *65*(10), 86–88.

Trezza, T. A., & Vergano, P. J. (1994). Grease resistance of corn zein coated paper. *Journal of Food Science*, *59*(4), 912–915.

Tryding, J. (1996). *In-plane fracture of paper*. Doctoral dissertation, Lund University.

Twede, D., & Harte, B. (2003). Logistical packaging for food marketing systems. *Food Packaging Technology*, 98–99.

Twede, D., & Selke, S. E. (2005). *Cartons, crates and corrugated board: Handbook of paper and wood packaging technology*. DEStech Publications, Inc.

Uchino, T., Nei, D., Hu, W., & Sorour, H. (2004). Development of a mathematical model for dependence of respiration rate of fresh produce on temperature and time. *Postharvest Biology and Technology*, *34*(3), 285–293.

Uesaka, T. E. T. S. U. (2002). Dimensional stability and environmental effects on paper properties. *Handbook of Physical Testing of Paper*, *1*, 115–171.

Uesaka, T., & Juntunen, J. (2012). Time-dependent, stochastic failure of paper and box. *Nordic Pulp & Paper Research Journal*, *27*(2), 370–374.

Urbanik, T. J. (1996). Machine direction strength theory of corrugated fibreboard. *Journal of Composites, Technology and Research*, *18*(2), 80–88.

Urbanik, T. J. (2001). Effect of corrugated flute shape on fibreboard edgewise crush strength and bending stiffness. *Journal of Pulp and Paper Science*, *27*(10), 330–335.

Urbanik, T. J., & Frank, B. (2006). Box compression analysis of world-wide data spanning 46 years. *Wood and Fibre Science*, *38*(3), 399–416.

Urbanik, T. J., & Saliklis, E. P. (2007). Finite element corroboration of buckling phenomena observed in corrugated boxes. *Wood and Fibre Science*, *35*(3), 322–333.

Vagenas, G. K., & Marinos-Kouris, D. (1991). Finite element simulation of drying of agricultural products with volumetric changes. *Applied Mathematical Modelling*, *15*(9), 475–482.

Vähä-Nissi, M., & Kuusipalo, J. (1997). Wetting and adhesion in paper and paperboard converting. *Papermaking Science and Technology*, *12*, 24-59.

Vaidya, R. (2012). *Structural analysis of poly ethylene terephthalate bottles using the finite element method*. Doctoral dissertation, Oklahoma State University.

Van Zeebroeck, M., Ramon, H., De Baerdemaeker, J., Nicolaï, B. M., & Tijskens, E. (2007). Impact damage of apples during transport and handling. *Postharvest Biology and Technology*, *45*(2), 157–167.

Venter, M. P., & Venter, G. (2012). Overview of the development of a numerical model for an inflatable paper dunnage bag. *Packaging Technology and Science*, *25*(8), 467–483.

Vergano, P. J., Testin, R. F., & Newall Jr, W. C. (1991). Peach bruising: susceptibility to impact, vibration, and compression abuse. *Transactions of the ASAE (USA)*, *34*(5): 2110–2116.

Vigneault, C., & de Castro, L. R. (2005). Produce-simulator property evaluation for indirect airflow distribution measurement through horticultural crop package. *International Journal of Food, Agriculture and Environment*, *3*(2), 67–72.

Vigneault, C., & Goyette, B. (2002). Design of plastic container opening to optimise forced-air precooling of fruits and vegetables. *Applied Engineering in Agriculture*, *8*(1), 73–76.

Vigneault, C., Thompson, J., & Wu, S. (2009). Designing container for handling fresh horticultural produce. *Postharvest Technologies for Horticultural Crops*, *2*, 25–47.

Viguié, J., & Dumont, P. J. J. (2013). Analytical post-buckling model of corrugated board panels using digital image correlation measurements. *Composite Structures*, *101*, 243-254.

Viguié, J., Dumont, P. J. J., Orgéas, L., Vacher, P., Desloges, I., & Mauret, E. (2011). Surface stress and strain fields on compressed panels of corrugated board boxes. An experimental analysis by using Digital Image Stereocorrelation. *Composite Structures*, *93*(11), 2861-2873.

Viguié, J., Dumont, P. J., Desloges, I., & Mauret, É. (2010). Some experimental aspects of the compression behaviour of boxes made up of G-flute corrugated boards. *Packaging Technology and Science*, *23*(2), 69–89.

Vishnuvarthanan, M., & Rajeswari, N. (2013). Additives for enhancing the drying properties of adhesives for corrugated boards. *Alexandria Engineering Journal*, *52*(1), 137–140.

Vishtal, A., & Retulainen, E. (2012). Deep-drawing of paper and paperboard: The role of material properties. *BioResources*, *7*(3), 4424–4450.

Vishtal, A., Hauptmann, M., Zelm, R., Majschak, J. P., & Retulainen, E. (2014). 3D forming of paperboard: The influence of paperboard properties on formability. *Packaging Technology and Science*, *27*(9), 677–691.

Vorakunpinij, A., Coffin, D. W., & Haberger, C. C. (2004). A new device for measuring tensile and compressive creep in paper. *Experimental Techniques*, *28*(3), 43–48.

Vursavuş, K. K., & Özgüven, F. (2004). Determining the effects of vibration parameters and packaging method on mechanical damage in golden delicious apples. *Turkish Journal of Agriculture and Forestry*, *28*(5), 311–320.

Walker, D. J. (1992). *World Food Programme: food storage manual*. Natural Resources Institute.

Wallace, J. R., Bromberek, A. E., & Young, S. N. (1995). High-density papers and corrugator runnability. *Tappi Journal*. *78*(4), 183–188.

Wang, D. M., Wang, J., & Liao, Q. H. (2013). Investigation of mechanical property for paper honeycomb sandwich composite under different temperature and relative humidity. *Journal of Reinforced Plastics and Composites*, *32*(13), 987–997.

Wang, L., & Sun, D. W. (2002). Modelling vacuum cooling process of cooked meat–part 1: analysis of vacuum cooling system. *International Journal of Refrigeration*, *25*(7), 854–861.

Wang, N., & Brennan, J. G. (1995). A mathematical model of simultaneous heat and moisture transfer during drying of potato. *Journal of Food Engineering*, *24*(1), 47–60.

Wang, Z. H., & Chen, G. (1999). Heat and mass transfer during low intensity convection drying. *Chemical Engineering Science*, *54*(17), 3899–3908.

Wang, Z. W. (2010). Effect of relative humidity on energy absorption properties of honeycomb paperboards. *Packaging Technology and Science*, *23*(8), 471–483.

Waterhouse, J. F. (1985). Paper properties and converting. *Technical Paper. IPC Technical Paper*, 162.

Wattrisse, B., Chrysochoos, A., Muracciole, J. M., & Némoz-Gaillard, M. (2001). Analysis of strain localization during tensile tests by digital image correlation. *Experimental Mechanics*, *41*(1), 29–39.

Wei, J., Junle, L., Jun, Y., Shihong, D., & Dean, Z. (2015). Analysis and validation for mechanical damage of apple by gripper in harvesting robot based on finite element method. *Transactions of the Chinese Society of Agricultural Engineering*, *31*(5), 17–22.

Wei, Z., Hua, G. J., & Zhao, D. J. (2011). Testing Research of Aspect Ratio on Corrugated Box Compression Strength. In *Applied Mechanics and Materials* (Vol. 48, pp. 1213-1216). Trans Tech Publications.

Weigel, T. G. (2001). *Modelling the dynamic interactions between wood pallets and corrugated containers during resonance*. Doctoral dissertation. Virginia Polytechnic Institute and State University, USA.

Wendler, S. (2006). *Washboarding of corrugated cardboard*. Doctoral Dissertation. Royal Melbourne Institute of Technology.

Whitsitt, W. J. (1988). Papermaking factors affecting box properties. *Tappi Journal*, *71*(12). 163–167.

Whitsitt, W. J., & McKee, R. C. (1972). Effect of relative humidity and temperature on stacking performance. *A summary report to the technical division of the FKBI, Inc., Project 2695-9.*

Whitsitt, W. J., Sprague, C. H., & Kloth, G. R. (1982). Fundamentals of the cold corrugating process-forming. *Tappi Journal*, *65*(10), 83–85.

Wilson, L. G., Boyette, M. D., & Estes, E. A. (1995). Part III: Handling. In: *Postharvest handling and cooling of fresh fruit, vegetables, and flowers for small farms*, North Carolina cooperative extension service, Horticulture information leaflet 804.

Wong, L., Kortschot, M. T., & Dodson, C. T. J. (1996). Effect of formation on local strain fields and fracture of paper. *Journal of pulp and paper science*, *22*(6), J213–J219.

World Packaging Organization. (2008). Market statistics and future trends in global packaging. World Packaging Organisation/PIRA International Ltd. www.worldpackaging.org/ (Accessed 26.06.17).

Wu, J., Li, F., Ge, Y., & Hu, R. (2013). Measurement of contact pressure of Korla pear under compression and bruising predication using finite element analysis. *Transactions of the Chinese Society of Agricultural Engineering*, *29*(6), 261–266.

Wu, N., & Pitts, M. J. (1999). Development and validation of a finite element model of an apple fruit cell. *Postharvest Biology and Technology*, *16*(1), 1–8.

Xia, B., & Sun, D. W. (2002). Applications of computational fluid dynamics (CFD) in the food industry: A review. *Computers and Electronics in Agriculture*, *34*(1), 5–24.

Xia, Q. (2002). *Mechanics of inelastic deformation and delamination in paperboard*. Doctoral dissertation, Massachusetts Institute of Technology.

Xia, Q. S., Boyce, M. C., & Parks, D. M. (2002). A constitutive model for the anisotropic elastic–plastic deformation of paper and paperboard. *International Journal of Solids and Structures*, *39*(15), 4053–4071.

Yang, W., Jia, C. C., Siebenmorgen, T. J., Howell, T. A., & Cnossen, A. G. (2002). Intra–kernel moisture responses of rice to drying and tempering treatments by finite element simulation. *Transactions of the ASAE*, *45*(4), 1037–1044.

Yang, Z. J., Harkin-Jones, E., Menary, G. H., & Armstrong, C. G. (2004). A non-isothermal finite element model for injection stretch-blow moulding of PET bottles with parametric studies. *Polymer Engineering and Science*, *44*(7), 1379–1390.

Ye, Z., Berdichevsky, V. L., & Yu, W. (2014). An equivalent classical plate model of corrugated structures. *International Journal of Solids and Structures*, *51*(11), 2073–2083.

Yoneyama, S., Kitagawa, A., Iwata, S., Tani, K., & Kikuta, H. (2007). Bridge deflection measurement using digital image correlation. *Experimental Techniques*, *31*(1), 34–40.

Yousefi, S., Farsi, H., & Kheiralipour, K. (2016). Drop test of pear fruit: Experimental measurement and finite element modelling. *Biosystems Engineering*, *147*, 17–25.

Yuan, W., Xu, W. C., Zhang, G. M., & Xie, L. H. (2013). The finite element study of the compressive strength of typical waveform corrugated box. *Applied Mechanics and Materials*, *262*, 390–394.

Yucesoy, C. A., Koopman, B. H., Huijing, P. A., & Grootenboer, H. J. (2002). Three-dimensional finite element modelling of skeletal muscle using a two-domain approach: Linked fibre-matrix mesh model. *Journal of Biomechanics*, *35*(9), 1253–1262.

Zeng, X., & Faghri, A. (1994). Experimental and numerical study of microwave thawing heat transfer for food materials. *Journal of Heat Transfer*, *116*(2), 446–455.

Zhang, Y. L., Chen, J., & Wu, Y. (2011). Analysis on hazard factors of the use of corrugated carton in packaging low-temperature yogurt during logistics. *Procedia Environmental Sciences*, *10*, 968–973.

Zhang, Z., Qiu, T., Song, R., & Sun, Y. (2014). Nonlinear finite element analysis of the fluted corrugated sheet in the corrugated cardboard. *Advances in Materials Science and Engineering*, *2014*, 1–8.

Zhao, L. L. (1993). *Evaluation of the performance of corrugated shipping containers: virgin versus recycled boards*. Doctoral dissertation, Victoria University of Technology.

Zhao, Y., Kolbe, E., & Craven, C. (1998). Computer simulation on on-board chilling and freezing of albacore tuna. *Journal of Food Science*, *63*(5), 751–755.

Zhou, J. W., Liu, D. H., Shao, L. Y., & Wang, Z. L. (2013). Application of digital image correlation to measurement of packaging material mechanical properties. *Mathematical Problems in Engineering*, 2013.

Zhou, L., Puri, V. M., Anantheswaran, R. C., & Yeh, G. (1995). Finite element modelling of heat and mass transfer in food materials during microwave heating–Model development and validation. *Journal of Food Engineering*, *25*(4), 509–529.

Zhou, Y., Pan, B., & Chen, Y. Q. (2012). Large deformation measurement using digital image correlation: A fully automated approach. *Applied optics*, *51*(31), 7674–7683.

Zou, Q., Opara, L. U., & McKibbin, R. (2006a). A CFD modelling system for airflow and heat transfer in ventilated packaging for fresh foods: I. Initial analysis and development of mathematical models. J*ournal of Food Engineering*, *77*(4), 1037–1047.

Zou, Q., Opara, L. U., & McKibbin, R. (2006b). A CFD modelling system for airflow and heat transfer in ventilated packaging for fresh foods: II. Computational solution, software development, and model testing. *Journal of Food Engineering*, *77*(4), 1048–1058.